Departament d'Enginyeria Química
Escola Tècnica Superior d'Enginyeria

P. San Valero

MODELACIÓN DEL PROCESO DE BIOFILTRO PERCOLADOR PARA EL TRATAMIENTO DE EMISIONES EN AIRE DE COMPUESTOS ORGÁNICOS VOLÁTILES DE ELEVADA SOLUBILIDAD EN AGUA

2016

MODELACIÓN DEL PROCESO DE BIOFILTRO PERCOLADOR PARA EL TRATAMIENTO DE EMISIONES EN AIRE DE COMPUESTOS ORGÁNICOS VOLÁTILES DE ELEVADA SOLUBILIDAD EN AGUA

TESIS DOCTORAL

PROGRAMA DE DOCTORADO EN INGENIERÍA QUÍMICA, AMBIENTAL Y DE PROCESOS

Autora:
Pau San Valero Tornero
Directora/es:
Dra. Carmen Gabaldón García
Dr. Josep Manuel Peñarrocha Oltra

VNIVERSITAT DE VALÈNCIA

VNIVERSITAT DE VALÈNCIA

Escola Tècnica Superior d'Enginyeria

Departament d'Enginyeria Química

MODELACIÓN DEL PROCESO DE BIOFILTRO PERCOLADOR PARA EL TRATAMIENTO DE EMISIONES EN AIRE DE COMPUESTOS ORGÁNICOS VOLÁTILES DE ELEVADA SOLUBILIDAD EN AGUA

PROGRAMA DE DOCTORADO EN INGENIERÍA QUÍMICA, AMBIENTAL Y DE PROCESOS

Memoria que, para optar al Título de Doctora por la Universitat de València, presenta **PAU SAN VALERO TORNERO**

Directores de tesis:
Dra. CARMEN GABALDÓN GARCIA
Dr. JOSEP M. PEÑARROCHA OLTRA

Valencia, febrero de 2016

Dra. CARMEN GABALDÓN GARCÍA, Profesora Titular del Departament d'Enginyeria Química de la Universitat de València, y

Dr. JOSEP MANUEL PEÑARROCHA OLTRA, Profesor Titular del Departament d'Enginyeria Química de la Universitat de València.

CERTIFICAN: Que Dña. Pau San Valero Tornero, con Título de Ingeniería Química y Máster Universitario en Ingeniería Ambiental, ha realizado bajo su dirección el trabajo que bajo el título de: "**MODELACIÓN DEL PROCESO DE BIOFILTRO PERCOLADOR PARA EL TRATAMIENTO DE EMISIONES EN AIRE DE COMPUESTOS ORGÁNICOS VOLÁTILES DE ELEVADA SOLUBILIDAD EN AGUA**" presenta en esta Memoria y que constituye su Tesis para optar al Título de Doctora por la Universitat de València en el Programa de Doctorado en Ingeniería Química, Ambiental y de Procesos.

Y para que conste a los efectos oportunos firman el presente certificado en Valencia a ___ de_____de 2016

Fdo.: Dra. Carmen Gabaldón García Fdo.: Dr. Josep Manuel Peñarrocha Oltra

AGRADECIMIENTOS

En primer lugar me gustaría agradecer a mis directores de tesis, Carmen Gabaldón y Josep Peñarrocha, por haber hecho posible la realización de esta tesis doctoral. Gracias por la dedicación y el apoyo de todos estos años. Por supuesto quiero extender este agradecimiento a Paula Marzal y Vicente Martínez-Soria que son dos pilares fundamentales del grupo de investigación.

Me gustaría agradecer a Javier Álvarez su dedicación e implicación en el desarrollo de esta tesis, especialmente su ayuda durante la modelación matemática. También agradecer a Marta Izquierdo todo el apoyo y el ánimo que me ha transmitido, tanto en el laboratorio como en la vida personal. Extender mi agradecimiento a Feliu Sempere por su disponibilidad para ayudar y su optimismo.

Gracias especialmente a Carlos por ser mi compañero y amigo todo este tiempo, a Jordi, por los buenos recuerdos, a M. Carmen y a Maria y al resto de compañeros, Pablo, Keisy, Dani Bravo, Nadine y Lidia. A todos los demás que han pasado por el laboratorio también gracias. Extender mi agradecimiento al resto de miembros del departamento que en algún un momento ha prestado su ayuda.

Quiero agradecer a la empresa PAS Solutions BV por permitirme realizar mi estancia en Zwolle y por la gran acogida durante los meses que estuve allí. Gracias especialmente a Salva por su motivación, y por todo lo que me enseñó en tan poco tiempo.

Me gustaría agradecerles a mis amigos que estén mi lado pase lo que pase. Gracias a Laia, a Paola. A Claudia, a Cate. A María, a Pablo, a Ana, a Pilar. Y, por supuesto a todo el resto de grandes amigos que tengo la suerte de tener: gracias por tantos años de amistad.

También agradecer a mi familia, a mis tíos y a mis primos, por poder contar siempre con ellos. Gracias a mis abuelos, por haber creido tanto en mí.

Gracias a Dani, porque conocerle fue una suerte, agradecerle la paciencia, la comprensión, y por ponerlo todo tan fácil. Extender mi agradecimiento a su familia por la ayuda durante este tiempo.

Gracias a mi hermano, Diego, por ser el mejor hermano del mundo.

Finalmente, me gustaría agradecerles y dedicarles esta tesis a mis padres, Arturo y Francisca. Gracias por enseñarme a luchar y a no rendirme, por enseñarme que no hay situación en la que no quepa una sonrisa. En definitiva, gracias por habérmelo enseñado todo, sin vosotros no lo habría conseguido.

RESUMEN

La contaminación del aire producida por las emisiones a la atmosfera de compuestos orgánicos volátiles (COV) es una de las causas más importantes asociadas al deterioro de la calidad ambiental. Una de las fuentes principales de emisión de COV son las industrias que utilizan disolventes. En este sentido, las industrias deben hacer un esfuerzo por adaptar sus procesos productivos para minimizar el impacto ambiental. Sin embargo, las propiedades de los disolventes los convierten en indispensables en algunas aplicaciones por lo que el tratamiento de las emisiones derivadas de su uso se convierte en una necesidad. El uso de biofiltros percoladores para la depuración de COV de elevada solubilidad en agua es una tecnología sostenible, habiéndose demostrado que es una alternativa viable técnica y económicamente, tal y como avalan las investigaciones realizadas en las últimas décadas. Sin embargo, el desarrollo de la investigación sobre esta tecnología requiere dar un paso más para lograr consolidarla en el entorno industrial.

Este trabajo de tesis doctoral tiene como objetivo principal el de desarrollar una herramienta matemática que incluya los principales mecanismos involucrados en la depuración de aire contaminado con COV de elevada solubilidad en agua mediante el proceso de biofiltro percolador en condiciones de operación típicas de la industria. Los COV de elevada solubilidad en agua están presentes de manera habitual en las emisiones gaseosas procedentes de la industria entre otras, de impresión flexográfica. Pese a que son compuestos con una biodegradabilidad relativamente elevada, la depuración de este tipo de COV suele verse limitada por la disponibilidad de oxígeno en el interior de la biopelícula, lo que favorece la acumulación de contaminante en el interior del sistema. En este sentido, una parte importante de la tesis doctoral ha consistido en profundizar en los mecanismos de transferencia de materia de contaminante y de oxígeno mediante la determinación de los coeficientes de transferencia de materia para ambos compuestos. La herramienta matemática desarrollada en la presente tesis doctoral tiene como finalidad simular y predecir la respuesta transitoria de los biofiltros percoladores sometidos a condiciones de carga variable y riego intermitente. El modelo matemático ha sido aplicado tanto a biofiltros percoladores utilizados en el laboratorio, en condiciones controladas de operación, como a biofiltros percoladores situados en instalaciones industriales, en los que se suele observar patrones de emisión más amortiguados.

En la primera etapa de este trabajo se llevó a cabo el estudio experimental a escala de laboratorio de eliminación de emisiones en aire que contenían

isopropanol, elegido éste como contaminante modelo. Para ello se utilizaron dos biofiltros percoladores empaquetados con diferente material de relleno: uno desordenado y otro estructurado. Durante este estudio se sometieron a los reactores a condiciones discontinuas de alimentación y de riego intermitente, y se evaluó la respuesta del biofiltro percolador a cambios en la concentración de alimentación de contaminante y de caudal de gas. Los resultados indicaron que el uso de patrones de riego intermitente provocaba una emisión fugitiva de contaminante en la corriente gaseosa de salida del biofiltro percolador que coincidía con el momento del riego. Para evaluar este efecto se aplicaron diferentes condiciones de riego al sistema, concluyendo que el patrón de riego podía utilizarse como estrategia para aumentar el rendimiento del reactor. Así mismo se sometió al reactor a un periodo de 7 semanas sin alimentación de COV. La capacidad de recuperación de los biofiltros percoladores puso de manifiesto la robustez del sistema.

La siguiente fase de la tesis se centró en el estudio de la transferencia de materia en los biofiltros percoladores. Para ello se determinaron los coeficientes de transferencia de materia de isopropanol y de oxígeno para diferentes velocidades superficiales de líquido y de gas y para varios materiales de relleno. Los datos obtenidos en este estudio permitieron desarrollar correlaciones empíricas para caracterizar la relación entre los coeficientes de transferencia de materia y las velocidades superficiales de gas y de líquido aplicadas en el biofiltro percolador. Así mismo, se evaluó un material de relleno de uso industrial en términos de transferencia de oxígeno con el objetivo de compararlo con los materiales de relleno empleados en el laboratorio, demostrándose que, en las velocidades de aplicación de los biofiltros percoladores industriales, la transferencia de oxígeno para este material era similar a la obtenida con los materiales utilizados en el laboratorio.

En la última parte del presente estudio se desarrolló un modelo matemático para la predicción de la respuesta transitoria de los biofiltros percoladores en condiciones de estado no estacionario de carga y de riego intermitente. El desarrollo del modelo se basó en balances de materia de isopropanol y de oxígeno en la fase gas, en la fase líquida y en la biopelícula. El modelo matemático se desarrolló asumiendo condiciones cíclicas de periodos con riego y de periodos sin riego, ya que ésta es la forma habitual de operación a nivel industrial. Durante los periodos con riego se consideró una fase líquida móvil, mientras que durante los periodos sin riego se consideró una fase líquida estancada. La calibración y validación del modelo matemático se realizó con datos de biofiltros percoladores utilizados a escala de laboratorio y a escala industrial.

Las principales hipótesis del modelo estuvieron relacionadas con la resistencia a la transferencia de materia tanto durante el riego (fase líquida móvil) como durante el no riego (fase líquida estancada). La calibración del modelo se llevó a cabo con datos de experimentos realizados a escala de laboratorio en biofiltros percoladores sometidos a riego discontinuo y carga de contaminante intermitente. Considerando despreciable la resistencia a la transferencia de materia producida por la fase líquida estancada durante los periodos sin riego, el modelo fue capaz de reproducir el rendimiento global del sistema así como el patrón de emisiones ocasionado por el riego discontinuo. Además, permitió identificar que la relación entre la concentración de carbono orgánico en el tanque de recirculación y la emisión fugitiva observada durante los periodos con riego estaba asociada al incremento de la resistencia a la transferencia de materia entre la fase gas y la fase líquida móvil con respecto a las determinaciones realizadas en condiciones abióticas. Este fenómeno se asoció al cambio de las propiedades físicas que ocasiona la presencia de biopelícula. La aplicación del modelo para la predicción de las emisiones de salida de un biofiltro percolador instalado en una industria de impresión flexográfica demostró la utilidad práctica del modelo. La aplicación del modelo para la simulación de esta corriente se basó en las hipótesis de la existencia de una resistencia a la transferencia de materia de la fase gas a la fase líquida móvil durante el riego y una resistencia adicional con respecto al biofiltro percolador de laboratorio a la transferencia de materia desde la fase gas a la fase líquida estancada durante los periodos sin riego. Se utilizó un mayor espesor de biopelícula que en los biofiltros percoladores empleados en el laboratorio ya que se identificó que ésta actuaba cíclicamente como fuente/sumidero asociado a los periodos diarios de fabricación/no fabricación. El elevado espesor de la biopelícula provocó que durante los periodos de alimentación de COV al sistema, la parte no degradada del contaminante se acumulara en la biopelícula, produciéndose su desorción en los periodos en los que circulaba aire limpio por el reactor. Todo ello demostró la capacidad del modelo para reproducir los fenómenos complejos involucrados en la respuesta dinámica de los biofiltros percoladores que tratan compuestos orgánicos volátiles de elevada solubilidad en agua.

El modelo matemático se integró en una herramienta informática mediante una GUI (Graphical User Inteface) desarrollada con MATLAB®. A fin de facilitar la comunicación con el usuario final, se generaron dos interfaces: una interfaz para introducir los datos para realizar las simulaciones y una interfaz de resultados. La herramienta desarrollada permite introducir de una manera sencilla patrones de concentraciones y caudales de gas variables, así como el uso de patrones de riego intermitente. Al terminar la simulación, la herramienta ofrece

una pantalla de resultados con la información más relevante para evaluar el funcionamiento de los biofiltros percoladores: gráficas de patrón de emisión de la concentración de contaminante en la fase gas a la entrada y a la salida del reactor y de la variación temporal de la concentración de carbono disuelto en el tanque de recirculación, así como datos promedio de concentración de contaminante en las emisiones gaseosas a la entrada y a la salida del bioreactor, de carga volumétrica y de capacidad de eliminación.

SUMMARY

Air pollution produced by the emission to the atmosphere of volatile organic compounds (VOCs) is one of the most important causes associated with deterioration of air quality. One of the main sources of VOC emissions are companies that use solvents. In this regard, they should make an effort to adapt their production processes in order to minimise environmental impact. However, the properties of solvents make them essential in certain applications, so the treatment of derivative emissions becomes a necessity. Use of biotrickling filters for the removal of highly water soluble VOCs is a sustainable technology, having been proven to be technologically and economically a viable alternative, as supported by research in the last few decades. However, research development on this technology requires one further step to achieve consolidation in the industrial environment.

The main objective of this dissertation is to develop a mathematical tool that includes the principal mechanisms involved in the removal of VOCs of high solubility in water from air emissions by the biotrickling filtration process in typical industry operating conditions. VOCs of high solubility in water are usually present in gaseous emissions from the flexographic printing industry, among others. Despite being compounds with a relatively high biodegradability, biological removal of such compounds is often limited by oxygen availability within biofilm, which leads to pollutant accumulation within the system. In this regard, an important part of the thesis was focused on the study of the mechanisms of mass transfer of pollutants and oxygen by means of the determination of the mass transfer coefficients for both compounds. The mathematical tool developed here aims to simulate and predict the transient response of the biotrickling filters under variable loading conditions and intermittent spraying. The mathematical model has been applied to biotrickling filters used in the laboratory, under controlled operating conditions, as well as to biotrickling filters located in industrial facilities, in which more buffered emission patterns are observed.

The first stage of this work comprises the removal of isopropanol in air emissions at the laboratory scale, selected as a model pollutant. For this purpose, two biotrickling filters filled with different packing materials were used: a random one and a structured one. The reactors were operated under discontinuous loading conditions and intermittent spraying. The response of the biotrickling filter to variations in the inlet concentration of pollutant, as well as in the gas flow, was evaluated. The results showed that intermittent spraying caused a fugitive pollutant emission in the outlet gaseous stream of the biotrickling during spraying.

To evaluate this effect, different spraying conditions were tested, concluding that the spray pattern could be used as a strategy to increase the reactor performance. Likewise, a starvation period of seven weeks was applied to both reactors. The resilience of the biotrickling filters showed the robustness of the system.

The next stage was focused on the study of mass transfer in biotrickling filters. For this purpose, the mass transfer coefficients of oxygen and of isopropanol were determined. Different superficial gas and liquid velocities as well as different packing materials were tested. Results allowed empirical correlations to be established, which characterised the relationship between the mass transfer coefficients and superficial velocities of liquid and of gas applied to the biotrickling filters. Likewise, a packing material for industrial use was evaluated in terms of oxygen mass transfer, in order to compare it to the packing materials applied in the laboratory. At typical industrial operating conditions, oxygen mass transfer for the industrial material was found to be similar to those obtained for the laboratory packing materials.

In the final stage, a mathematical model was developed in order to predict the transient response of the biotrickling filters under non-steady conditions of pollutant loading and of intermittent spray. The model development was based on the mass balances of isopropanol and of oxygen in the gas phase, in the liquid phase and in the biofilm. The mathematical model was built assuming cyclic conditions of spraying/non-spraying periods, the common industrial operational protocol. During spraying periods, a mobile liquid phase was considered, while during non-spraying periods, a stagnant liquid phase was considered. The calibration and validation of the mathematical model was performed using data from biotrickling filters operated at laboratory and industrial scales. The main hypotheses of the model were related to mass transfer resistance during spraying (mobile liquid phase) and mass transfer resistance during non-spraying (stagnant liquid phase). Model calibration was carried out with laboratory biotrickling filters operated under discontinuous spraying and intermittent pollutant loading. By assuming negligible mass transfer resistance for the stagnant liquid phase during non-spraying, the model was able to reproduce the average system performance and the emission pattern occasioned by the discontinuous spraying. In addition, the relationship between VOC concentration in the recirculation tank and the fugitive emission observed during spraying periods was related to higher mass transfer resistance between the gas and the mobile liquid phase during spraying than that obtained during abiotic determinations. This phenomenon was associated with variations in the physical properties caused by the presence of biofilm. The model application for predicting outlet emissions of a biotrickling filter

installed in the flexographic printing industrial facility demonstrated its practical usefulness. Model application for simulating this industrial air flow was based on the hypotheses of mass transfer resistance for the mobile liquid phase during spraying and an additional mass transfer resistance from the stagnant liquid phase during non-spraying with respect to laboratory experiments. It was identified that the biofilm acted as a source/sink associated with daily periods of manufacturing/ non-manufacturing. Thus, a greater thickness of biofilm than in the laboratory biotrickling filters was fixed. The thick biofilm caused the accumulation of the non-degraded pollutant during periods with VOCs feeding to the system. The stored pollutant in the biofilm led to desorption during periods when clean air circulated through the reactor. The model capability to reproduce the complex phenomena involved in the dynamic response of the biotrickling filters treating volatile organic compounds with high water solubility was demonstrated.

The mathematical model was integrated into an informatics tool using a GUI (Graphical User Interface) developed with MATLAB®. In order to facilitate communication with the end user, two interfaces were generated: an interface to enter data for simulations, and a results interface. The developed tool allows for the introduction of variable patterns of concentration and gas flows in a simple way, and also the use of intermittent spraying patterns. When the simulation ends, the tool offers a results screen with the most relevant information to evaluate the performance of the biotrickling filters: graphic information regarding the pattern of the gaseous emissions at the inlet and at the outlet of the reactor, as well as graphic information regarding the variation of dissolved organic carbon in the recirculation tank. Average data regarding the concentration in the gaseous emission at the inlet and at the outlet of the bioreactor, and the inlet load and the elimination capacity, are also provided.

ÍNDICE

1 JUSTIFICACIÓN, OBJETIVOS Y ESTRUCTURA

1.1 JUSTIFICACIÓN

La emisión a la atmosfera de compuestos orgánicos volátiles (COV) continúa siendo una de las causas más importantes de contaminación en aire. Esta problemática hace necesario promover el uso de tecnologías de tratamiento de bajo coste y respetuosas con el medio ambiente. El biofiltro percolador es una de las tecnologías que ha recibido mayor atención en las últimas décadas para la depuración de emisiones gaseosas contaminadas con compuestos orgánicos volátiles, especialmente si se trata de COV de elevada solubilidad en agua. Numerosos estudios a escala de laboratorio y algunos ejemplos a escala industrial demuestran la capacidad de estos sistemas para conseguir un tratamiento eficaz de estas emisiones. Sin embargo, debido a la dificultad para establecer las condiciones óptimas de funcionamiento o para establecer criterios robustos de diseño, todavía existen dificultades para implantar de manera generalizada este tipo de sistemas en el entorno industrial. Por este motivo, para lograr consolidar esta tecnología, es necesario profundizar en los principales fenómenos físico-químicos y biológicos que se producen durante la aplicación de los biofiltros percoladores al tratamiento de COV. El uso de modelos matemáticos basados en una descripción fenomenológica del sistema puede ayudar al investigador en la identificación de las etapas limitantes del proceso, permitiendo elaborar estrategias que mejoren el rendimiento global. En este sentido, es necesario el desarrollo de modelos matemáticos encaminados hacia una descripción más realista de las condiciones de operación que se utilizan en los sistemas industriales. Es en este contexto donde se fundamenta la presente tesis doctoral, cuya finalidad es el desarrollo de un modelo matemático que ayude al investigador a entender el funcionamiento de los biofiltros percoladores e identificar las limitaciones de esta tecnología. Para conseguirlo se debe profundizar en el conocimiento de las interacciones entre los diferentes fenómenos que se producen durante la degradación de COV (transferencia de materia, transporte convectivo y dispersivo, difusión y consumo de contaminante por parte de la biomasa). El modelo matemático se ha integrado en una interfaz gráfica de usuario (GUI) de MATLAB®, a través de la cual el usuario final puede definir de manera intuitiva las características de la corriente a tratar. Esta herramienta posibilita la simulación de patrones intermitentes y oscilantes de concentración y caudal de gas así como la simulación de condiciones de riego discontinuo con el fin de evaluar su influencia en la respuesta transitoria del sistema. Todo ello tiene como propósito final el desarrollo de una herramienta predictiva que ayude en la

identificación de las etapas limitantes del proceso y en la toma de decisiones durante el diseño y operación de los biofiltros percoladores.

1.2 OBJETIVOS

El objetivo general de esta tesis es el desarrollo de un modelo matemático para la simulación del proceso de biofiltro percolador para la eliminación de compuestos orgánicos volátiles de elevada solubilidad en agua en emisiones gaseosas generadas en los procesos industriales.

Para conseguir este objetivo general se han definido los siguientes objetivos parciales:

1. **Estudio experimental a escala de laboratorio de la depuración de COV de elevada solubilidad mediante biofiltros percoladores.** Para llevar a cabo este objetivo se ha seleccionado isopropanol como contaminante representativo de las emisiones gaseosas de la industria de impresión flexográfica. El sector flexográfico es pionero en Europa en la implantación de esta tecnología como solución final de tratamiento de emisiones de COV. Para ello se han planificado una serie de experimentos basados en el estudio de reactores tipo a escala de laboratorio. Se han empleado condiciones de alimentación de características similares a las propias de las emisiones procedentes de la industria de impresión flexográfica. Así mismo se han utilizado patrones de riego discontinuos con el objetivo de simular las condiciones habituales de operación de los biofiltros percoladores industriales. Este experimento tiene como objetivo específico obtener información sobre la influencia de los principales parámetros de operación como tiempo de residencia, carga volumétrica de contaminante y patrones de riego. Esta investigación incluye las siguientes etapas:

   - Evaluación preliminar de la transferencia de oxígeno en un biofiltro percolador con un relleno desordenado y otro estructurado.
   - Comparación del rendimiento del biofiltro percolador entre los dos rellenos seleccionados en función de diferentes parámetros y variables de operación del sistema: carga volumétrica de isopropanol, concentración en la corriente de entrada de COV, tiempo de residencia de volumen vacío y tipo de empaquetamiento del material de relleno en condiciones de alimentación discontinua de contaminante habituales de las emisiones industriales.

- Evaluación de la influencia del patrón de riego en las fluctuaciones de las emisiones gaseosas de contaminante a la salida del bioreactor.
- Evaluación de la respuesta de los biofiltros percoladores a un largo periodo sin alimentación de isopropanol simulando, con ello, paradas programadas de funcionamiento en instalaciones industriales.

2. **Modelación de la transferencia de materia en biofiltros percoladores para la eliminación de isopropanol.** La solubilidad en agua del isopropanol, de la misma manera que la de otros compuestos hidrofílicos, es menor que la solubilidad del oxígeno. Por este motivo, habitualmente la disponibilidad de oxígeno en el líquido y en la biopelícula puede limitar la biodegradación. Este fenómeno tendría como consecuencia la acumulación de contaminante en el sistema lo que podría provocar un empeoramiento en el rendimiento global asociado a la desorción del COV desde la fase líquida a la fase gas. Por este motivo es importante realizar un estudio de la transferencia de oxígeno, además de la del contaminante, cuando se estudia la transferencia de materia en biofiltros percoladores que van a tratar compuestos de elevada solubilidad en agua. El estudio de la transferencia de materia realizado en esta tesis doctoral tiene como objetivos específicos determinar una correlación entre las velocidades superficiales de gas y de líquido y los coeficientes de transferencia de materia para los intervalos de operación típicos de los biofiltros percoladores. El estudio de la transferencia de materia se ha desglosado en los siguientes puntos:

- Desarrollo de una metodología sencilla para determinar los coeficientes de transferencia para compuestos hidrofílicos utilizando isopropanol como contaminante de referencia.
- Determinación de los coeficientes globales de transferencia de materia de oxígeno y de isopropanol para diferentes tipos de materiales de relleno en las condiciones de operación típicas de los biofiltros percoladores.
- Determinación de la influencia de las velocidades superficiales de líquido y de gas en la transferencia de materia de isopropanol y oxígeno en las condiciones de operación típicas de los biofiltros percoladores.
- Desarrollo de correlaciones empíricas entre los coeficientes de trasferencia de materia y las condiciones de operación.

- Estudio comparativo para cambio de escala referente al comportamiento de diferentes materiales de relleno habituales en el laboratorio, en planta piloto y en escala industrial en términos de transferencia de oxígeno.

3. **Desarrollo de un modelo matemático en condiciones no estacionarias** que permita su uso como herramienta de predicción en tareas de diseño y operación. Partiendo de los datos obtenidos en la consecución de los dos objetivos anteriores, el desarrollo del modelo matemático incluye los siguientes elementos:

- Determinación de la relación dinámica que existe entre la fuga gaseosa de contaminante a la salida del bioreactor y la acumulación de sustratos orgánicos en la disolución de recirculación utilizando diferentes patrones de riego. Este estudio experimental tiene como objetivo obtener información sobre el perfil de la variación temporal de contaminante del gas a la salida del bioreactor y el perfil de la variación temporal de carbono disuelto en el tanque de recirculación.
- Desarrollo de un modelo matemático para la simulación y predicción de la respuesta transitoria en un biofiltro percolador, tanto de la fase gas como de la evolución del carbono disuelto en la disolución de riego. Este modelo permitirá la simulación con patrones intermitentes y oscilantes de concentración y caudal de gas, así como la simulación de condiciones de riego discontinuo. El modelo estará basado en la descripción de los principales procesos involucrados en la eliminación biológica de COV. Para estimar los coeficientes de transferencia de materia en función de las condiciones de operación y del material de relleno se utilizarán las correlaciones empíricas obtenidas en el desarrollo del objetivo parcial 2.
- Calibración de los parámetros del modelo a partir de los perfiles experimentales de variación de concentración de contaminante en la fase gas a la salida del reactor y de carbono disuelto en el tanque de recirculación.
- Validación del modelo matemático utilizando datos experimentales de laboratorio e industriales. Los datos a escala industrial se obtendrán de un biofiltro percolador (tecnología VOCUS^{TM}, PAS Solutions BV, Países Bajos) instalado en una industria de impresión flexográfica.

4. **Integración del modelo matemático en una herramienta informática** utilizando el programa MATLAB® para facilitar la comunicación con el usuario a través de una interfaz gráfica. Este trabajo se ha concretado en los siguientes elementos:

- Diseño y desarrollo de una interfaz gráfica de usuario que permita la introducción de manera intuitiva de las características de la corriente gaseosa a depurar, así como de todos los parámetros necesarios para llevar a cabo la simulación: patrones de concentración, patrones de caudal de aire, contaminantes, dimensiones del biofiltro percolador, características hidrodinámicas, frecuencia de riego, propiedades del biopelícula, constantes cinéticas, material de relleno, entre otros.
- Diseño y desarrollo de una interfaz gráfica de usuario que proporcione los resultados de la simulación: gráficas de evolución temporal de la concentración de contaminante en la fase gas a la entrada y a la salida del reactor, concentración de carbono disuelto en el tanque de recirculación, así como datos promedio de interés para el usuario (concentración de contaminante en las emisiones gaseosas a la entrada y a la salida del bioreactor, carga volumétrica y capacidad de eliminación).
- Aplicación de la interfaz gráfica de usuario para la simulación de los datos experimentales de los patrones pseudoestacionarios de concentración de contaminante de la fase gas a la salida del biofiltro percolador obtenidos en la consecución del objetivo 1.
- Simulación de diversas situaciones habituales a nivel industrial que permitan comparar la respuesta del biofiltro percolador ante corrientes variables en carga y en concentración con la información experimental obtenida.

1.3 ESTRUCTURA DE LA TESIS

Esta tesis doctoral se presenta por compendio de 5 artículos científicos dispuestos en 5 capítulos (capítulos 6-10). Los artículos originales se presentan en forma de anexo al final del presente documento. La memoria de tesis incluye un capítulo donde se realiza un resumen y discusión de los resultados más relevantes obtenidos durante el desarrollo de la presente tesis doctoral (capítulo 5). Estos resultados se encuentran ampliados en cada uno de los artículos científicos. Además, el documento de memoria de tesis consta de 12 capítulos: en el capítulo 1 se presentan la justificación de la tesis, objetivos y estructura; en los capítulos 2 y 3 se presenta el marco teórico de la tesis donde se realiza una introducción incluyendo una revisión bibliográfica del estado del arte actual; en el capítulo 4 se presenta un resumen de la metodología utilizada a lo largo del desarrollo experimental. Las conclusiones del presente trabajo junto con las perspectivas y trabajo futuro se presentan en el capítulo 11 y su versión en inglés en el capítulo 12.

Las referencias completas de los artículos científicos son las siguientes:

- **Artículo I (capítulo 6):** San-Valero, P., Penya-roja, J. M., Sempere, F. y Gabaldón, C. (2013). Biotrickling filtration of isopropanol under intermittent loading conditions. *Bioprocess and Biosystems Engineering, 36*(7), 975–984.
- **Artículo II (capítulo 7):** San-Valero, P., Penya-roja, J. M., Álvarez-Hornos, F. J. y Gabaldón, C. (2014). Modelling mass transfer properties in a biotrickling filter for the removal of isopropanol. *Chemical Engineering Science, 108*(0), 47–56.
- **Artículo III (capítulo 8):** San-Valero, P., Gabaldón, C., Penya-roja, J. y Pérez, M. C. (2012). Study of mass oxygen transfer in a biotrickling filter for air pollution control. *Procedia Engineering*, *42*, 1726–1730.
- **Artículo IV (capítulo 9):** San-Valero, P., Penya-roja, J. M., Álvarez-Hornos, F. J., Marzal, P y Gabaldón, C. (2015) Dynamic mathematical modelling of the removal of hydrophilic VOCs by biotrickling filters. *International Journal of Environmental Research and Public Health, 12,* 746–766.
- **Artículo V (capítulo 10):** San-Valero, P., Alcántara, S., Penya-roja, J. M., Álvarez-Hornos, F. J. y Gabaldón, C. (2016). A tool for predicting the dynamic response of biotrickling filters for VOC removal. *Chemical Engineering Communications 203 (4),* 476-487.

Springer Science BV y Business Media, Elsevier B.V., MDPI y Taylor & Francis han concedido el derecho de incluir los artículos científicos en la presente tesis doctoral.

En el **capítulo 6** se presentan los resultados sobre el estudio experimental a escala de laboratorio de la depuración de isopropanol mediante biofiltros percoladores. El isopropanol es un compuesto que se utiliza de manera habitual en los procesos de producción que utilizan tintas y disolventes, como es el caso de las industrias de impresión flexográfica. Este tipo de instalaciones industriales suelen trabajar en uno o dos turnos de producción, y, por tanto, presentan patrones de emisión discontinuos. Las condiciones de operación utilizadas en el desarrollo experimental están basadas en los procesos productivos que utilizan estas industrias. Así mismo, en la operación de los biofiltros percoladores se ha trabajado con un patrón de riego intermitente como es habitual a nivel industrial ya que disminuye los costes de operación y puede utilizarse como estrategia para controlar el crecimiento excesivo de la biomasa y de las pérdidas de presión.

En el **capítulo 7** se presentan los resultados relativos a la modelación de la transferencia de materia en biofiltros percoladores para la eliminación de isopropanol. La transferencia de materia, tanto de oxígeno como de contaminante, puede ser la etapa limitante del proceso. Por ello, es necesario conocer el papel de cada uno de los parámetros de operación como son la superficie específica y la estructura del material de relleno y las velocidades superficiales de líquido y de gas, para obtener las ecuaciones matemáticas que definen el sistema. En este capítulo se presenta la determinación de los coeficientes globales de transferencia de materia. Así mismo, este trabajo se ha enfocado a la obtención de correlaciones matemáticas con el objetivo de incluirlas en el modelo matemático desarrollado.

En el **capítulo 8** se muestran los resultados sobre el estudio comparativo en términos de transferencia de oxígeno del comportamiento de diferentes materiales de relleno habituales en el laboratorio, en planta piloto y en escala industrial.

En el **capítulo 9** se presenta el modelo matemático para la simulación y predicción de la respuesta transitoria de un biofiltro percolador sometido a condiciones de carga intermitente y utilizando patrones de riego discontinuos. Tras establecer las hipótesis del modelo, se presentan las ecuaciones matemáticas basadas en la descripción fenomenológica de los principales procesos involucrados en la eliminación biológica de COV. Así mismo, se describe el método utilizado para la resolución numérica de los balances de materia en cada una de las fases (gas, líquido, biopelícula) para los diferentes periodos de riego y de no riego. En

este capítulo se presenta la calibración y validación del modelo matemático con reactores de laboratorio. Para ello se utilizan los resultados de los experimentos llevados a cabo para la determinación de la relación dinámica existente entre la fuga gaseosa de contaminante a la salida del bioreactor y la acumulación de compuestos orgánicos en la disolución de recirculación utilizando diferentes patrones de riego. La utilidad del modelo se corrobora con la aplicación del modelo para la simulación del comportamiento de un biofiltro percolador (tecnología VOCUS^{TM}, PAS Solutions BV) instalado en una industria de impresión flexográfica que está sometido a condiciones variables e intermitentes de carga y donde se utilizan patrones de riego discontinuo.

La integración del modelo matemático en una interfaz gráfica de usuario utilizando el programa MATLAB® se muestra en el **capítulo 10**. En este capítulo se presentan ejemplos de su aplicación para la simulación de las respuestas dinámicas del biofiltro percolador en forma de patrón diario de fuga de contaminante gaseoso en la salida de los biofiltros percoladores obtenidos en la realización de los experimentos presentados en el capítulo 6. Así mismo se muestra la utilidad de la herramienta matemática para la simulación de diversos escenarios habituales de la industria utilizando diferentes variaciones de concentración y caudal de aire.

1.4 CONTRIBUCIÓN A LOS ARTÍCULOS

En los artículos presentados en este trabajo fui responsable del desarrollo de los experimentos en el laboratorio, evaluación crítica de los resultados, obtención de conclusiones y escritura de los artículos bajo la supervisión de mis directores de tesis, la Dra. Gabaldón y el Dr. Peñarrocha. Esta tesis doctoral se ha realizado en el marco del proyecto europeo NEXT AIR BIOTREAT: "*Developing the next generation air treatment based on replacing non-renewable resources by microbiology*" (Grant Agreement nº 284949). Se trata de un proyecto de investigación colaborativo academia e industria del programa PEOPLE, que tiene como finalidad el intercambio de personal y conocimiento entre los miembros del proyecto. El proyecto está coordinado por el grupo GI^{2}AM de la Universitat de València al que pertenezco. Uno de los socios del proyecto es la empresa PAS Solutions BV que se dedica al desarrollo de tecnologías biológicas para el tratamiento de diversos contaminantes en aire, entre ellos COV. Esto ha permitido el flujo de información entre la empresa y la universidad obteniéndose una visión realista de las necesidades de la industria respecto a esta tecnología para facilitar su consolidación en el mercado. En el marco del proyecto NEXT AIR BIOTREAT he

realizado una estancia de investigación de 3 meses de duración en la empresa PAS Solutions BV (Países Bajos). Durante la estancia de investigación realicé la recopilación y el análisis de los datos referentes al biofiltro percolador industrial. Los datos recogidos constituyen una parte fundamental del artículo IV (capítulo 9). Así mismo durante mi estancia, bajo la supervisión del Dr. Alcántara, llevé a cabo el desarrollo de la interfaz gráfica de usuario así como la generación de los escenarios teóricos de simulación que constituyen el artículo V (capítulo 10). El trabajo y la escritura del artículo fueron supervisados por el Dr. Alcántara junto con mis directores de tesis. La realización de esta estancia junto con los resultados obtenidos me ha permitido optar a incluir en el título de doctor la mención de "Doctor Internacional".

2 INTRODUCCIÓN

2.1 IMPORTANCIA DEL TRATAMIENTO DE LAS EMISIONES GASEOSAS DE COV

El desarrollo industrial ha derivado en un progresivo empobrecimiento de la calidad del aire, especialmente en las zonas urbanas. Los niveles de contaminación alcanzados se han convertido así en un gran riesgo para la salud y para el medio ambiente. En este sentido, la contaminación atmosférica es la primera causa de muerte prematura en la Unión Europea (UE). La Organización para la Cooperación y el Desarrollo Económicos (OCDE) estima que, si se continúa en la tendencia actual, en el 2050 la contaminación del aire se habrá convertido en la principal causa de mortalidad en todo el mundo.

Los contaminantes atmosféricos más problemáticos en términos de exposición para los seres humanos son el ozono troposférico y las partículas en suspensión (European Environment Agency, 2013). Sólo en el año 2012 el ozono troposférico causó alrededor de 17 000 muertes prematuras en Europa y un número considerable de enfermedades, de afecciones respiratorias y de empeoramiento de problemas cardiovasculares (European Environment Agency, 2015). Los principales precursores del ozono troposférico son los óxidos de nitrógeno y los COV. En el marco del Convenio de Ginebra (1979) relativo a la reducción de la acidificación, de la eutrofización y del ozono en la troposfera como consecuencia de transporte de contaminantes atmosféricos transfronterizos, se firmó el Protocolo de Gotemburgo (1999) cuyo objetivo fue controlar y reducir las emisiones de dióxido sulfúrico, de óxido de nitrógeno, de COV y de amoniaco. El protocolo de Gotemburgo entró en vigor en el año 2005, siendo ese mismo año cuando España lo ratificó. El protocolo fijaba los límites de emisión máximos para 2010, imponiendo a España una reducción de 39 % en la emisión de COV. Este protocolo se ha actualizado en el año 2012. Los nuevos objetivos del Protocolo supondrán una reducción de las emisiones de 30% de COV en el año 2020 respecto al año 2005. Así mismo, la crisis financiera que comenzó en 2008 en Europa ha promovido la búsqueda de otro tipo de desarrollos más allá del económico. Por ello ha cobrado importancia el concepto de *Economía verde* cuyo objetivo es solucionar al mismo tiempo dos de los problemas fundamentales ocasionados por la crisis financiera: el declive de la economía y el continuo deterioro del medio ambiente. Este concepto se ha convertido así en uno de los pilares fundamentales de la acción política europea (European Environment Agency, 2014b) y debe ser entendido como un camino para alcanzar al desarrollo sostenible.

En este contexto, se ha creado el "*Programa de Aire Puro para Europa*" cuyo objetivo es asegurar el cumplimiento de las normas vigentes de calidad ambiental en el año 2020 como fecha límite. Este programa fija una acción suplementaria para reducir las emisiones en el origen cuyo objetivo es la reducción de los impactos sobre la salud y sobre el medio ambiente con fecha límite 2030. Para conseguir este objetivo el principal instrumento es la Directiva de Techos Nacionales de Emisión que tiene fijado el horizonte político en ese mismo año. La propuesta incluye la obligación de reducción de las emisiones nacionales de los cuatro contaminantes atmosféricos que contribuyen a la contaminación transfronteriza, entre ellos los COV. Según la evolución prevista bajo la hipótesis de una aplicación plena de la legislación, en el 2030 los impactos sobre la salud relacionados con las partículas y el ozono deberían haberse reducido un 40% en relación a los de 2005. Además, los nuevos objetivos de la política sobre calidad del aire a largo plazo cifran esta reducción en un 52% si se aplican todas las medidas previstas.

La emisión de contaminantes atmosféricos, incluyendo los COV, actualmente está regulada por la Directiva 75/2010 en la cual se marcan las normas sobre la prevención y el control integrados de la contaminación procedente de las actividades industriales, modificando las anteriores directivas. La Directiva 75/2010 ha sido transpuesta al estado español a través de la Ley 5/2013, de 11 de junio, por la que se modifican la Ley 16/2002, de prevención y control integrados de la contaminación y la Ley 22/2011, de residuos contaminados.

Así pues, atendiendo a la Directiva 75/2010, Artículo 3, se define compuesto orgánico volátil como:

"*Todo compuesto orgánico, así como la fracción de creosota, que tenga a 293.15 K una presión de vapor de 0,01 kPa o más, o que tenga una volatilidad equivalente en las condiciones particulares de uso*."

Entendiendo compuesto orgánico como:

"*Compuesto orgánico: todo compuesto que contenga carbono y uno o más de los siguientes elementos: hidrógeno, halógenos, oxígeno, azufre, fósforo, silicio o nitrógeno, salvo los óxidos de carbono y los carbonatos y bicarbonatos inorgánicos.*"

Por otra parte, la Agencia Europea del Medio Ambiente los define como:

"*Compuestos orgánicos que bajo condiciones normales de operación son gaseosos o pueden vaporizarse o entrar en la atmosfera. Los compuestos orgánicos incluyen compuestos como el metano, benceno, xileno, propano y butano. El metano es primariamente emitido por la agricultura (por rumiantes y cultivos), mientras que los compuestos orgánicos volátiles diferentes del metano (COVNM), son principalmente emitidos por el transporte, los procesos industriales y el uso de disolventes*".

Sin embargo, no todos los compuestos tienen la misma reactividad fotoquímica. En este sentido, la Agencia Europea de Medio Ambiente distingue entre COV metánico y COV no metánico (COVNM). Así mismo, la Agencia Protección Ambiental de EEUU (Environmental Protection Agency, 2003) excluye algunos compuestos de carbono debido a que se ha demostrado que tienen una reactividad fotoquímica despreciable, entre ellos se encuentran el metano, etano y algunos compuestos halogenados, entre otros. Derivado de las descripciones anteriores se deduce la diferenciación entre compuestos orgánicos volátiles metánicos y no metánicos. En referencia al desarrollo de la presente tesis doctoral se entenderá COV como COV no metánicos.

En sí mismo, algunos COV constituyen un peligro para la salud de los seres humanos. Según la Agencia de Protección Ambiental de EEUU los signos claves o síntomas asociados con la exposición a los COV más comunes incluyen irritación conjuntival, nasal y molestias de garganta, dolor de cabeza, reacción alérgica de la piel, disnea, disminución de los niveles de colinesterasa sérica, náuseas, vómitos, epistaxis, fatiga y mareos. Algunos compuestos orgánicos pueden causar cáncer en animales y algunos se sospecha o se sabe que causan cáncer en los seres humanos.

Las mayores fuentes emisoras de COV son de origen antropogénico, destacando las fuentes difusas y las actividades industriales. En la Figura 2-1 se muestran las categorías clave en la emisión de COV. Como se observa, el 44% de los compuestos orgánicos volátiles emitidos a la atmósfera provienen del uso de disolventes. Durante los últimos años las industrias que utilizan disolventes en sus procesos productivos han tenido como prioridad reemplazar progresivamente el uso de disolventes orgánicos por otro tipo de disolventes. Esto ha supuesto una disminución de las emisiones de COV de 42% entre el año 1990 y el año 2012 en esta categoría (European Environment Agency, 2014a).

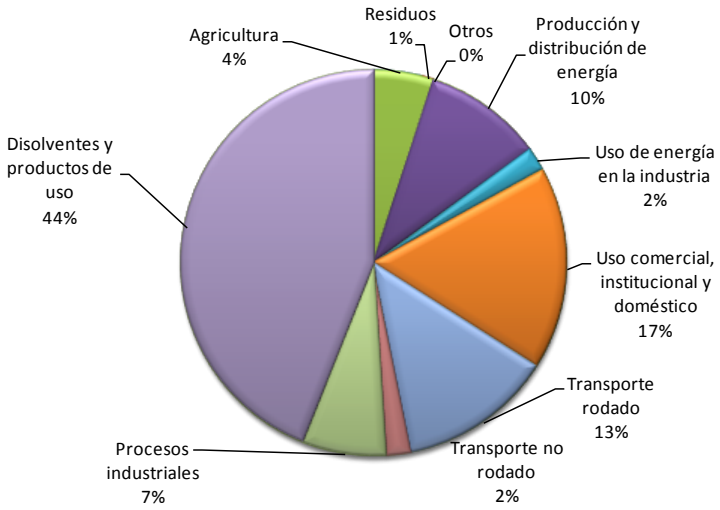

Figura 2-1 Distribución de las categorías clave en la UE–28 para las emisiones de COV. *Adaptada de European Environment Agency* (2014a).

Los cambios en la política actual prevén que se alcancen los objetivos de emisión establecidos para el 2020, lo que no estaba previsto antes de la crisis económica (European Environment Agency, 2014b). En este sentido, hay que destacar que las medidas existentes y previstas de la UE aplicables al control de la fuente de emisión contribuirán al logro de las reducciones exigidas.

Entre el año 1990 y el año 2012 las emisiones a la atmosfera de COV se han reducido en torno al 60% en el total de la UE. En el caso de España la reducción global de las emisiones de COV a la atmosfera ha sido de un 43% en este mismo periodo. En general, la reducción de las emisiones de COV se ha asociado a cambios en el modelo productivo así como a cambios en la política medioambiental europea. Sin embargo, los motivos de esta reducción no están claros. En Francia y en Reino Unido estas reducciones se asociaron con una política más restrictiva y mayor control. No obstante, la crisis económica europea ha afectado a los ritmos de disminución de la contaminación ambiental. Como ejemplo, en Alemania se asoció la reducción de las emisiones de COV a la crisis económica entre 2008 y 2009; sin embargo, las emisiones de COV en el año 2011 para este mismo país volvían a estar en niveles similares a los de 2008.

2.2 TECNOLOGÍAS DE TRATAMIENTO DE LAS EMISIONES GASEOSAS DE COV

Uno de los papeles más importantes que juega la Unión Europea es su capacidad para difundir el conocimiento de manera internacional fomentando aquellos proyectos basados en la eco-innovación (European Environment Agency, 2014b) con el objetivo de promover las tecnologías más sostenibles. Así mismo, existen instrumentos legales que obligan a las instalaciones industriales a tomar las medidas adecuadas de prevención de la contaminación, en particular mediante la aplicación de las Mejores Técnicas Disponibles (MTD).

La depuración de las emisiones gaseosas que contienen COV es considerada en sí mismo una MTD según el documento de referencia (European Commission, 2003), recientemente actualizado y en estado de borrador final (European Commission, 2014). La técnica de control a aplicar depende del proceso del que se emiten y de la peligrosidad que representa. A modo de resumen, en la Tabla 2-1 se muestran algunas de las técnicas disponibles más utilizadas para la depuración de emisiones gaseosas que contienen COV, presentando también las principales características de operación, y las principales ventajas y limitaciones de cada una de las técnicas propuestas. La selección de la tecnología más adecuada para el tratamiento de COV depende, entre otros factores, del caudal y de la concentración de las emisiones gaseosas. De manera orientativa, habitualmente se tiene en cuenta los criterios recomendados de caudal y de concentración de contaminante mostrados en la Figura 2-2 (Revah y Morgan-Sagastume, 2005). Sin embargo, para la selección final deberían emplearse otro tipo de factores como costes de inversión, de mantenimiento y de operación así como posibles impactos ambientales secundarios.

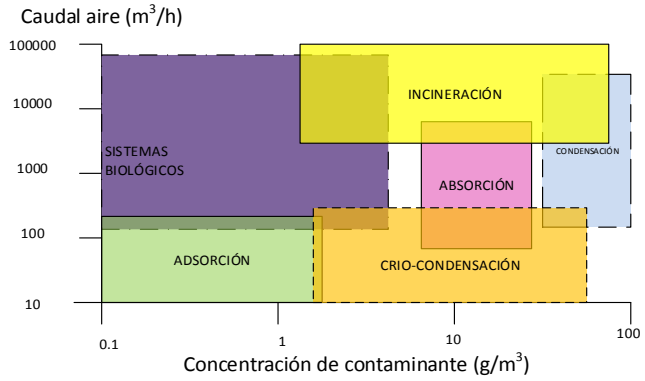

Figura 2-2 Intervalos recomendados para la preselección de las técnicas de depuración de COV. *Adaptado de Revah y Morgan-Sagastume (2005)*.

Tabla 2-1 Características, ventajas y limitaciones de las principales técnicas de recuperación y eliminación de COV. *Adaptada de Delhomenie y Heitz (2005).*

Tecnología	*Principio de funcionamiento y características*	*Rendimiento*	*Limitaciones*	*Uso*
Separación por membranas	• Separación de mezclas de gases a través de membranas semipermeables • Materiales: Polímeros (fibras de vidrio, siliconas) cerámicas porosas • Flujo de gas comprimido antes de la membrana de separación	• Conversión: 50–98% • Los COV se concentran 5–100 veces • Posible valorización • Membranas selectivas resistentes a compuestos halogenados	• Altas pérdidas de presión • Altas presiones de operación • Se requiere la limpieza de la membrana	PT
Condensación	• Licuefacción de COV con alto punto de ebullición (>38 ºC) vía calentamiento y/o compresión • Refrigeración/Sistemas criogénicos: Agua (5 ºC), salmuera (→-35ºC), nitrógeno líquido (→-185 ºC)	• Conversión:50–99% • Recuperación y valorización	• Solo adaptado para COV saturados • Eliminación de condensados • Problemas con los depósitos de hielo	FT PT
Adsorción	• Transferencia de VOC a una superficie solida porosa, fija o fluidizada • Materiales: carbón activado, zeolitas y polímeros • Instalación doble: Ciclos de adsorción y desorción • Temperatura de operación <50–60 ºC.	• Conversión: 90–99% • Posible recuperación de VOC • Amplio rango de caudal y periodos de apagado	• Necesitan tratamientos de regeneración • Humedad del efluente<50% • Pérdidas de presión • Envenenamiento del lecho con ciertos COV	FT
Absorción	• Transferencia de COV del gas al líquido • Columna de platos, columna de burbujas, columna empacada, atomizador • Disolventes: Agua (con ajuste de pH, hidrocarburos de punto de ebullición alto, aminas, etc. • Operación en contracorriente	• Conversión: 90–98% • Posible recuperación y valorización de los COV disueltos	• Inadecuados para COV de baja solubilidad • Producción de aguas residuales	FT

Tecnología	*Principio de funcionamiento y características*	*Rendimiento*	*Limitaciones*	*Uso*
Biotratamientos	• Oxidación biocatalítica de COV • Microorganismos: Bacterias y hongos • 30 s<Tiempo de residencia< Varios minutos • Temperatura de operación: 20–40 º C	• Conversión: 80–95% • Costes de instalación y operación moderados • Bajo mantenimiento	• Necesidad de un control estricto de los parámetros biológicos (pH, T, humedad, nutrientes, etc.) • Necesidades de espacio relativamente elevadas • Problemas de pérdidas de presión	FT
Incineración	• Oxidación térmica de COV • 760<T<1200 º C • Tiempos de residencia entre 0.3 y 2s • Concentración de COV<25% limite explosión. • Necesidad de O_2 ~10%	• Conversión: 98–99.5% • Posible recuperación de energía • Eliminación de COV halogenados o sulfurados con el equipo adecuado	• Altos costes de inversión y operación • Productos tóxicos de salida: CO, NOx, dioxinas, furanos, etc. • Baja eficiencia energética para concentraciones bajas de COV	FT
Oxidación catalítica	• Oxidación térmica, catalítica de COV • 300<T<650 º C • 0.07<Tiempo de residencia<1 s • Catalizadores: Metales nobles (Pt, Pd, Rh) en soportes (Alúmina y otras cerámicas) o óxidos de metal (Cu, Ti, Mn, etc.) • O_2 requerido ~2%	• Conversión: 90–99% • Menos requerimientos de energía • Subproductos menos tóxicos	• Problemas de desactivación de los catalizadores (*clogging*, envenenamiento, sobrecalentamien-to) • Subproductos de combustión • Eliminación del catalizador	FT
Oxidación fotocatalítica	• Oxidación completa por agentes oxidantes (O_3, H_2O_2) e iniciado por radiación UV • Posible utilización de fotocatalizadores • Temperatura de operación: ambiente	• Conversión: 90–98% • Costes energéticos moderados	• Inadecuados para COV halogenados • Depósito de subproductos de oxidación en la superficie de los catalizadores	FT

FT: Técnica de final de tubería / PT: Pretratamiento

Pese a que las medidas de prevención y control de la contaminación deben basarse en el uso de tecnologías eficientes de mínimo impacto ambiental, actualmente la oxidación térmica es una de las técnicas para el control de las emisiones de COV más utilizadas debido a sus elevadas eficacias de eliminación. Esta tecnología cuenta con grandes desventajas como son los elevados costes económicos e impactos ambientales asociados al uso de combustible auxiliar necesario para llevar a cabo el proceso.

En este sentido, en la guía sobre MTD se indica explícitamente que de las técnicas de final de tubería, en caso de tener que ser aplicadas, deben priorizarse las que tienen menor consumo energético; y entre este tipo de técnicas se puede identificar a los bioprocesos. El uso de estas tecnologías para el control de las emisiones de gas contaminadas con COV es adecuado cuando las emisiones presentan concentraciones bajas de contaminante (0.1–1 g m^{-3}) y caudales de aire elevados (10^2–10^4 Nm^3 h^{-1}) (Devinny et al., 1999). En general, los disolventes más adecuados para tratarse mediante este tipo de reactores son aquellos de mayor solubilidad y menor peso molecular, como alcoholes (metanol, etanol, isopropanol,…), aldehídos, cetonas y algunos compuestos aromáticos. Entre las ventajas de este tipo de tecnologías frente al uso de tecnologías convencionales está el ser uno de los métodos más económicos y con menos impacto ambiental (Delhomenie y Heitz, 2005; Devinny et al., 1999). Otra de las grandes ventajas es que pueden utilizarse a presión atmosférica y en el rango mesófilo de temperaturas (Revah y Morgan-Sagastume, 2005).

El uso de biotecnologías para el tratamiento de aire contaminado se remonta a mediados del siglo XX, sin embargo, no fue hasta a mediados de los años 70 que se empezaron a aplicar extensamente para el control de olores. En la actualidad son técnicas consolidadas en el campo de la eliminación de olores y comienzan a implantarse para el control de COV. Existen diferentes técnicas disponibles para el biotratamiento de aire contaminado con COV. Estas se diferencian en el método de retención de la biomasa en el reactor y en las condiciones de flujo de la fase líquida. Tal y como está especificado en el documento MTD (European Commission, 2003, 2014), entre los bioprocesos más aceptados y establecidos se encuentran el biofiltro, el biofiltro percolador y el biolavador (Figura 2-3). Los biofiltros son reactores de lecho fijo, normalmente de naturaleza orgánica, donde los microorganismos encargados de llevar a cabo la biodegradación se encuentran inmovilizados. En esta configuración el flujo de aire contaminado se hace pasar a través del lecho, de modo que los contaminantes son degradados por los microorganismos que están en la fase líquida inmóvil, llamada biopelícula, que se encuentra en la superficie del relleno. Por otra parte, los

biofiltros percoladores utilizan como material de relleno un soporte sintético (normalmente plástico) sobre el que se forma una película fina de biomasa; el relleno puede utilizarse desordenado o estructurado y son muy similares a los utilizados en la operación unitaria de absorción. Se establece un flujo líquido móvil, que puede ser en paralelo o en contracorriente al flujo de aire contaminado, que permite introducir los nutrientes y el agua necesaria para el desarrollo de la película de biomasa, así como para controlar la humedad y el pH. En cambio, los biolavadores se componen de dos etapas. La primera es una torre de absorción donde los contaminantes del aire se transfieren a una fase líquida. En la segunda etapa, el líquido contaminado se regenera en un reactor biológico aerobio de cultivo en suspensión, de forma que una vez reducido el contenido orgánico, se recircula a la torre de absorción. En el reactor biológico se realiza el control del pH y la adición de nutrientes para el crecimiento de los microorganismos encargados de la degradación de los contaminantes. La aplicación de esta técnica está limitada a la eliminación de contaminantes que presenten una solubilidad en agua adecuada.

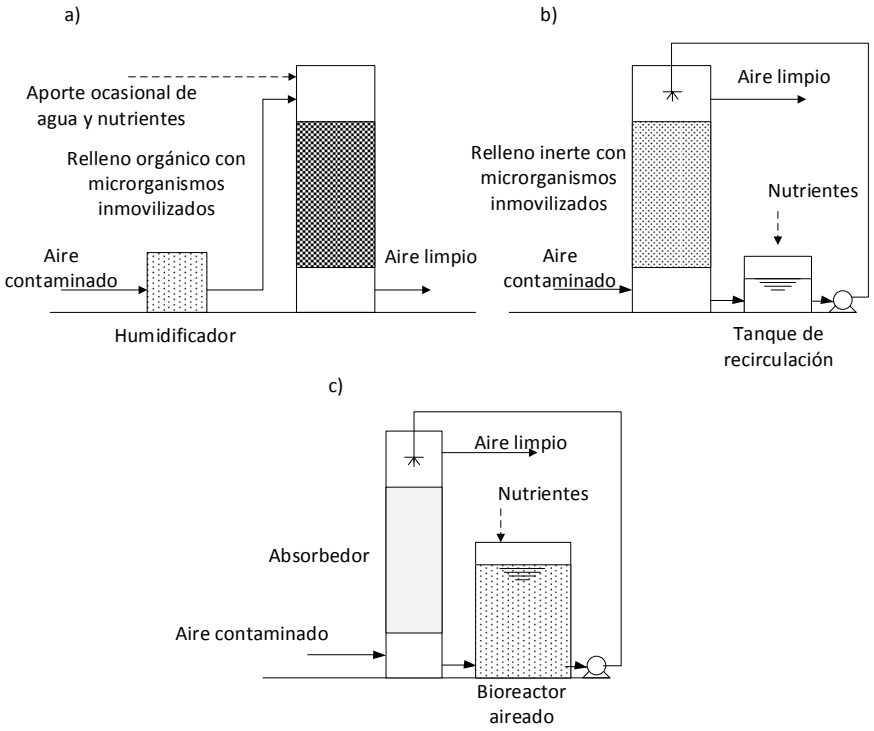

Figura 2-3 Esquema de los principales biotratamientos para la eliminación de COV. a) Biofiltro b) Biofiltro Percolador c) Biolavador.

2.3 BIOFILTROS PERCOLADORES

Los biofiltros percoladores empezaron a utilizarse a finales de los años 80 pero no fue hasta finales de la década de los 90 que esta tecnología empezó a ser utilizada para el tratamiento de contaminantes atmosféricos. En general, los biofiltros percoladores son adecuados para compuestos con una solubilidad en agua media o alta, con constantes de Henry inferiores a 0.1 (Kennes y Thalasso, 1998). Debido a sus múltiples ventajas esta tecnología ha generado un mayor interés en las últimas dos décadas frente a los biofiltros convencionales. Los biofiltros percoladores son capaces de obtener rendimientos superiores debido a que los materiales de relleno que se utilizan tienen mayor superficie específica y volumen de vacío. Así mismo, los biofiltros percoladores tienen mayor capacidad de respuesta a los cambios en la carga volumétrica de entrada de contaminante. Otra de las características que lo diferencian del biofiltro convencional, es la facilidad para el control de los parámetros físico-químicos del proceso como son humedad, temperatura, pH y salinidad a través de la corriente de recirculación del líquido. A nivel industrial, la aplicación del biofiltro percolador cuenta con la ventaja de necesitar menor superficie para su implantación debido a que se suele realizar la construcción en altura. Por último, las características del soporte sintético permiten ampliar la vida útil del relleno hasta un mínimo 10 años sin necesidad de ser reemplazado ni reacondicionado (Deshusses y Gabriel, 2005; Martínez-Soria et al., 2009).

2.3.1 Principales factores de operación

Existen diversos parámetros físico-químicos y de operación que influyen en el funcionamiento del proceso tanto a nivel económico como en la estabilidad a largo plazo. A continuación se describen los más importantes:

- Líquido de recirculación

En los biofiltros percoladores la fase líquida se introduce por la parte superior del reactor para aprovechar el efecto de la gravedad. Este líquido móvil permite mejorar el control de los parámetros físico-químicos, como disponibilidad de nutrientes y pH. En este sentido, la presencia del líquido de recirculación ofrece la capacidad de regular la relación de nutrientes para tener una dosificación más precisa (Kennes y Veiga, 2013). Las velocidades superficiales de líquido en un biofiltro percolador son más pequeñas que en el caso de los absorbedores químicos; valores habituales están comprendidos entre 0.05 y 20 m h^{-1} (Cox y Deshusses, 2001; Kennes y Veiga, 2013).

Las características del líquido de recirculación afectan al rendimiento global del sistema (Zhu et al., 1998). En general, el efecto del líquido de recirculación depende, entre otros, del contaminante y del material de relleno. Diversos estudios demuestran que su efecto sobre el rendimiento no está completamente definido. Por ejemplo, el aumento del caudal de líquido puede tener efectos positivos sobre el sistema como mejorar la transferencia de materia en el sistema (Hartmans y Tramper, 1991) y aumentar la superficie mojada de la biopelícula (Diks y Ottengraf, 1991b). Por contrapartida, puede provocar que la velocidad de desprendimiento de la biomasa se acelere.

A nivel industrial utilizar una corriente de recirculación continua resultaría económica y técnicamente inviable debido al aumento de los costes de operación y al crecimiento excesivo de la biomasa. Por este motivo, en los biofiltros percoladores es inevitable interrumpir la recirculación del líquido en algunos momentos (Devinny y Ramesh, 2005). Existen numerosos ejemplos de biofiltros percoladores industriales que utilizan de manera habitual el riego de agua de manera intermitente, siendo una práctica común en la industria (Cox y Deshusses, 2001; Sempere et al., 2012). En este sentido, se ha demostrado que en algunos casos puede aumentar el rendimiento del sistema y favorecer el control de las pérdidas de presión (Sempere et al., 2008). Además, utilizar riego intermitente puede favorecer la transferencia de materia, ya que en estos periodos se reduce el espesor de la capa de líquido que rodea a la biopelícula (Pol et al., 1998).

- Material de relleno

Los materiales de relleno utilizados en los biofiltros percoladores son inertes. Pueden ser de diversos materiales, siendo los materiales plásticos los más adecuados. En general, las propiedades más importantes para la selección del material son: elevada superficie específica, elevada porosidad, elevada estabilidad química y estructural, bajo peso, superficie adecuada para favorecer la fijación y el crecimiento de las bacterias y bajo coste económico (Cox y Deshusses, 2001).

La superficie específica del material de relleno es fundamental en el proceso de transferencia de materia, elevadas superficies específicas mejoran la transferencia de contaminante y oxígeno a la biopelícula, mejorando el rendimiento del sistema. Otra característica importante es la rugosidad de la superficie, materiales con mayor rugosidad permiten que los microorganismos se adhieran con mayor facilidad. Otro factor clave es el volumen de vacío, generalmente grandes volúmenes de vacío implican menores pérdidas de presión y facilitan el flujo de gas y de líquido a través del reactor. La densidad aparente también tiene un papel fundamental ya que el soporte interior en el bioreactor

debe ser capaz de sostener el peso. Así mismo, el tamaño del material de relleno es un aspecto clave, especialmente en el caso de los rellenos desordenados, donde si el tamaño es pequeño el aumento de la pérdida de presión puede evolucionar más rápido.

El relleno puede ser estructurado o desordenado. El relleno estructurado consiste en una serie de elementos regulares que están combinados juntos para formar un bloque. Normalmente estos bloques están fabricados de materiales de paredes delgadas, lo que reduce la densidad aparente del medio. Por otra parte, el relleno desordenado puede ser de varios materiales, tamaños y formas, desde anillos tipo *Pall* a otros como espumas, fibras, etc. Una de las principales ventajas de los materiales estructurados frente a los materiales desordenados radica en que, bajo condiciones optimizadas, el exceso de biomasa puede ser eliminado de manera más fácil, con tan solo aumentar la velocidad del líquido de recirculación durante un periodo corto de tiempo (Jin et al., 2008). Esto es debido a que en los rellenos estructurados se puede utilizar la fuerza cortante del líquido ya que están formados por canales definidos. Como consecuencia, se provocaría una turbulencia que ocasionaría el desprendimiento de la biomasa. Esto podría hacer factible el uso de materiales estructurados cuando se prevé que la acumulación de biomasa en el sistema pueda ser muy alta. Por contrapartida, estos materiales suelen tener un coste económico más elevado. Es por ello que en la actualidad los rellenos desordenados son más habitualmente utilizados.

- Inoculación y ecología microbiana

Para la puesta en marcha del proceso es necesaria la inoculación del sistema. La selección del inóculo adecuado depende del material de relleno y de la biodegradabilidad de los contaminantes. En la práctica los inóculos más habituales son: cultivos mixtos procedentes de suelos contaminados, biomasa de otros reactores que degradan los mismos contaminantes o similares, fangos activados de depuradoras y cultivos puros o consorcios de microorganismos adaptados a degradar el contaminante de interés.

En cuanto a la selección del inóculo atendiendo a la biodegradabilidad del contaminante, existen autores que indican que utilizar cultivos puros o adaptados con bacterias cuya capacidad de degradar el contaminante seleccionado haya sido demostrada influye en los periodos iniciales de puesta en marcha del proceso, disminuyendo considerablemente el tiempo de arranque (Cox y Deshusses, 2001). En cambio otros autores indican que para la degradación de estireno en un biofiltro, la utilización de una cepa de *P. putida* con capacidad degradadora no ofrece ninguna ventaja frente a un biofiltro percolador inoculado con fango de

depuradora (Pérez et al., 2014). En este sentido, hay que tener en cuenta que estos reactores biológicos son sistemas abiertos por lo que es inevitable la invasión de otras especies contenidas en el aire a depurar.

Los fangos activados contienen una gran variedad de microorganismos que ya han sido expuestos a contaminantes químicos presentes en las aguas residuales. En este sentido, se prevé que en el medio existan microorganismos que sean capaces de degradar COV (Devinny et al., 1999). El uso de fangos activados tiene evidentes ventajas frente a otros tipos de inóculos, como puede ser la facilidad para conseguirlo en grandes cantidades y el relativo bajo coste económico. En este sentido, diversos autores han demostrado la capacidad de este tipo de inóculo para adaptarse a disolventes orgánicos cómo, por ejemplo, etileno, etanol, acetato de etilo, metil etil cetona, entre otros (Lee et al., 2010; Sempere et al., 2008).

- Pérdidas de presión

La alimentación continua de un medio rico en nutrientes y contaminantes orgánicos conlleva la acumulación de la biomasa en el sistema. La acumulación excesiva de biomasa puede llegar a la colmatación del lecho provocando un aumento de las pérdidas de presión así como un empeoramiento del rendimiento del sistema (Kennes et al., 2009). Además, el exceso de biomasa provoca la disminución del tiempo de residencia efectivo y facilita la formación de zonas anaerobias con olores desagradables, así como la formación de caminos preferenciales. Así mismo, la distribución de la biomasa a lo largo del reactor normalmente no es uniforme llegando en ocasiones a producirse el 80–90 % de la eliminación en la primera mitad del reactor (Lu et al., 2001).

La obturación del sistema por acumulación de biomasa es uno de los mayores problemas asociados a la operación de los biofiltros percoladores. Existen diversas técnicas para evitar la acumulación excesiva de biomasa en el reactor. En este sentido, el riego intermitente y la operación discontinua como método de control del crecimiento de la biomasa parece una de las prácticas más sencillas para integrarse en instalaciones industriales. Por ejemplo, Cai et al. (2007) demostraron que períodos cíclicos con falta de alimentación de 2 a 7 días podían utilizarse para controlar el crecimiento de la biomasa en un bioreactor a escala de laboratorio para una mezcla gaseosa que contenía tolueno, estireno, metil etil cetona y metil isobutil cetona. Así mismo, el grupo de investigación GI^{2}AM de la Universitat de València viene trabajando en el desarrollo de esta técnica tanto a escala de laboratorio (Sempere et al., 2008) como a escala industrial (Martínez-

Soria et al., 2009) obteniendo resultados satisfactorios para el control de la biomasa en biofiltros percoladores.

- Temperatura

La temperatura es uno de los parámetros más importantes en los procesos biológicos, ya que puede afectar tanto a la reacción biológica como a la transferencia de materia. En el caso de la reacción biológica, en el rango mesófilo un aumento de la temperatura conlleva un aumento de la actividad biológica. Por otra parte en el caso de la transferencia de materia intervienen diversos fenómenos contrapuestos. Por una parte, un aumento de la temperatura implica un aumento en la constante de Henry, y por tanto, disminuye la solubilidad del contaminante y del oxígeno en la fase líquida. Por otro lado, el coeficiente de difusión del contaminante y del oxígeno en el interior de la biopelícula se ve favorecido al aumentar la temperatura facilitando la difusión en el interior de la biopelícula. Algunos estudios señalan que ambos efectos pueden contrarrestarse entre ellos, y sería posible no observar variaciones en el rendimiento de los reactores a cambios de temperatura en el intervalo de 18 a 30 ^{o} C (Diks y Ottengraf, 1991; Hartmans y Tramper, 1991). Sin embargo, otros estudios indican que el efecto de un incremento de temperatura sería generalmente favorable al proceso de transferencia en el intervalo de temperaturas habitualmente empleadas (Cox y Deshusses, 2001; Cox et al., 2001).

- Concentración de oxigeno

La constante de Henry del oxígeno en agua es varios órdenes de magnitud superior a la constante de Henry de COV hidrofílicos. Por este motivo la degradación de este tipo de compuestos puede estar limitada por la disponibilidad de oxígeno en la biopelícula. En consecuencia, la limitación por oxígeno por difusión es habitual, causando etapas anaerobias en las partes más profundas de biopelícula. En general, la limitación se acentúa en biopelículas con espesor grueso y con emisiones de concentraciones elevadas de disolventes hidrofílicos. Todo ello sugiere que el espesor de biopelícula activo está controlado, en ciertas situaciones, también por la cantidad de oxígeno y no solo por la disponibilidad de COV.

Existen diversos autores que han determinado la concentración oxígeno en la biopelícula. Kirchner et al. (1992) observaron que la difusión de oxígeno en la biopelícula podía ser la etapa limitante para el tratamiento de acetona y propionaldehído, ambos compuestos hidrofílicos. Zhu et al. (2004) concluyeron que para compuestos con elevadas constantes de Henry, como hexano y tolueno, la transferencia de COV entre la fase líquida y la fase gas era la etapa limitante;

pero que la transferencia de oxígeno podría ser la etapa limitante en el tratamiento de COV con bajas constantes de Henry, como butanol, especialmente con cargas orgánicas elevadas. Alonso et al. (1998b) confirmaron que es posible que la penetración del oxígeno en el agua y/o biopelícula sea menor que la del contaminante, causando zonas anaerobias. Para ello usaron una técnica de microelectrodos de oxígeno con la que se observó la escasez de oxígeno a una profundidad de 400 µm en la biopelícula de un biofiltro percolador que trataba dietil éter. Recientemente, Guimerà et al. (2014) presentaron un novedoso microsensor para determinar el oxígeno disuelto en el interior de la biopelícula. En este estudio encontraron que la difusividad efectiva relativa de oxígeno disminuía a largo de la biopelícula, por ejemplo, para una velocidad superficial de líquido de 9.88 m h^{-1}, la concentración de oxígeno variaba desde 3 mg L^{-1} hasta 0 mg L^{-1}.

- pH

En general, el metabolismo de los microorganismos heterótrofos capaces de consumir COV requiere pH neutros entre 6.5 y 7.5 (van Lith et al., 2011). Algunos autores han observado disminuciones en la eficacia de eliminación con pH inferiores a 4.5 (Prado et al., 2006). El pH puede ser regulado a través de la solución de nutrientes, o mediante la adición de ácidos y bases. Por ejemplo, Lu et al. (2002) observaron que en un biofiltro de riego por goteo tratando una mezcla de benceno, tolueno etil-benceno y o-xileno (BTEX) se incrementaba la eficacia de eliminación conforme se aumentaba el pH de los nutrientes entre 5 y 8. Sin embargo cuando se aumentaba por encima de 8, la eficacia de eliminación disminuía. Otros autores trabajaron con pH relativamente bajos, entre 3.5 y 7 (Veiga et al., 1999). Incluso hay estudios que han demostrado que algunas bacterias son capaces de degradar metanol hasta pH tan bajo como 2 (Jin et al., 2008). Así mismo hay que tener en cuenta que el pH puede variar a lo largo de la operación del biofiltro percolador debido a la producción de metabolitos intermedios como ácido acético y otros ácidos grasos volátiles, produciendo un empeoramiento del rendimiento del sistema (Devinny y Hodge, 1995).

- Nutrientes

Otro de los parámetros clave a tener en cuenta a la hora de emplear cualquier proceso biológico es el aporte de los nutrientes, ya que una mala distribución puede ocasionar rendimientos bajos (Lee et al., 2010). En general, para la degradación de COV el nutriente mayoritario es el nitrógeno, algunos autores recomiendan un coeficiente másico de carbono alimentado y nitrógeno alimentado entre 13 y 70 (Kennes y Veiga, 2002). También suelen ser necesarios otros elementos como fosforo, potasio, magnesio, hierro, manganeso y otros

elementos traza (micronutrientes). Para calcular la concentración óptima de nutrientes se puede utilizar el coeficiente de rendimiento de carbono para cada uno de los nutrientes. Sin embargo, debido a los costes económicos derivados de cualquier reactivo químico, en las plantas industriales es más común utilizar fertilizantes agrícolas o efluentes de decantadores secundarios de plantas de tratamiento de agua residuales (Cox y Deshusses, 2001).

2.3.2 Parámetros que definen la eficacia del proceso

Los principales parámetros que se utilizan para definir la eficacia del proceso se presentan a continuación. Se incluye la nomenclatura en inglés debido a que es la forma utilizada en los artículos que constituyen esta tesis doctoral.

- Tiempo de residencia a volumen de vacío (TRVV) o *Empty Bed Residence Time (EBRT):*

$$TRVV(s) = \frac{V_r}{Q_G} \cdot 3600 \tag{2-1}$$

donde V_r es el volumen de relleno del lecho (m^3) y Q_G es el caudal volumétrico de gas ($m^3\ h^{-1}$).

- Carga másica volumétrica de contaminante (CV) o *Inlet Load* (IL):

$$CV\left(g\ m^{-3}\ h^{-1}\right) = \frac{C_{ent}}{V_r} Q_G \tag{2-2}$$

donde C_{ent} es la concentración de contaminante en la fase gas a la entrada del biofiltro percolador ($g\ m^{-3}$).

- Capacidad de eliminación (CE) o *Elimination Capacity* (EC):

$$CE\left(g\,m^{-3}\,h^{-1}\right) = \frac{C_{ent} - C_{sal}}{V_r} Q_G \tag{2-3}$$

donde C_{sal} es la concentración de contaminante en la fase gas en el efluente del biofiltro percolador ($g\ m^{-3}$).

- Eficacia de eliminación (EE) o *Removal efficiency* (RE):

$$EE\,(\%) = \frac{C_{ent} - C_{sal}}{C_{ent}}\,100 \qquad (2\text{-}4)$$

Durante la operación del biofiltro percolador una parte del contaminante se acumula en el líquido de recirculación. En la práctica es habitual purgar una parte del líquido de forma periódica. Por ello, para determinar la eficacia de eliminación del proceso debe tenerse en cuenta la cantidad de contaminante absorbido en el agua de recirculación y la cantidad de contaminante eliminado con la purga.

La capacidad de eliminación definida en la ecuación (2-3) es el parámetro más importante a la hora de evaluar el funcionamiento del proceso. Sin embargo desde el punto de vista legislativo los parámetros más importantes son la concentración de contaminante en las emisiones de los gases depurados y la EE ya que en el Artículo 59 de la Directiva 75/2010 se especifica:

"*Los Estados miembros adoptarán las medidas necesarias para asegurar que cada instalación cumple uno de los siguientes requisitos:*

a) la emisión de compuestos orgánicos volátiles de las instalaciones no supera los valores límite de emisión en los gases residuales y los valores límite de emisión fugitiva o bien se respetan los valores límite de emisión total, y se cumplen los demás requisitos establecidos en las partes 2 y 3 del anexo VII;

b) *los requisitos del sistema de reducción especificado en la parte 5 del anexo VII, siempre y cuando se consiga una reducción en las emisiones equivalente en comparación con la alcanzada mediante la aplicación de los valores límites de emisión mencionados en la letra a).*"

En el Anexo VII de dicha directiva se establecen las disposiciones técnicas relativas a las instalaciones y actividades que utilizan disolventes orgánicos en la que se incluyen diversos tipos de industrias. En la parte 2 de dicho anexo se establecen los umbrales y valores límite de emisión mencionados en el apartado a). En general, para empresas consumidoras de disolventes de más de 15 Tn/año los valores límites de emisión están comprendidos entre 75 y 100 mg C Nm^{-3}. Por otra parte, la opción b) plantea un sistema de reducción basado en el cálculo de la reducción equivalente en Tn/año. Para verificar el cumplimiento de la legislación se utiliza el plan de gestión de disolventes planteados en el punto 3, de la parte 7

del mencionado anexo basado en el balance de consumo de disolventes. Así mismo, la Directiva concede al titular de la instalación libertad en la selección del sistema de reducción, siempre y cuando se consiga la reducción establecida.

2.3.3 Mecanismos involucrados en el proceso de biofiltro percolador

Para conseguir la degradación de los contaminantes gaseosos en el proceso de biofiltro percolador es necesario que el compuesto sea transferido desde la fase gas a la fase líquida, y en última instancia, a la biopelícula donde se produce la transformación del contaminante. Esto implica que el proceso se compone de varias etapas en serie, tal y como se esquematiza en la Figura 2-4. En estos sistemas, el contaminante orgánico y el oxígeno se transfieren desde la fase gas hasta la película biológica a través de la fase líquida, mientras que los productos de reacción se transfieren desde la biopelícula hacia el exterior.

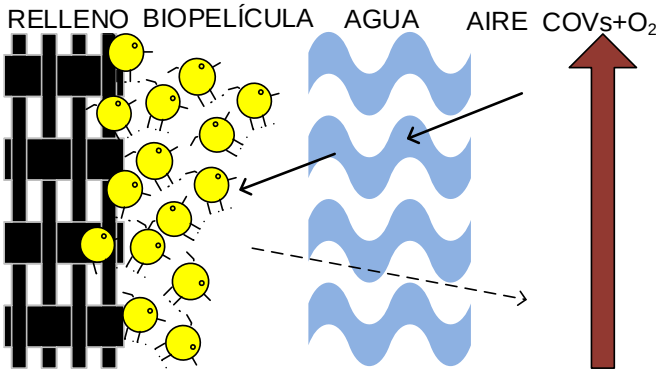

Figura 2-4 Fases implicadas en el proceso de eliminación de COV en un biofiltro percolador.

La primera etapa consiste en la transferencia de los contaminantes y del oxígeno desde la fase gas a la fase líquida. Diversos estudios (Alonso et al., 1998a; Baltzis et al., 2001; Zhu et al., 1998) han demostrado que la resistencia a la transferencia de materia se produce en la interfase, siendo despreciable la resistencia en el seno de la fase gas. Por este motivo se considera que en la interfase gas–líquido ambas concentraciones se encuentran en equilibrio, y, por tanto se puede considerar que se cumple la ley de Henry.

Una vez que el contaminante y el oxígeno han sido transferidos a la fase líquida, se produce la transferencia a la biopelícula. Diversos autores (Baltzis et al.,

2001; Baquerizo et al., 2005; Sharvelle et al., 2008) consideran despreciable la resistencia a la transferencia entre líquido y biopelícula y que la transferencia de materia entre ambas fases se produce por difusión, según la primera ley de Fick. Otros autores, entre ellos Kim y Deshusses (2003) han identificado que cuando el contaminante es muy soluble pueden producirse limitaciones a la transferencia de materia entre ambas fases.

En el interior de la biopelícula se produce la difusión y la biodegradación de los compuestos. Habitualmente se considera que la difusión se produce acorde con la segunda Ley de Fick. Sin embargo, existe controversia en este aspecto debido a la incertidumbre producida por la ausencia de datos sobre la difusión efectiva de contaminante y oxígeno en el interior de la biopelícula (Devinny y Ramesh, 2005). Durante la biodegradación de los COV están involucradas transformaciones microbiológicas y enzimáticas que convierten los contaminantes en metabolitos intermedios y finales. Cuando se produce la biodegradación de este tipo de compuestos, el objetivo principal es producir agua y CO_2 como productos finales. Sin embargo, en función de la naturaleza de los compuestos, pueden formarse otro tipo de metabolitos, como por ejemplo ácidos grasos volátiles. Durante este proceso, también se forma biomasa. Los microorganismos heterótrofos consiguen la energía necesaria para sus funciones vitales de la oxidación de las moléculas orgánicas, y asimilan parte del carbono orgánico como tejido celular.

La importancia relativa de cada una de las etapas marcará el funcionamiento del reactor. El proceso de biofiltro percolador puede estar limitado por la cinética microbiana, por la transferencia de materia o por ambas, dependiendo de la naturaleza del compuesto a degradar y de las condiciones de funcionamiento. Por ejemplo, en los compuestos de elevada solubilidad la etapa limitante suele ser la disponibilidad de oxígeno en la biopelícula que a su vez, limita la cinética microbiana. Por el contrario, para compuestos de menor solubilidad la etapa limitante suele ser la transferencia de contaminante entre la fase gas y la fase líquida.

2.3.4 Aplicaciones de los biofiltros percoladores para la depuración de COV de elevada solubilidad en agua

La aplicación de los biofiltros percoladores para la eliminación de COV de elevada solubilidad en agua ha sido demostrada en diversos estudios. En la Tabla 2-2 se muestran algunos ejemplos de aplicación de biofiltros percoladores para el tratamiento de emisiones gaseosas de compuestos orgánicos de elevada solubilidad en agua en diferentes escalas de aplicación.

El isopropanol es el compuesto seleccionado como contaminante modelo en la presente tesis doctoral. Es un compuesto utilizado de manera habitual en las empresas de impresión flexográfica. Los estudios disponibles en la bibliografía sobre este compuesto son escasos y corresponden a biofiltros convencionales y biofiltros de riego por goteo sometidos a condiciones de alimentación continua y en estado estacionario. Chang y Lu (2003) encontraron una CE comprendida entre 45 – 89 g C m^{-3} h^{-1} para cargas de isopropanol comprendidas entre 50–90 g C m^{-3} h^{-1} y TRVV comprendidos entre 20 – 30 s. Krailas et al. (2004) obtuvieron una CE máxima de 165 g C m^{-3} h^{-1} con una producción de acetona de 35 g C m^{-3} h^{-1} para una carga volumétrica de 204 g C m^{-3} h^{-1}. Otro compuesto típico de las industrias de impresión flexográfica comparable al isopropanol por su elevada solubilidad es el etanol. Existen diversos estudios sobre tratamiento de etanol en biofiltros percoladores realizados con alimentación continua de contaminante. Por ejemplo, Cox et al (2001) encontraron una carga crítica de 37 g C m^{-3} h^{-1} y un TRVV de 57 s mientras que Morotti et al. (2011) determinaron una capacidad máxima de eliminación de 24 g C m^{-3} h^{-1} utilizando un TRVV de 66 s y una concentración de entrada de 1100 g etanol m^{-3}.

Tabla 2-2 Ejemplos de aplicación de biofiltros percoladores para la eliminación de COV de elevada solubilidad en agua en emisiones gaseosas.

Contaminante	*Alimentación*	*Material de relleno*[a]	*CV* ($g\ m^{-3}\ h^{-1}$)	*TRVV* (s)	*EE* (%)	CE_{max} ($g\ m^{-3}\ h^{-1}$)	*Escala*[c]	
Acetona	Continua	Plexiglás fibra de coco	33-120	75-114	20-100	96	Lab	(Pielech-Przybylska et al., 2006)
Metanol	Continua	Cerámico	16-350	30	75-100	234	Lab	(Jin et al., 2008)
Metil Etil Cetona	Continua	Esferas PP	5-95	88	53-100	55	Lab	(Chou y Huang, 1997)
Metil Etil Cetona	Continua	Espuma PU	13-25	45-60	>99	25	Lab	(Moe y Li, 2004)
Isopropanol, acetona	Continua	Carbón	12-159	20-90	82-100	130	Lab	(Chang y Lu, 2003)
Metil Etil Cetona	Intermitente	Espuma PU, carbón activado	56-282	20-40	99-56		Lab	(Li y Moe, 2003)
Etanol, acetato etilo, metil etil cetona	Intermitente	Anillos PP	25-140[b]	15-60	58-95	96[b]	Lab	(Sempere et al., 2008)
Etanol, acetato de etilo	Intermitente	Anillos PP	50-90[b]	25-60	40-100	60[b]	Lab	(Sempere et al., 2009)
Etanol, n-propanol, isopropanol acetato de etilo	Intermitente	Esferas PP	312	14	89	278	Pil	(Popov et al., 2004)
Etanol, n-propanol, n-propil acetato , 1-metoxi 2-propanol	Intermitente	Anillos PP	0-160[b]	26-36	50-100	122[b]	Ind	(Sempere et al., 2012)

[a] *PP: Polipropileno / PU: Poliuretano*
[b] *($g\ C\ m^{-3}\ h^{-1}$)*
[c] *Lab: Laboratorio/ Pil: Piloto / Ind: Industrial*

Uno de los retos fundamentales de este proceso es su aplicación industrial. La mayoría de los procesos de fabricación que utilizan disolventes suelen caracterizarse por emisiones con patrones discontinuos e intermitentes resultando en variaciones en la concentración y en la velocidad de gas. En los últimos años ha habido un aumento en el número de investigaciones en el laboratorio que simulan condiciones típicas del entorno industrial. En este sentido, el grupo de investigación GI^{2}AM de la Universitat de València, en el cual he desarrollado esta tesis doctoral, cuenta con amplia experiencia en la aplicación de esta tecnología para tratar emisiones de COV con elevada solubilidad en agua en condiciones similares a las propias de la industria. En general, los estudios bibliográficos demuestran que en condiciones no estacionarias el rendimiento del proceso biológico se ve afectado negativamente. En trabajos previos llevados a cabo en el laboratorio, Sempere et al. (2009) aplicaron condiciones de carga volumétrica discontinua (12 h por día, 5 días por semana) para el tratamiento de una mezcla 1:1 de acetato de etilo y etanol, obteniéndose CE máximas de 48.5 g C m^{-3} h^{-1} para cargas de entrada de 70.5 g C m^{-3} h^{-1} y TRVV de 40 s. En otro estudio realizado por Sempere et al. (2008) se aplicaron condiciones de alimentación de contaminante intermitentes (16 h por día, 5 días por semana) para depurar una corriente equimásica 1:1:1 de etanol, acetato de etilo y metil etil cetona obteniéndose CE máximas de 96 g C m^{-3} h^{-1} para una CV de 141 g C m^{-3} h^{-1} y TRVV de 15 s. Además, la experiencia del grupo de investigación GI^{2}AM en la depuración de COV ha permitido constatar que existe una discrepancia en los patrones de emisión de los gases residuales obtenidos a nivel industrial respecto a los patrones de emisión obtenidos en los experimentos con biofiltros percoladores en el laboratorio. A nivel de laboratorio es habitual observar fuga de contaminante cuando hay riego mientras que a nivel de laboratorio es habitual un patrón de emisión más amortiguado.

El uso de biofiltros percoladores a escala de planta piloto y a escala industrial es todavía escaso para el tratamiento de COV de elevada solubilidad, aunque en la bibliografía se pueden encontrar algunos casos de éxito. En el estudio presentado por Popov et al. (2004) se instaló un biofiltro percolador en una industria de impresión flexográfica para tratar una corriente formada por etanol, n-propanol, isopropanol y acetato de etilo, obteniéndose una eficacia de eliminación de 89% con TRVV de 14 s y concentración de entrada de 814 mg C m^{-3}. Sempere et al. (2012) ha publicado el único ejemplo en Europa de aplicación de un biofiltro percolador como solución final en industrias de impresión flexográfica. En este trabajo se estudió el rendimiento del biofiltro percolador durante un periodo de 12 meses para la depuración de emisiones que contenían etanol, n-propanol, n-

propil acetato y 1-metoxi 2-propanol obteniéndose una capacidad de eliminación de 50 ± 11 g C m^{-3} h^{-1} para CV de 56 ± 15 g C m^{-3} h^{-1} y TRVV de 32 ± 7 s. Así mismo, en este estudio se obtuvo una capacidad de eliminación máxima de 122 g C m^{-3} h^{-1} para una CV de 138 g C m^{-3} h^{-1}. Cabe destacar que los protocolos desarrollados en el laboratorio por el grupo de investigación GI^{2}AM, así como los estudios realizados en planta piloto han sido un referente en la implantación industrial de esta tecnología tanto para el tratamiento de emisiones gaseosas de COV de elevada solubilidad en el sector de la industria flexográfica como para el tratamiento de emisiones del sector de recubrimientos de la madera con corrientes gaseosas compuestas por COV de distinta naturaleza (Martínez-Soria et al., 2009; Sempere et al., 2010).

2.4 BIBLIOGRAFÍA

Alonso, C., Suidan, M. T., Kim, B. R. y Kim, B. J. (1998a). Dynamic mathematical model for the biodegradation of VOCs in a biofilter: biomass accumulation study. *Environmental Science & Technology*, *32*(20), 3118–3123.

Alonso, C., Zhu, X., Suidan, M. T., Kim, B. R. y Kim, B. J. (1998b). Modelling of the biodegradation process un a gas phase bioreactor-estimation of intrinsic parameters. En: F. E. Reynolds Jr. (Ed.), *Proc. 1998 USC-TRG Conference on Biofiltration* (pp. 211–218). Tustin, CA: The Reynolds Group.

Baltzis, B. C., Mpanias, C. J. y Bhattacharya, S. (2001). Modeling the removal of VOC mixtures in biotrickling filters. *Biotechnology and Bioengineering*, *72*(4), 389–401.

Baquerizo, G., Maestre, J. P., Sakuma, T., Deshusses, M. A., Gamisans, X., Gabriel, D. y Lafuente, J. (2005). A detailed-model of a biofilter for ammonia removal: Model parameters analysis and model validation. *Chemical Engineering Journal*, *113*(2-3), 205–214.

Cai, Z., Kim, D. y Sorial, G. A. (2007). A comparative study in treating two VOC mixtures in trickle bed air biofilters. *Chemosphere*, *68*(6), 1090–1097.

Chang, K. S. y Lu, C. S. (2003). Biofiltration of isopropyl alcohol by a trickle-bed air biofilter. *Biodegradation*, *14*(1), 9–18.

Chou, M. S. y Huang, J. J. (1997). Treatment of methylethylketone in air stream by biotrickling filters. *Journal of Environmental Engineering-Asce*, *123*(6), 569–576.

Cox, H. H. J. y Deshusses, M. A. (2001). Biotrickling filters. En: C. Kennes y M. C. Veiga (Eds.), *Bioreactors for waste gas treatment* (pp. 99–131). Dordrecht, The Netherlands: Kluwer Academic Publisher.

Cox, H. H. J., Sexton, T., Shareefdeen, Z. M. y Deshusses, M. A. (2001). Thermophilic biotrickling filtration of ethanol vapors. *Environmental Science & Technology*, *35*(12), 2612–2619.

Delhomenie, M. C. y Heitz, M. (2005). Biofiltration of air: A review. *Critical Reviews in Biotechnology*, *25*(1-2), 53–72.

Deshusses, M. A. y Gabriel, D. (2005). Biotrickling filter technology. En: Z. Shareefdeen y A. Singh (Eds.), *Biotechnology for Odor and Air Pollution Control*. Heidelberg, Germany: Springer.

Devinny, J. S., Deshusses, M. A. y Webster, T. S. (1999). *Biofiltration for Air Pollution Control*. Boca Raton, USA: CRC-Lewis Publishers.

Devinny, J. S. y Hodge, D. S. (1995). Formation of acidic and toxic intermediates in overloaded ethanol biofilters. *Journal of the Air & Waste Management Association*, *45*(2), 125–131.

Devinny, J. S. y Ramesh, J. (2005). A phenomenological review of biofilter models. *Chemical Engineering Journal*, *113*(2-3), 187–196.

Diks, R. M. M. y Ottengraf, S. P. P. (1991). Verification studies of a simplified model for the removal of dichloromethane from waste gases using a biological trickling filter. 2. *Bioprocess Engineering*, *6*(4), 131–140.

Environmental Protection Agency. (2003). Code of Federal Regulations 51.100. Washington, DC, USA.: U.S. Government Printing Office.

European Commission. (2003). *IPPC Reference Document on Best Available Techniques in Common Waste Water and Waste Gas Treatment/Management Systems in the Chemical Sector*. (E. I. Bureau, Ed.). Sevilla.

European Commission. (2014). *Best Available Techniques (BAT) Reference Document for Common Waste water and Waste Gas Treatment/Management Systems in the Chemical Sector (Final Draft)*. (E. I. Bureau, Ed.). Sevilla.

European Environment Agency. (2013). Air quality in Europe -2013 report. En: *EEAA Technical report 9/2013*. Luxembourg: Publications Office of the European Union.

European Environment Agency. (2014a). *European Union emission inventory report 1990–2012 under the UNECE Convention on Long-range Transboundary Air Pollution (LRTAP)*. *Technical report Nº 12/2014*. Luxembourg: Publications Office of the European Union.

European Environment Agency. (2014b). Resource-efficient green economy and EU policies. En: *EEAA Report Nº2/2014*. Luxembourg: Publications Office of the European Union.

European Environment Agency. (2015). Air quality in Europe -2015 report. En: *Technical report Nº5/2015*. Luxembourg: Publications Office of the European Union.

Guimerà, X., Moya, A., Dorado, A. D., Villa, R., Gabriel, D., Gabriel, G. y Gamisans, X. (2014). Biofilm dynamics characterization using a novel DO-MEA sensor: mass transport and biokinetics. *Applied Microbiology and Biotechnology*, 55–66.

Hartmans, S. y Tramper, J. (1991). Dichloromethane removal from waste gases with a trickle-bed bioreactor. *Bioprocess Engineering*, *6*(3), 83–92.

Jin, Y., Veiga, M. C. y Kennes, C. (2008). Removal of methanol from air in a low-pH trickling monolith bioreactor. *Process Biochemistry*, *43*(9), 925–931.

Kennes, C., Rene, E. R. y Veiga, M. C. (2009). Bioprocesses for air pollution control. *Journal of Chemical Technology and Biotechnology*, *84*(10), 1419–1436.

Kennes, C. y Thalasso, F. (1998). Waste gas biotreatment technology. *Journal of Chemical Technology and Biotechnology*, *72*(4), 303–319.

Kennes, C. y Veiga, M. C. (2002). Inert filter media for the biofiltration of waste gases - characteristics and biomass control. *Reviews in Environmental Science and Biotechnology*, *1*(3), 201–214.

Kennes, C. y Veiga, M. C. (2013). Biotrickling filters. En: C. Kennes y M. C. Veiga (Eds.), *Air pollution prevention and control: Bioreactors and Bioenergy*. United Kingdom: John Wiley & Sons, Ltd.

Kim, S. y Deshusses, M. A. (2003). Development and experimental validation of a conceptual model for biotrickling filtration of H_2S. *Environmental Progress*, *22*(2), 119–128.

Kirchner, K., Wagner, S. y Rehm, H. J. (1992). Exhaust-gas purification using biocatalysts (fixed bacteria monocultures) - the influence of biofilm diffusion rate (O_2) on the overall reaction-rate. *Applied Microbiology and Biotechnology*, *37*(2), 277–279.

Krailas, S., Tongta, S. y Meeyoo, V. (2004). Macrokinetic determination of isopropanol removal using a downward flow biofilter. *Songklanakarin Journal Science Technology*, (26 (Suppl. 1)), 55–64.

Lee, S.-H., Li, C., Heber, A. J. y Zheng, C. (2010). Ethylene removal using biotrickling filters: Part I. Experimental description. *Chemical Engineering Journal*, *158*(2), 79–88.

Li, C. y Moe, W. M. (2003). Sequencing batch biofilter operation for treatment of methyl ethyl ketone (MEK) contaminated air. *Environmental Technology*, *24*(5), 531–44.

Lu, C., Lin, M.-R. y Chu, C. (2002). Effects of pH, moisture, and flow pattern on trickle-bed air biofilter performance for BTEX removal. *Advances in Environmental Research*, *6*(2), 99–106.

Lu, C. S., Lin, M. R. y Wey, I. H. (2001). Removal of pentane and styrene mixtures from waste gases by a trickle-bed air biofilter. *Journal of Chemical Technology and Biotechnology*, *76*(8), 820–826.

Martínez-Soria, V., Gabaldón, C., Penya-roja, J. M., Palau, J., Álvarez-Hornos, F. J., Sempere, F. y Soriano, C. (2009). Performance of a pilot-scale biotrickling filter in controlling the volatile organic compound emissions in a furniture manufacturing facility. *Journal of the Air & Waste Management Association*, *59*(8), 998–1006.

Moe, W. M. y Li, C. (2004). Comparison of Continuous and Sequencing Batch Operated Biofilters for Treatment of Gas-Phase Methyl Ethyl Ketone. *Journal of Environmental Engineering*, *130*(3), 300–313.

Morotti, K., Ramirez, A. A., Jones, J. P. y Heitz, M. (2011). Analysis and comparison of biotreatment of air polluted with ethanol using biofiltration and biotrickling filtration. *Environmental Technology*, *33*(15-16), 1967–1973.

Pérez, M. C., Álvarez-Hornos, F. J., Portune, K. y Gabaldón, C. (2014). Abatement of styrene waste gas emission by biofilter and biotrickling filter: comparison of packing materials and inoculation procedures. *Applied Microbiology and Biotechnology*, 19–32.

Pielech-Przybylska, K., Ziemiński, K. y Szopa, J. S. S. (2006). Acetone biodegradation in a trickle-bed biofilter. *International Biodeterioration & Biodegradation*, *57*(4), 200–206.

Pol, A., van Haren, F. J. J., den Camp, J. H. M. O. y van der Drift, C. (1998). Styrene removal from waste gas with a bacterial biotricking filter. *Biotechnology Letters*, *20*(4), 407–410.

Popov, V. O., Bezborodov, A. M., Cavanagh, M. y Cross, P. (2004). Evaluation of industrial biotrickling filter at the flexographic printing facility. *Environmental Progress*, *23*(1), 39–44.

Prado, O. J., Veiga, M. C. y Kennes, C. (2006). Effect of key parameters on the removal of formaldehyde and methanol in gas-phase biotrickling filters. *Journal of Hazardous Materials*, *138*(3), 543–548.

Revah, S. y Morgan-Sagastume, J. M. (2005). Methods of odor and VOC control. En: Z. Shareefdeen y A. Singh (Eds.), *Biotechnology for Odor and Air Pollution Control*. Alemania: Heidelberg.

Sempere, F., Gabaldón, C., Martínez-Soria, V., Marzal, P., Penya-roja, J. M. y Álvarez-Hornos, F. J. (2008). Performance evaluation of a biotrickling filter treating a mixture of oxygenated VOCs during intermittent loading. *Chemosphere*, *73*(9), 1533–1539.

Sempere, F., Gabaldón, C., Martínez-Soria, V., Penya-roja, J. M. y Álvarez-Hornos, F. J. (2009). Evaluation of a combined activated carbon prefilter and biotrickling filter system treating variable ethanol and ethyl acetate gaseous emissions. *Engineering in Life Sciences*, *9*(4), 317–323.

Sempere, F., Martínez-Soria, V., Penya-roja, J. M., Waalkens, A. y Gabaldón, C. (2012). Control of VOC emissions from a flexographic printing facility using an industrial biotrickling filter. *Water Science and Technology : A Journal of the International Association on Water Pollution Research*, *65*(1), 177–82.

Sempere, F., Martínez-Soria, V., Penya-roja, J.-M., Izquierdo, M., Palau, J. y Gabaldón, C. (2010). Comparison between laboratory and pilot biotrickling filtration of air emissions from painting and wood finishing. *Journal of Chemical Technology & Biotechnology*, *85*(3), 364–370.

Sharvelle, S., Arabi, M., McLamore, E. y Banks, M. (2008). Model development for biotrickling filter teatment of graywater simulant and waste Gas. I. *Journal of Environmental Engineering*, *134*(10), 813–825.

van Lith, C., Leson, G. y Michelsen, R. (2011). Evaluating design options for biofilters. *Journal of the Air & Waste Management Association*, *47*(1), 37–48.

Veiga, M. C., Fraga, M., Amor, L. y Kennes, C. (1999). Biofilter performance and characterization of a biocatalyst degrading alkylbenzene gases. *Biodegradation*, *10*(3), 169–176.

Zhu, X. Q., Alonso, C., Suidan, M. T., Cao, H. W. y Kim, B. R. J. (1998). The effect of liquid phase on VOC removal in trickle-bed biofilters. *Water Science and Technology*, *38*(3), 315–322.

Zhu, X. Q., Suidan, M. T., Pruden, A., Yang, C. P., Alonso, C., Kim, B. J. y Kim, B. R. (2004). Effect of substrate Henry's constant on biofilter performance. *Journal of the Air & Waste Management Association*, *54*(4), 409–418.

3 MODELACIÓN DEL PROCESO DE BIOFILTRO PERCOLADOR

La complejidad de los procesos que gobiernan un sistema biológico requiere utilizar herramientas matemáticas que permitan profundizar en el funcionamiento de los mismos. Desde que se empezó a trabajar en el desarrollo de estas tecnologías se ha realizado un gran esfuerzo por parte de los investigadores para intentar reproducir su funcionamiento. En general, los modelos desarrollados para describir los bioprocesos son modelos fenomenológicos basados en balances de materia. La dificultad en la modelación de este tipo de procesos radica en la complejidad de los fenómenos que intervienen tanto físicos–químicos como biológicos y en el acoplamiento e interacción de cada uno de ellos. En este capítulo de la tesis se presenta la descripción de la modelación matemática de los principales mecanismos involucrados en el proceso de biofiltro percolador, así como una revisión bibliográfica de los modelos matemáticos más relevantes publicados hasta la fecha.

3.1 DESCRIPCIÓN MATEMÁTICA DE LOS PRINCIPALES MECANISMOS DE BIOFILTRACIÓN

3.1.1 Transporte convectivo

En la modelación de los biofiltros percoladores habitualmente se considera flujo de pistón para reproducir el movimiento de la fase líquida y de la fase gaseosa en el interior del reactor. En estas condiciones el transporte se produce en la dirección axial de acuerdo con las ecuaciones (3-1) y (3-2) para la fase gas y para la fase líquida, respectivamente:

$$\theta_G \frac{\partial C_G}{\partial t} = \pm v_G \frac{\partial C_G}{\partial z} \tag{3-1}$$

$$\theta_L \frac{\partial C_L}{\partial t} = \pm v_L \frac{\partial C_L}{\partial z} \tag{3-2}$$

donde C_G es la concentración del componente en la fase gas (g m^{-3}), t es el tiempo (s), θ_G es la fracción volumétrica ocupada por la fase gas, v_G es la velocidad superficial de gas referida a volumen vacío (m s^{-1}), z es la altura del reactor (m), C_L es la concentración del componente en la fase líquida (g m^{-3}), θ_L es la fracción volumétrica ocupada por la fase líquida y v_L es la velocidad superficial del líquido referida a volumen vacío (m s^{-1}).

3.1.2 Dispersión axial

En ocasiones, la dispersión axial debe ser evaluada en referencia a su influencia en el rendimiento del proceso. Sin embargo, algunos autores indicaron que el efecto de ésta era insignificante, excepto en biofiltros que trabajan a tiempos de residencia de unos pocos segundos (Hodge y Devinny, 1995). La dispersión axial se expresa según:

$$\frac{\partial C_G}{\partial t} = D_{G,axial} \frac{\partial^2 C_G}{\partial z^2} \tag{3-3}$$

$$\frac{\partial C_L}{\partial t} = D_{L,axial} \frac{\partial^2 C_L}{\partial z^2} \tag{3-4}$$

donde $D_{G,\ axial}$ y $D_{L,\ axial}$ son los coeficientes de dispersión axial en la fase gas y en la fase líquida, respectivamente ($m^2\ s^{-1}$).

3.1.3 Transferencia de materia entre la fase líquida y la fase gas

La transferencia de contaminantes y de oxígeno desde la fase gas hacia la fase líquida ocurre según leyes físicas fundamentales. De acuerdo con la teoría de la doble película se considera que la diferencia de concentración en el interior de cada fase es despreciable excepto en las interfase de las mismas. Las concentraciones en la interfase están en equilibrio y la resistencia a la transferencia de compuesto se concentra en pequeñas películas a cada lado de la interfase. En este contexto, la dirección de transferencia de materia entre fases depende del gradiente de concentraciones y de la relación de equilibrio, siendo el factor controlante la velocidad de difusión a través de las dos películas.

En equilibrio, la relación entre la concentración en el aire y en el agua se rige por la ley de Henry, tal como representa la ecuación:

$$C_G = H \cdot C_L \tag{3-5}$$

donde H es la constante de Henry adimensional que depende del compuesto y de las condiciones ambientales.

El equilibrio es un fenómeno local ya que normalmente las concentraciones de componente varían sustancialmente según si éste se encuentra en regiones cerca o lejos de la salida del sistema, o si está en la interfase agua–aire o cerca de la biopelícula. Tradicionalmente se considera que la resistencia a la transferencia de materia externa que ofrece la fase gas es despreciable (Alonso et al., 1998; Baltzis et al., 2001; Zhu et al., 1998). Se puede asumir que la concentración en la fase gas es prácticamente la misma que en la interfase a causa del flujo convectivo que tiende a mezclar esta fase. En general, la capacidad de eliminación de contaminantes mediante el biofiltro percolador disminuye cuando los contaminantes presentan mayores constantes de Henry, ya que la solubilidad del compuesto en la fase acuosa es menor. De acuerdo con esta perspectiva, la transferencia de materia entre la fase líquida y la fase gas depende de los coeficientes globales de transferencia de materia y del gradiente de concentración entre ambas fases, de acuerdo con la ecuación:

$$N_a = K_L a \cdot \left(C_L^* - C_L \right) \tag{3-6}$$

donde N_a es la velocidad de transferencia de materia (g m^{-3} s^{-1}), C_L^* es la concentración de compuesto en la interfase de la fase líquida en equilibrio con la concentración de la fase gas (g m^{-3}) y $K_L a$ es el coeficiente global de transferencia de materia volumétrico basado en la fuerza impulsora en el líquido (s^{-1}).

El coeficiente global de transferencia de materia expresado en la fase líquida se relaciona con el coeficiente de materia expresado en la fase gas a través de la constante de la ley de Henry; ambos coeficientes se definen en función de los coeficientes individuales de transferencia de materia según la ecuación (3-7):

$$\frac{1}{K_L a} = \frac{1}{H\, K_G a} = \frac{1}{k_L a} + \frac{1}{H\, k_G a} \tag{3-7}$$

siendo $K_G a$ el coeficiente global de transferencia de materia volumétrico expresado en la fase gas (s^{-1}) y $k_L a$ *y* $k_G a$ los coeficientes individuales de transferencia de materia volumétricos para la fase líquida y la fase gas (s^{-1}), respectivamente.

La determinación de los coeficientes globales de transferencia de materia es uno de los puntos clave en la modelación del funcionamiento de los biofiltros percoladores. En este sentido, para una caracterización correcta del sistema debe tenerse en cuenta la influencia en la transferencia de materia tanto de la fase

líquida como de la fase gas (Pérez et al., 2006). Para determinar los coeficientes de transferencia de materia habitualmente se utilizan correlaciones empíricas desarrolladas para procesos de absorción. Las correlaciones más utilizadas fueron desarrolladas por Onda et al. (1968) y han sido utilizadas en numerosos trabajos de modelación (Baltzis et al., 2001; Kim y Deshusses, 2003):

$$k_G = 5.23\frac{D_G}{d_p^2 a_p}\left(\frac{\rho_G v_G}{\mu_G a_p}\right)^{0.7}\left(\frac{\mu_G}{\rho_G D_G}\right)^{1/3} \tag{3-8}$$

donde k_G es el coeficiente individual de transferencia de materia de la fase gas (m s^{-1}), a_p es la superficie específica del material de relleno (m^2 m^{-3}), d_p es el diámetro de partícula (m), D_G es el coeficiente de difusión de la fase gas (m^2 s^{-1}), ρ_L es la densidad de la fase gas (kg m^{-3}) y μ_G es la viscosidad del gas (kg m^{-1} s^{-1}),

$$k_L = 0.0051\left(a_p d_p\right)^{0.4}\left(\frac{\mu_L g}{\rho_L}\right)^{1/3}\left(\frac{\rho_L v_L}{a_e \mu_L}\right)^{2/3}\left(\frac{\mu_L}{\rho_L D_L}\right)^{-0.5} \tag{3-9}$$

donde k_L es el coeficiente individual de transferencia de materia de la fase líquida (m s^{-1}), a_e es la superficie especifica efectiva del material de relleno (m^2 m^{-3}), D_L es el coeficiente de difusión de la fase líquida (m^2 s^{-1}), ρ_L es la densidad de la fase líquida (kg m^{-3}) y μ_L es la viscosidad del líquido (kg m^{-1} s^{-1}).

Así mismo, otras de las ecuaciones empíricas utilizadas en el campo de la biofiltración fueron propuestas por van Krevelen y Hoftijzer (1948):

$$k_G = 0.2\frac{D_G}{d_c}\left(\frac{\rho_G v_G}{\mu_G a_p}\right)^{0.8}\left(\frac{\mu_G}{\rho_G D_G}\right)^{1/3} \tag{3-10}$$

donde d_c es el diámetro interno de la columna (m).

$$k_L = 0.015 D_L\left(\frac{\mu_L^2}{\rho_L^2 g}\right)^{-1/3}\left(\frac{\rho_L v_L}{a_e \mu_L}\right)^{2/3}\left(\frac{\mu_L}{\rho_L D_L}\right)^{1/3} \tag{3-11}$$

donde g es la constante gravitacional (m s^{-2}).

Diversos autores han demostrado que el uso de este tipo de correlaciones puede conducir a desviaciones debido a la diferencia en las condiciones hidrodinámicas de los biofiltros percoladores con respecto a los absorbedores químicos (Dorado et al., 2009; Kim y Deshusses, 2008b; Pérez et al., 2006). En este sentido, Kim y Deshusses (2008a) realizaron un estudio sistemático con el fin de desarrollar ecuaciones empíricas para los intervalos típicos de velocidades superficiales de líquido y de gas en los biofiltros percoladores. Este estudio se realizó para diversos materiales utilizados en el campo de la biofiltración. Las ecuaciones se presentaron de la forma:

$$\log(k_G a_w) = \log C_2 + i_2 \log v_G \tag{3-12}$$

$$\log(k_L a_w) = \log C_3 + i_3 \log v_L \tag{3-13}$$

donde $k_G a_w$, $k_L a_w$ son los coeficientes de transferencia de materia de la fase gas y en la fase líquida para los biofiltros percoladores expresados en h^{-1}; log C_2, i_2 y log C_3, i_3 son parámetros específicos de los diferentes materiales de relleno utilizados (Tabla 3-1).

Tabla 3-1 Parámetros empíricos para calcular los coeficientes de transferencia de materia individuales en biofiltros percoladores (Kim y Deshusses, 2008a).

Material de relleno	i_2	$\log C_2$	i_3	$\log C_3$
Roca de lava	0.19	2.94	0.85	1.29
Espuma de poliuretano	0.18	2.34	0.86	0.54
Pall ring	0.33	2.05	0.83	0.69
Esfera de cerámica porosa	0.36	2.75	0.94	1.43
Anillos de cerámica porosa	0.13	2.98	0.59[a]	0.99 [a]
			0.93[b]	1.26[b]

[a] Parámetros para velocidades superficiales menores de 720 m h^{-1}.
[b] Parámetros para velocidades superficiales mayores de 720 m h^{-1}.

Así mismo, otros autores como Dorado et al. (2009) han señalado la importancia de determinar los coeficientes de materia con el contaminante de referencia para una correcta caracterización de la transferencia de materia en los procesos de biodegradación.

3.1.4 Difusión en la fase líquida y en la biopelícula

Tradicionalmente se considera que la transferencia de contaminante entre la fase gas y la fase líquida está limitada por la difusión en la fase líquida. En los biofiltros percoladores, la transferencia en la fase líquida móvil es más lenta que el transporte en el aire y más rápida que en la biopelícula (Devinny y Ramesh, 2005). Normalmente se considera que la concentración en la superficie de la biopelícula está determinada por la concentración de contaminante en la fase líquida y que el flujo de contaminante y oxígeno está controlado por la resistencia a la difusión en la interfase de la biopelícula de acuerdo con la primera ley de Fick:

$$J_x = D_b \left[\frac{\partial S}{\partial x} \right]_{x=0} \tag{3-14}$$

siendo J_x es el flujo de compuesto por unidad de área (g m^{-2} s^{-1}), S concentración del compuesto en la biopelícula (g m^{-3}), D_b es el coeficiente de difusión del componente en la biopelícula (m^2 s^{-1}) y x es la coordenada perpendicular a la superficie de la biopelícula que es 0 en la interfase líquido-biopelícula (m).

Sin embargo, cuando la solubilidad del contaminante es alta y la biodegradación es rápida, algunos investigadores han observado resistencia a la transferencia de materia en la interfase (Kim y Deshusses, 2003). En esos casos la transferencia de materia ocurre por fuerza impulsora entre la concentración de ambas fases:

$$J_x = k_L \left(S^* - S \right) \tag{3-15}$$

donde S^* es la concentración en la interfase líquido–biopelícula (g m^{-3}).

3.1.5 Difusión de contaminante en el interior del biopelícula

Una vez transferidos los contaminantes y el oxígeno desde la fase gas a la fase líquida, estos se difunden a través de la fase líquida y de la biopelícula, o través de la biopelícula en el caso que el flujo líquido no esté en contacto con él. Esta difusión se rige por la Ley de Fick:

$$\frac{\partial S}{\partial t} = D_b \frac{\partial^2 S}{\partial x^2} \tag{3-16}$$

Pese a que la ecuación (3-16) está ampliamente aceptada, hay bastante incertidumbre sobre los valores del coeficiente de difusión adecuados para este tipo de procesos. En este sentido, la presencia de células y polisacáridos puede reducir la sección de paso disponible del agua para la difusión y restringir la difusión de contaminante a través de caminos preferenciales (Devinny y Ramesh, 2005). Por este motivo, algunos investigadores utilizan correlaciones empíricas para corregir el coeficiente de difusión en agua. Una de las correlaciones empíricas más utilizadas es la ecuación propuesta por Fan et al. (1990), que desarrollaron una ecuación para la estimación de los coeficientes de difusión en la biopelícula a partir de los coeficientes en agua y de la concentración de la biomasa:

$$D_b = D_w \left(1 - \frac{0.43\left(X_v 10^{-3}\right)^{0.92}}{11.19 + 0.27\left(X_v 10^{-3}\right)^{0.99}} \right) \tag{3-17}$$

donde D_w es el coeficiente de difusión del compuesto en agua ($m^2\ s^{-1}$) y X_v es la concentración de biomasa en la biopelícula ($g\ m^{-3}$).

En el interior de la biopelícula la etapa controlante del proceso puede venir dada por la limitación de la difusión interna, es decir, si todo el compuesto transferido es asimilado por la biopelícula; o bien por parte de la reacción de biodegradación en el caso de que no se elimine todo el compuesto que se transfiere a la biopelícula. Este último caso suele ser el más habitual para compuestos de elevada solubilidad en agua.

3.1.6 Biodegradación de los contaminantes

El crecimiento microbiano es particular para cada especie y depende de la concentración de carbono, de la fuente de energía y de otras sustancias limitantes como pueden ser la concentración de oxígeno, los nutrientes y las condiciones micro-ambientales. Los microorganismos que predominan en la eliminación de compuestos orgánicos son microorganismos heterótrofos. Estos microorganismos consiguen la energía necesaria para sus funciones vitales de la oxidación de las moléculas orgánicas, y asimilan parte del carbono orgánico como tejido celular. De

esta manera, la degradación de COV mediante microorganismos heterótrofos en presencia de oxígeno se puede expresar según:

$$COV + O_2 + \text{nutrientes} \longrightarrow \text{microorganismos} + \text{energía} + CO_2 + H_2O \quad (3\text{-}18)$$

Así mismo, el proceso de crecimiento de los microorganismos es un proceso autocatalítico que se describe según la ecuación (3-19):

$$\frac{dX_v}{dt} = \mu \cdot X_v \quad (3\text{-}19)$$

donde μ es la velocidad específica de crecimiento celular (s^{-1}).

La cinética microbiana más utilizada para describir la relación entre el crecimiento microbiano y la concentración de contaminante limitante fue propuesta por Monod (1942):

$$\mu = \mu_{\max} \frac{S}{K_s + S} \quad (3\text{-}20)$$

donde μ_{max} es la velocidad máxima de crecimiento (s^{-1}) y K_s es la constante de semisaturación (g m^{-3}). La ecuación de Monod predice que a concentraciones de contaminantes altas el crecimiento puede llegar a alcanzar velocidades máximas (cinética de orden cero) mientras que a concentraciones bajas, el crecimiento se puede asimilar a una cinética de primer orden.

Es habitual encontrar en la bibliografía variaciones en la cinética de Monod asociadas a la limitación por algún componente, como el propio contaminante, el oxígeno y /o los nutrientes. En los casos en los que el oxígeno puede llegar a ser un compuesto limitante, debido por ejemplo a la elevada solubilidad del contaminante frente a él, a la cinética de Monod anteriormente propuesta se le suele añadir el término:

$$\frac{S_o}{K_o + S_o} \quad (3\text{-}21)$$

donde S_O es la concentración de oxígeno en el interior del biopelícula (g m^{-3}) y K_O es la constante de semisaturación de oxígeno (g m^{-3}).

La velocidad de consumo de sustrato asociada al metabolismo microbiano es proporcional a la velocidad de crecimiento celular a través del coeficiente de rendimiento celular (*Y*) que representa la cantidad de biomasa producida por unidad de sustrato consumido por los microorganismos:

$$\frac{dS}{dt} = -\frac{1}{Y}\frac{dX_v}{dt} \tag{3-22}$$

Combinando la ecuación de velocidad, (3-19), con la ecuación (3-22) se obtiene como resultado la ecuación de consumo de contaminante en la biopelícula:

$$\frac{dS}{dt} = -\frac{X_v}{Y}\mu \tag{3-23}$$

3.1.7 Adsorción en el material de relleno

Existen situaciones en las que el compuesto puede ser adsorbido por el material de relleno, especialmente en casos en el que el material tiene alta capacidad de adsorción como puede ser el caso del carbón activado, y en particular en condiciones de operación intermitente. En estos casos el fenómeno de adsorción no puede menospreciarse y debe ser incluido utilizando expresiones que cuantifiquen dicho proceso.

3.2 MODELOS APLICADOS EN EL CAMPO DE LA BIOFILTRACIÓN

Los modelos fenomenológicos propuestos para describir el funcionamiento del biofiltro percolador están basados en los mismos mecanismos que se utilizan para describir el funcionamiento de los biofiltros convencionales. Por ello, para entender el desarrollo de la modelación de este tipo de configuraciones es necesario abarcar los modelos más importantes desarrollados para los biofiltros, así como para otras configuraciones similares como es la del biofiltro de riego por goteo.

La modelación de los procesos de biofiltración para el tratamiento de emisiones de aire contaminado se remonta a principios de los años 80. En esta primera fase, Ottengraf y van Den Oever (1983) extendieron las teorías utilizadas por Jennings et al. (1976) para la modelación de filtros biológicos sumergidos

estableciendo las bases del futuro de la modelación de este tipo de procesos. Posteriormente, Ottengraf (1986) propuso un modelo que continúa actualmente siendo uno de los más aplicados y referenciados. Este modelo asume estado estacionario e incluye la modelación de la cinética de reacción utilizando diferentes cinéticas: de orden cero con limitación de la reacción, de orden cero con limitación de la difusión y cinética de primer orden. Este modelo asume flujo de pistón en la fase gas, concentración en equilibrio en la interfase gas–biopelícula y geometría plana. La difusión de los contaminantes en el interior de la biopelícula está definida por un término de difusión efectiva. Este modelo ha sido validado por otros autores en diferentes condiciones de aplicación (van Lith et al., 1990). Como principales limitaciones cabe destacar que no tiene en cuenta la limitación de oxígeno en el sistema y fue desarrollado para solo un contaminante. Este modelo fue modificado posteriormente para añadirle la limitación por oxígeno (Shareefdeen y Baltzis, 1994b).

Desde el comienzo de los años 90, el interés general se ha centrado en el desarrollo de modelos dinámicos con el objetivo de simular y predecir el comportamiento de los biofiltros en condiciones de estado no estacionario. Uno de los primeros trabajos fue desarrollado por Shareefdeen y Baltzis (1994a). Este modelo fue una extensión de su trabajo previo (Shareefdeen y Baltzis, 1994b). En él cabe destacar la consideración del fenómeno de adsorción, demostrando que tiene un papel más importante durante la puesta en marcha del proceso y en condiciones de operación fluctuantes. En este trabajo se consideró que el material de relleno no estaba completamente cubierto por la biopelícula por lo que parte del aire contaminado estaba en contacto directo con el material, asumiendo que el proceso de adsorción seguía una isoterma de Freundlich.

Poco después Hodge y Devinny (1995) desarrollaron un modelo simplificado en el que se asumió que la transferencia en el agua y la adsorción en el medio eran rápidas en comparación con la convección y la biodegradación. En su modelo incorporaron la dispersión axial y describieron también la producción de dióxido de carbono utilizando una cinética de primer orden. El primer modelo dinámico en biofiltros y que incluía los procesos de difusión en el biopelícula fue propuesto por Deshusses et al. (1995). En este modelo se asumió que existía un volumen disperso de agua en la matriz donde se absorbía el contaminante, también se podía producir acumulación de contaminante siempre y cuando antes se hubiera difundido al interior de la biopelícula. La cinética asumida fue de tipo Monod con competición entre los sustratos: metil etil cetona y metil isobutil cetona. Otros autores han desarrollado modelos matemáticos para la modelación de los

biofiltros, Dorado et al. (2008) desarrollaron un modelo basado en los balances de materia de la fase gas y la biopelícula y lo aplicaron para la eliminación de tolueno mediante biofiltros que utilizaban bacterias y biofiltros que utilizaban hongos para la degradación. Estos mismos autores, en un trabajo posterior ampliaron el modelo matemático para la predicción de la acumulación de la biomasa dentro del reactor (Dorado et al., 2012). Otros autores incluyeron diferentes cinéticas y diferentes fenómenos. Álvarez-Hornos et al. (2009) desarrolló un modelo dinámico para simular la degradación de tolueno y acetato de etilo utilizando una cinética tipo Monod con doble limitación sustrato y oxígeno y en las que se incluyeron los efectos de inhibición por elevadas concentraciones de sustrato en la degradación de acetato de etilo e inhibición competitiva en la degradación de tolueno. En este modelo se incluyó una distribución creciente de la biomasa a lo largo del lecho con el fin de simular los perfiles experimentales de contaminante a través del lecho.

En relación a los modelos utilizados para describir el comportamiento de los biofiltros percoladores, generalmente están basados en los modelos previos utilizados para describir el funcionamiento de los biofiltros convencionales. Así mismo, la modelación de los biofiltros percoladores está influenciada por los modelos desarrollados para los reactores de riego de lecho utilizados en la industria química. Uno de los primeros trabajos en el campo de la modelación de los biofiltros percoladores fue desarrollado por Diks y Ottengraf (1991a, 1991b), estos autores propusieron un modelo en estado estacionario con una cinética de orden cero. En este modelo no se consideraron las limitaciones de oxígeno y se asumió que no había resistencia a la transferencia de materia en la interfase líquido–biopelícula.

Mpanias y Baltzis (1998) fueron los primeros en presentar un modelo en estado estacionario considerando porciones mojadas y no mojadas de la biopelícula, pese a que la transferencia desde la fase gas solo se llevaba a cabo a través de la fase mojada, introduciendo además la limitación de oxígeno en el biopelícula para concentraciones elevadas de sustrato (clorobenceno en este caso). En un trabajo posterior ampliaron su modelo a mezclas de COV y consideraron inhibición cruzada durante la biodegradación de una mezcla de clorobencenos. Este trabajo sugería un arrastre por aire considerable de contaminante en el gas emitido cuando se utilizaba riego en contracorriente (Baltzis et al., 2001).

El modelo propuesto en estado estacionario por Barton et al. (1998) mostró que el funcionamiento del biofiltro percolador podía estar condicionado por una

doble limitación a la resistencia a la transferencia de materia y a la biodegradación.

Pese a que la modelación de los biofiltros percoladores se remonta a principios de los años 90, no fue hasta finales de esta década y primeros del año 2000 cuando los investigadores se centraron en la modelación de biofiltros percoladores en estado no estacionario tanto para compuestos orgánicos como inorgánicos. Este hecho está relacionado con el avance en las herramientas informáticas para resolver ecuaciones más complejas.

Okkerse et al. (1999) desarrollaron un modelo trifásico detallado (gas–líquido–biopelícula) para el tratamiento de COV acidificantes que incluía el crecimiento de la biomasa, tanto activa como inerte, el efecto del pH y del oxígeno disuelto. Este modelo podía ser utilizado para predecir la colmatación del lecho. Alonso et al (1998) y Zhu et al. (1998) pusieron en evidencia que la resistencia a la transferencia de materia producida por la fase líquida en el comportamiento de este tipo de configuraciones es un parámetro crítico en el funcionamiento de los mismos. Para ello propusieron un modelo dinámico conceptual en el que se diferenciaba entre biomasa activa y biomasa inactiva y que tenía en cuenta el crecimiento y muerte de la biomasa. Lee y Heber (2010) modificaron el modelo propuesto por Alonso et al. (1998) para aplicarlo al tratamiento de etileno, este trabajo se centró en el desarrollo de un algoritmo genético para la optimización de los parámetros. Para modelar el crecimiento de la biomasa, en los últimos años se han desarrollado otros modelos. Por ejemplo, Mannucci et al. (2012) desarrollaron un modelo simplificado para estimar la cantidad de biomasa producida en el lecho en función de la cantidad de ácido sulfúrico eliminada y de las condiciones de operación. Este trabajo se centró en el crecimiento y muerte de la biomasa y en la predicción de la eficacia de eliminación, mientras que la transferencia de materia gas–líquido, la difusión y la oxidación química no se estudiaron en detalle.

Kim y Deshusses (2003) desarrollaron un modelo conceptual para la eliminación de H_2S centrándose en la transferencia de materia. En este modelo se consideró que la biopelícula no estaba completamente mojada, por lo que una fracción del contaminante se transfería directamente de la fase gas a la biopelícula y la otra fracción, para llegar, al biopelícula se transfería a través de la fase líquida. Para determinar los coeficientes de transferencia de materia se utilizaron las correlaciones propuestas por Onda et al. (1968). Recientemente, Arellano-García et al.(2014) han modelado los efectos de la acumulación de la biomasa en términos de hidrodinámica y espacio vacío para tratar vapores de dimetil

disulfuro. El modelo está basado en el propuesto por Kim y Deshusses (2003) e incluye el término de dispersión en la fase líquida. En este estudio se concluye que el contenido de la biomasa óptimo es de 20%.

Li et al. (2002) desarrollaron un modelo conceptual, incluyendo una descripción detallada de la transferencia de materia en las diferentes interfases. Este modelo se desarrolló en base a dos categorías: un modelo de tres fases (aire, agua y biopelícula) para biofiltros percoladores y un modelo de dos fases (aire y biopelícula) para biofiltros convencionales. Este modelo se desarrolló para emisiones de ácido sulfhídrico pero podría ser extendido al tratamiento de COV. En este trabajo se hizo un análisis de los principales parámetros de sensibilidad. Se detectó, entre otros fenómenos, que la existencia de la fase líquida en el modelo desarrollado para biofiltros percoladores provocaba una disminución en la eficacia del proceso comparado con el modelo desarrollado para el biofiltro. En este sentido, Iliuta et al. (2005) desarrollaron un modelo predictivo dinámico para un bioreactor de riego por goteo basado en las ecuaciones de balance de materia y balances de cantidad de movimiento. El objetivo del trabajo fue ilustrar la influencia que la acumulación de biomasa dentro del reactor. En este trabajo se llegó a la conclusión que la fase líquida podía actuar como barrera a la transferencia de materia.

Los modelos matemáticos señalados anteriormente aportan información muy valiosa para entender los principales fenómenos que se desarrollan durante la depuración de COV en reactores biológicos de lecho fijo. Sin embargo, actualmente no existe todavía un modelo general aceptado. En este sentido, en el campo de la modelación de biofiltros percoladores es necesario avanzar hacia modelos que tengan en cuenta las características de funcionamiento de los biofiltros percoladores industriales, así como en modelos que profundicen en las diferencias que se observan entre los reactores de laboratorio y los reactores industriales.

3.3 BIBLIOGRAFÍA

Alonso, C., Suidan, M. T., Kim, B. R. y Kim, B. J. (1998). Dynamic mathematical model for the biodegradation of VOCs in a biofilter: biomass accumulation study. *Environmental Science & Technology*, *32*(20), 3118–3123.

Álvarez-Hornos, F. J., Gabaldón, C., Martínez-Soria, V., Marzal, P. y Penya-roja, J.-M. (2009). Mathematical modeling of the biofiltration of ethyl acetate and toluene and their mixture. *Biochemical Engineering Journal*, *43*(2), 169–177.

Arellano-García, L., Dorado, A. D., Morales-Guadarrama, A., Sacristan, E., Gamisans, X. y Revah, S. (2015). Modeling the effects of biomass accumulation on the performance of a biotrickling filter packed with PUF support for the alkaline biotreatment of dimethyl disulfide vapors in air. *Applied Microbiology and Biotechnology*, *99*(1), 97–107.

Baltzis, B. C., Mpanias, C. J. y Bhattacharya, S. (2001). Modeling the removal of VOC mixtures in biotrickling filters. *Biotechnology and Bioengineering*, *72*(4), 389–401.

Barton, J. W., Hartz, S. M., Klasson, K. T. y Davison, B. H. (1998). Microbial removal of alkanes from dilute gaseous waste streams: Mathematical modeling of advanced bioreactor systems. *Journal of Chemical Technology and Biotechnology*, *72*(2), 93–98.

Deshusses, M. A., Hamer, G. y Dunn, I. J. (1995). Behavior of biofilters for waste air biotreatment. 1. Dynamic-model development. *Environmental Science & Technology*, *29*(4), 1048–1058.

Devinny, J. S. y Ramesh, J. (2005). A phenomenological review of biofilter models. *Chemical Engineering Journal*, *113*(2-3), 187–196.

Diks, R. M. M. y Ottengraf, S. P. P. (1991a). Verification studies of a simplified model for the removal of dichloromethane from waste gases using a biological trickling filter. 1. *Bioprocess Engineering*, *6*(3), 93–99.

Diks, R. M. M. y Ottengraf, S. P. P. (1991b). Verification studies of a simplified model for the removal of dichloromethane from waste gases using a biological trickling filter. 2. *Bioprocess Engineering*, *6*(4), 131–140.

Dorado, A. D., Lafuente, J., Gabriel, D. y Gamisans, X. (2012). Biomass accumulation in a biofilter treating toluene at high loads - Part 2: Model

development, calibration and validation. Chemical Engineering Journal, 209, 670–676.

Dorado, A. D., Baquerizo, G., Maestre, J. P., Gamisans, X., Gabriel, D. y Lafuente, J. (2008). Modeling of a bacterial and fungal biofilter applied to toluene abatement: Kinetic parameters estimation and model validation. *Chemical Engineering Journal*, *140*(1-3), 52–61.

Dorado, A. D., Rodriguez, G., Ribera, G., Bonsfills, A., Gabriel, D., Lafuente, J. y Gamisans, X. (2009). Evaluation of mass transfer coefficients in biotrickling filters: Experimental determination and comparison to correlations. *Chemical Engineering & Technology*, *32*(12), 1941–1950.

Fan, L.-S., Leyva-Ramos, R., Wisecarver, K. D. y Zehner, B. J. (1990). Diffusion of phenol through a biofilm grown on activated carbon particles in a draft-tube three-phase fluidized-bed bioreactor. *Biotechnology and Bioengineering*, *35*(3), 279–286.

Hodge, D. S. y Devinny, J. S. (1995). Modeling removal of air contaminants by biofiltration. *Journal of Environmental Engineering*, *121*(1), 21–32.

Iliuta, I., Iliuta, M. C. y Larachi, F. (2005). Hydrodynamics modeling of bioclogging in waste gas treating trickle-bed bioreactors. *Industrial & Engineering Chemistry Research*, *44*(14), 5044–5052.

Jennings, P. A., Snoeyink, V. L. y Chian, E. S. K. (1976). Theoretical model for a submerged biological filter. *Biotechnology and Bioengineering*, *18*(9), 1249–1273.

Kim, S. y Deshusses, M. A. (2003). Development and experimental validation of a conceptual model for biotrickling filtration of H_2S. *Environmental Progress*, *22*(2), 119–128.

Kim, S. y Deshusses, M. A. (2008a). Determination of mass transfer coefficients for packing materials used in biofilters and biotrickling filters for air pollution control - 2: Development of mass transfer coefficients correlations. *Chemical Engineering Science*, *63*(4), 856–861.

Kim, S. y Deshusses, M. A. (2008b). Determination of mass transfer coefficients for packing materials used in biofilters and biotrickling filters for air pollution control. 1. Experimental results. *Chemical Engineering Science*, *63*(4), 841–855.

Lee, S. H. y Heber, A. J. (2010). Ethylene removal using biotrickling filters: part II. Parameter estimation and mathematical simulation. *Chemical Engineering Journal*, *158*(2), 89–99.

Li, H., Crittenden, J. C., Mihelcic, J. R. y Hautakangas, H. (2002). Optimization of biofiltration for odor control: Model development and parameter sensitivity, *Water Environment Research*, *74*(1), 5–16.

Mannucci, A., Munz, G., Mori, G. y Lubello, C. (2012). Biomass accumulation modelling in a highly loaded biotrickling filter for hydrogen sulphide removal. *Chemosphere*, *88*(6), 712–7.

Monod, J. (1942). *Research of the growth of bacterial cultures*. París, Francia: Herman et Cie.

Mpanias, C. J. y Baltzis, B. C. (1998). An experimental and modeling study on the removal of mono-chlorobenzene vapor in biotrickling filters. *Biotechnology and Bioengineering*, *59*(3), 328–343.

Okkerse, W. J. H., Ottengraf, S. P. P., Osinga-Kuipers, B. y Okkerse, M. (1999). Biomass accumulation and clogging in biotrickling filters for waste gas treatment. Evaluation of a dynamic model using dichloromethane as a model pollutant. *Biotechnology and Bioengineering*, *63*(4), 418–430.

Onda, K., Takeuchi, H. y Okumoto, Y. (1968). Mass transfer coefficients between gas and liquid phases in packed columns. *Journal of Chemical Engineering of Japan*, *1*(1), 56–62.

Ottengraf, S. P. P. (1986). Exhaust gas purification. En: H. J. Rehm y G. Reed (Eds.), *Biotechnology, V.8*. Weinheim, Alemania: VCH Verlagsgeseellschaft.

Ottengraf, S. P. y van Den Oever, A. H. (1983). Kinetics of organic-compound removal from waste gases with a biological filter. *Biotechnology and Bioengineering*, *25*(12), 3089–3102.

Pérez, J., Montesinos, J. L. y Gòdia, F. (2006). Gas–liquid mass transfer in an up-flow cocurrent packed-bed biofilm reactor. *Biochemical Engineering Journal*, *31*(3), 188–196.

Shareefdeen, Z. y Baltzis, B. C. (1994a). Biofiltration of toluene vapor under steady-state and transient conditions - Theory and experimental results. *Chemical Engineering Science*, *49*(24A), 4347–4360.

Shareefdeen, Z. y Baltzis, B. C. (1994b). Biological removal of hydrophobic solvent vapors from airstreams. En: E. Galindo y O. Ramirez (Eds.), *Advances in bioprocess engineering* (pp. 397–404). Dordrecht: Kluwer.

van Krevelen, D. W. y Hoftijzer, P. J. (1948). Kinetics of simultaneous absorption and chemical reaction. *Chemical Engineering Progress*, *44*, 529–536.

van Lith, C., David, S. L. y Marsh, R. (1990). Design criteria for biofilters. *Transactions of the Institution of Chemical Engineers and the Chemical Engineer*, *68*, 127–132.

Zhu, X. Q., Alonso, C., Suidan, M. T., Cao, H. W. y Kim, B. R. J. (1998). The effect of liquid phase on VOC removal in trickle-bed biofilters. *Water Science and Technology*, *38*(3), 315–322.

4 MATERIALES Y MÉTODOS

En el presente capítulo se describen los principales equipamientos, técnicas analíticas, y protocolos experimentales de determinación de parámetros de operación utilizados durante el desarrollo de la tesis doctoral. También se presentan las técnicas analíticas utilizadas, así como los protocolos determinar los principales parámetros de operación. Además, se presenta el procedimiento de resolución del modelo matemático. La información ampliada está en los capítulos científicos que componen esta tesis doctoral.

4.1 MATERIAL

4.1.1 Material de relleno

Durante el desarrollo de la tesis se utilizaron cuatro tipos de relleno, uno estructurado y tres rellenos desordenados de diferentes tamaños en función de la escala de aplicación. Los rellenos utilizados fueron: PAS Winded Media (PAS Solutions BV, Países Bajos), anillos de polipropileno de idéntica geometría y diámetros de 15 mm (Refilltech, Alemania), de 25 mm y de 50 mm (Koch-Glitsch B.V.B.A, Bélgica). En la Figura 4-1 se presenta una fotografía de los materiales plásticos desordenados. Las principales propiedades de los materiales de relleno utilizados durante la realización de la presente tesis doctoral se presentan en la Tabla 4-1. Los anillos de polipropileno de 15 mm y el relleno estructurado PAS Winded Media se utilizaron en el estudio experimental a escala de laboratorio de la depuración de isopropanol mediante biofiltros percoladores (capítulo 6). El estudio de transferencia de isopropanol se llevó a cabo con los anillos de polipropileno de 25 mm y con el material de relleno estructurado PAS Winded Media (capítulo 7). El estudio de transferencia de oxígeno se llevó a cabo con los materiales de relleno PAS Winded Media, los anillos de polipropileno de 15 mm, de 25 mm (capítulo 7) y de 50 mm (capítulo 8). En los experimentos realizados para la determinación de la relación dinámica entre la emisión gaseosa de contaminante a la salida del bioreactor y la acumulación de compuestos orgánicos en la disolución de recirculación se utilizaron los anillos de polipropileno de 25 mm (capítulo 9). En el biofiltro industrial se utilizaron los anillos de polipropileno de 50 mm (capítulo 9).

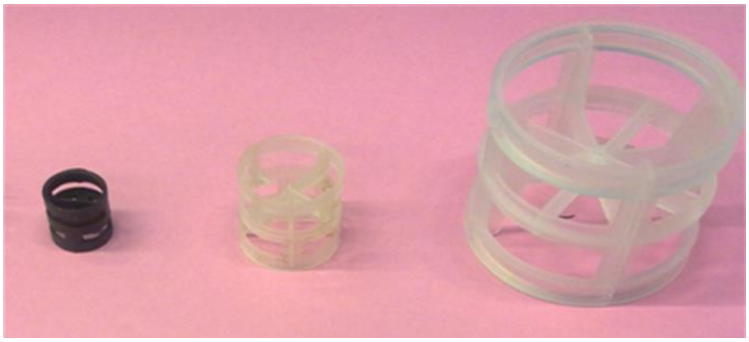

Figura 4-1 Detalle de los anillos de polipropileno: a) diámetro 15 mm; b) diámetro 25 mm; c) diámetro 50 mm.

Tabla 4-1 Propiedades físicas de los diferentes rellenos utilizados en la presente tesis doctoral.

Relleno	Tipo de relleno	Tamaño[a] (mm)	Densidad[a] (Kg m^{-3})	Porosidad[a] (%)	Superficie específica[a] (m^2 m^{-3})
PAS Winded media	Estructurado	----	----	93	410
Refilltech	Anillos PP	15	110.7	91	348
Flexiring	Anillos PP	25	71	92	207
Flexiring	Anillos PP	50	60	93	102

[a] Información proporcionada por los distribuidores.

4.1.2 Compuestos

Para todos los experimentos llevados a cabo en el laboratorio se ha seleccionado el isopropanol como contaminante representativo de la industria de impresión flexográfica (capítulos 6–10). Las propiedades físicas del isopropanol se detallan en la Tabla 4-2. Las emisiones industriales proceden de una industria de impresión flexográfica (capítulo 9). Las emisiones estuvieron constituidas por una mezcla de COV formada por etanol (63%), acetato de etilo (22%) y 1-etoxi-2-propanol (13%). Las proporciones se refieren a valores promedios obtenidos de 3 análisis por cromatografía gaseosa.

Tabla 4-2 Propiedades físicas del isopropanol.

CAS	67-63-0
Masa molecular	60.1 g mol^{-1}
Punto de ebullición	82.5 ° C
Densidad relativa (agua = 1)	0.785
Solubilidad en agua	100%
Constante de Henry	3.14 10^{-4}
Presión de vapor, a 20°C	32.4 mmH_2O
Densidad relativa de vapor (aire = 1)	2.08
Densidad relativa de la mezcla vapor/aire a 20°C	1.05
Punto de inflamación	11.7°C
Temperatura de autoignición	455°C
Límites de explosividad, % en volumen en el aire	2–12
Biodegradabilidad del compuesto	3

4.1.3 Nutrientes

A lo largo del desarrollo experimental de la presente tesis doctoral se han utilizado diferentes formulaciones de nutrientes. Se prepararon disoluciones concentradas ajustando el pH de la disolución a un valor neutro. La disolución se administró al tanque de recirculación de manera que la relación másica C: N estuviera comprendida entre 20–35 manteniendo una concentración de nitrógeno disuelto en el tanque como mínimo de 10 mg N L^{-1} con el fin de evitar que limitara la bioreacción.

En el estudio experimental a escala de laboratorio de la depuración de isopropanol mediante biofiltros percoladores (capítulo 6) se utilizó la formulación de nutrientes presentada en la Tabla 4-3. En esta formulación se utilizaba nitrato potásico como fuente de nitrógeno y fosfato trisódico como fuente de fósforo. En los experimentos realizados para la determinación de la relación dinámica entre la fuga gaseosa de contaminante a la salida del bioreactor y la acumulación de compuestos orgánicos en la disolución de recirculación (capítulo 9) se utilizó la formulación de nutrientes que se presenta en la Tabla 4-4. En este caso se modificó la composición de los nutrientes para utilizar como fuente de nitrógeno amonio y amonio fosfato disódico, siendo este último también la fuente de fosforo. En el biofiltro percolador a escala industrial (capítulo 9) se adicionó una solución de nutrientes suministrada por la empresa PAS Solutions BV (Países Bajos).

Tabla 4-3 Composición de nutrientes de la disolución suministrada a los biofiltros percoladores para el tratamiento de isopropanol (capítulo 6).

Compuestos	**Concentración, g L^{-1}**
$Na_3PO_4 \cdot 12H_2O$	4.6
KNO_3	21.7

Vitaminas	**Concentración, µg L^{-1}**
Beta-caroteno	20.0
B1	70.0
B2	70.0
B6	95.0
B9	10.0
B12	0.1
C	3.0
D	0.3
E	500
Biotina	2
Niacina	900

	Concentración, µg L^{-1}
Ca	12000
Fe	1500
Mg	2650
Zn	605
Co	60
Mo	60
Ni	55
Cu	50
B	45
Mn	40
I	8
Se	3
Cr	1

Tabla 4-4 Composición de nutrientes de la disolución suministrada en los experimentos para evaluar la relación dinámica entre la fuga gaseosa de contaminante y el carbono disuelto en el tanque (capítulo 9).

Compuestos	**Concentración, g L^{-1}**
NH_4Cl	9.7
$MgSO_4$ 7H2O	0.9
$(NH4)_2HPO_4$	2.2
$NaHCO_3$	0.5
NaOH	0.4
KCl	0.6
Micronutrientes	**Concentración, mg L^{-1}**
$CaCl_2$	12.7
$Fe_2(SO_4)_3$	4.8
$ZnSO_4 \cdot 7H_2O$	0.2
$CoCl_2 \cdot 6H_2O$	0.2
$MnCl_2 \cdot 4H_2O$	0.1
$Na_2MoO_4 \cdot 2H_2O$	0.1
$NiSO_4 \cdot 6H2O$	0.24
H_3BO_3	0.2
Vitaminas	**Concentración, µg L^{-1}**
A	40
C	3000
D	0.2
E	500
K	1.3

Vitaminas	**Concentración, µg L^{-1}**
B1	70
B2	80
Niacina	900
B6	100
B9	10
B12	0.1
Biotina	1.5
B5	300
Ca	600
Mg	4000
Fe	700
Cu	45
I	3.8
Zn	400
Mn	90
K	1160
Se	2.5
Cr	1.3
Mo	2.3
Cl	1075
coenzima Q10	150

4.2 MONTAJE EXPERIMENTAL DE LOS BIOFILTROS PERCOLADORES

4.2.1 Biofiltro percolador a escala de laboratorio

Los biofiltros percoladores utilizados en el laboratorio (capítulos 6 y 9) estaban formados por una columna de metacrilato de 120 cm de altura, 14.4 cm de diámetro y dividida en 3 módulos iguales. En la Figura 4-2 se presenta un esquema del montaje experimental. El sistema estaba equipado en la parte superior y en la parte inferior con dos puertos para la toma de muestras de aire. La columna se completaba con dos tapas de 20 cm de altura colocadas una en la parte superior y una en la parte inferior. Además, en la parte superior del reactor se dispuso de un desnebulizador con el fin de separar las gotas de líquido arrastradas por la corriente gaseosa. Para la correcta distribución del líquido de recirculación se utilizó un inyector (FullJet HH, Spraying Systems Co., EEUU). El montaje se completaba con un tanque de recirculación de 10 L de capacidad máxima que contenía el líquido de recirculación, el cual se introducía en la columna por la parte superior, en contracorriente con el flujo de aire. El aire provenía de un compresor y se acondicionaba mediante dos etapas en serie de filtrado y secado. El caudal se controlaba mediante un controlador de flujo másico (EL-FLOW F-201AV, Bronkhorst Hi-Tec, Países Bajos). El aire se contaminaba con isopropanol utilizando una bomba de jeringa de inyección y recarga automática (NE 1000, New Era Pump Systems Inc., EEUU). Además se disponía de un tanque de nutrientes y una bomba peristáltica (Watson-Marlow, EEUU) que dosificaba la disolución al tanque de recirculación.

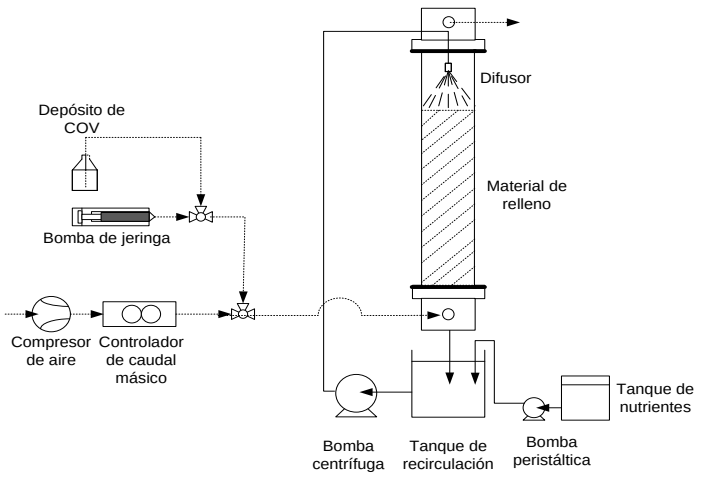

Figura 4-2 Esquema de funcionamiento del biofiltro percolador a escala de laboratorio.

4.2.2 Biofiltro percolador a escala industrial (VOCUS^{TM})

El grupo de investigación GI^{2}AM de la Universitat de València, en el cual se desarrolla la presente tesis doctoral, colabora con la empresa holandesa PAS Solutions BV en la transferencia de tecnología para la depuración de emisiones gaseosas de biofiltro percolador. Fruto de esta colaboración se han instalado unidades de biofiltro percolador para tratar emisiones de COV en empresas de diversos sectores, entre ellos, el sector de impresión flexográfica (Sempere et al., 2012). La planta industrial VOCUS^{TM} (PAS Solutions, BV, Países Bajos) que se utiliza en la presente tesis doctoral es otro ejemplo de ello (capítulo 9). Se trata de una unidad de biofiltro percolador instalada en una empresa de impresión flexográfica de empaquetados plásticos para el sector alimentario. Esta instalación se utiliza como solución final de depuración desde 2009. El reactor biológico está formado por una columna cilíndrica cónica de plástico reforzado con fibra de vidrio y empaquetado con un relleno desordenado de polipropileno en su interior con un volumen útil de 49 m^3 y un tanque de recirculación con un volumen máximo para el líquido de recirculación de 15 m^3. Un ventilador controlado por un variador de frecuencia permite succionar el caudal de aire de los diversos focos de emisión durante las horas de fabricación de la empresa (de 6 a 24h) durante 5 días a la semana. Durante las 6 horas restantes se introduce aire limpio al biofiltro percolador.

La planta está equipada con sensores de temperatura, pH, nivel de líquido y de presión. La instrumentación se completa con un analizador de hidrocarburos total (RS 53-T, Ratfisch Analysensyteme GmbH, Alemania). El caudal de aire se mide continuamente utilizando un tubo *pitot* (19" tubo pitot, Testo AG, Alemania). Tanto la adquisición y visualización de los datos de los instrumentos de medida, como el control de la instalación se realiza de forma telemática. En este sentido, los datos industriales fueron seleccionados durante mi estancia de investigación en la empresa PAS Solutions BV (Países Bajos), en el marco del proyecto europeo Marie Curie IAPP Next Air Biotreat.

Figura 4-3 Fotografía del exterior de la planta industrial VOCUS^{TM}. Cortesía de PAS Solutions BV (Países Bajos).

4.3 MONTAJES EXPERIMENTALES PARA LA DETERMINACIÓN DE LOS COEFICIENTES DE TRANSFERENCIA DE MATERIA

4.3.1 Montaje experimental para la determinación de los coeficientes globales de transferencia de isopropanol

Para la determinación de los coeficientes globales de transferencia de isopropanol (capítulo 7) se utilizó el biofiltro percolador de laboratorio que consistía en una columna de metacrilato de 14.4 cm de diámetro interno y 120 cm de altura y un tanque de recirculación con un volumen de agua de 5 L. La altura del relleno utilizado fue de 100 cm para ambos materiales. Por la parte inferior de la columna se introdujo un caudal de aire que provenía de un compresor, filtrado y seco y con un caudal ajustado mediante un controlador de flujo másico (Bronkhorst Hi-Tec, Países Bajos). El agua de recirculación se impulsaba mediante una bomba centrífuga (HPRT10/15, ITT, Gran Bretaña) en contracorriente con el flujo de gas.

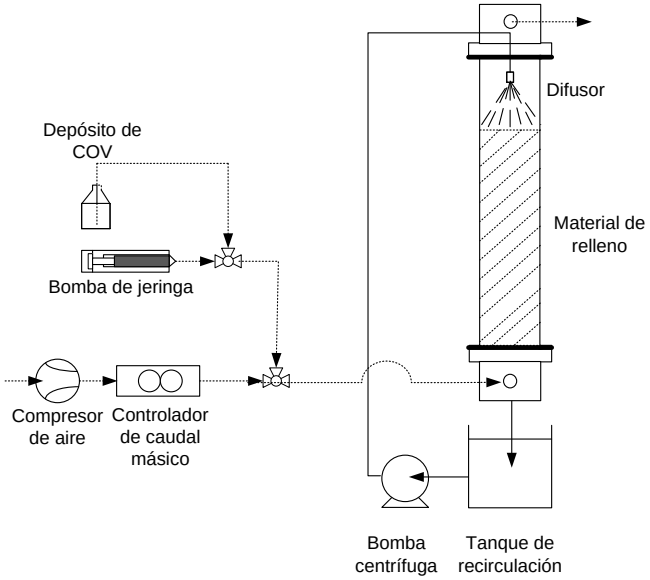

Figura 4-4 Esquema del montaje experimental para la determinación del coeficiente de transferencia de isopropanol**.**

4.3.2 Montaje experimental para la determinación de los coeficientes globales de transferencia de oxigeno

Para el estudio de la transferencia de oxigeno (capítulos 6, 7 y 8) se utilizó una columna de metacrilato de 14.4 cm de diámetro interno y 80 cm de altura y un tanque de recirculación de 10 L de volumen máximo, el esquema del sistema se puede observar en la Figura 4-5. La altura efectiva del lecho varió entre 20 y 40 cm dependiendo del tipo de relleno utilizado. Por la parte inferior de la columna se introdujo un caudal prefijado de aire proveniente de un compresor, filtrado y seco y con un caudal ajustado mediante un controlador de flujo másico (Bronkhorst Hi-Tec, Países Bajos). El agua de recirculación se impulsaba mediante una bomba centrífuga (HPRT10/15, ITT, Gran Bretaña) en contracorriente con el flujo de gas. La concentración de oxígeno en el tanque se registró mediante un oxímetro (Cellox® 325i, WTW, Alemania) conectado a un sistema de adquisición de datos.

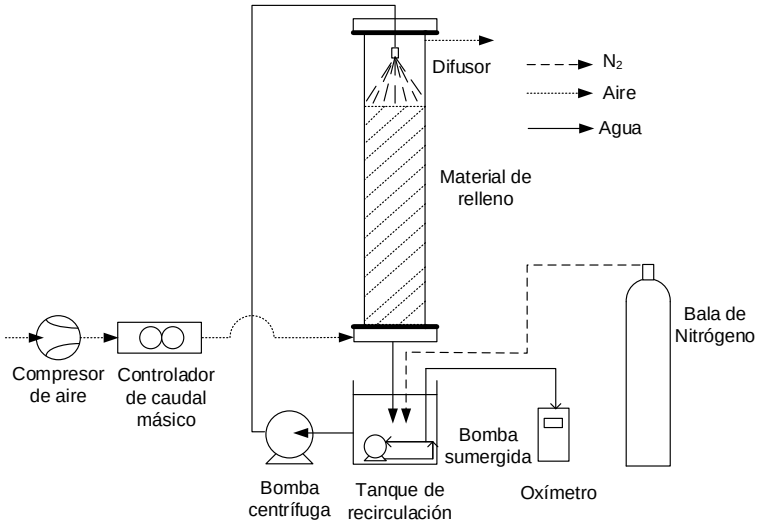

Figura 4-5 Esquema del montaje experimental para la determinación del coeficiente de transferencia de oxígeno.

4.4 TÉCNICAS ANALÍTICAS UTILIZADAS EN EL LABORATORIO

4.4.1 Determinación de las concentraciones de COV en aire

Para determinar las concentraciones COV en aire se han utilizado dos equipos distintos, un analizador de hidrocarburos totales, el cual permitía un seguimiento en continuo del proceso, y un cromatógrafo de gases, que se ha utilizado para determinar el factor de respuesta del analizador de hidrocarburos total para isopropanol.

Analizador de hidrocarburos total

La concentración de COV se midió con un analizador de hidrocarburos totales (Nira Mercury modelo 901, Spirax SARCO, España) equipado con un detector de ionización de llama y una bomba incorporada para la succión de la muestra de gas. Este equipo se calibraba periódicamente utilizando una bala patrón de propano en el intervalo 0 – 1000 mg C Nm^{-3}.

La frecuencia de análisis del equipo era de 11 segundos, y la duración de las medidas realizadas variaba desde un mínimo de 15 minutos hasta seguimientos de días enteros. El analizador se utilizó para obtener las concentraciones de entrada y salida de COV en la fase gaseosa.

Cromatógrafo de gases

El cromatógrafo de gases (modelo 7890, Agilent Technologies, EE UU) estaba equipado con un sistema automático de válvula de inyección, un detector de llama de ionización y una columna capilar Rtx®-VMS (30 m x 0.25 mm x 1.4 µm). El gas portador fue helio y las condiciones del análisis fueron: 250 °C en el puerto de inyección, 100 °C en el horno y 240 °C en el detector. Este equipo se calibró periódicamente utilizando una bala patrón de acetato de etilo y tolueno (Carburos Metálicos, España). La calibración del cromatógrafo frente al isopropanol se realizaba analizando la respuesta relativa de muestras que contenían mezclas de composición conocidas de isopropanol y tolueno.

4.4.2 Determinación de la concentración de dióxido de carbono en aire

Para la medida de la concentración de dióxido de carbono en las corrientes gaseosas de entrada y salida se utilizó un analizador de CO_2 por infrarrojo no dispersivo (GMP222, Vaisala, Finlandia), equipado con sensor de CO_2 para un intervalo de concentración comprendido entre 0 y 3000 ppmv. El analizador disponía de un filtro de partículas integrado al equipo.

Para la calibración se utilizaba una bala patrón (Carburos Metálicos, España) de una mezcla sintética de CO_2 y oxígeno en nitrógeno con una concentración de CO_2 de 2018 ppmv.

4.4.3 Pérdida de presión en el lecho de relleno

La pérdida de presión a través de la columna del reactor de laboratorio se midió con un manómetro digital (MP101, KIMO Instruments, España) con un intervalo de medida comprendido entre 0 y 1000 mmH_2O.

4.4.4 Determinación de la porosidad del biofiltro percolador

La determinación de la porosidad del biofiltro percolador se realizó a partir de la determinación de la fracción volumétrica ocupada por la fase líquida, la biopelícula y el material de relleno.

La fracción volumétrica ocupada por la fase líquida se determinó experimentalmente a partir de la diferencia entre el volumen en el tanque de recirculación antes del riego y durante el riego.

La fracción volumétrica ocupada por la biopelícula se determinó cogiendo muestras de los anillos y midiendo el contenido de biopelícula por anillo. La cantidad total de biopelícula en el reactor se estimó a partir del contenido por anillos y el número total de anillos. Para el volumen de biopelícula se asumió que la densidad de la biopelícula era igual a la del agua.

4.4.5 Determinación de la calidad del líquido de recirculación

Para determinar la calidad del líquido de recirculación en los ensayos de laboratorio se midió la temperatura, pH y conductividad, y durante toda la experimentación se determinó periódicamente la concentración de sólidos en suspensión (SS), sólidos en suspensión volátiles (SSV), concentración de nitrógeno, demanda química de oxígeno soluble (DQO_{sol}), concentración en la fracción soluble de carbono orgánico total (TOC), carbono inorgánico (IC) y carbono total (TC).

El seguimiento de la temperatura, pH y conductividad a escala de laboratorio se realizó mediante un equipo multiparamétrico (pH / Cond 340i, WTW, Alemania). Los SS y SSV se determinaron de acuerdo con el método 2540 D y 2540 E, respectivamente, según el Standard Methods (American Public Health Association, American Water Works Association and Water Environment Federation, 1998). Estos métodos consisten, en filtrar la muestra en un filtro de fibra de vidrio, secándose posteriormente en estufa a 105°C para la determinación de los SS, y una vez cuantificados los SS calcinar a 550°C para la determinación de los SSV.

La cantidad de COV absorbida en el líquido de recirculación se determinó midiendo en una muestra filtrada la materia orgánica (DQO_{sol} y TOC). La muestra filtrada se analizó con el test fotométrico en cubetas de DQO Speqtroquant® (114540 Speqtroquant®, Merck KGaA, Alemania). El análisis de la fracción soluble de TOC, de IC y de TC se realizó con un analizador de carbono para muestras líquidas (Total Organic Carbon Analyzer, TOC-V_{CHS}, Shimadzu Corporation, Kyoto, Japón). El equipo se calibraba periódicamente para el carbono total y para el carbono inorgánico. Para calibrar carbono total se utilizaba un patrón preparado a partir de hidrogenoftalato de potasio. Para calibrar el carbono inorgánico se utilizaba un patrón compuesto por carbonato sódico y bicarbonato sódico. Ambos análisis se calibraban para intervalos comprendidos entre 0 y 100 mg C L^{-1}. El carbono orgánico se determinaba por diferencia entre ambos.

La concentración de nitrógeno se realizaba mediante test fotométrico (114773, Spectroquant®, Merck KGaA, Alemania).

4.5 RESOLUCIÓN NUMÉRICA DEL MODELO

El conjunto de ecuaciones diferenciales que definen el modelo constituyen dos sistemas de ecuaciones diferenciales de segundo grado no lineales. Para la resolución se escogió el Método de las Líneas (MOL), obteniéndose dos sistemas de ecuaciones diferenciales ordinarias (EDO). El método MOL permite que la discretización en el tiempo sea independiente de la discretización en el espacio añadiendo flexibilidad a la resolución. Para la aplicación del método MOL se siguieron los siguientes pasos:

- Se generó un mallado en las dimensiones espaciales (x, z). Para ello, la altura total del reactor se dividió en N secciones, generando N+1 nodos. Análogamente, el espesor de la biopelícula se dividió en M secciones con M+1 nodos.
- Para cada nodo en el mallado, se reemplazó cada derivada parcial por su correspondiente aproximación por diferencias finitas.
- El sistema de ecuaciones diferenciales ordinarias se resolvió utilizando métodos numéricos estándar.

El uso del método MOL permitió resolver los sistemas EDO utilizando los métodos de resolución disponibles en MATLAB®. Los sistemas de ecuaciones obtenidos fueron moderadamente rígidos (*stiff*) como resultado de la aplicación del método MOL. Para escoger el método de resolución del sistema de EDO se tuvo en cuenta que la resolución numérica de este tipo de sistemas exige una disminución significativa del paso de integración con el objetivo de evitar inestabilidades. En este sentido, el método *ode23t* integrado en MATLAB® es adecuado para problemas moderadamente rígidos. Se probaron otros métodos de resolución pero en la práctica este último dio los mejores resultados en tiempo de resolución. Para la resolución numérica del modelo se utilizaron 20 secciones de la altura de la columna y 40 secciones para la biopelícula. Esto resultó en dos sistemas EDO, con 2 (N+1) (M+3) ecuaciones cada uno. El esquema conceptual de la resolución del modelo se presenta en la Figura 4-6.

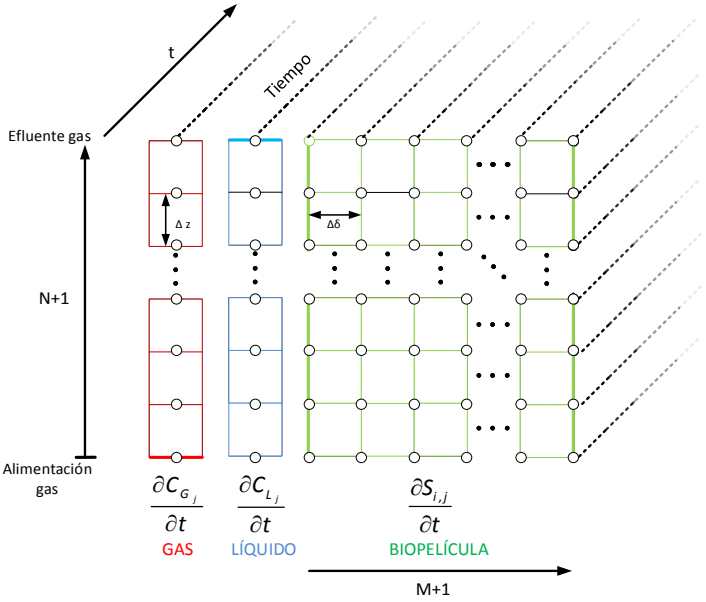

Figura 4-6 Esquema de la semidiscretización del método MOL para las fases gas–líquido–biopelícula. Las condiciones de contorno están marcadas mediante una línea más ancha.

4.6 BIBLIOGRAFÍA

American Public Health Association, American Water Works Association y Water Environment Federation. (1998). *Standard Methods for the Examination of Water and Wastewater*. (L. S. Clesceri, A. E. Greenberg, y A. D. Eaton, Eds.). Washington.

Sempere, F., Martínez-Soria, V., Penya-Roja, J. M., Waalkens, A. y Gabaldón, C. (2012). Control of VOC emissions from a flexographic printing facility using an industrial biotrickling filter. *Water Science and Technology : A Journal of the International Association on Water Pollution Research*, *65*(1), 177–82.

5 RESULTADOS PRINCIPALES Y DISCUSIÓN GENERAL

En este capítulo se muestra de forma resumida los resultados experimentales obtenidos durante el desarrollo de la presente tesis doctoral, incluyendo algunas figuras para facilitar su seguimiento. Toda la información está recogida en los artículos científicos que componen esta tesis doctoral.

5.1 TRATAMIENTO DE ISOPROPANOL MEDIANTE BIOFILTROS PERCOLADORES EN CONDICIONES DE OPERACIÓN INTERMITENTES

En la primera parte de esta tesis doctoral (**capítulo 6**) se ha llevado a cabo el estudio experimental a escala de laboratorio de dos biofiltros percoladores empleados para la depuración de emisiones gaseosas contaminadas con isopropanol. Los experimentos se realizaron en condiciones de operación típicas de la industria de impresión flexográfica. En este tipo de industria se suele trabajar en uno o dos turnos de operación y, por tanto, suelen emitir un patrón de emisiones discontinuo y de concentración variable. Así mismo, una de las prácticas más habituales en la operación de los biofiltros percoladores a nivel industrial es la aplicación de patrones de riego discontinuos con el objetivo de reducir los costes de operación y controlar el crecimiento excesivo de la biomasa. Para simular esta situación se trabajó en condiciones de alimentación intermitente y de riego discontinuo. La corriente contaminada con isopropanol se introdujo en el reactor 16 h al día durante 5 días a la semana. Además se utilizó un patrón de riego discontinuo de 15 min cada 1.5 h durante los periodos de alimentación de corriente contaminada con COV. El resto del tiempo (8 h al día de lunes a viernes y los fines de semana) se introducía aire limpio, manteniendo constante el TRVV, a fin de simular las paradas nocturnas y de fin de semana de las fábricas que trabajan con dos turnos de trabajo. Con el fin de simular la puesta en marcha de un biofiltro percolador a escala industrial, donde el proceso de adaptación de los microorganismos al compuesto a degradar no resulta viable económicamente, el fango activado no fue adaptado previamente a la degradación de isopropanol. Se utilizó un fango activado que provenía de la depuradora de aguas residuales de Carlet (España). Se emplearon dos biofiltros percoladores operados en paralelo utilizando diferente material de relleno: anillos de polipropileno de 15 mm de diámetro y un material de relleno estructurado (PAS Winded Media), y se evaluó el rendimiento de ambos biofiltros percoladores ante variaciones en la concentración de COV de la corriente de entrada y en el TRVV. Para ello se aplicaron 3 cargas volumétricas para diferentes TRVV comprendidos entre 14 s y 160 s. El experimento se llevó a cabo para concentraciones de isopropanol en la corriente

gaseosa de entrada de 1000, 500 y 250 mg C Nm^{-3} (Fases A, B y C). Para cada una de estas concentraciones se utilizaron a su vez 3 TRVV de manera que se obtuvieron CV de 20, 35 y 65 g C m^{-3} h^{-1}, excepto para la concentración de entrada de 250 mg C Nm^{-3} en que no se aplicó la CV más baja. En la Tabla 5-1 se presenta la planificación de las condiciones de operación en el estudio experimental a escala de laboratorio de la depuración de isopropanol mediante biofiltros percoladores (capítulo 6). Posteriormente se evaluó la respuesta del biofiltro percolador a un periodo sin alimentación de COV de 7 semanas, tras el cual se restauró la alimentación de COV aplicando una CV de 35 g C m^{-3} h^{-1} (Fase D).

Tabla 5-1 Planificación de las condiciones de operación para el estudio experimental a escala de laboratorio de la depuración de isopropanol mediante biofiltros percoladores (capítulo 6).

	Días	$C_{entrada}$ (mg C Nm^{-3})	CV (g C $m^{-3}h^{-1}$)	TRVV (s)
Fase A				
A–I	0 – 48	1000	20	160
A–II	49 – 69	1000	35	90
A–III	70 –90	1000	65	50
Fase B				
B–I	91– 97	500	20	90
B–II	98–104	500	35	50
B–III	105 – 125	500	65	25
Fase C				
C–II	126 – 132	250	35	25
C–III	133 – 163	250	65	14

En la Figura 5-1 se presenta la evolución de la eficacia de eliminación y de la concentración en la corriente gaseosa a la entrada y en la salida de los biofiltros percoladores durante toda la experimentación. La puesta en marcha del proceso se llevó a cabo con una CV de 20 g C m^{-3} h^{-1} durante el periodo de alimentación de COV y un TRVV alrededor de 160 segundos. Después de 4–6 días de operación se obtuvieron rendimientos superiores al 70 %. Tras este periodo de adaptación, durante la fase A–I, se obtuvieron rendimientos de 80 % para ambos reactores. En las fases A-II y A–III (concentración de entrada 1000 mg C Nm^{-3}, CV 35 y 65 g C m^{-3} h^{-1}, respectivamente), ambos biofiltros percoladores funcionaron de manera similar, obteniéndose eficacias de eliminación entre 60 y 85 %. En la siguiente fase se disminuyó la concentración de entrada a 500 mg C Nm^{-3} para la CV de 20 y 35 g

C m^{-3} h^{-1} (fases B–I y B–II), obteniéndose rendimientos superiores a 90 %. Por el contrario, al aumentar la carga volumétrica hasta 65 g C m^{-3} h^{-1} (fase B–III), la eficacia de eliminación disminuyó hasta valores de 60 – 70 %. Durante la fase C, los bioreactores trabajaron con una concentración en la corriente de entrada de 250 mg C Nm^{-3}. En la etapa C–II, con una CV de 37–39 g C m^{-3} h^{-1}, se obtuvieron altas eficacias de eliminación: 80 % para el biofiltro percolador que contenía el material estructurado y 88 % para el biofiltro percolador relleno con anillos de polipropileno de 15 mm. Al incrementar la carga a 65 g C m^{-3} h^{-1} (fase C–III, TRVV = 14 s), el rendimiento del proceso empeoró, obteniéndose eficacias de eliminación de 49% para el material estructurado y de 60% para el material desordenado. La máxima CE fue de 51 g C m^{-3} h^{-1} para una CV de 65 g C m^{-3} h^{-1} y un TRVV de 50 s y utilizando el material de relleno desordenado, mientras que la CE máxima para el material estructurado en estas condiciones de aplicación fue ligeramente menor, 45 g C m^{-3} h^{-1}.

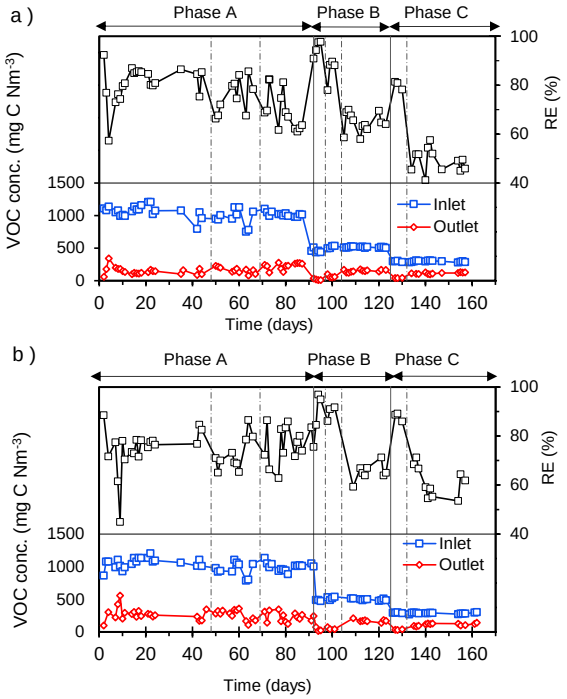

Figura 5-1 Evolución de los biofiltros percoladores para la eliminación de isopropanol. La línea discontinua representa un incremento en la CV de 1.8. a) Biofiltro percolador con material estructurado; b) biofiltro percolador con anillos de polipropileno de 15 mm de diámetro. *Corresponde con la Figura 6-6 del capítulo 6.*

El riego intermitente produjo fugas de contaminante en la emisión gaseosa de salida del biofiltro percolador coincidiendo con el momento del riego. En la Figura 5-2 se muestra la influencia del patrón de riego en las emisiones de salida de la fase gas. La operación del biofiltro percolador utilizando condiciones de entrada de contaminante discontinuas (16 h al día, 5 días a la semana) provocó que la concentración máxima aumentara en cada uno de los riegos hasta alcanzar un máximo después del tercer riego del día. Durante los periodos sin riego se obtuvieron eficacias de eliminación casi completas, excepto cuando el reactor trabajaba a las CV más elevada (65 g C m^{-3} h^{-1}). En los periodos en los que se introducía corriente gaseosa contaminada con isopropanol, el riego produjo la absorción y acumulación de una parte del contaminante tanto en el agua de recirculación como en el interior de la biopelícula. Este fenómeno es especialmente importante para compuestos muy solubles en agua, como es el caso del isopropanol, donde se pueden alcanzar concentraciones elevadas del compuesto en el agua y en el interior de la biopelícula que actuarán como fuente/sumidero. A su vez se produjo la desorción de contaminante desde la fase líquida a la fase gas durante los periodos con riego, lo que causaba una fuga de contaminante cíclica coincidiendo con el riego.

Para evaluar la influencia del patrón de riego en las emisiones de salida de la fase gas se disminuyó la frecuencia de riego desde 15 min cada 1.5 h (Figura 5-2a) hasta 15 min cada 3 h (Figura 5-2b), y se comparó la concentración de contaminante promedio en la emisión gaseosa a la salida del reactor durante las 16 h de entrada de contaminante al sistema. Con ello se obtuvo una disminución en el promedio de la concentración de salida, desde 86 a 59 mg C Nm^{-3} para una concentración de entrada de 500 mg C Nm^{-3}. En este sentido, al disminuir el número de riegos el fenómeno de fuga de contaminante se repite con menor frecuencia por lo que lleva asociado la reducción de la concentración promedio de COV en la corriente de salida. Desde el punto de vista de la operación industrial, disminuir el número de riego disminuiría los costes de explotación del proceso y ayudaría a controlar el crecimiento excesivo de la biomasa. Sin embargo, habría que llegar a un compromiso para garantizar el aporte de nutrientes y de humedad. De forma adicional, se evaluó el efecto de utilizar el riego también durante el periodo sin alimentación de COV a fin de que el biofiltro percolador degradara durante ese periodo el isopropanol que se acumulaba en el agua de recirculación durante las 16 h de alimentación de isopropanol. La extensión del riego a las 24 h diarias supuso una mejora en el rendimiento del reactor, obteniéndose una

concentración en la emisión gaseosa de 44 mg C Nm^{-3} (Figura 5-2c), es decir prácticamente la mitad de la obtenida con la configuración inicial.

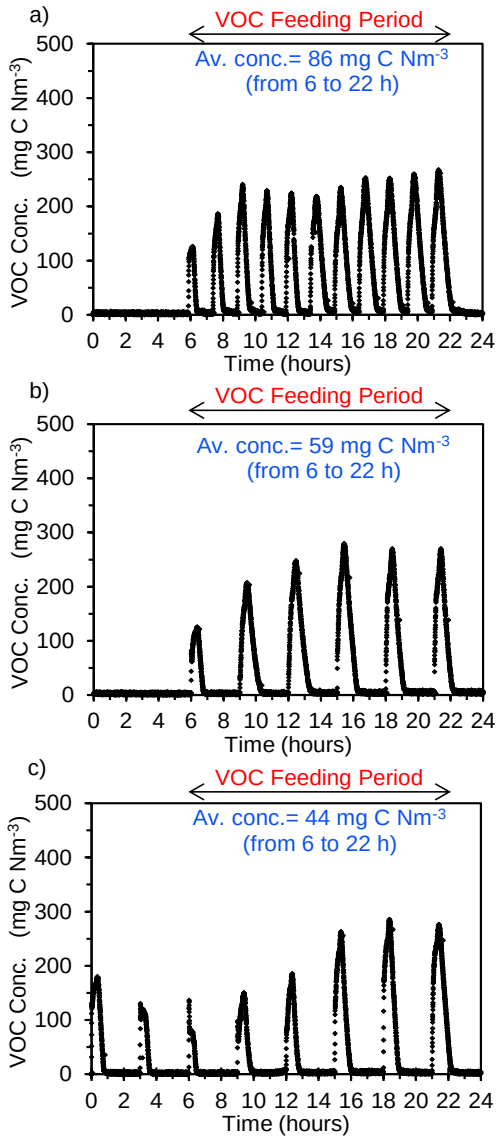

Figura 5-2 Influencia del régimen de riego en el patrón de emisión gaseosa a la salida del biofiltro percolador: a) riego de 15 min cada 1.5 h; b) riego de 15 min cada 3 h; c) riego de 15 min cada 3 h durante 24 h. *Corresponde con Figura 6-9 del capítulo* 6.

Finalmente se sometió a los dos bioreactores a un periodo de 7 semanas sin alimentación de COV, manteniendo la aireación y el riego intermitente, con el objetivo de simular una parada programada de producción de las empresas debida, por ejemplo, a cierres vacacionales. Para ello, se utilizó un TRVV de 60 segundos y un régimen de riego de 15 minutos al día a fin de asegurar condiciones de humedad de la biopelícula y de aporte de nutrientes adecuadas. Para reanudar el aporte de contaminante al sistema se utilizó un patrón de alimentación de 16 horas diarias, tal y como se llevó a cabo en el resto de experimentos. El régimen de riego utilizado fue de 15 minutos cada 4 horas, menos intenso que el utilizado en las fases A, B y C, para reducir el riesgo de desprendimiento de biomasa. Se seleccionaron condiciones de CV y TRVV intermedias entre las ensayadas (35 g C m^{-3} h^{-1}, 60 segundos) similares a las de la fase B-II, ya que en estas se había observado un rendimiento óptimo del sistema. Para ambos reactores tras 5–6 días de operación se obtuvieron eficacias de eliminación superiores a 80%. Después de 10 días se alcanzó una eficacia de eliminación de 90 % similar a la obtenida en la fase B–II. El comportamiento observado en ambos bioreactores demostró que la actividad biológica se recuperó de manera favorable en pocos días. Esta recuperación indica que la población bacteriana puede sobrevivir durante largos periodos de tiempo si se mantienen las condiciones de aireación, humedad y nutrientes adecuados, demostrando que no es necesaria una posterior reinoculación tras una interrupción prolongada en la alimentación de COV. En este sentido, es importante destacar que previamente no se habían probado periodos tan largos sin alimentación de COV en biofiltros percoladores. Los resultados obtenidos en este trabajo son de especial interés ya que la robustez del sistema es un parámetro clave para su aplicación industrial.

5.2 MODELACIÓN DE LA TRANSFERENCIA DE MATERIA EN BIOFILTROS PERCOLADORES PARA LA ELIMINACIÓN DE ISOPROPANOL

Los sistemas biológicos pueden verse limitados tanto por la transferencia de materia como por la cinética microbiana. Debido a la baja constante de Henry de los COV de elevada solubilidad en comparación con la constante de Henry del oxígeno, la etapa limitante del proceso puede ser la transferencia de oxígeno lo que puede causar la aparición de zonas anaerobias en las zonas más profundas de la biopelícula. Por este motivo, se ha llevado a cabo el estudio y modelación de la transferencia de isopropanol y de oxígeno como paso previo al desarrollo del

modelo matemático de biofiltro percolador. La metodología utilizada en el presente trabajo puede ser aplicada para la determinación de los coeficientes de transferencia de materia para cualquier otro compuesto orgánico volátil de elevada solubilidad.

Para la determinación del coeficiente de transferencia de materia del isopropanol (**capítulo 7**) se utilizó el coeficiente global de transferencia de materia en la fas gas ($K_G a$). En este estudio se determinó la influencia de las velocidades superficiales de líquido y de gas para dos materiales de relleno: anillos de polipropileno de 25 mm de diámetro (a= 207 m^2 m^{-3}) y material de relleno estructurado PAS Winded Media (a= 410 m^2 m^{-3}). Los experimentos para determinar el valor de coeficiente transferencia de materia fueron llevados a cabo a unas velocidades superficiales de gas de 100, 150 y 300 m h^{-1} y a velocidades superficiales de líquido de 2, 4, 7 y 13 m h^{-1}. En la Figura 5-3 se presenta la influencia de la velocidad superficial de gas y de líquido en el coeficiente global de transferencia de materia de la fase gas para los dos materiales de relleno estudiados. Dependiendo del material de relleno y de las condiciones hidrodinámicas, se obtuvieron coeficientes de transferencia de materia de isopropanol comprendidos entre 500 y 1800 h^{-1}. En las condiciones estudiadas la transferencia de materia de isopropanol estuvo fuertemente afectada por la velocidad superficial del gas, obteniéndose variaciones de 40% en el coeficiente de transferencia de materia para variaciones de 50% de la velocidad superficial del gas. Por contrapartida, no se observó influencia de la velocidad superficial de líquido ni del material de relleno utilizado en la transferencia de materia. La escasa influencia de la velocidad superficial de líquido en la transferencia de materia de isopropanol está asociada a la elevada solubilidad del isopropanol en agua, y por tanto, la resistencia a la transferencia de materia reside en la fase gas. El estudio incluyó la determinación de la influencia de la temperatura en la constante de Henry de isopropanol. Para describir el comportamiento de la constante de Henry con la temperatura se utilizó la ecuación de Van't Hoff. Los valores de la constante de Henry a 25 ^{o}C y de la entalpia de la disolución se obtuvieron mediante la aplicación del método de mínimos cuadrados minimizando las diferencias entre los datos experimentales y la ecuación de Van´t Hoff. La aplicación de la ecuación empírica dio como resultado un aumento de un factor de 1.8 por cada 10 ^{o}C en la constante de Henry adimensional del isopropanol.

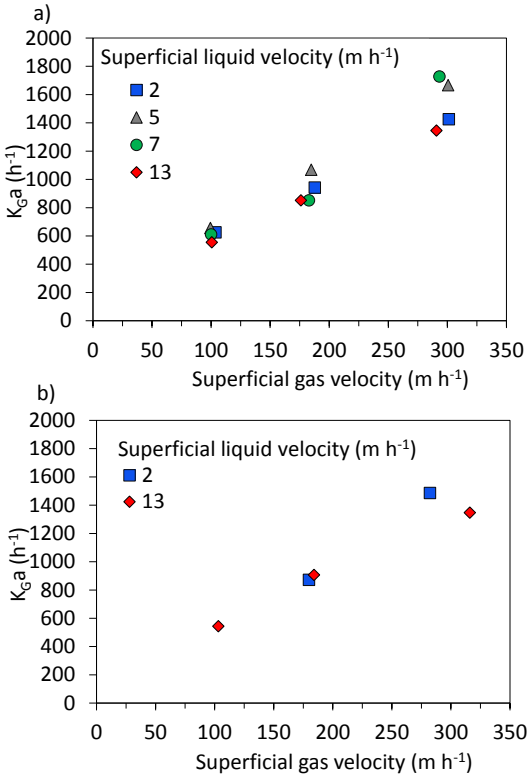

Figura 5-3 Influencia de la velocidad superficial de gas y de líquido en el coeficiente global de transferencia de isopropanol en la fase gas para diferentes materiales de relleno*:* a) anillos de polipropileno de 25 mm de diámetro; b) estructurado PAS Winded Media. *Corresponde con Figura 7-5 del capítulo 7.*

Para la determinación del coeficiente de transferencia de oxígeno (**capítulo 7**) se utilizó el coeficiente global de transferencia de materia en la fase líquida (K_La). Se seleccionaron dos velocidades superficiales de gas de 100 y 300 m h^{-1} y velocidades superficiales de líquido comprendidas entre 3 y 33 m h^{-1}. Estos experimentos se llevaron a cabo para el material de relleno estructurado PAS Winded Media (a= 410 m^2 m^{-3}) y para los anillos de polipropileno de diámetros 15 mm (a= 348 m^2 m^{-3}) y 25 mm (a= 207 m^2 m^{-3}). En la Figura 5-4 se presenta la influencia de la velocidad superficial de gas y de líquido en el coeficiente global de transferencia de oxígeno en la fase líquida para los materiales de relleno estudiados. Dependiendo del material de relleno y de las condiciones hidrodinámicas se obtuvieron valores de coeficientes de transferencia de materia

que variaron entre 20 y 200 h^{-1}. La influencia de la superficie específica y de la estructura del material de relleno sólo fue apreciable para velocidades superficiales de líquido superiores a 15 m h^{-1}. Para una velocidad de 30 m h^{-1} los mayores valores de coeficiente de transferencia de oxígeno se obtuvieron para el relleno estructurado (K_La = 175 h^{-1}); mientras que para los anillos de polipropileno su valor disminuyó al disminuir la superficie específica de éstos: K_La = 130 h^{-1} para anillos de polipropileno de 15 mm de diámetro y K_La = 100 h^{-1} para anillos de polipropileno de 25 mm de diámetro. Por tanto, desde el punto de vista de la transferencia de oxígeno desde la fase gas a la fase líquida, la biodegradación del compuesto se verá favorecida utilizando rellenos con elevada superficie específica y velocidades superficiales de líquido superiores a 15 m h^{-1}. Sin embargo, estas condiciones de operación serian de difícil aplicación industrial ya que incrementarían los costes de explotación del proceso. Al triplicar la velocidad superficial de aire (312 m h^{-1}) no se observó influencia significativa en la transferencia de oxígeno. La escasa influencia de la velocidad superficial de gas está asociada a que la resistencia a la transferencia de materia reside mayoritariamente en la fase líquida debido a la baja solubilidad del oxígeno en agua. Desde el punto de vista del proceso de eliminación de COV, esto implica que la transferencia de oxígeno no debe verse prácticamente afectada con las variaciones del caudal de aire, siempre y cuando se mantengan el resto de propiedades constantes.

Con los datos experimentales obtenidos se determinaron correlaciones empíricas entre los coeficientes de transferencia de materia y las velocidades superficiales de gas y de líquido (**capítulo 7**). Para el coeficiente de transferencia de materia de isopropanol se estableció una correlación única para los dos materiales de relleno que dependía solamente de la velocidad superficial de gas. Para el coeficiente de transferencia de oxígeno se estableció una correlación diferente para cada material de relleno en función de la velocidad superficial de líquido. Los resultados obtenidos fueron comparados con las correlaciones para absorbedores químicos propuestas por Onda et al. (1968) y por van Krevelen y Hoftijzer (1948) y con la correlación propuesta por Kim y Deshusses (2008) para biofiltros percoladores con anillos Pall ring 1". Ninguna de las correlaciones de la bibliografía reprodujo correctamente los resultados experimentales obtenidos en el estudio de transferencia de isopropanol. Para el estudio de transferencia de oxígeno sólo la ecuación propuesta por Onda et al. (1968) fue capaz de predecir los coeficientes de transferencia obtenidos experimentalmente. Por tanto, los resultados obtenidos demostraron la necesidad de establecer correlaciones empíricas en los intervalos de variación de velocidades superficiales de líquido y de

gas de los biofiltros percoladores a fin de caracterizar correctamente los procesos de transferencia de materia.

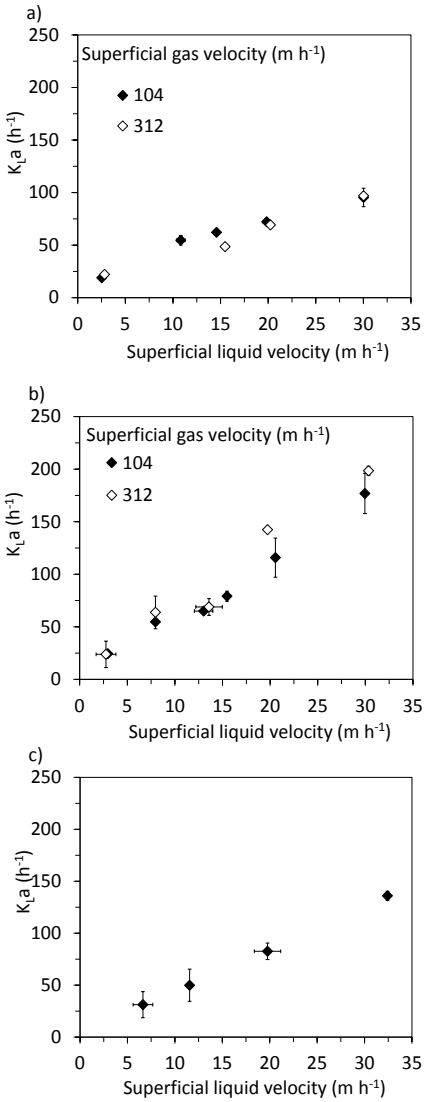

Figura 5-4 Influencia de la velocidad superficial de gas y de líquido en el coeficiente global de transferencia de oxígeno en la fase líquida para diferentes materiales de relleno*:* a) anillos de polipropileno de 25 mm de diámetro; b) estructurado PAS Winded Media; c) anillos polipropileno de 15 mm de diámetro. *Corresponde con Figura 7-7 del capítulo 7.*

Teniendo en cuenta que la superficie específica y la configuración del material de relleno tiene impacto en la transferencia de oxígeno, se realizó un estudio adicional comparando los tres materiales de relleno estudiados en el laboratorio con los anillos de polipropileno de 50 mm de diámetro (a = 102 m^2 m^{-3}), que son lo que se utilizan habitualmente en la industria (**capítulo 8**). Para ello, se seleccionaron dos intervalos de velocidades superficiales de líquido: 3–6 m h^{-1}, que corresponde con velocidades superficiales habituales en la operación industrial y 30 m h^{-1} que corresponde con la velocidad superficial donde se observaron las mayores diferencias entre los materiales ensayados en el laboratorio. En la Figura 5-5 se muestran los resultados obtenidos. Este experimento mostró que para velocidades de 30 m h^{-1} el coeficiente global de transferencia de oxígeno en la fase líquida del material de relleno utilizado en la industria era sustancialmente menor que el obtenido para el resto de materiales de relleno. Sin embargo, en el intervalo inferior de velocidades superficiales de líquido la transferencia de oxígeno era similar a la del resto de materiales de relleno. Por tanto, cuando se realiza el cambio de escala de este proceso desde el laboratorio a la industria y en el intervalo de velocidades superficiales de líquido que se utilizan en la aplicación industrial (3–6 m h^{-1}), la transferencia de oxígeno obtenida con los anillos de polipropileno de 50 mm sería comparable a la transferencia de oxígeno obtenida con los materiales de laboratorio.

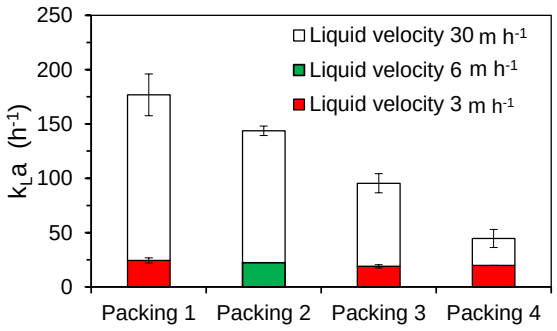

Figura 5-5 Influencia de la velocidad superficial de líquido en la transferencia de oxígeno para diferentes materiales de relleno. Relleno 1: material estructurado PAS Winded Media, Rellenos 2, 3 y 4: Anillos de polipropileno de diámetros 15, 25 y 50 mm, respectivamente. *Corresponde con Figura 8-3 del capítulo 8.*

5.3 MODELACIÓN MATEMÁTICA DEL PROCESO DE BIOFILTRO PERCOLADOR

En esta tesis doctoral se ha desarrollado un modelo dinámico cuyo objetivo es la predicción de la respuesta transitoria de los biofiltros percoladores sometidos a condiciones de carga variable y de riego intermitente (**capítulo 9**), como es habitual en la operación industrial. A fin de simular este comportamiento se asumió que los biofiltros percoladores funcionaban en condiciones cíclicas de riego/no riego. Para ello, se definieron dos conjuntos de ecuaciones diferenciales independientes acoplados entre ellos mediante las condiciones iniciales y finales. Para describir ambos periodos se planteó un modelo trifásico (gas–líquido–biopelícula) basado en las ecuaciones de balance de materia y teniendo en cuenta los mecanismos más relevantes que tienen lugar durante la depuración de COV mediante biofiltro percolador: transporte convectivo, transferencia de materia, y consumo de contaminante por parte de la biomasa. El flujo másico gas–líquido y líquido–biopelícula se expresó a través del coeficiente de transferencia de materia y del gradiente de concentraciones. Durante los periodos con riego, se asumió que existía una fase líquida móvil entre la fase gas y la biopelícula mientras que en los periodos sin riego se asumió que existía una fase líquida estancada. Durante los periodos de riego el contaminante y el oxígeno eran transferidos desde la fase gas a la fase líquida móvil y, finalmente, a la biopelícula, donde tenía lugar la biodegradación de los contaminantes. En estos periodos se utilizó como condición de contorno en la fase líquida una ecuación adicional que representaba el balance de materia en el tanque de recirculación. De manera análoga a los periodos con riego, durante los periodos sin riego se asumió que el contaminante y el oxígeno se transferían desde la fase gas a la fase líquida estancada y posteriormente a la biopelícula. Una de las novedades del modelo desarrollado fue la capacidad para reproducir comportamientos diferentes en términos de transferencia de materia en la fase líquida estancada mediante la incorporación de una función *switch*. Esta función fue incluida en las ecuaciones de balance de materia de la fase gas y de la fase líquida en los periodos sin riego mediante el parámetro α_2. A este parámetro se le podían asignar solo dos valores: 100 indicando que la resistencia a la transferencia de materia entre el gas–líquido era despreciable o 1 indicando que la resistencia a la transferencia de materia gas – líquido contribuía a reducir el flujo másico hasta/desde la biopelícula.

En primer lugar se determinó la relación dinámica que existía entre la fuga gaseosa de contaminante a la salida del bioreactor y la acumulación de compuestos orgánicos en la disolución de recirculación (**capítulo 9**). Para ello se utilizó un biofiltro percolador de laboratorio empaquetado con el material de relleno de anillos de polipropileno de 25 mm diámetro y se utilizó isopropanol como contaminante modelo. Se utilizaron condiciones de alimentación intermitente (16 h por día durante 7 días a la semana) y el patrón de riego se aplicó durante 24 horas al día. El biofiltro percolador fue inoculado con fango activado de depuradora y fue operado con una CV de 30 g C m^{-3} h^{-1}, TRVV de 60 s y riego intermitente durante más de 3 meses. Manteniendo esta CV se ensayaron dos patrones de riego intermitente (1 h cada 4 h y 30 min cada 4 h) que fueron utilizados un mínimo de 2 semanas cada uno. Además, se llevó a cabo un tercer experimento incrementando la CV hasta 60 g C m^{-3} h^{-1} y utilizando el patrón de riego de 1 h cada 4 h. Cada uno de estos experimentos comenzó con agua limpia en el tanque de recirculación para obtener datos sobre la acumulación de carbono orgánico disuelto en el tanque de recirculación. A modo de ejemplo, en la Figura 5-6 se presenta la evolución de la emisión gaseosa de contaminante y de la concentración de carbono orgánico disuelto en el tanque de recirculación del biofiltro percolador operado a una CV de 30 g C m^{-3} h^{-1} y riego 1 h cada 4 h, el tiempo 0 h representa el lunes a las 8.00 a.m. En esta figura se presenta la evolución semanal de lunes a viernes (Figura 5-6a) y el detalle correspondiente al miércoles (Figura 5-6b) como día representativo del patrón diario de emisión de contaminante de la fase gas y de la evolución de la concentración de carbono del tanque de recirculación. El patrón de concentración de COV en la fase gas producido por el riego intermitente fue similar al obtenido en los experimentos previos (**capítulo 6**), con emisiones fugitivas de contaminante en la fase gaseosa durante los periodos de riego y eliminaciones completas durante los periodos sin riego. Durante las 16 horas al día en las que se alimentaba la corriente gaseosa contaminada con COV se observó que la fuga de contaminante durante el riego aumentaba con el número de ciclos de riego, produciéndose un total de 6 picos por día. Este patrón de emisión de contaminante era similar para todos los días de la semana. Como ejemplo de patrón de comportamiento representativo se ha seleccionado el miércoles (Figura 5-6.b.1). Como se observa en esta figura, el primer pico de fuga de contaminante era mucho menor que los demás (48 h). La fuga aumentaba durante el segundo pico del día (Figura 5-6.b.1, 52 h) obteniéndose una fuga de contaminante prácticamente estable después del tercer pico de riego (Figura 5-6.b.1, 56 h y 60 h). Además, el pico inmediatamente posterior a la parada en la alimentación era similar a los demás picos del día

(Figura 5-6.b.1, 64 h). Después de unas horas alimentando aire limpio al reactor la emisión fugitiva de COV durante el riego disminuía drásticamente (Figura 5-6.b.1, 68 h). Para determinar la relación de la emisión gaseosa de contaminante con la acumulación de compuestos orgánicos en la fase líquida se realizó el seguimiento de la evolución de la concentración de carbono disuelto en el tanque de recirculación durante los ciclos de riego en días alternos de la semana (lunes, miércoles y viernes). Este seguimiento mostró que la concentración de carbono disuelto en el tanque aumentaba con cada riego realizado durante el periodo de alimentación de COV (16 h al día), indicando que el carbono se absorbía en el agua de recirculación (Figura 5-6 a.2 y b.2). Así mismo, se observó que la concentración de carbono orgánico disuelto en el tanque de recirculación tras 8 h sin alimentación de COV disminuía notablemente. Por ejemplo, el lunes después del riego de las 8 h, la concentración de carbono en el tanque de recirculación era aproximadamente 200 mg C L^{-1} y el miércoles a las 52 h volvía estar alrededor de 100 mg C L^{-1} (Figura 5-6.a.2). Esto indicó que el carbono orgánico se transfería y se degradaba en el bioreactor durante los riegos en los periodos sin entrada de contaminante al reactor. El seguimiento de manera paralela de la concentración de salida de COV en aire y de la toma de muestras de agua del tanque de recirculación permitió determinar que la concentración de COV a la salida del reactor era más de 3 veces superior a la concentración de equilibrio del agua del tanque de recirculación. Esta observación implicaba que la fuga de contaminante observada en la emisión gaseosa no se debía únicamente a la desorción de contaminante desde la fase líquida a la fase gas, sino que se podía asociar a un aumento de la resistencia a la transferencia de materia entre ambas fases.

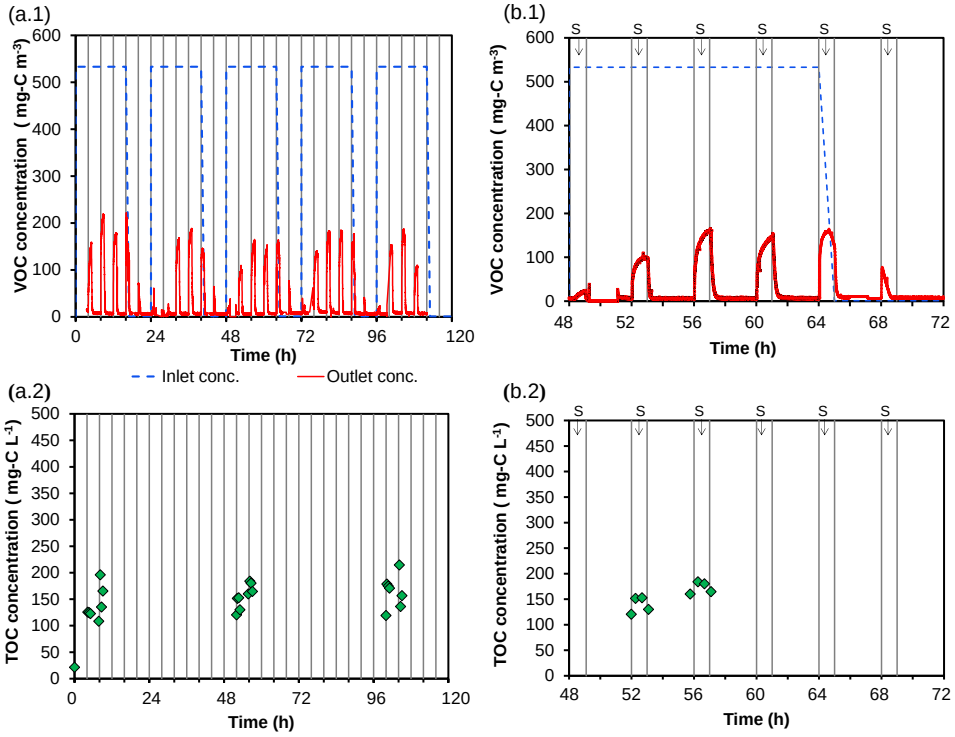

Figura 5-6 Evolución semanal (lunes a viernes) y detalle del miércoles del biofiltro percolador para una CV de 30 g c m^{-3} h^{-1} y riego 1 h cada 4 h. (a) Evolución semanal: Las líneas verticales indican el inicio de un riego. (a.1) Concentración de COV en la fase gas; (a.2) concentración de carbono disuelto en el tanque de recirculación. (b) Miércoles: S representa el periodo de riego: (b.1) Concentración de COV en la fase gas; (b.2) concentración de carbono en el tanque de recirculación. *Corresponde con Figura 9-2 del capítulo 9*

Para la calibración del modelo matemático se utilizaron los datos del experimento llevado a cabo con una CV de 30 g C m^{-3} h^{-1} y riegos intermitentes de 1 h cada 4 h (**capítulo 9**). Los valores de las difusividades en agua y constantes de Henry se obtuvieron de la bibliografía. Los coeficientes globales de transferencia de materia en condiciones abióticas para el isopropanol y el oxígeno se obtuvieron de las correlaciones propuestas en el capítulo 7. Se asumió un espesor de biopelícula constante (60 µm). Así mismo, se asumió que la resistencia ofrecida por la fase líquida estancada durante los periodos sin riego era despreciable (α_2= 100). La calibración se llevó a cabo en dos etapas. Primero se determinaron los

valores del espesor de la interfase líquido-biopelícula (β) y de los parámetros cinéticos (μ_{max}, K_s) capaces de reproducir la evolución experimental de la variación de la concentración de contaminante de la fase gas y del carbono orgánico disuelto en el tanque de recirculación. De esta etapa de la calibración se determinaron valores de β= 3.8 10^{-6} m, μ_{max}= 2 10^{-5} s^{-1} y K_s= 350 g C m^{-3}, consiguiéndose un error relativo de 6.7 % entre la CE experimental y la CE obtenida con el modelo. Con estos parámetros, el patrón simulado de la variación dinámica de concentración de COV en la fase gas a la salida del reactor subestimaba la fuga de contaminante durante los periodos con riego. Experimentalmente se observó que el patrón diario de fuga de contaminante en la emisión gaseosa durante el riego se repetía de forma cíclica durante toda la experimentación: aumentando desde el primer al tercer riego tras una noche sin alimentación, manteniéndose estable a partir de éste, y disminuyendo a lo largo de los riegos realizados durante los periodos sin entrada de contaminante. En base a esta observación se planteó una hipótesis: la alimentación intermitente junto con el patrón discontinuo de riego causaban cambios transitorios en las propiedades físicas de la biopelícula, produciéndose la acumulación de agua y de polímeros extracelulares a lo largo del día, lo que causaba una barrera transitoria a la transferencia de materia entre la fase gas y la fase líquida. Para simular este fenómeno se redujo el flujo de transferencia de materia por un factor (α_1) y se llevó a cabo la calibración de su variación diaria. A modo ilustrativo, en la Figura 5-7 se muestra los resultados de la calibración de la variación del flujo de transferencia de materia. Durante el segundo ciclo de riego del día el flujo de transferencia de materia se corrigió en un factor de 0.3 (tiempo 52 h, tras 4 h de entrada de COV) mientras que en el resto de ciclos se corrigió en un factor de 0.23 (tiempo 56 y 60 h), incluyendo el riego inmediatamente posterior al corte de suministro de contaminante (tiempo 64 h). En los demás riegos durante los periodos sin entrada de contaminante y el primer riego tras su reanudación se mantuvieron los coeficientes de transferencia de materia calibrados para condiciones abióticas (tiempo 48 h y 68 h). Por tanto, este fenómeno implicó que la transferencia de materia en el biofiltro percolador con biomasa fuera hasta 4 veces inferior a la transferencia de materia calibrada en condiciones abióticas. Con esta propuesta se obtuvo un error relativo de 2.3 % entre la CE simulada y la CE experimental y se reprodujo la variación de la emisión de contaminante de la fase gas, mejorando el resultado respecto a la primera etapa de la calibración (α_1=1).

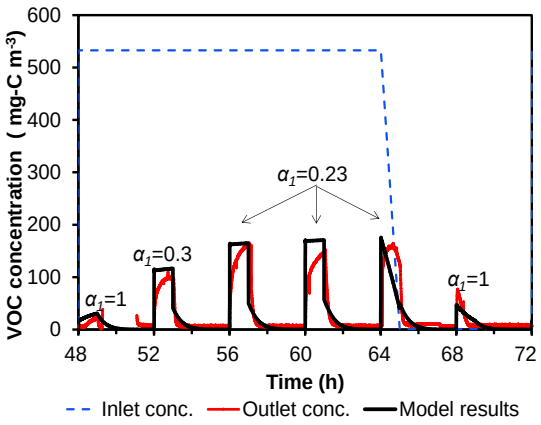

Figura 5-7 Calibración de la variación diaria del flujo de transferencia de materia. α_1 es el factor corrector. *Adaptada de Figura 9-4 del capítulo 9.*

La validación del modelo matemático se llevó a cabo con dos conjuntos de datos experimentales independientes: disminuyendo el riego al 50 % (30 min cada 4 horas) y aumentando la CV hasta 60 g C m^{-3} h^{-1}. En la Figura 5-8 se muestran los datos experimentales relativos a la validación del modelo matemático: en la Figura 5-8a se presentan los resultados del experimento llevado a cabo con CV 30 g C m^{-3} h^{-1} y riego 30 min cada 4 h, y en la Figura 5-8b se presentan los resultados del experimento llevado a cabo con CV 60 g C m^{-3} h^{-1} y riego 1 h cada 4 h. Para ambos experimentos se obtuvieron errores relativos menores de 4% entre las CE simuladas por el modelo y las CE obtenidas experimentalmente. La aplicación del modelo permitió simular tanto las variaciones diarias en la emisión gaseosa de salida como las variaciones en la concentración de carbono orgánico disuelto en el tanque de recirculación. Por ejemplo, durante el experimento realizado una CV 60 g C m^{-3} h^{-1} se realizó una purga en el tanque de recirculación a las 52 h (Figura 5-8.b.2), y el modelo fue capaz de predecir el incremento en la concentración de carbono orgánico disuelto desde 55 mg C L^{-1} hasta aproximadamente 400 mg C L^{-1}. Esta purga intermedia tuvo un impacto despreciable en la emisión gaseosa de contaminante (Figura 5-8.b.1), corroborando que la emisión durante el riego estaba asociada al incremento en la resistencia a la transferencia de materia entre la fase gas y la fase líquida.

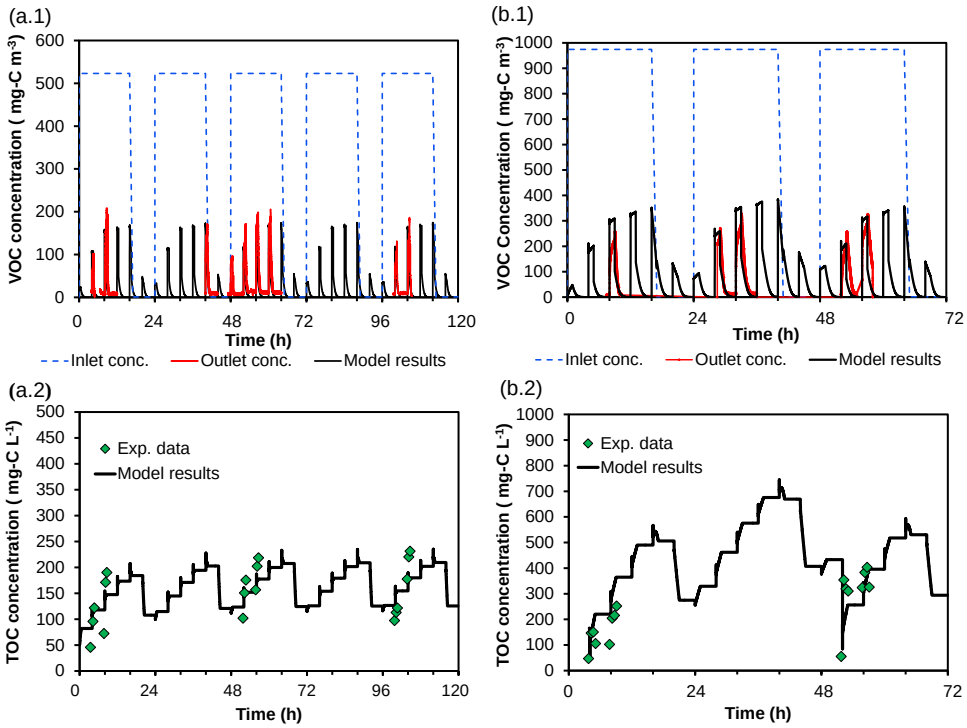

Figura 5-8 Evolución semanal de los datos experimentales y predicción del modelo (a) CV 30 g C m^{-3} h^{-1} y riego 30 min cada 4 h: (a.1) fase gas, (a.2) carbono orgánico disuelto en el tanque de recirculación. (b) CV 60 g C m^{-3} h^{-1} y riego 1 h cada 4 h: (b.1) fase gas, (b.2) carbono orgánico disuelto en el tanque de recirculación. *Corresponde con la Figura 9-5 del capítulo 9.*

El modelo matemático se utilizó para explicar el comportamiento de un biofiltro percolador instalado para la depuración de las emisiones de COV en aire en una industria de impresión flexográfica **(capítulo 9)**. El turno de fabricación y, por tanto, de emisión contaminada con COV de la industria era de 18 h al día (desde las 6 hasta las 24 h) durante 5 días a la semana. El biofiltro percolador empezó a operar en junio de 2009. Se seleccionaron dos series de datos con diferente patrón de riego y 2 años de diferencia entre ellos (octubre 2009 y enero de 2011). En octubre de 2009 se utilizaba un patrón de riego de 6 min cada 21 min durante todo el día, mientras que en enero de 2011 se utilizaba un patrón de riego de 6 min cada 1 h durante los periodos nocturnos (de 0 a 6 h) y 6 min cada 3 h el resto del tiempo (desde las 6 hasta las 24 h). En contraste con los resultados

experimentales obtenidos en el laboratorio, la concentración de salida del bioreactor presentaba un patrón amortiguado. Durante toda la operación de este biofiltro no se observaba influencia en la emisión de contaminante a la salida de variaciones en la carga volumétrica de contaminante ni del régimen de riego utilizado, sino que se observaba un aumento gradual de la concentración de COV durante las horas de entrada de corriente contaminada al bioreactor. Los datos experimentales indicaron que el biofiltro percolador estaba actuando como un sistema de absorción durante los periodos de entrada de contaminante y como un sistema de desorción durante los periodos de entrada de aire limpio al reactor, respectivamente. Para ilustrar el comportamiento del biofiltro percolador industrial se presenta la Figura 5-9 que corresponde al detalle de los datos experimentales correspondiente un lunes y un martes de enero de 2011, como representativos del patrón de emisión de fuga de contaminante del reactor industrial. En las emisiones de salida del biofiltro percolador se podían distinguir dos situaciones: de martes a viernes (Figura 5-9a) cuando se había producido una interrupción en la producción de la fábrica y, por tanto, una interrupción de suministro de contaminante de 6 h, y, los lunes (Figura 5-9b) cuando se había producido una interrupción en la producción de la fábrica por el fin de semana con entrada de aire limpio de más de 48 horas. De martes a viernes (Figura 5-9a), durante los periodos nocturnos (de 0 a 6 h), se observaba una emisión fugitiva de contaminante que disminuía lentamente. Esto se debía a que 6 horas no eran suficientes para desorber y/o degradar la materia orgánica disuelta acumulada durante los periodos de entrada de contaminante al sistema en el tanque de recirculación y en la biopelícula. Sin embargo, los lunes de 0 a 6 h (Figura 5-9b) la emisión de contaminante a la salida era despreciable, debido a la eliminación completa durante el fin de semana de la materia orgánica disuelta acumulada en el agua del tanque de recirculación y en el interior de la biopelícula. Así mismo, al reanudar la entrada de contaminante al sistema (Figura 5-9b, a partir de las 6 h), la fuga observada durante el tiempo de operación era menor que durante el resto de días a la semana. Esto se debía a que, tras eliminar la materia orgánica disuelta acumulada, la biopelícula era capaz de absorber parte de contaminante en su interior.

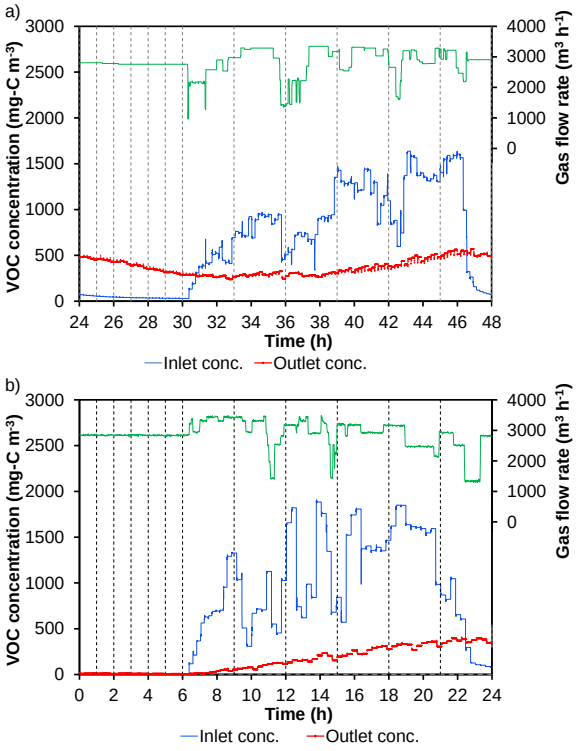

Figura 5-9 Datos experimentales correspondientes al biofiltro percolador industrial para datos correspondiente a enero de 2011. Las líneas de puntos indican riego: (a) martes; (b) lunes. *Adaptada de detalle de la Figura 9-7b del capítulo 9.*

La aplicación del modelo para la simulación del comportamiento del biofiltro percolador industrial se basó en dos hipótesis en relación al proceso a escala de laboratorio. La primera fue que la fase líquida estancada que permanecía en el interior del reactor durante los periodos sin riego ofrecía una resistencia a la transferencia de materia adicional que no se observaba en los biofiltros percoladores de laboratorio (α_2= 1). Este fenómeno fue representado en el modelo mediante dos resistencias en serie (gas–líquido, líquido–biopelícula). La segunda fue que se asumió una biopelícula con un espesor casi 10 veces superior al espesor de la biopelícula de los biofiltros percoladores de laboratorio (500 µm) que actuaba como fuente/sumidero de compuestos orgánicos. A partir de la composición de la mezcla de COV y de las propiedades físicas de los compuestos

individuales (difusividad, constante de Henry) se obtuvieron las propiedades físicas de la mezcla de COV. Los coeficientes globales de transferencia de materia de contaminante fueron estimados para cada velocidad de gas a partir de la correlación propuesta para el isopropanol en el capítulo 7 y se corrigieron utilizando el valor medio ponderado de la constante de Henry con la composición de la corriente de entrada. Para el coeficiente de transferencia de oxígeno se utilizó el valor obtenido preliminarmente (capítulo 8). A fin de representar el incremento de la resistencia a la transferencia de materia de un sistema con biomasa respecto a la transferencia de materia en condiciones abióticas se asumió que ésta se reducía en un factor de 0.23, que era el caso más desfavorable obtenido en el laboratorio. Las simulaciones empezaban con agua limpia en el reactor ya que el sistema venía de trabajar con aire limpio durante un periodo superior a 48h. A modo ilustrativo se presenta la Figura 5-10 donde se muestra la evolución semanal (de lunes a jueves) del biofiltro percolador industrial en una semana representativa en enero de 2011 y el resultado de la aplicación del modelo matemático para la simulación del proceso. El error relativo entre los datos experimentales y los simulados fue inferior a 2.5%. La aplicación del modelo para la simulación de los datos experimentales permitió confirmar que durante las horas de entrada de contaminante al sistema la fracción que no se degradaba se acumulaba en el interior de la biopelícula, mientras que, cuando entraba aire limpio se expulsaba lentamente de la biopelícula, produciendo un efecto de fuente/sumidero.

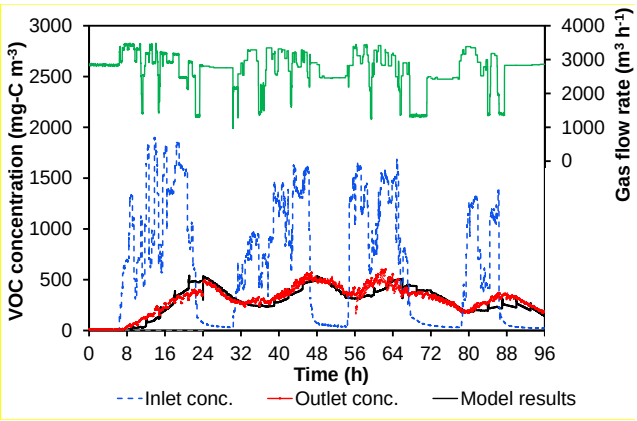

Figura 5-10 Comparación entre los datos experimentales y el modelo dinámico del biofiltro percolador industrial instalado en una industria de impresión flexográfica (enero 2011). *Adaptada de la Figura 9-7b del capítulo 9.*

El modelo matemático se ha integrado en un software mediante el diseño de una interfaz gráfica de usuario utilizando el programa MATLAB® a través del uso de la herramienta GUI **(capítulo 10).** El software es flexible, intuitivo y fácil de utilizar. La interfaz gráfica desarrollada permite el uso de patrones variables de concentración y caudales de gas, incluyendo periodos prolongados sin alimentación de COV, así como la combinación de hasta dos patrones de riego en un mismo periodo de 24 horas. Al terminar las simulaciones, la herramienta ofrece otra interfaz gráfica con los resultados de la simulación: una representación gráfica de las variaciones de la concentración de entrada y de la concentración de salida, y de la variación del carbono orgánico disuelto en el tanque de recirculación. Así cómo los resultados promedio de las concentraciones, de la carga volumétrica y de las capacidades de eliminación.

La herramienta matemática se aplicó para la simulación de los perfiles de concentración de contaminante de la fase gas y de los datos puntuales de concentración de carbono orgánico disuelto en el tanque de recirculación obtenidos durante el estudio de tratamiento de isopropanol llevado a cabo previamente en el capítulo 6 **(capítulo 10)**. Se utilizaron tres perfiles pseudoestacionarios de emisión de contaminante de la fase gas, correspondientes a dos experimentos utilizando una CV de 32 g C m^{-3} h^{-1} y aplicando dos regímenes de riego diferentes (15 min cada 1.5 h y 15 min cada 3 h) y un experimento a CV de 65 g C m^{-3} h^{-1} y régimen de riego de 15 min cada 1.5 h. Para todos los casos se obtuvo un error relativo entre la CE obtenida experimentalmente y la CE simulada menor de 4 %. Este resultado pone de manifiesto la capacidad del modelo para reproducir los perfiles pseudoestacionarios obtenidos en estos experimentos a diferentes condiciones de riego y de carga.

El modelo se utilizó para predecir el comportamiento del proceso de biofiltro percolador bajo diferentes condiciones de operación habituales en la operación de estos sistemas a nivel industrial, como son las variaciones en la concentración de entrada de contaminante y en el caudal de gas producidas por variaciones en el proceso de fabricación. Para ello se estudiaron tres escenarios diferentes. Primero se evaluó la respuesta del biofiltro percolador ante variaciones en las concentraciones de entrada. Al escenario anterior, se le añadió un periodo sin entrada de contaminante y se estudió la influencia de la extensión del régimen de riego a este periodo. En el tercer escenario se evaluó la respuesta del sistema ante variaciones en el caudal de gas. A modo de ejemplo en la Figura 5-11 se muestra la simulación correspondiente a la simulación del biofiltro percolador

utilizando concentraciones oscilantes combinadas con riego intermitente en periodos sin entrada de contaminante. En esta simulación se observa como el patrón de emisión a la salida del reactor depende principalmente del régimen del riego. En esta simulación se observaba, en menor medida, influencia de las variaciones en la entrada de contaminante, produciéndose oscilaciones en la concentración de salida durante estos periodos (Figura 5-11a). Así mismo, se observó cómo variaciones en la concentración de contaminante a la entrada del reactor ocasionaban la absorción y desorción del contaminante en el tanque de recirculación (Figura 5-11b). Esta simulación demostró como el riego en los periodos sin entrada de contaminante al reactor permitía eliminar el COV acumulado, mostrándose como una estrategia efectiva de operación.

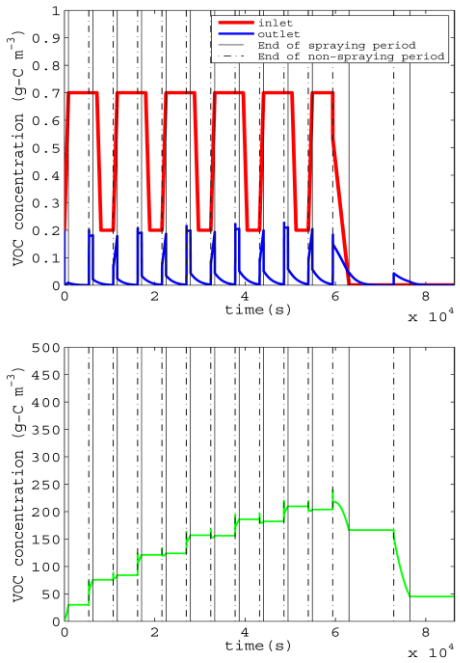

Figura 5-11 Simulación de la respuesta dinámica de un biofiltro percolador sometido a concentraciones oscilantes combinadas con riego intermitente tanto al periodo de aporte de COV como al periodo sin entrada de COV: (a) evolución de la concentración de COV en la fase gas; (b) evolución del carbono orgánico disuelto en el tanque de recirculación. *Corresponde con Figura 10-10 del capítulo 10.*

En general, las simulaciones realizadas demostraron que el efecto en la emisión de contaminante a la salida del reactor de las variaciones en la concentración de entrada y en el caudal está amortiguado por el sistema y están

mínimamente afectados por la acumulación de compuestos orgánicos en el tanque de recirculación. Todo ello pone en evidencia la utilidad del modelo matemático, así como de la interfaz gráfica de usuario que se ha desarrollado en esta tesis, para ayudar en la elaboración de estrategias para el diseño y la optimización de la operación de los biofiltros percoladores.

5.4 BIBLIOGRAFÍA

Kim, S. y Deshusses, M. A. (2008). Determination of mass transfer coefficients for packing materials used in biofilters and biotrickling filters for air pollution control - 2: Development of mass transfer coefficients correlations. *Chemical Engineering Science*, *63*(4), 856–861.

Onda, K., Takeuchi, H. y Okumoto, Y. (1968). Mass transfer coefficients between gas and liquid phases in packed columns. *Journal of Chemical Engineering of Japan*, *1*(1), 56–62.

van Krevelen, D. W. y Hoftijzer, P. J. (1948). Kinetics of simultaneous absorption and chemical reaction. *Chemical Engineering Progress*, *44*, 529–536.

6 BIOTRICKLING FILTRATION OF ISOPROPANOL UNDER INTERMITTENT LOADING CONDITIONS

BIOTRICKLING FILTRATION OF ISOPROPANOL UNDER INTERMITTENT LOADING CONDITIONS

Pau San-Valero, Josep M. Penya-roja, Feliu Sempere & Carmen Gabaldón*

Research Group GI²AM, Department of Chemical Engineering, University of Valencia, Avda. Universitat s/n, 46100 Burjassot, Spain

*Corresponding author: carmen.gabaldon@uv.es

Abstract

This paper investigates the removal of isopropanol by gas-phase biotrickling filtration. Two plastic packing materials, one structured and one random, have been evaluated in terms of oxygen mass transfer and isopropanol removal efficiency. Oxygen mass transfer experiments were performed at gas velocities of 104 and 312 m h^{-1} and liquid velocities between 3 and 33 m h^{-1}. Both materials showed similar mass transfer coefficients up to liquid velocities of 15 m h^{-1}. At greater liquid velocities, the structured packing exhibited greater oxygen mass transfer coefficients. Biotrickling filtration experiments were carried out at inlet loads (IL) from 20 to 65 g C m^{-3} h^{-1} and empty bed residence times (EBRT) from 14 to 160 s. To simulate typical industrial emissions, intermittent isopropanol loading (16 h/day, 5 day/week) and intermittent spraying frequency (15 min/1.5 h) were applied. Maximum elimination capacity of 51 g C m^{-3} h^{-1} has been obtained for the random packing (IL of 65 g C m^{-3} h^{-1}, EBRT of 50 s). The decrease in irrigation frequency to 15 min every 3 h caused a decrease in the outlet emissions from 86 to 59 mg C Nm^{-3} (inlet of 500 mg C Nm^{-3}). The expansion of spraying to night and weekend periods promoted the degradation of the isopropanol accumulated in the water tank during the day, reaching effluent concentrations as low as 44 mg C Nm^{-3}. After a 7-week starvation period, the performance was recovered in less than 10 days, proving the robustness of the process.

Keywords

Biotrickling filter; intermittent loading; isopropanol; oxygen mass transfer; volatile organic compounds

Bioprocess Biosyst Eng (2013) 36:975–984

6.1 INTRODUCTION

Isopropanol is one of the main solvents used in chemical industries, and its manufacture worldwide exceeds 1×10^6 tonnes per year. This results in a significant production of solvent organic wastes, including emissions to the atmosphere as volatile organic compounds (VOC). Since the abatement of VOC is a factor in the protection of the environment and of public health in Europe (European Union, 2010), treatment technologies for VOC removal are required. When emissions are characterised by high flow rates and low VOC concentrations, biotreatments are suitable alternatives to conventional physicochemical technologies and have been classified as best available technologies (BAT) (European Commission, 2003) owing to their low operational costs and the minimisation of negative cross-media effects (Devinny et al., 1999). Compared to a conventional biofilter, a biotrickling filter (BTF) allows better control of the physicochemical parameters, offers a smaller footprint and higher removal rates. The BTF uses an inert packing material and involves the continuous or intermittent trickling of water. In this configuration, the biomass attaches to the media and develops a biofilm; thus, the pollutant and the oxygen must be transferred from the gas phase to the trickling liquid and then to the biofilm, where the biodegradation takes place.

To enhance the performance of the BTF, it is necessary to understand the rate limiting steps of the process. One of the most important limiting factors may be the mass transfer from gas to liquid and biofilm (Barton et al., 1999; Kirchner et al., 1992; Popat and Deshusses, 2010). However, correlations commonly used for absorption in chemical processes do not correctly represent the phenomenon occurring in BTFs due to the different hydrodynamic conditions of chemical absorption. Absorption is marked by higher superficial velocities of the gas and liquid in comparison with BTF (Kim and Deshusses, 2008b). Treatment of hydrophilic compounds such as isopropanol, characterised by low Henry's constants, could typically be limited by oxygen transference. Consequently, oxygen mass transfer should be systematically studied in these cases (Kim and Deshusses, 2008b).

Despite being widely used in industrial and chemical processes, there are no previous studies on the removal of isopropanol by biotrickling filtration. Literature data about the removal of isopropanol by biofilters is also scarce compared with other solvents (Chang and Lu, 2003; Krailas et al., 2004). These

works have been performed under continuous and constant loading; the removal of isopropanol under oscillating and/or discontinuous emissions has not been previously reported. Most gaseous emissions from industrial processes are intermittently generated due to short-time shut-off periods during the night and/or weekends. In fact, previous studies show that the operation of biofiltration under discontinuous VOC feeding regime can produce a degeneration of the system's performance, although the literature in this field is still limited. Cox and Deshusses (2002) reported that non-use periods cause a starvation condition on the microorganisms, which has been identified as one of factors that causes a reduction in pollutant removal. These researchers observed that after 2 days of starvation, the endogenous respiration activity dropped by about 60 % and remained relatively constant thereafter.

The influence of long-term starvation periods, without VOC feeding, also requires further study to advance the applicability of this technology. In our previous work, the reacclimation period, after 3 weeks without VOC feeding, was lower than 24 h working at 60 s of empty bed residence time (EBRT) in a BTF treating a mixture of ethanol, ethyl acetate and methyl-ethyl ketone (MEK), and operating under discontinuous loading (Sempere et al., 2008).

The purpose of the present study was to investigated the removal of isopropanol using a BTF, taking into consideration the following objectives: (1) to determine the oxygen mass transfer coefficient of a structured and a random packing material, establishing a relationship between the mass transfer coefficient, the trickling flow rate and the specific surface area; (2) to compare the performance of the process, in terms of EC and RE, under isopropanol discontinuous loading conditions at several EBRT by using two BTFs operating in parallel, one filled with the structured and the other with the random material; (3) to evaluate the influence of spraying frequency on the RE, and (4) to evaluate the response of the BTFs to a long-term starvation period representative of a holiday closure at an industrial site.

6.2 MATERIALS AND METHODS

6.2.1 Experimental setup for the determination of oxygen mass transfer

The system consisted of a column of methacrylate (14.4 cm internal diameter, 80 cm height) and a recirculation tank (10 L of water volume). The schematic of the experimental setup is shown in Figure 6-1. The column was filled with two inert packing materials: a novel plastic cross-flow structured packing material (Odourpack, Pure Air Solution, The Netherlands) with 410 m^2 m^{-3} specific surface area and a random packing material (Refill-Tech, Italy) consisting of polypropylene rings with a nominal diameter of 5/8 in. and a specific surface area of 348 m^2 m^{-3}. The packing height was 20 cm for the structured packing and 40 cm for the rings. The air stream (compressed, filtered and dried) was introduced through the bottom of the columns, with the flow rate adjusted using a mass flow controller (Bronkhorst Hi-Tec, The Netherlands). The experiments were carried out at two air superficial velocities of 104 and 312 m h^{-1}. The trickling water was recirculated using a centrifugal pump (HPR10/ 15, ITT, Great Britain) in counter-current mode with respect to the air flow rate, with a superficial velocity of the water between 3 and 33 m h^{-1}. The equipment is completed with a dissolved oxygen probe (Cellox® 325i, WTW, Germany). An internal pump installed in the recirculation tank ensured the ideal mixing condition. The experiments were carried out at room temperature (21.2 ± 0.7 °C).

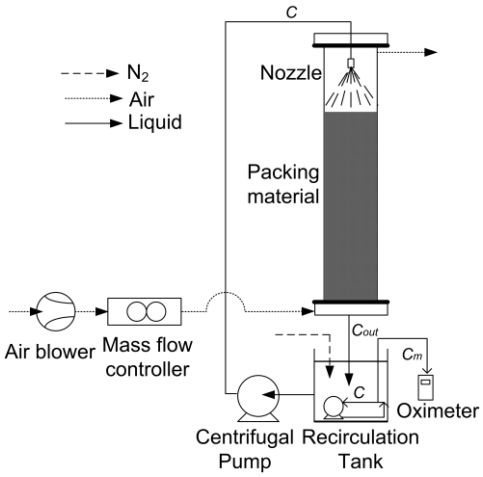

Figure 6-1 Schematic of the experimental setup for the determination of k_La.

For the determination of k_La, a dynamic method under inert conditions was used. The method consists of measuring the increase in the oxygen concentration with time in a tank in which the oxygen has been previously displaced by bubbling nitrogen gas. The experiment starts when the air blower and the recirculation pump are switched on; oxygen is transferred from the air to the water in the packed column causing an increase in the dissolved oxygen concentration in the recirculation tank. Under these conditions, oxygen mass balances are as follows:

- In the packed column:

$$C_{out} = C^* - \frac{C^* - C}{\exp(\frac{L}{v} k_L a)} \tag{6-1}$$

where C_{out} is the predicted dissolved oxygen concentration at the bottom of the column, C is the predicted dissolved oxygen concentration in the recirculation tank, C^* is the oxygen solubility and L and v are the height of the column and the velocity of the trickling water, respectively.

- In the tank:

$$\frac{dC}{dt} = \frac{1}{\theta}\left(C_{out} - C\right) \tag{6-2}$$

where θ is the residence time in the tank.

The combination of Eqs. (6-1) and (6-2) permits obtaining the variation of the predicted oxygen concentration with time:

$$\frac{dC}{dt} = \frac{1}{\theta}\left(C^* - \left(\frac{C^* - C}{\exp(\frac{L}{v} k_L a)} - C \right) \right) \tag{6-3}$$

Because the dynamics of the probe is not fast enough, it is necessary to take into account the response time constant of the probe, τ, defined as time that the probe achieves 63 % of the end value measured when the probe is subjected to a step input assay (Van't Riet, 1979). The response time of the probe was determined by transferring the oxygen probe from an ideal mixed tank in which

the dissolved oxygen concentration was displaced by bubbling nitrogen gas to a second tank which is saturated with dissolved oxygen. A first-order dynamic was assumed according to Eq. (6-4) (Weiland and Onken, 1981).

$$\frac{dC_m}{dt} = \frac{(C - C_m)}{\tau} \tag{6-4}$$

where C_m is the measured dissolved oxygen concentration in the recirculation tank by the oxygen probe.

The value of k_La of the packed column was calculated by minimising the sum of squares of the difference between the measured data recorded for dissolved oxygen concentration in the recirculation tank and the value obtained from the mathematical resolution of Eqs. (6-3) and (6-4).

6.2.2 Experimental setup for the removal of isopropanol

The experiment was performed using two identical laboratory-scale BTFs operating in parallel, named BTF1 and BTF2. The experimental setup is shown in Figure 6-2. Each bioreactor was composed of three cylindrical methacrylate modules in series, with a total bed length of 100 cm and an internal diameter of 14.4 cm. BTF1 was filled with the structured material and BTF2 with the random packing, in each using a volume of 16.32 L. The bioreactors were also provided with 20 cm of top and bottom free spaces. The stream contaminated with isopropanol was introduced through the bottom of the column of the BTFs. A recirculation solution of 3 L, partially renewed every week, was fed into the bioreactor in counter-current mode with respect to the air flow using a centrifugal pump at 2.5–3 L min^{-1}. A nutrient solution buffered at pH 7 (21.65 g KNO_3 L^{-1}, 4.6 g $Na_3PO_4 \cdot 12H_2O$ L^{-1} and Ca, Fe, Zn, Co, Mn, Na, Ni, B, I, Se, Cr, Cu and vitamins at trace doses) was supplied to the recirculation tank using a peristaltic pump. The nutrient solution flow rate was set to maintain a supplied mass ratio of carbon and nitrogen (C/N) of 35, in order to assure that the nitrogen concentration in the recirculation solution was not limiting the biodegradation process. C/N mass ratios between 13 and 70 are suggested in the literature for the operation of bioreactors (Kennes et al., 2009).

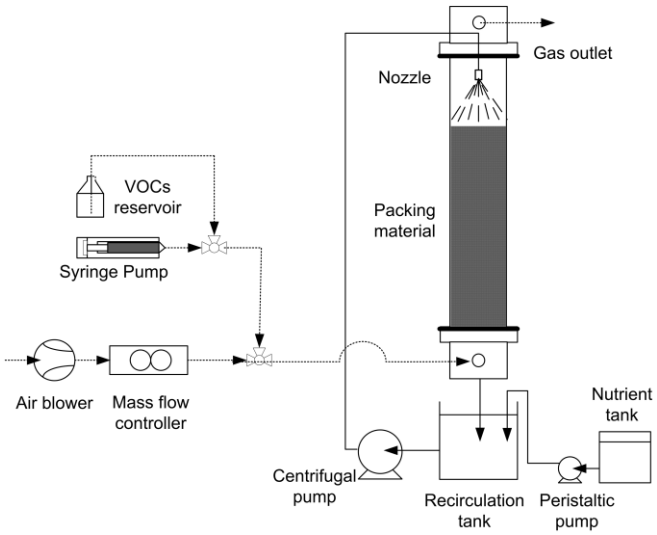

Figure 6-2 Schematic of the experimental setup for the elimination of isopropanol.

6.2.3 Influence of IL and EBRT on the removal of isopropanol

The operation of the bioreactors to determine the influence of IL and EBRT on the removal of isopropanol was structured in three phases (A, B, C) of a twofold step decrease in inlet concentration. Phase A started with 1000 mg C Nm^{-3}. For each phase, several 1.8-fold IL step increases were carried out, resulting in EBRTs from 15 to 160 s. The design parameters of the experiments are summarised in Table 6-1. Intermittent feeding of VOC was programmed to simulate shift working conditions, which consisted of a regime of a period with VOC feeding of 16 h per day (from 6 to 22 h) for 5 days a week, and night and weekend periods without VOC supply. The air flow rate was kept constant during both periods. Water was trickled for 15 min every 1.5 h during the VOC feeding period. During non-VOC feeding periods, the trickling of water was stopped.

Table 6-1 Experimental plan for the removal of isopropanol under intermittent loading conditions.

	Days	C_{in} (mg C Nm^{-3})	*IL* (g C $m^{-3}h^{-1}$)	*EBRT* (s)
Phase A				
A–I	0 – 48	1000	20	160
A–II	49 – 69	1000	35	90
A–III	70 –90	1000	65	50
Phase B				
B–I	91– 97	500	20	90
B–II	98–104	500	35	50
B–III	105 – 125	500	65	25
Phase C				
C–II	126 – 132	250	35	25
C–III	133 – 163	250	65	14

6.2.4 Influence of spraying frequency on the removal of isopropanol

The influence of the spraying frequency on the global performance of the system was evaluated by testing several patterns at an IL of 30 g C m^{-3} h^{-1} and EBRT of 60 s on the random packing material. Three frequency regimes were tested. Two of them were only applied during VOC feeding (16 h per day, 5 days per week) with trickling water frequencies of 15 min every 1.5 h or 15 min every 3 h; spraying was stopped during the night and weekend periods. The expansion of spraying to the non-VOC feeding periods was tested by trickling 15 min every 3 h over the whole day (24 h per day, 7 days per week).

6.2.5 Influence of long-term starvation on the removal of isopropanol

The influence of a long period without VOC feeding on the performance of the BTF was evaluated by stopping the supply of isopropanol for a period of 7 weeks. During this time, the air flow rate was maintained at an EBRT of 60 s and the water trickling was set to 15 min per day, to provide the minimum amount of nutrients and moisture that assures biomass viability. After that, the supply of isopropanol was restored using the same discontinuous VOC feeding mode (16 h per day, 5 days per week) that was applied before the VOC interruption; IL of 35 g C m^{-3} h^{-1}, EBRT of 60 s and a trickling water frequency of 15 min every 4 h were set.

6.2.6 Analytical methods

The oxygen concentration in the liquid was determined using a dissolved oxygen probe (Cellox® 325i, WTW, Germany). The concentration of isopropanol was measured using a total hydrocarbon analyser (Nira Mercury 901, Spirax Sarco, Spain). The response factor of the total hydrocarbon analyser was determined by gas chromatograph (model 7890, Agilent Technologies, EEUU). The CO_2 concentration was analysed using a nondispersive infrared carbon dioxide analyser (GMP222, Vaisala, Finland). The inlet and outlet gas streams were monitored daily. The pressure drop was monitored daily (MP101, KIMO Instruments, Spain). To determine the quality of the recirculation solution, conductivity and pH (ph/Cond 340i, WTW, Germany), soluble chemical oxygen demand (COD), nitrate and suspended solids (SS) concentrations were measured prior to the weekly purge. Soluble COD and nitrate concentrations were measured using Merck Speqtroquant kits (Merck KGaA, Germany): 114540 (COD) and 114773 (nitrate). The SS concentrations were determined according to the Standard Methods for Examination of Water and Wastewater (American Public Health Association et al., 1998).

6.3 RESULTS AND DISCUSSION

6.3.1 Determination of oxygen mass transfer coefficients

The determination of oxygen mass transfer coefficients was carried out for the two packing materials at several liquid velocities. The k_La coefficients were obtained using the least squares method to minimise the differences between the experimental data and the concentration of oxygen provided by the simple mathematical model established by Eqs. (6-3) and (6-4). The response time of the probe (τ) was determined earlier by means of a step input assay, resulting in a value of 19.4 ± 1.5 s. The effect of liquid velocity on mass transfer is shown in Figure 6-3. The two packing materials presented a relationship between the liquid flow rate and the k_La values for a gas velocity of 104 m h^{-1} with similar values up to 15 m h^{-1}. For liquid velocities higher than this value, the structured material showed greater values of k_La. That difference cannot be explained by the slightly higher specific surface area of this material alone, but it could be attributed to the different air and water flow paths in both materials. Selecting a liquid velocity of 10 m h^{-1} as representative of the operation of the BTFs in this study, a k_La approximately of 45 h^{-1} was obtained for both packing materials, without

differences between them. The values obtained herein are of the same order of magnitude as those found by Kim and Deshusses (2008b) in previous papers. These authors reported a value of about 25 h^{-1} for liquid velocities around 10 m h^{-1} using 1 in. Pall rings (210 m^2 m^{-3}). These authors showed that Onda's correlation overestimated the k_La values on biotrickling filtration by a factor of about 20 (Kim and Deshusses, 2008a), indicating the need for determining oxygen mass transfer in the typical range of velocities of biotreatments.

The influence of gas velocity on the oxygen mass transfer coefficients was determined with an additional test conducted at a gas velocity of 312 m h^{-1}. As an example, the results obtained for the structured packing material are shown in Figure 6-4. As can be expected, these experiments demonstrated that k_La values were not significantly affected by gas velocities in the typical values of operation of BTFs.

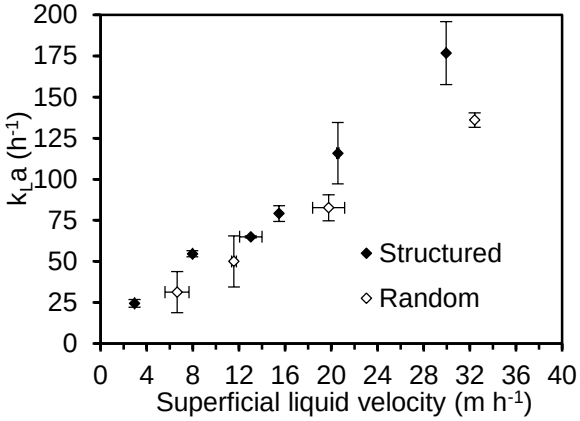

Figure 6-3 Influence of superficial liquid velocity on the oxygen mass transfer coefficient in BTFs.

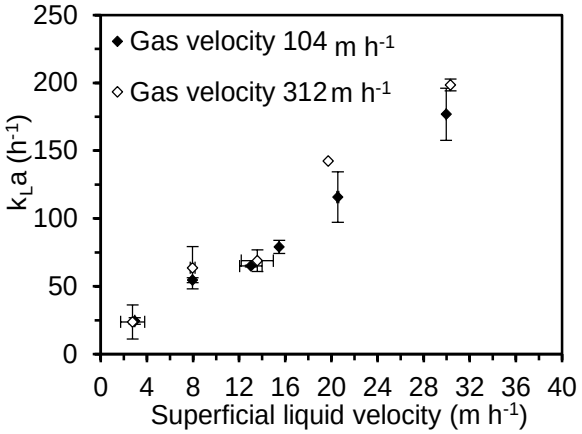

Figure 6-4 Influence of superficial gas velocity on the oxygen mass transfer coefficient for the structured packing material.

6.3.2 Influence of inlet load and EBRT on the removal of isopropanol

The influence of inlet load on the removal of isopropanol in terms of EC and RE was evaluated. To simulate the emissions of industrial facilities, an intermittent VOC loading regime and a discontinuous trickling pattern were used. As an example, 24 h of a typically daily evolution of VOC concentration in the outlet gas stream of the BTF2 is shown in Figure 6-5. This figure represents the outlet emission pattern for two different stages where inlet concentrations of 1000 mg C Nm^{-3} (IL of 65 g C m^{-3} h^{-1}, stage A-III, Figure 6-5a) and 500 mg C Nm^{-3} (IL of 35 g C m^{-3} h^{-1}, stage B-II, Figure 6-5b) were applied. As can be observed, the operating regime resulted in peaks of concentration coinciding with the irrigation of the bed (15 min every 1.5 h). These peaks are related to the accumulation of the pollutant in the trickling water and subsequent desorption when trickling starts, resulting in outlet emission peaks. The comparison between both stages shows the influence of loading in the emission pattern. In the periods between trickling, a complete removal of pollutant was achieved for the lowest loading condition (Figure 6-5b), while leakage of pollutant occurred for the highest load (Figure 6-5a).

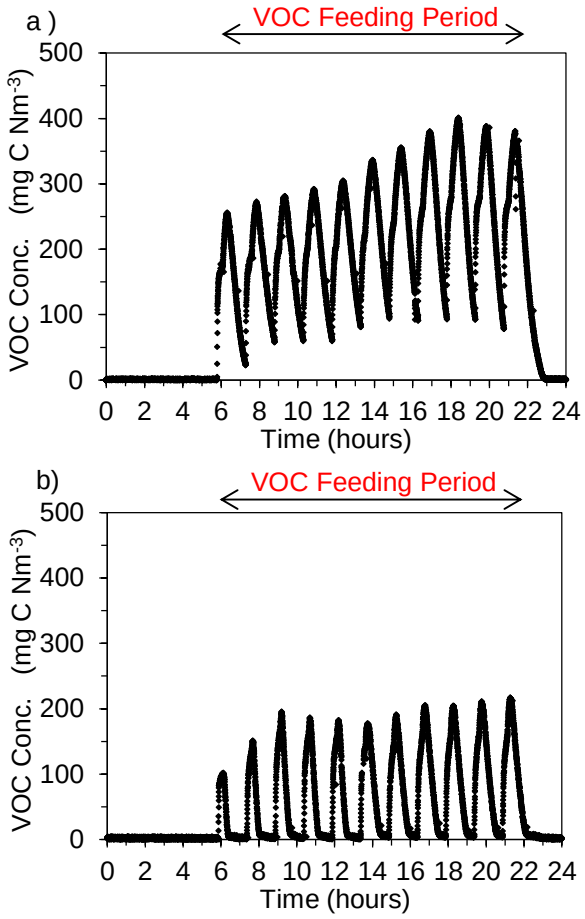

Figure 6-5 Outlet pattern emission during 24 h monitoring of the biotrickling filtration of isopropanol under intermittent loading conditions for BTF2: a) phase A-III; b) phase B-II.

The monitoring of the quality of the trickling water was carried out twice per week for the whole experimental period. The average values along with the standard deviation are shown in Table 6-2. As shown in Table 6-2, the pH and conductivity were kept at normal values for the development of the biological process during the whole period. Nitrate in the water tank was kept above 10 mg N L^{-1} making sure that nutrients were not limiting the bioprocess. Soluble COD values ranged between 700 and 1800 mg COD L^{-1} depending on the loading conditions. The operational protocols regarding the quality of the

trickling water included a weekly purge of 1.5 L of water. In all cases, solvent removal with the purge represents less than 5 % of the total amount of fed isopropanol during the week. In consequence, the organic carbon in the purge was considered negligible for evaluation of the BTF performance in terms of inlet load (IL), elimination capacity (EC) and removal efficiency (RE). About suspended solids, concentrations higher than 500 mg L^{-1} were only observed since month 3, indicating that significant detachment of solids from the packing materials started as the biofilm thickened. Average values of the suspended solids concentration from day 90 until the end of the experimentation period resulted in 3151 and 1022 mg L^{-1} for BTF1 and BTF2, respectively. The higher suspended solid concentrations in BTF1 than in BTF2 can be associated with the capability of the structured packing material to drag the biomass, in comparison with the random packing where biomass is detached with greater difficulty. In both bioreactors, the pressure drop was kept below 48 Pa m^{-1}, indicating that nonexcessive accumulation of biomass occurred. The accumulation of acetone as an intermediate product was not observed.

Table 6-2 Quality of trickling water during the whole experiment.

	BTF1		BTF2	
	Average	SD	Average	SD
pH	8.91	0.23	9.01	0.23
Conductivity (mS cm^{-1})	5.22	1.33	5.23	1.14
Nitrate conc.(mg N L^{-1})	30	23	38	33
Soluble COD (mg L^{-1})	1200	498	1107	540

To quantify the outlet concentration of VOC, the most unfavourable conditions were selected. So, the average values of the previous 7 h during VOC feeding (from 15 to 22 h: last five spraying cycles) was used. The performance of BTF1 and BTF2 is shown in Figure 6-6a, b, respectively. A similar evolution of both BTFs during the whole experiment was observed. The start-up was carried out using activated sludge from the secondary clarifier of the municipal wastewater treatment plant of Carlet (Spain). In order to simulate the procedure of the industrial BTFs, the inoculum was not previously adapted to degrade isopropanol. The systems were started by setting an EBRT of 160 s for BTF1 and 152 s for BTF2 and an inlet concentration of 1000 mg C Nm^{-3} (phase A-I, day 0–48). After 4–6 days of operation, REs of 70 % were obtained. After that the performance was stable, with REs around 80 % for both BTFs. On day 49 (phase A-II) and on day 70 (phase A-III) the EBRT was

consecutively decreased to 90 and 50 s, increasing the IL to 35 and 65 g C m^{-3} h^{-1}, respectively. During these stages, both BTFs presented similar variability in their performance with REs ranging between 60 and 85 %. In phase B, an inlet concentration of 500 mg C Nm^{-3} was set. REs greater than 90 % were achieved by applying ILs of 18 (phases B-I, days 91–97) and 33 g C m^{-3} h^{-1} (phase B-II, days 98–104). In phase B-III (days 105–125), with an IL of 64 g C m^{-3} h^{-1}, the REs significantly decreased to 60–70 %. Finally, the inlet concentration applied in phase C was 250 mg C Nm^{-3}. Working with an IL of 37 g C m^{-3} h^{-1} for BTF1, and 39 g C m^{-3} h^{-1} for BTF2 (days 126–132), high REs with values around 80 % for BTF1 and 88 % for BTF2 were observed. When the IL was increased to 65 g C m^{-3} h^{-1} (days 133–163), the performance of the BTFs decreased to reach an RE of 49 % for BTF1 and 60 % for BTF2, coinciding with the minimum EBRT applied (14 s).

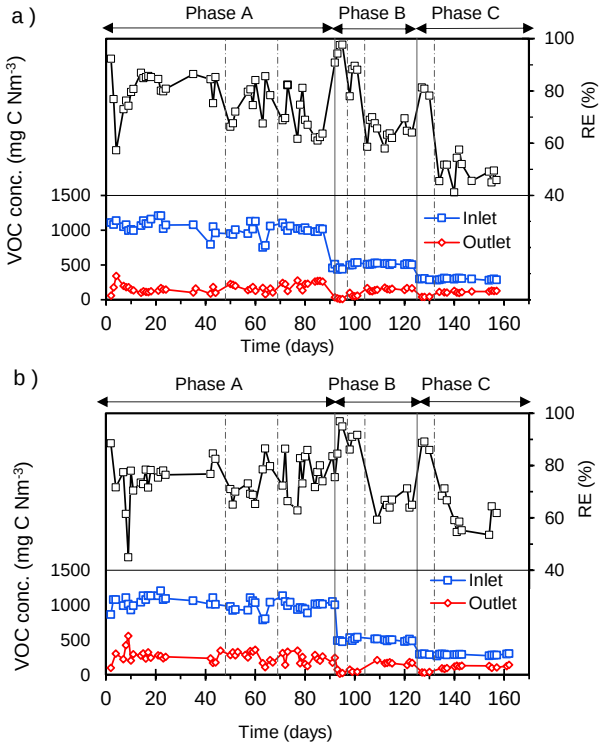

Figure 6-6 Performance of the BTFs on the removal of isopropanol. The *discontinuous line* represents a 1.8 step increase in the inlet load. a) BTF1; b) BTF2.

The elimination capacity versus the inlet load is presented in Figure 6-7 for the different EBRTs (BTF1 in Figure 6-7a and BTF2 in Figure 6-7b). Both BTF performed near complete degradation up to a critical IL of 30 g C m^{-3} h^{-1} for all tested inlet concentrations (EBRT > 25 s). Maximum ECs of 44.7 ± 5.3 and 50.8 ± 3.4 g C m^{-3} h^{-1} were obtained for BTF1 and BTF2, respectively (IL of 65 g C m^{-3} h^{-1} and EBRT of 50 s).

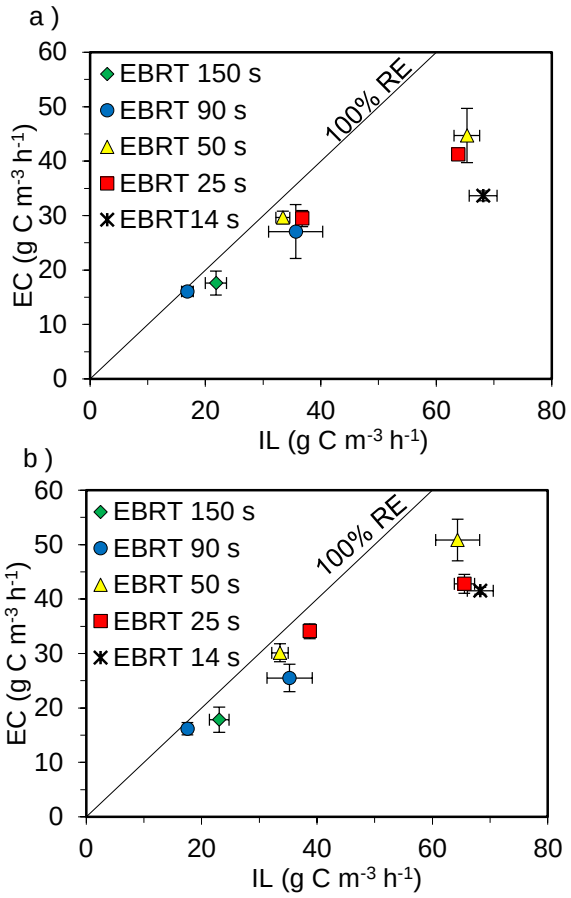

Figure 6-7 Isopropanol elimination capacity versus inlet load: a) BTF1; b) BTF2.

No data related to the biodegradation of isopropanol under intermittent loading conditions have previously been published in the literature. Previous studies on the removal of isopropanol under continuous loading conditions are also scarce and correspond with biofilters and trickled bed biofilters. Chang and Lu (2003) found ECs between 45–89 g C m^{-3} h^{-1} for

isopropanol loadings of 50–90 g C m^{-3} h^{-1} with EBRT of 20–30 s. Krailas et al. (2004) reported a maximum isopropanol elimination capacity of 276 g m^{-3} h^{-1} (equivalent to 165 g C m^{-3} h^{-1}) and an acetone production rate of 56 g m^{-3} h^{-1} (equivalent to 35 g C m^{-3} h^{-1}) at an inlet load of 342 g m^{-3} h^{-1} (equivalent to 204 g C m^{-3} h^{-1}) using a biofilter. As can be seen, data reported in the present study show lower values of EC than those from the literature, due to the discontinuous operation used to mimic an industrial pattern. Results can also be compared with the removal of other hydrophilic compounds by biotrickling filtration, such as ethanol. Working under continuous loading conditions, Cox et al. (2001) found a critical IL of 70 g ethanol m^{-3} h^{-1} (equivalent to 37 g C m^{-3} h^{-1}) at an EBRT of 57 s, and Morotti et al. (2011) determined a maximum EC of 46 g ethanol m^{-3} h^{-1} (equivalent to 24 g C m^{-3} h^{-1}) using an EBRT of 66 s and an inlet concentration of 1100 mg ethanol m^{-3}. Working under intermittent loading conditions, there are limited studies with BTF. In our previous work (Sempere et al., 2009), a maximum EC of 48.5 g C m^{-3} h^{-1} was obtained with an IL of 70.5 g C m^{-3} h^{-1} and an EBRT of 40 s, treating a mixture 1:1 of ethyl acetate and ethanol working with fluctuating conditions for 12 h per day, 5 days at week using 1″ polypropylene rings as the packing material. Thus, the data presented in the present work are comparable with those previously reported for the fluctuating conditions of other oxygenated solvents, showing the capability of the system to adapt itself to the typical operation of industrial facilities characterised by discontinuous VOC emissions.

The variation in the rate of carbon dioxide production with its elimination capacity is shown in Figure 6-8a, b for BTF1 and BTF2, respectively. No significant differences were obtained between the bioreactors. An average yield of 0.25 ± 0.09 and 0.29 ± 0.09 g C-CO_2 produced per g C degraded for BTF1 and BTF2 was obtained during the entire experiment, respectively. These values are similar to the data in the literature on treating oxygenated compounds. Sempere et al. (2008) obtained an average yield coefficient between 0.18 and 0.40 g C-CO_2 produced per g C degraded treating a mixture of ethanol, ethyl acetate and methyl-ethyl ketone. Other researchers reported carbon mineralisation between 17 % (Morotti et al., 2011) and 46 % (Cox et al., 2001) on treating ethanol.

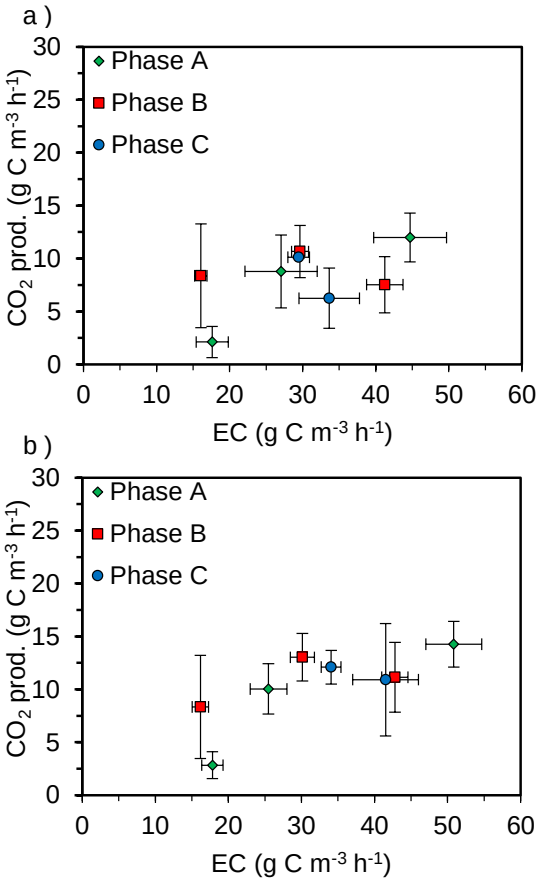

Figure 6-8 Production of carbon dioxide versus elimination capacity of isopropanol: a) BTF1, b) BTF2.

6.3.3 Influence of spraying frequency on the removal of isopropanol

As discussed previously, the discontinuous regime of the spraying of the bed resulted in emissions of isopropanol during irrigation, increasing the average outlet concentrations in the emission. A minimum irrigation is required to supply the nutrients, but, due to the high solubility of non-degraded isopropanol in water, the accumulation in the trickling liquid caused a fugitive emission that could be minimised by optimising the frequency of the spraying. The effect of this variable on the average outlet concentration was evaluated for the random packing material. Three regimes of spraying were applied at IL of 32 g C m^{-3} h^{-1} and EBRT of 60 s. Figure 6-9a, b shows the results of spraying for 15 min every 1.5 h and every

3 h, respectively, only during the VOC feeding period (16 h per day). Figure 6-9c corresponds to a continuous trickling of 15 min every 3 h over a 24 h period, including the period without VOC.

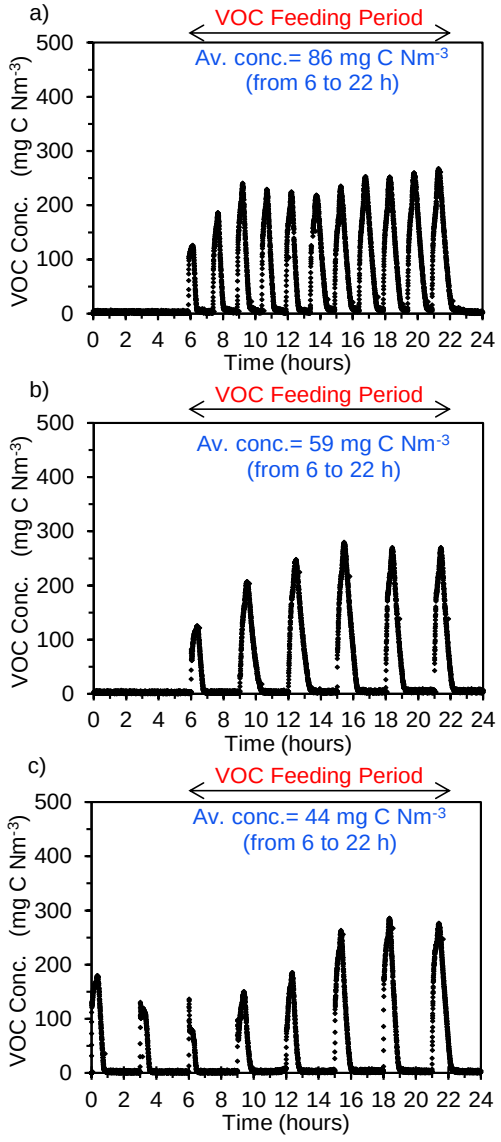

Figure 6-9 Influence of the spraying regime on the outlet pattern emission: a) spraying for 15 min every 1.5 h during VOC feeding period; b) spraying for 15 min every 3 h during VOC feeding period; c) 15 min every 3 h during 24 h.

From Figure 6-9a, b, it can be observed that by decreasing the spraying frequency per day it was possible to reduce the average daily outlet concentration from 86 to 59 mg C Nm^{-3} during the VOC feeding period. This decrease in the average daily outlet concentration is related to the fewer peaks of the spraying pattern of 15 min every 3 h. The expansion of spraying at nights (Figure 6-9c) caused a decrease in the average outlet emission from 59 to 44 mg C Nm^{-3} during the isopropanol feeding period. Spraying during non-VOC feeding periods facilitated the VOC transfer to the biofilm and thus enhanced the degradation of the accumulated isopropanol in the water tank. Therefore, the transfer from water to the air during spraying decreases. These results indicated that for the removal of hydrophilic compounds, the spraying frequency is a critical parameter to achieve low emissions under discontinuous and oscillating patterns.

6.3.4 Influence of long-term starvation on the removal of isopropanol

The BTFs were submitted to a starvation period to simulate a holiday industrial closure, to evaluate their response after restoring VOC feeding. During the long-term starvation, the air flow rate was maintained at an EBRT of 60 s, and water trickling was set to 15 min per day to assure biomass viability conditions. The BTFs were kept under these conditions for up to 7 weeks. The VOC feeding was restored using the same intermittent pattern of 16 h per day that was applied before the VOC interruption. An IL of around 35 g C m^{-3} h^{-1}, EBRT of 60 s and a trickling water of 15 min every 4 h was set. The monitoring of the inlet and outlet VOC concentrations of BTF1 and BTF2 is presented in Fig. 10a, b, respectively, once the VOC feeding was restored. As can be observed, REs of 80 % were obtained 5 days after the re-start up for both BTFs. After 10 days of operation, both BTFs achieved REs of 90 %, similar values to those obtained in phase B-II, indicating that the performance of the two bioreactors was fully recovered. These results show that the bacterial population can survive with endogenous metabolism for more than 7 weeks if proper adequate operational conditions are adjusted. Zhang and Bishop (2003) suggested that extracellular polymeric substances can be a substrate during starving periods. Shorter starvation periods have also been tested on the degradation of other compounds in BTFs. Sempere et al. (2008) reported on the successful reacclimation of a BTF degrading a mixture of oxygenated compounds after a 3-week starvation period. Cox and Deshusses (2002) found a great reactivation of toluene-degrading BTFs after periods of 2–9 days without VOC feeding. The long starvation period tested in this study is of interest due to the fact it has never previously been applied in

biotrickling filtration. It demonstrates the sturdiness of the biofiltration techniques to adapt to conditions found in industrial facilities, avoiding the necessity for system re-inoculation with the subsequent saving of costs.

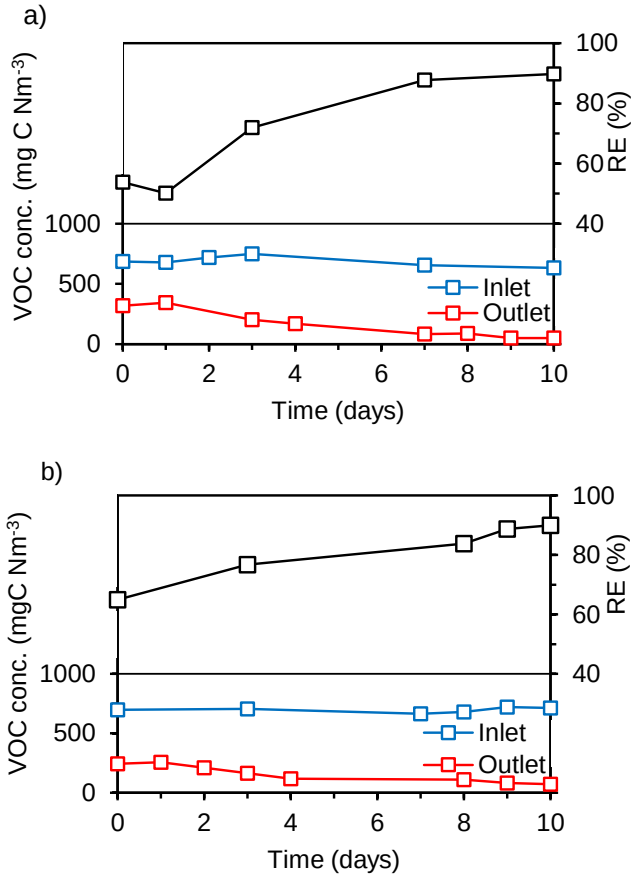

Figure 6-10 Performance of the BTFs on the removal of isopropanol after 7 weeks of starvation: a BTF1; b BTF2.

6.4 CONCLUSIONS

The removal of isopropanol in two biotrickling filters with two packing materials of similar specific surface area, one structured and one random, was investigated. Oxygen mass transfer coefficients were determined, showing similar values for liquid velocities up to 15 m h^{-1} at gas velocities of 104 and 312 m h^{-1}. At

higher liquid velocities, the structured packing material showed a greater mass transfer coefficient attributed to the different air and water flow paths in both materials. Biotrickling filtration has been shown as an effective technology for the removal of isopropanol in waste gases under intermittent loading conditions (16 h per day, 5 days per week), typical of industrial sites with night and weekend shut-offs. Stable performance has been obtained with complete removal up to an inlet load of 30 g C m^{-3} h^{-1}. At high loads, the random packing material showed a slightly higher removal capacity. Due to the low Henry coefficient of isopropanol, it tends to accumulate in the water tank, causing a peak in the outlet emission during intermittent spraying. Thus, this fact indicates that the frequency of irrigation is a crucial parameter to achieve low emissions under intermittent loading of highly soluble compounds. Outlet emissions were reduced by half by decreasing the spraying frequency during isopropanol feeding and expanding the irrigation to nights and weekends. This strategy allows the minimisation of peak emissions from liquid-mass transfer during isopropanol feeding periods and promotes the biodegradation of isopropanol accumulated in water during nonfeeding periods. A fast re-start-up after a 7-week starvation period, one of the longest reported, corroborated that biotrickling filtration of soluble compounds under intermittent loading is a robust technology for industrial applications.

Acknowledgments

The research leading to these results has received funding from the People Programme (Marie Curie Actions) of the European Union's Seventh Framework Programme FP7/2007-2013/under REA grant agreement no. 284949. Financial support from the Ministerio de Ciencia e Innovación (Project CTM2010-15031/ TECNO) and Generalitat Valenciana (ACOMP/2012/209), Spain, is also acknowledged. Pau San-Valero acknowledges the Generalitat Valenciana, Spain (ACIF/2011/067 contract).

6.5 REFERENCES

American Public Health Association, American Water Works Association and Water Environment Federation. (1998). *Standard Methods for the Examination of Water and Wastewater*. (L. S. Clesceri, A. E. Greenberg, and A. D. Eaton, Eds.). Washington.

Barton, J. W., Davison, B. H., Klasson, K. T. and Gable, C. C. (1999). Estimation of mass transfer and kinetics in operating trickle-bed bioreactors for removal of VOCs. *Environmental Progress*, *18*(2), 87–92.

Chang, K. S. and Lu, C. S. (2003). Biofiltration of isopropyl alcohol by a trickle-bed air biofilter. *Biodegradation*, *14*(1), 9–18.

Cox, H. H. J. and Deshusses, M. A. (2002). Effect of starvation on the performance and re-acclimation of biotrickling filters for air pollution control. *Environmental Science & Technology*, *36*(14), 3069–3073.

Cox, H. H. J., Sexton, T., Shareefdeen, Z. M. and Deshusses, M. A. (2001). Thermophilic biotrickling filtration of ethanol vapors. *Environmental Science & Technology*, *35*(12), 2612–2619.

Devinny, J. S., Deshusses, M. A. and Webster, T. S. (1999). *Biofiltration for Air Pollution Control*. Boca Raton, USA: CRC-Lewis Publishers.

European Union. (2010). *Directive 2010/75/EU of the European Parliament and of the council of 24 November 2010 on industrial emissions (integrated pollution prevention and control) (Recast)*. *Official Journal of the European Union* (Vol. L334).

European Commission. (2003). *IPPC Reference Document on Best Available Techniques in Common Waste Water and Waste Gas Treatment/Management Systems in the Chemical Sector*. (E. I. Bureau, Ed.). Sevilla.

Kennes, C., Rene, E. R. and Veiga, M. C. (2009). Bioprocesses for air pollution control. *Journal of Chemical Technology and Biotechnology*, *84*(10), 1419–1436.

Kim, S. and Deshusses, M. A. (2008a). Determination of mass transfer coefficients for packing materials used in biofilters and biotrickling filters for air pollution control -2: Development of mass transfer coefficients correlations. *Chemical Engineering Science*, *63*(4), 856–861.

Kim, S. and Deshusses, M. A. (2008b). Determination of mass transfer coefficients for packing materials used in biofilters and biotrickling filters for air pollution control. 1. Experimental results. *Chemical Engineering Science*, *63*(4), 841–855.

Kirchner, K., Wagner, S. and Rehm, H. J. (1992). Exhaust-gas purification using biocatalysts (fixed bacteria monocultures) -the influence of biofilm diffusion rate (O_2) on the overall reaction-rate. *Applied Microbiology and Biotechnology*, *37*(2), 277–279.

Krailas, S., Tongta, S. and Meeyoo, V. (2004). Macrokinetic determination of isopropanol removal using a downward flow biofilter. *Songklanakarin Journal Science Technology*, (26 (Suppl. 1)), 55–64.

Morotti, K., Ramirez, A. A., Jones, J. P. and Heitz, M. (2011). Analysis and

comparison of biotreatment of air polluted with ethanol using biofiltration and biotrickling filtration. *Environmental Technology*, *33*(15-16), 1967–1973.

Popat, S. C. and Deshusses, M. A. (2010). Analysis of the rate-limiting step of an anaerobic biotrickling filter removing TCE vapors. *Process Biochemistry*, *45*(4), 549–555.

Sempere, F., Gabaldón, C., Martínez-Soria, V., Marzal, P., Penya-roja, J. M. and Álvarez-Hornos, F. J. (2008). Performance evaluation of a biotrickling filter treating a mixture of oxygenated VOCs during intermittent loading. *Chemosphere*, *73*(9), 1533–1539.

Sempere, F., Gabaldón, C., Martínez-Soria, V., Penya-roja, J. M. and Álvarez-Hornos, F. J. (2009). Evaluation of a combined activated carbon prefilter and biotrickling filter system treating variable ethanol and ethyl acetate gaseous emissions. *Engineering in Life Sciences*, *9*(4), 317–323.

Van't Riet, K. (1979). Review of Measuring Methods and Results in Nonviscous Gas-Liquid Mass Transfer in Stirred Vessels. *Industrial & Engineering Chemistry Process Design and Development*, *18*(3), 357–364.

Weiland, P. and Onken, U. (1981). Fluid dynamics and mass transfer in an airlift fermenter with external loop. *German Chemical Engineering*, *4*, 42–50.

Zhang, X. Q. and Bishop, P. L. (2003). Biodegradability of biofilm extracellular polymeric substances. *Chemosphere*, *50*(1), 63–69.

7 MODELLING MASS TRANSFER PROPERTIES IN A BIOTRICKLING FILTER FOR THE REMOVAL OF ISOPROPANOL

MODELLING MASS TRANSFER PROPERTIES IN A BIOTRICKLING FILTER FOR THE REMOVAL OF ISOPROPANOL

Pau San-Valero, Josep M. Penya-roja, F. Javier Álvarez-Hornos & Carmen Gabaldón*

Research Group GI²AM, Department of Chemical Engineering, University of Valencia, Avda. Universitat s/n, 46100 Burjassot, Spain

*Corresponding author: carmen.gabaldon@uv.es

Abstract

A study was carried out to model mass transfer properties in biotrickling filters, treating isopropanol as the target pollutant. This study was extended to the mass transfer of oxygen related to the fact that the treatment of hydrophilic compounds by biotrickling filtration is often limited by oxygen. A simple method for each compound was developed based on their physical properties. The influence of temperature on Henry's law constant of isopropanol was determined. An increase of 1.8 per 10 ^{o} C for the dimensionless Henry's law constant was obtained. The determination of the overall mass transfer coefficients of isopropanol ($K_G a$) was carried out, obtaining values between 500 and 1800 h^{-1} for gas velocities of 100 and 300 m h^{-1}. No significant influences were observed for either the liquid velocity or packing material. Also, the determination of overall mass transfer coefficients of oxygen ($K_L a$) were carried out, obtaining values between 20 and 200 h^{-1} depending on the packing material for liquid velocities between 2 and 33 m h^{-1}. Structured packing materials exhibited greater mass transfer coefficients, while for random packing materials, the mass transfer coefficients clearly benefited from the high specific surface area. Mathematical correlations found in the literature were compared with the empirical data, showing that neither was capable of reproducing the mass transfer coefficients obtained empirically. Thus, empirical relationships between the mass transfer coefficients and the gas and liquid velocities are proposed to characterise the system.

Keywords

Bioreactors; mass transfer; mathematical modelling; bioprocess; hydrodynamics

Chem Eng Sci 108 (2014) 47–56

7.1 INTRODUCTION

In recent decades, there has been an emergent interest in research into biotreatment as an alternative for the treatment of volatile organic compounds (VOC), which includes the biotrickling filter as one of the most applicable technologies (Devinny et al., 1999). The use of biotrickling filtration for the treatment of VOC it is frequent and has been shown to be capable of achieving high removal efficiencies. Considering that biotrickling filtration involves a series of complex physical, chemical and biological processes further work is needed to determine the mechanisms that contribute to the observed behaviour (Iranpour et al., 2005). The most representative mechanisms in a biotrickling filter are mass transfer, diffusion and biological degradation. Typically, the process may be limited by mass transfer as well as kinetics. Unfortunately, research has been mainly focused on biodegradation kinetics rather than mass transfer (Dorado et al., 2009; Lebrero et al., 2012) and, despite being a key step in the process, the optimisation of mass transfer between the gas and the liquid/ biofilm remains one of the most difficult aims to achieve. Relating to this, several authors (Dorado et al., 2009; Kim and Deshusses, 2008b) have emphasised the need to determine the mass transfer coefficients in order to develop simulations for the design and optimisation of biotrickling filters. Also, determining the mass transfer coefficient would facilitate the selection of the packing material and the modelling of bioreactors used for air pollution control.

As pointed by other authors (Dorado et al., 2009; Kim and Deshusses, 2008b; Pérez et al., 2006), the hydrodynamic conditions used in biofiltration are markedly different than those used in absorption processes, so the typical correlations used in these systems are not useful for predicting the phenomena occurring in biotrickling filters. Dorado et al. (2009) confirmed that using experimental global mass transfer coefficients appears to be the most suitable way to represent mass transfer in biotrickling filter systems; they pointed out the need for using the target pollutant for the determination of mass transfer coefficients.

Isopropanol is a hydrophilic compound typified by its high volatility and relatively low hazardous properties in comparison with other solvents. As a result, it is one of the most commonly used solvents in chemical industries as coating, printing, cleaning, among others, resulting in a large amount of emissions to the atmosphere that should be treated. Due to its low Henry's law constant in comparison with Henry's law constant of oxygen, its treatment by biofiltration

implies that the process could be typically limited by the low concentration of oxygen in the biofilm. This could imply that that the penetration depth of oxygen in water or the biofilm is lower than that of the pollutant, causing anaerobic zones in the deeper parts of the biofilm close to the substratum (Shareefdeen and Singh, 2005). Experiments based on the physical properties of the gas and liquid phases have shown that the volumetric mass transfer coefficient could be influenced by the liquid phase at a similar level of contribution than the influence of the gas (Pérez et al., 2006). So, both influences should be assessed in order to characterise and improve the process.

The purpose of this research was to determine the mass transfer coefficients for the treatment of hydrophilic compounds using isopropanol and oxygen as reference components for various packing materials. To carry out this purpose, the following objectives were developed: (1) to establish a simple method to determine the mass transfer coefficients of typical hydrophilic compounds using isopropanol as the target pollutant, (2) to establish a simple method to determine the mass transfer coefficients of oxygen, (3) to determine the influence of gas and liquid velocities on the mass transfer coefficients and (4) to establish a mathematical relationship between the mass transfer coefficients and the operational conditions.

7.2 MATERIALS AND METHODS

7.2.1 Theory

The overall mass transfer coefficient expressed in the liquid phase is defined as a function of the individual mass transfer coefficients, and is related to the overall mass transfer coefficient expressed in the gas phase:

$$\frac{1}{K_L a} = \frac{1}{HK_G a} = \frac{1}{k_L a} + \frac{1}{Hk_G a} \qquad (7\text{-}1)$$

Depending on Henry's law constant of the substance, the main resistance to the transfer could be controlled only by one of these phases. Liss and Slater (1974) established that for Henry's law constants over 250 atm (mole fraction)$^{-1}$, the main resistance is controlled by the liquid film, while for Henry's law constants between 1 and 250 atm (mole fraction)$^{-1}$, the main resistance is a mix between the two phases, and for Henry's law constants up to 1 atm (mole fraction)$^{-1}$, the

resistance is controlled by the gas film. Due to the existing differences between Henry's law constant of isopropanol (0.460 ± 0.124 atm (mole fraction)$^{-1}$ (Sander, 2005)) and oxygen (43922 ± 1679 atm (mole fraction)$^{-1}$), two different methods were developed to measure the mass transfer coefficients for each compound.

7.2.2 Determination of the mass transfer coefficient of isopropanol

7.2.2.1 *Experimental setup*

As shown in Figure 7-1, the system consisted of a column of methacrylate (14.4 cm internal diameter, 120 cm height) and a recirculation tank (5 L water volume). Two packing materials, one random (Flexiring 25 mm) and one structured (PAS Winded Media), were investigated; the characteristics of these materials are shown in Table 7-1. The packing height was 100 cm. The air stream (compressed, filtered and dried) was introduced through the bottom of the column, with the flow rate adjusted using a mass flow controller (Bronkhorst Hi-Tec, The Netherlands). The experiments were carried out at three superficial air velocities around 100, 150 and 300 m h^{-1} and the trickling water was recirculated using a centrifugal pump (HPR10/15, ITT, Great Britain) in counter-current mode with respect to the air flow rate, with a superficial water velocity of 2, 4, 7 and 13 m h^{-1}. The operational conditions were selected in order to evaluate the wide range used in biotrickling filters. The experiments were carried out at room temperature (21.5 ± 1.3 ^{o} C). For isopropanol, these changes in temperature imply variations in Henry's law constants of up to 20–25% (Sander, 2005); thus, the dependence of *H* on temperature had to be obtained for an accurate study of mass transfer.

The concentration of isopropanol was measured using a total hydrocarbon analyser (Nira Mercury 901, Spirax Sarco, Spain). The response factor of the total hydrocarbon analyser was determined by gas chromatography (model 7890, Agilent Technologies, EEUU). The determination of the total organic carbon (TOC) in water was measured using a total organic carbon analyser (TOC -V_{CHS}, Shimadzu Corporation, Japan).

Table 7-1 Characteristics of the packing materials.

Packing material		Diameter[a] (mm)	Density[a] (kg m^{-3})	Bed Porosity[a] (%)	Specific surface area[a] (m^2 m^{-3})
PAS Winded Media[b]	Structured	----	----	93	410
Flexiring	Random	25	71	92	207[c]
Refilltech	Random	15	110.7	91	348

[a] Packing material supplied by PAS Solutions BV / [b] Data provided by the suppliers / [c] Larachi et al. (2008)

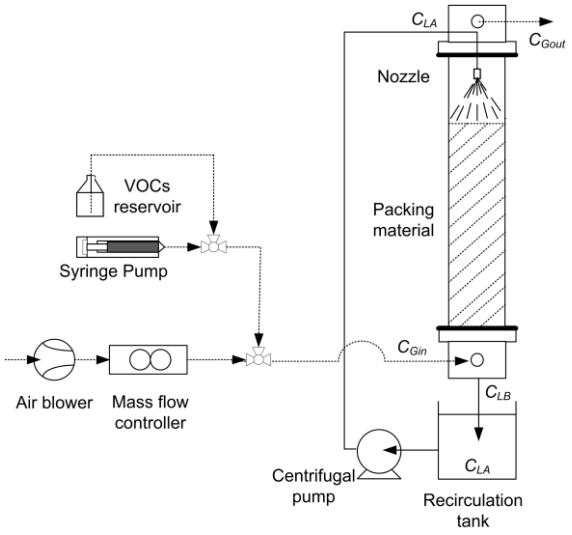

Figure 7-1 Experimental setup for the determination of the mass transfer coefficient of isopropanol.

7.2.2.2 *Experimental procedure*

A method under inert conditions was used for the determination of the overall mass transfer coefficients of isopropanol. This method consisted of monitoring the concentration of isopropanol in the gas phase during entire experiment and periodically taking samples from the bottom of the column and water tank. To minimise the effect of adsorption in the packing surface and the absorption in the water inside the reactor, the system was previously wetted and saturated with isopropanol. When the inlet concentration was equal to the outlet concentration, a continuous trickle began from the tank to the top of the column. The first 20 min of each experiment were neglected to ensure that stable

conditions were achieved. After 20 min, the gas concentration as well as the liquid concentration at the bottom of the column and in the tank were considered as the initial points of the experiment and were used to estimate the value of the mass transfer coefficients. Under these conditions, mass balances of isopropanol were developed based on the following assumptions: (1) the behaviour of the column was described as a plug flow regime; (2) the water tank was perfectly mixed; (3) reaction in pipes was negligible, so, the concentration of the water tank was the same as the concentration of the inlet of the column.

7.2.2.2.1 Mass balance in the packed column

For each time point and for a differential column of the reactor, the total amount of carbon transferred from the gas to the liquid phase in the column is defined by:

$$dC_{G,IPA} = -\frac{Q_L}{Q_G} dC_{L,IPA} \tag{7-2}$$

where $C_{G,IPA}$ and $C_{L,IPA}$ are the gas/liquid concentrations and Q_G and Q_L are the volumetric flow rates in the gas/liquid phases, respectively.

From the integration of Eq. (7-2), the following equation is obtained:

$$C_{L_B,IPA} = C_{L_A,IPA} + \frac{Q_G}{Q_L} \cdot \left(C_{G_{in},IPA} - C_{G_{out},IPA} \right) \tag{7-3}$$

To determine the outlet concentration in the gas phase, the mass balance is described as:

$$Q_G \cdot dC_{G,IPA} = -H_{IPA} K_G a \cdot (C^*_{L,IPA} - C_{L,IPA}) \cdot dV_c \tag{7-4}$$

where V_c is the volume of the column, H_{IPA} is the dimensionless Henry's law constant of isopropanol expressed as concentration of gas phase/concentration of the liquid phase and $C^*_{L,IPA}$ is defined by Henry's Law according to the following equation:

$$C^{*}_{L,IPA} = \frac{C_{G,IPA}}{H_{IPA}} \tag{7-5}$$

Taking into account Eq. (7-5) and that the cross-sectional area of the column is constant, Eq. (7-4) can be written as follows:

$$Q_G \frac{dC_{G,IPA}}{dz} = -H_{IPA} K_G a \cdot S \left(\frac{C_{G,IPA}}{H_{IPA}} - C_{L,IPA} \right) \tag{7-6}$$

where *S* and *z* are the surface and the distance from the bottom of the column, respectively. The following boundary conditions were assumed. At the bottom of the column (*z*=0):

$$\begin{aligned} C_{G,IPA} &= C_{G_{in},IPA} \\ C_{L,IPA} &= C_{L_B,IPA} \end{aligned} \tag{7-7}$$

while at the top of the column (*z*=*Z*):

$$\begin{aligned} C_{G,IPA} &= C_{G_{out},IPA} \\ C_{L,IPA} &= C_{L_A,IPA} \end{aligned} \tag{7-8}$$

where $C_{G\,in,IPA}$ and $C_{G\,out,IPA}$ are the inlet/outlet concentrations in the gas phase and $C_{L\,A,IPA}$ and $C_{L\,B,IPA}$ are the liquid concentrations at the top and at the bottom of the column. The concentration at the top of the column is assumed to be equal to the concentration in the tank. Integrating Eq. (7-6) and with the conditions presented in Eqs. (7-7) and (7-8), the following equation was obtained:

$$\ln \frac{\left(C_{G_{out},IPA} - H_{IPA} \cdot C_{L_A,IPA} \right)}{\left(C_{G_{in},IPA} - H_{IPA} \cdot C_{L_B,IPA} \right)} = -\left(1 + H_{IPA} \frac{Q_G}{Q_L} \right) \frac{K_G a}{Q_G} \cdot S \cdot Z \tag{7-9}$$

Combining Eq. (7-9) and Eq. (7-3), the outlet concentration is described by:

$$C_{G_{out},IPA} = \frac{\left(1 - H_{IPA}\frac{Q_G}{Q_L}\right)\exp\left(-\left(1 + H_{IPA}\frac{Q_G}{Q_L}\right)\frac{K_G a}{Q_G}\cdot S\cdot Z\right)C_{G_{in},IPA} + \left(1 - \exp\left(-\left(1 + H_{IPA}\frac{Q_G}{Q_L}\right)\frac{K_G a}{Q_G}\cdot S\cdot Z\right)\right)\cdot H_{IPA}\cdot C_{L_A,IPA}}{1 - H_{IPA}\frac{Q_G}{Q_L}\exp\left(-\left(1 + H_{IPA}\frac{Q_G}{Q_L}\right)\frac{K_G a}{Q_G}\cdot S\cdot Z\right)} \quad (7\text{-}10)$$

7.2.2.2.2 Mass balance in the tank

The variation of $C_{L\,A,IPA}$ and $C_{L\,B,IPA}$ is described by the mass balance in the tank as follows:

$$\frac{dC_{L_A,IPA}}{dt} = \frac{Q_L}{V_T}\left(C_{L_B,IPA} - C_{L_A,IPA}\right) \quad (7\text{-}11)$$

where V_T is the volume of the tank.

As was previously mentioned, the variations in temperature during the experiment imply variations in Henry's law constants up to 20–25% (Sander, 2005). For this reason, the estimation of the parameters was divided into two stages. First, the estimation of $K_G a$ and H was carried out for the experiments with Flexiring 25 mm. These fitted values of H were related to the temperature and an empirical correlation between H and T was obtained. Second, the empirical correlation between H and T was used in each experiment of the structured packing material, thus the $K_G a$ was the only parameter to be fitted in this step.

7.2.3 Determination of the mass transfer coefficient of oxygen

7.2.3.1 *Experimental setup*

As is shown in Figure 7-2, a similar setup as that used for the determination of the mass transfer coefficient of isopropanol was used but with a volume of 10 L in the recirculation tank. In this case, the study was extended to three packing materials, two random (Flexiring 25 mm and Refilltech 15 mm) and one structured (PAS Winded Media); the characteristics are shown in Table 7-1. The packing height was 40 cm for the random packing materials and 20 cm for the structured packing material. The experiments were carried out at two superficial air velocities of 104 m h^{-1} and 312 m h^{-1}. The trickling water was recirculated using a centrifugal pump with a superficial water velocity between 3 and 33 m h^{-1}. The

equipment was supplemented with a dissolved oxygen probe (Cellox® 325i, WTW, Germany) to measure the dissolved oxygen concentration in the tank. An internal pump installed in the recirculation tank ensured the ideal mixing conditions. The experiments were carried out at room temperature (21.2 ± 0.7 ° C). For oxygen, this implies variations in Henry's law constant up to 2% (Sander, 2005), thus the dependence of *H* on temperature was neglected.

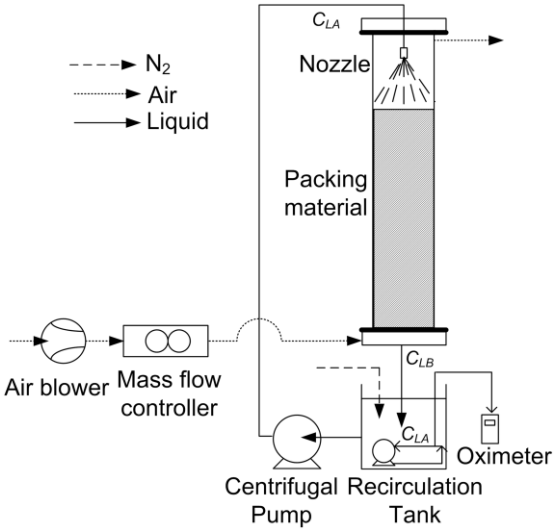

Figure 7-2 Experimental setup for the determination of the mass transfer coefficient of oxygen.

7.2.3.2 *Experimental procedure*

For the determination of K_La, a dynamic method under inert conditions was used as described elsewhere (San-Valero et al., 2013). The method consisted of measuring the increase in the oxygen concentration over time in a tank in which the oxygen was previously displaced by bubbling nitrogen gas. The experiment started when the air blower and the recirculation pump were switched on; oxygen was transferred from the air to the water in the packed column, causing an increase in the dissolved oxygen concentration in the recirculation tank. The oxygen mass balances were developed using the same assumptions as isopropanol.

7.2.3.2.1 Mass balance in the packed column

$$C_{L_B,OXY} = C^*_{L,OXY} - \frac{C^*_{L,OXY} - C_{L_A,OXY}}{\exp(\frac{Z}{v} K_L a)} \tag{7-12}$$

where $C_{LB,OXY}$ is the predicted dissolved oxygen concentration at the bottom of the column, $C_{LA,OXY}$ is the predicted dissolved oxygen concentration in the recirculation tank, $C^*_{L,OXY}$ is the oxygen solubility and Z and v are the height of the column and the velocity of the trickling water, respectively.

In the tank:

$$\frac{dC_{L_A,OXY}}{dt} = \frac{Q_L}{V_T}\left(C_{L_B,OXY} - C_{L_A,OXY}\right) \tag{7-13}$$

The combination of Eqs. (7-12) and (7-13) permits obtaining the variation of the predicted oxygen concentration over time (Van't Riet, 1979):

$$\frac{dC_{L_A,OXY}}{dt} = \frac{Q_L}{V_T}\left(C^*_{L,OXY} - \frac{C^*_{L,OXY} - C_{L_A,OXY}}{\exp(\frac{Z}{v} K_L a)} - C_{L_A,OXY} \right) \tag{7-14}$$

The response time constant of the probe, τ, is defined as the time at which the probe achieves 63% of the end value measured when the probe is subjected to a step input assay (Van't Riet, 1979). It was determined by transferring the oxygen probe from an ideal mixed tank in which the dissolved oxygen concentration was displaced by bubbling nitrogen gas to a second tank which was saturated with dissolved oxygen. First order dynamics were assumed a according to Eq. (7-15) (Weiland and Onken, 1981):

$$\frac{dC_{L_m,OXY}}{dt} = \frac{(C_{L_A,OXY} - C_{L_m,OXY})}{\tau} \tag{7-15}$$

where $C^*_{Lm,\ OXY}$ is the dissolved oxygen concentration in the recirculation tank measured by the oxygen probe.

The value of K_La of the packed column was calculated by minimising the sum of squares of the difference between the measured data recorded for the dissolved oxygen concentration in the recirculation tank and the value obtained from the mathematical resolution of Eqs. (7-14) and (7-15).

7.3 RESULTS AND DISCUSSION

7.3.1 Determination of the mass transfer coefficient of isopropanol

7.3.1.1 *Correlation between Henry's law constant and the temperature*

The determination of the mass transfer coefficient of isopropanol was carried out for two packing materials: Flexiring 25 mm and PAS Winded Media. As the influence of the temperature on Henry's law constant of isopropanol should not be neglected, the first set of experiments with the packing material Flexiring 25 mm were used for the estimation of K_Ga and H. This estimation allowed for obtaining the exact temperature dependence of the system with Henry's law constant. The values of $H^*_{298\,K}$ and the enthalpy of the solution divided by the ideal gas law constant were obtained by using the least squares method in order to minimise the differences between the experimental data and the Van't Hoff equation. The parameters $H^*_{298\,K}$ and the enthalpy of the solution divided by the ideal gas law constant obtained are shown as:

$$H^*_{T,IPA} = 146 \cdot \exp\left(5501 \cdot \left(\frac{1}{T} - \frac{1}{298}\right)\right) \tag{7-16}$$

where $H^*_{T,IPA}$ is Henry's law constant expressed in M atm^{-1} and T is the temperature expressed in K. The dimensionless Henry's law constant could be related with Henry's law constant expressed in M atm^{-1} by the following equation:

$$H_{IPA} = \frac{1}{H^*_{T,IPA} RT} \tag{7-17}$$

where R is the universal gas constant (0.082 atm K^{-1} M^{-1}).

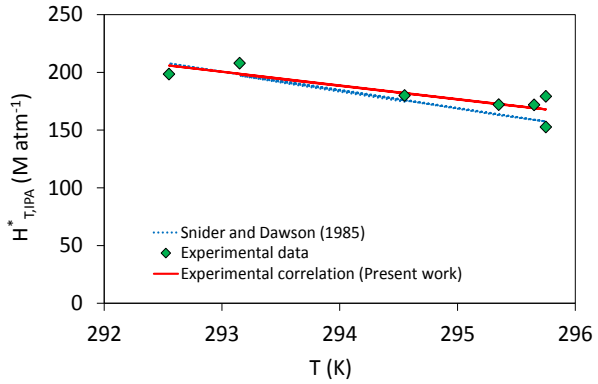

Figure 7-3 Dependence of Henry's law constant on temperature.

Figure 7-3 shows the experimental data with the results provided by the empirical correlation described by the Eq. (16). The available data from literature is also plotted (Snider and Dawson, 1985). The general variation range of the dimensionless Henry's law constant for VOC from 1.12 to 3.55 per 10 ^{o}C rise in temperature, with an average value of 1.88 found by Staudinger and Roberts (2001). The empirical correlation of Eq. (16) presented an increase in the dimensionless Henry's law constant of 1.8 per each 10 ^{o}C while Snider and Dawson (1985) provides a variation of 2.25 per 10 ^{o}C rise. It is common to find some discrepancies in the literature for the same compound related with the influence of non-temperature effects on Henry's law constant such as pH, dissolved salts, etc (Staudinger and Roberts, 1996). Regarding this, Staudinger and Roberts (2001) pointed out that it appears prudent to determine the exact temperature of each case. Thus, the empirical correlation obtained in Eq. (7-16) was used to obtain the value of *H* in the experiments carried out with the structured packing material.

7.3.1.2 *$K_G a$ calculations*

Typical examples of the raw data obtained from the experiments for each packing material and the results of the data obtained with the mathematical model are shown in Figure 7-4. The experiment presented in Figure 7-4a corresponds to one test carried out with the packing material Flexiring 25 mm operating at a gas velocity of 180 m h^{-1} and a liquid velocity of 6.3 m h^{-1} while the experiment presented in Figure 7-4b corresponds to one test carried out with the

packing material PAS Winded Media operating at a gas velocity of 180 m h^{-1} and a liquid velocity of 1.8 m h^{-1}. These examples were representative of all tests done. The goodness of fit of the experimental data and the data provided by the mathematical model were tested by using the relative error of the concentration of each phase. An average value of the relative error of 6% for the gas phase and an average error of 5% for the liquid phase (C_{LA}, C_{LB}) were obtained. The relative error obtained indicated that the method was accurate for the determination of the mass transfer coefficient of isopropanol.

The effect of the gas and liquid velocities for both packing materials is shown in Figure 7-5. Depending on the packing material and the conditions, $K_G a$ values were obtained in a range between 500 and 1800 h^{-1} for gas velocities between 100 and 300 m h^{-1} and for liquid velocities between 2 and 13 m h^{-1}. These data are on the same order of magnitude as the data presented by Kim and Deshusses (2008b). These authors showed that for biotrickling filters operating at a typical range of gas velocities below 500 m h^{-1}, the $k_G a$ values were between 500 and 2000 h^{-1}. As shown in Figure 7-5, the mass transfer coefficient of isopropanol was strongly influenced by the gas velocity. As an example, a 50% variation in the gas velocity would imply a variation of around 40% in the mass transfer coefficient. This behaviour is in agreement with that found by other authors in the literature (Dorado et al., 2009; Kim and Deshusses, 2008b; Piche et al., 2001). To evaluate the effect of the liquid velocity on the mass transfer coefficient of isopropanol, further experiments were carried out at several liquid velocities. No significant influence of the liquid velocity was observed. This could have occurred since the packing material was completely wet. Kim and Deshusses (2008b) observed that when wetting was almost complete, the effect of liquid velocity was slight or constant. The same behaviour was observed by Piche et al. (2001). No differences between packing materials were found (Figure 7-5). Regarding this, Dorado et al. (2009) suggested that when pollutant diffusion is in the gas phase, as is the case with isopropanol, neither the liquid side resistance nor the packing material characteristics affect the global system performance.

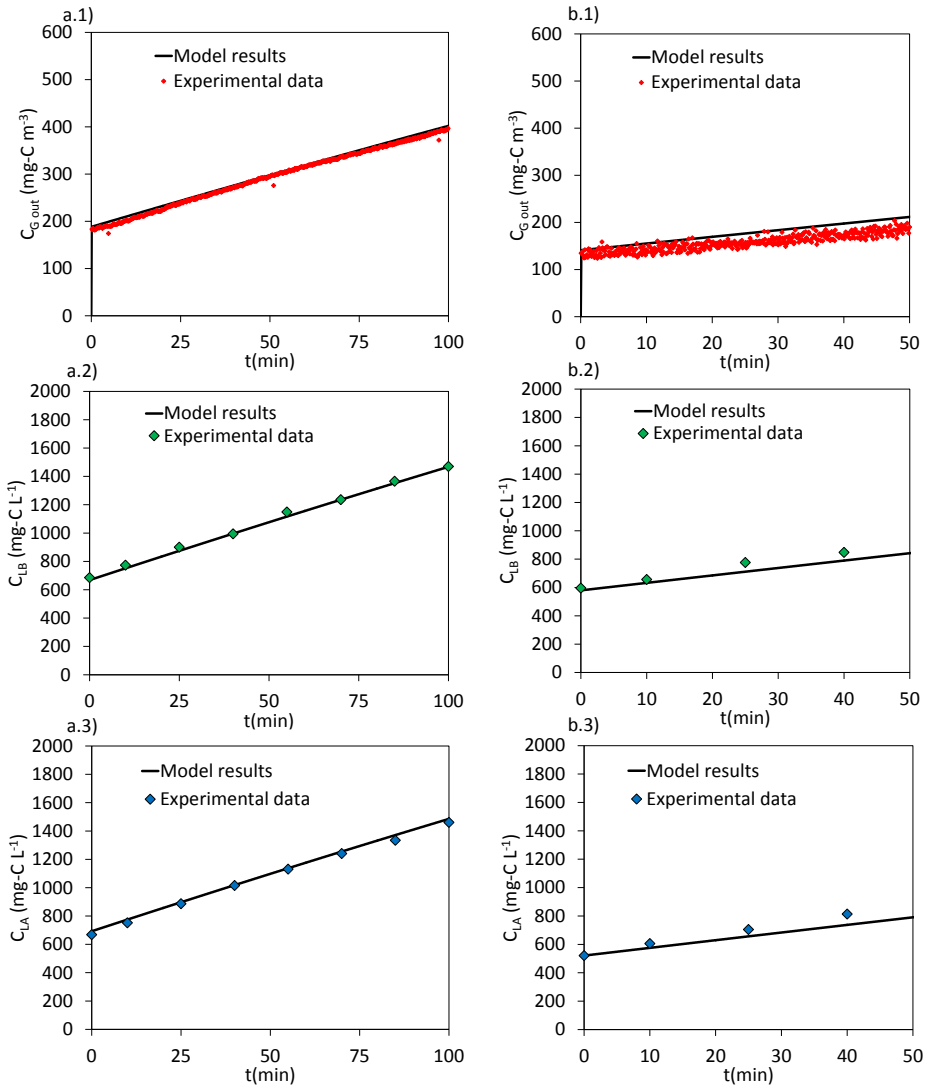

Figure 7-4. Experimental data and model results for the experiments of the mass transfer coefficient of isopropanol. (a) Flexiring 25 mm: (1) C_{Gout} (2) C_{LB} (3) C_{LA} and (b) PAS Winded Media: (1) C_{Gout} (2) C_{LB} (3) C_{LA}.

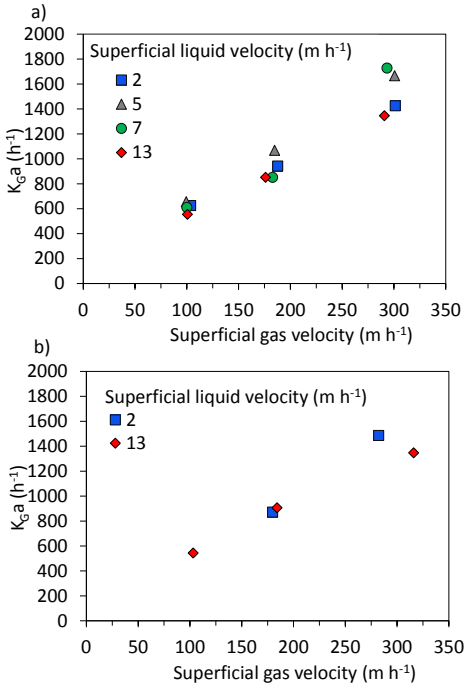

Figure 7-5 Influence of the superficial gas and liquid velocities on the mass transfer coefficient of isopropanol: (a) Flexiring 25 mm and (b) PAS Winded Media.

7.3.2 Determination of the mass transfer coefficient of oxygen

The determination of the mass transfer coefficient of oxygen was extended to the three packing materials shown in Table 7-1 at several liquid velocities (from 2 to 33 m h^{-1}) and two gas velocities (104 and 312 m h^{-1}). The K_La coefficients were obtained using the least squares method in order to minimise the differences between the experimental data and the concentration of oxygen provided by the mathematical model established by Eqs. (7-14) and (7-15). The response time of the probe (τ) was determined by means of a step input assay, resulting in a value of 19.4 ± 1.5 s (San-Valero et al., 2013).

A typical example of the raw data obtained during one of the experiments and the result of the mathematical procedure described above is shown in Figure 7-6. The same mathematical procedure was used for all packing materials, so only one example is shown as a representative of the other packing materials. This corresponds to one test carried out with the packing material Flexiring 25 mm operating at a gas velocity of 104 m h^{-1} and a liquid velocity of 11 m h^{-1}. Similarly to

the experiments using isopropanol, the experimental data and the data provided by the mathematical model were evaluated by using the relative error of the concentrations, obtaining an average value less than 2% for all tests done. This confirms that the method was accurate for the determination of the mass transfer coefficient of oxygen.

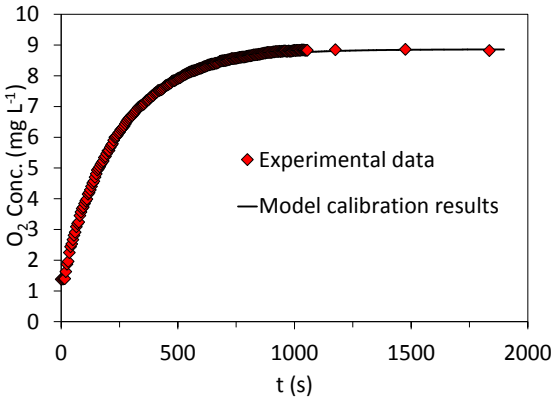

Figure 7-6 Experimental data and model results for the experiments of the mass transfer coefficients of oxygen.

The effect of the gas and liquid velocities on the mass transfer coefficient is shown in Figure 7-7 for each packing material. Depending on the packing material and the conditions, K_La values were obtained in a range between 20 and 200 h^{-1} for liquid velocities between 2 and 33 m h^{-1}. These results are consistent with the data obtained by other authors (Kim and Deshusses, 2008b; Piche et al., 2001). As may be seen in this figure, oxygen transfer was enhanced at high liquid velocities. A clear dependence can be observed between the global coefficients and liquid velocities. In addition, these data show that there was not a significant influence of gas velocity on the mass transfer coefficient of oxygen. This is in accordance with the literature (Piche et al., 2001; Kim and Deshusses, 2008b), and is related to the fact that oxygen is a poorly soluble gas in water and the main resistance is located in the liquid phase, in contrast to what occurs with isopropanol.

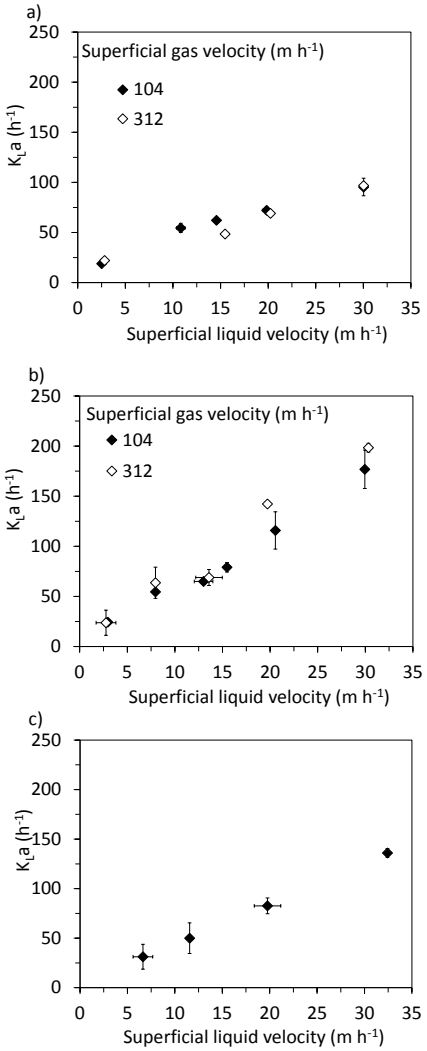

Figure 7-7 Influence of gas and liquid velocities on the mass transfer coefficients of oxygen. (a) Flexiring 25 mm (b) PAS Winded Media and (c) Refilltech 15 mm.

The influence of the packing material was extended to three materials: two random with different specific surface area and one structured. The experimental data from San-Valero et al. (2013) are compiled herein for this purpose. The most important differences in the behaviour of the packing material were observed at liquid velocities above 15 m h^{-1}. This could be due to the fact that turbulence is higher at higher liquid velocities than at lower liquid velocities, thus increasing the interfacial area and facilitating the mass transfer of oxygen

between phases, in contrast to the mass transfer of isopropanol where the main resistance was located in the gas phase. For the comparison between packing materials, a velocity of 30 m h^{-1} was chosen since this was the velocity where differences were most evident. In this regard, the structured packing material with a specific surface area of 410 m^3 m^{-2} exhibited the maximum mass transfer coefficient of oxygen with a value around 175 h^{-1}. For the random packing materials, K_La values of 130 and 100 h^{-1} were obtained for Refilltech 15 mm and Flexiring 25 mm, with specific surface areas of 348 and 207 m^3 m^{-1}, respectively. These data show that a high specific surface area improves the mass transfer of oxygen. The structured packing material exhibited a higher mass transfer coefficient than those obtained with the random packing material with a similar specific surface area. This could be attributed to the effect of different flow paths within the packing materials on the mass transfer of oxygen. Random packing materials could promote channelling more readily than structured packing materials.

7.3.3 Mathematical correlation

Mathematical correlations were developed in order to characterise the influence of the gas and liquid velocities on the mass transfer coefficients of isopropanol and oxygen. For the mass transfer of isopropanol, non-significant influences of the packing materials and liquid velocities were observed. Thus, the experimental data can be fitted to a relationship between the mass transfer coefficient and the gas velocity. For the mass transfer of oxygen, two important influences were observed, i.e. the packing material and the liquid velocity. So, it was considered necessary to develop empirical correlations for each of the packing materials. Power law relationships according to Eqs. (18) and (19) between gas or liquid velocity and K_Ga or K_La could be the most suitable way to represent this phenomenon for isopropanol and for oxygen:

$$K_G a_{IPA} = c_1 \cdot v_G^{c_2} \tag{7-18}$$

$$K_L a_{OXY} = c_1 \cdot v_L^{c_2} \tag{7-19}$$

where K_Ga and K_La are expressed in h^{-1}, and v_G and v_L in m h^{-1}.

The parameters obtained for each correlation are shown in Table 7-2. In order to analyse the accuracy of the empirical correlations proposed herein, the

observed and predicted values of the mass transfer coefficient for isopropanol and oxygen are presented in Figure 7-8. In both cases, the experimental data fit (r^2 > 0.94) the predicted data; the greatest observed difference was 20% for the entire data set. These uncertainties are similar to those reported by other authors (Kim and Deshusses, 2008a; Onda et al., 1968).

Table 7-2 Empirical coefficients for the correlations described by Eqs. (7-18) and (7-19).

Packing material	$K_G a$ isopropanol (h^{-1})		
	c_1 $(m^{-c2}\,h^{(c2-1)})$	c_2 *(dimensionless)*	r^2
PAS Winded Media Flexiring 25 mm	11.59	0.85	0.94
	$K_L a$ oxygen (h^{-1})		
	c_1 $(m^{-c2}\,h^{(c2-1)})$	c_2 *(dimensionless)*	r^2
Flexiring 25 mm	10.72	0.65	0.99
PAS Winded Media	9.54	0.84	0.95
Refilltech 15 mm	5.29	0.93	0.99

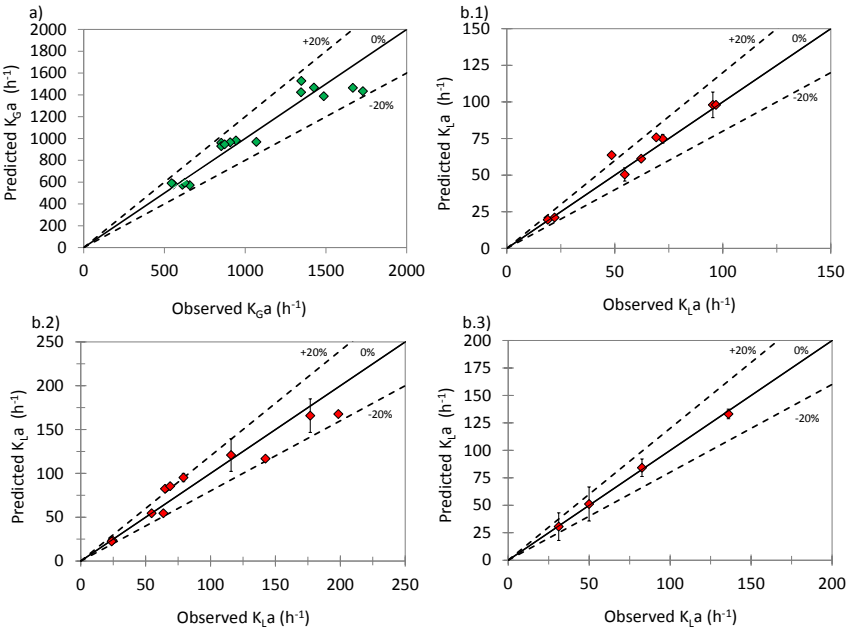

Figure 7-8 Comparison of correlation results and experimental data for mass transfer coefficients: (a) isopropanol and (b) oxygen: (1) Flexiring 25 mm (2) PAS Winded Media (3) Refilltech 15 mm. Dotted lines indicate an uncertainty of ± 20%.

The most general correlations were those proposed by Onda et al. (1968) and van Krevelen and Hoftijzer (1948) for conventional absorption packing columns. These correlations are described as follows:

Onda

$$k_G = 5.23\frac{D_G}{d_p^2 a_p}\left(\frac{\rho_G v_G}{\mu_G a_p}\right)^{0.7}\left(\frac{\mu_G}{\rho_G D_G}\right)^{1/3} \tag{7-20}$$

$$k_L = 0.0051\left(a_p d_p\right)^{0.4}\left(\frac{\mu_L g}{\rho_L}\right)^{1/3}\left(\frac{\rho_L v_L}{a_e \mu_L}\right)^{2/3}\left(\frac{\mu_L}{\rho_L D_L}\right)^{-0.5} \tag{7-21}$$

van Krevelen and Hoftijzer

$$k_G = 0.2\frac{D_G}{d_c}\left(\frac{\rho_G v_G}{\mu_G a_p}\right)^{0.8}\left(\frac{\mu_G}{\rho_G D_G}\right)^{1/3} \tag{7-22}$$

$$k_L = 0.015 D_L\left(\frac{\mu_L^2}{\rho_L^2 g}\right)^{-1/3}\left(\frac{\rho_L v_L}{a_e \mu_L}\right)^{2/3}\left(\frac{\mu_L}{\rho_L D_L}\right)^{1/3} \tag{7-23}$$

The assumed supposition that the main resistance to the mass transfer of isopropanol is in the gas phase and for oxygen is in the liquid phase was checked applying the Onda and van Krevelen and Hoftijzer equations, taking into account both resistances and neglecting one of them for each compound. The error committed neglecting one of the phases was very small (in all cases less than 6%). The hydrodynamics under which these correlations were developed are markedly different than these used in biofiltration, characterised by lower gas and liquid velocities. For this reason, Kim and Deshusses (2008a) developed specific correlations for biotrickling filters for different packing materials.

Kim and Deshusses (For Pall ring 1")

$$\log\left(k_G a\right) = 2.05 + 0.33\log\left(v_G\right) \tag{7-24}$$

$$\log\left(k_L a\right) = 0.69 + 0.83\log\left(v_L\right) \tag{7-25}$$

The results obtained herein were compared with these three correlations for the experiments with Flexiring 25 mm. In the case of the equations proposed by Onda and van Krevelen and Hoftijzer, the wetted area and the effective gas-liquid interface were considered the same as that of the packing material. In the case of Kim and Deshusses, since Pall rings 1" and Flexiring 25 mm have a similar specific surface area, the values of the coefficients proposed in their research were used for comparison purposes.

Figure 7-9 shows the comparison between the experimental data and correlations for the packing material Flexiring 25 mm. For the mass transfer coefficient of isopropanol (Figure 7-9a) it is clear that neither correlation found in the literature was capable of simulating the mass transfer coefficients obtained experimentally. The Onda equation overestimated the values of $K_G a$ by a factor between 2 and 3, while the values provided by the van Krevelen and Hoftijzer equation underestimated the experimental data. In the case of the equation from Kim and Deshusses, the experimental data were successfully predicted only at low gas velocities.

For the mass transfer coefficient of oxygen, the prediction of the Onda correlation fit accurately with the experimental data, and the results predicted by Kim and Deshusses were slightly smaller in comparison. In this case, the results of van Krevelen and Hoftijzer were clearly quite different from the empirical data.

These results show how theoretical and general correlations are not accurate for the prediction of the mass transfer coefficients in biotrickling filters. So, as was proposed by Dorado et al. (2009), using experimental global mass transfer coefficients appears the most suitable way to represent mass transfer. The correlations proposed in this paper are useful for the mathematical modelling of the treatment of vapour emissions of isopropanol with biotrickling filters.

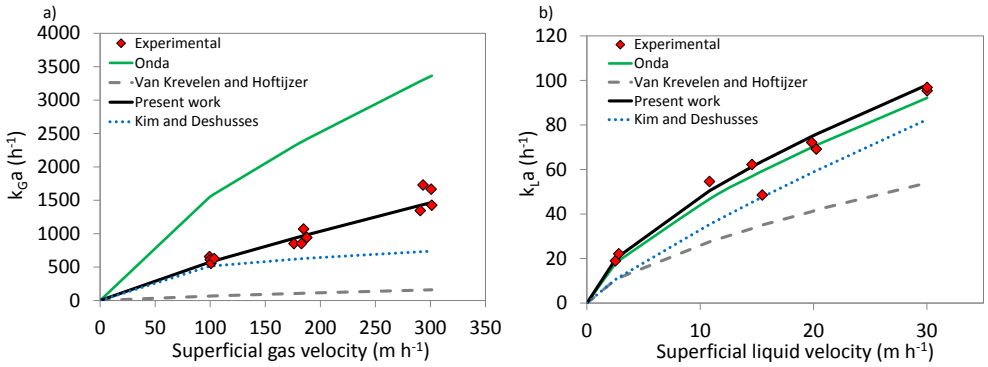

Figure 7-9 Comparison between experimental data and empirical correlations for Flexiring 25 mm. (a) Isopropanol; (b) oxygen.

7.4 CONCLUSIONS

Mass transfer properties for isopropanol and oxygen were determined for several packing materials in the liquid and gas velocity ranges typically used in biotrickling filtration. Henry's law constant of isopropanol was clearly influenced by the temperature in the ambient range. An empirical correlation based on the Van't Hoff equation was obtained by using experiments with the random packing material Flexiring 25 mm. This correlation was validated with the experiments carried out with the structured packing material PAS Winded Media. The influence of the gas and liquid velocities and the packing materials on the mass transfer coefficients of isopropanol and oxygen was determined. The mass transfer coefficient of isopropanol increased almost linearly with gas velocity, while the influences of the liquid velocity and packing material were not significant. The mass transfer coefficient of oxygen was influenced by the packing material and by the liquid velocity. No significant influence of the gas velocity was observed. Based on the data obtained in the present study, power law relationships between the mass transfer coefficient and the gas and liquid velocities were proposed in each case. Three mathematical correlations found in the literature were compared with the empirical data; none of the correlations were capable of reproducing the mass transfer coefficients obtained empirically.

The data presented in this paper contain valuable information for modelling the mass transfer coefficients of isopropanol and oxygen. This

information is useful for mathematical modelling of physical phenomena that take place during the removal of isopropanol by biotrickling filtration. This paper provides a simple methodology that can be extended to any hydrophilic volatile organic compound.

7.5 NOMENCLATURE

a	Specific interfacial area
a_e	Effective specific interfacial area
a_p	Packing specific surface area
C	Mass concentration
c_1	Empirical coefficient of power law
c_2	Empirical coefficient of power law
D	Diffusion coefficient
d_c	Column inner diameter
d_p	Particle diameter
H	Henry's law constant
K	Overall mass transfer coefficient
k	Individual mass transfer coefficient
Q	Volumetric flow rate
S	Surface of the column
t	Time
V	Volume
V_R	Volume of the reactor
V_T	Volume of the tank
z	Distance from the bottom of the column
Z	Height of the column
ρ	Density
τ	Response time of the probe
μ	Viscosity

Subscripts

G	Gas
IPA	Isopropanol
L	Liquid
OXY	Oxygen

Sub-subscripts

A	Inlet to the column of the liquid phase
B	Outlet of the column of the liquid phase
in	Inlet to the column of the gas phase
m	Measured
out	Outlet of the column of the gas phase

Acknowledgements

The research leading to these results has received funding from the People Programme (Marie Curie Actions) of the European Union0s Seventh Framework Programme FP7/2007-2013/ under REA grant agreement no. 284949. Financial support from the Ministerio de Economía y Competitividad (Project CTM2010-15031/TECNO) and Generalitat Valenciana (PROMETEO/2013/053) Spain is also acknowledged. Joaquim Castro Blanch is also acknowledged for his laboratory support. Pau San-Valero acknowledges the Ministerio de Educación, Cultura y Deporte Spain for her FPU contract (AP2010-2191).

7.6 REFERENCES

Devinny, J. S., Deshusses, M. A. and Webster, T. S. (1999). *Biofiltration for Air Pollution Control*. Boca Raton, USA: CRC-Lewis Publishers.

Dorado, A. D., Rodriguez, G., Ribera, G., Bonsfills, A., Gabriel, D., Lafuente, J. and Gamisans, X. (2009). Evaluation of mass transfer coefficients in biotrickling filters: Experimental determination and comparison to correlations. *Chemical Engineering & Technology*, *32*(12), 1941–1950.

Iranpour, R., Cox, H. H. J., Deshusses, M. A. and Schroeder, E. D. (2005). Literature review of air pollution control biofilters and biotrickling filters for odor and volatile organic compound removal. *Environmental Progress*, *24*(3), 254–267.

Kim, S. and Deshusses, M. A. (2008a). Determination of mass transfer coefficients for packing materials used in biofilters and biotrickling filters for air pollution control -2: Development of mass transfer coefficients correlations. *Chemical Engineering Science*, *63*(4), 856–861.

Kim, S. and Deshusses, M. A. (2008b). Determination of mass transfer coefficients for packing materials used in biofilters and biotrickling filters for air pollution control. 1. Experimental results. *Chemical Engineering Science*, *63*(4), 841–855.

Larachi, F., Lévesque, S. and Grandjean, B. P. A. (2008). Seamless mass transfer correlations for packed beds bridging random and structured packings. *Industrial & Engineering Chemistry Research*, *47*(9), 3274–3284.

Lebrero, R., Estrada, J. M., Muñoz, R. and Quijano, G. (2012). Toluene mass transfer characterization in a biotrickling filter. *Biochemical Engineering Journal*, *60*(0), 44–49.

Liss, P. S. and Slater, P. G. (1974). Flux of gases across the air-sea interface. *Nature*, *247*, 181–184.

Onda, K., Takeuchi, H. and Okumoto, Y. (1968). Mass transfer coefficients between gas and liquid phases in packed columns. *Journal of Chemical Engineering of Japan*, *1*(1), 56–62.

Pérez, J., Montesinos, J. L. and Gòdia, F. (2006). Gas–liquid mass transfer in an up-flow cocurrent packed-bed biofilm reactor. *Biochemical Engineering Journal*, *31*(3), 188–196.

Piche, S., Grandjean, B. P. A., Iliuta, I. and Larachi, F. (2001). Interfacial mass transfer in randomly packed towers: A confident correlation for environmental applications. *Environmental Science & Technology*, *35*(24), 4817–4822.

Sander, R. (2005). Henry's law constants in NIST chemistry WebBook, NIST standard referencedatabase number 69. In: P. J. Linstrom and W. G. Mallard (Eds.), *National Institute of Standards and Technology*. Gaithersburg MD 208999, USA.

San-Valero, P., Penya-roja, J. M., Sempere, F. and Gabaldón, C. (2013). Biotrickling filtration of isopropanol under intermittent loading conditions. *Bioprocess and Biosystems Engineering*, *36*(7), 975–984.

Shareefdeen, Z. and Singh, A. (Eds.). (2005). *Biotechnology for odor and air pollution control*. Heidelberg, Germany: Springer.

Snider, J. R. and Dawson, G. A. (1985). Tropospheric light alcohols, carbonyls, and acetonitrile: Concentrations in the southwestern United States and Henry's Law data. *Journal of Geophysical Research: Atmospheres*, *90*(D2), 3797–3805.

Staudinger, J. and Roberts, P. V. (1996). A critical review of Henry's law constants for environmental applications. *Critical Reviews in Environmental Science and Technology*, *26*(3), 205–297.

Staudinger, J. and Roberts, P. V. (2001). A critical compilation of Henry's law constant temperature dependence relations for organic compounds in dilute aqueous solutions. *Chemosphere*, *44*(4), 561–576.

van Krevelen, D. W. and Hoftijzer, P. J. (1948). Kinetics of simultaneous absorption and chemical reaction. *Chemical Engineering Progress*, *44*, 529–536.

Van't Riet, K. (1979). Review of Measuring Methods and Results in Nonviscous Gas-Liquid Mass Transfer in Stirred Vessels. *Industrial & Engineering Chemistry Process Design and Development*, *18*(3), 357–364.

Weiland, P. and Onken, U. (1981). Fluid dynamics and mass transfer in an airlift fermenter with external loop. *German Chemical Engineering*, *4*, 42–50.

8 STUDY OF MASS OXYGEN TRANSFER IN A BIOTRICKLING FILTER FOR AIR POLLUTION CONTROL

STUDY OF MASS OXYGEN TRANSFER IN A BIOTRICKLING FILTER FOR AIR POLLUTION CONTROL

Pau San-Valero, Carmen Gabaldón, Josep M. Penya-roja* & M. Carmen Pérez

Research Group GI^{2}AM, Department of Chemical Engineering, University of Valencia, Avda. Universitat s/n, 46100 Burjassot, Spain

*Corresponding author: josep.penarrocha@uv.es

Abstract

Biotrickling filtration is a potential and cost effective alternative for the treatment of volatile organic compound (VOC) emissions in air, so it is necessary to deepen into the key aspects of design and operation for the optimization of this technology. One of these factors is the oxygen mass transfer of the process. This study would facilitate the selection of the packing material and the mathematical modelling and simulation of bioreactors. Four plastic packing materials with a different specific surface area have been evaluated in terms of oxygen mass transfer. For the tested range of superficial liquid velocities, data show a relationship between the k_La and the superficial liquid velocity in all packing materials used, except for the biggest plastic rings. No significant differences in mass transfer coefficients at low liquid velocities were observed, however dependency between oxygen transfer and specific surface area increased considerably for high liquid velocities. No significant influences of the superficial air velocity were observed.

Keywords

Mass transfer; biotrickling filter; oxygen; volatile organic compounds

Procedia Eng 42 (2012) 1726 – 1730

8.1 INTRODUCTION

The abatement of volatile organic compound (VOC) emissions is a factor of protection of the environment and public health in Europe (European Union, 2010). As a consequence of these increasingly restrictive environmental regulations, treatment technologies for VOC removal are required. Since late 1990s there has been an emergent interest of research towards the biotrickling filter (BTF), which allows better control of the pH and offers smaller footprint compared to conventional biofilters. BTF uses an inert packing material and involves continuous or intermittent trickling of water. In this configuration, the biomass attaches to the media and develops a biofilm, thus, the pollutant and the oxygen will be transferred from the gas phase to the trickling liquid and then to the biofilm, where the biodegradation takes place. As it was pointed out (Popat y Deshusses, 2010; Kirchner et al., 1992) the mass transfer could be limiting the performance of the process, so the choice of a suitable packing is very important. In the same way, oxygen limitation could be occur (Kirchner et al., 1992; Alonso et al., 1998). This limitation could be especially vital for the treatment of high loads of VOCs hydrophilic compounds due to their higher partition coefficient than partition coefficient of the oxygen. In order to optimize the cost and efficiency of the BTF at industrial scale, a good gas-liquid contact is necessary. Determining the mass transfer coefficient would facilitate the selection of the packing material and the modelling of bioreactors used for air pollution control. Correlations commonly used for chemical absorption processes do not represent correctly the phenomenon occurred in BTFs due to the different hydrodynamic conditions of chemical absorption (Kim and Deshusses, 2008; Dorado et al., 2009).

8.2 MATERIALS AND METHODS

In this study, a dynamic method was used for the determination of $k_L a$. This method consists of measuring the evolution of the concentration of dissolved oxygen in the recirculation tank in which the oxygen has been previously displaced by bubbling nitrogen gas. The system consisted of a column of methacrylate (14.4 cm internal diameter, 80 cm height) and a recirculation tank. The column was filled with different propylene packing materials to be tested. In this case one structured

and three random packing materials with different size and superficial area have been used as can be seen in Table 8-1.

Table 8-1 Characteristics of the packing materials used*

			Size (mm)	Superficial area (m^2 m^{-3})
Packing 1		Structured	----	410
Packing 2	Plastic Rings	Random	15	348
Packing 3	Plastic Rings	Random	25	207
Packing 4	Plastic Rings	Random	50	110

As shown in Figure 8-1, the air stream was introduced through the bottom of the column. The flow rate was adjusted using a mass flow controller (Bronkhorst Hi-Tec, The Netherlands). The experiments were carried out for two air superficial velocities of 104 m h^{-1} and 312 m h^{-1} to evaluate the influence of air flow rate. The trickling water was recirculated in counter current mode, with a water superficial velocity between 3 and 33 m h^{-1}. The oxygen concentration in the liquid was determined using a dissolved oxygen probe (Cellox® 325i, WTW, Germany), for which the response time was considered.

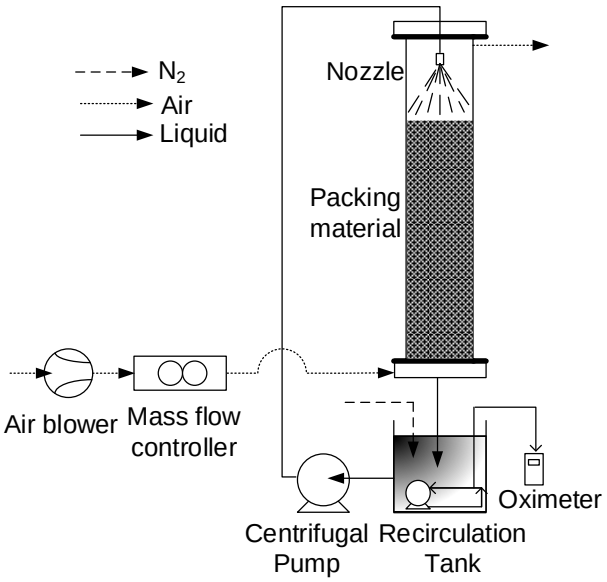

Figure 8-1 Experimental setup.

The value of k_La was calculated adjusting experimental data of dissolved oxygen concentration in the recirculation tank with theoretical values obtained from the oxygen mass balance in the tank, using the following equations:

$$\frac{dC}{dt} = \frac{1}{\theta}\left(C^* - \frac{\left(C^* - C\right)}{\exp\left(\frac{L}{v}k_L a\right)} - C \right) \tag{8-1}$$

$$\frac{dC_m}{dt} = \frac{\left(C - C_m\right)}{\tau} \tag{8-2}$$

where C is the real dissolved oxygen concentration in the recirculation tank, C_m is the measured dissolved oxygen concentration in the recirculation tank, C^* is the oxygen solubility experimentally determined, θ is the hydraulic residence time in the tank, τ is the response time constant of the probe (time that the probe achieves the 63.2% of the final value) and L and v are the height of the column and the velocity of the trickling water, respectively.

8.3 RESULTS AND DISCUSSION

The determination of oxygen mass transfer coefficients was carried out for each packing material at several liquid velocities, where k_La coefficients were obtained using least squares method to minimize the differences between the experimental data and the concentration of oxygen provided by the simple mathematical model established by the equations (1) and (2). Previously, the response time of the probe (τ) was determined by means of a step input assay, resulting in a value of 19.4 ±1.5 s.

For the tested range of superficial liquid velocities, data show a clear dependence of the k_La with the superficial liquid velocity for all tested packing material, except for the biggest plastic rings. As an example, besides, the influence of superficial liquid velocity versus the mass transfer coefficient for the two gas velocity tested in packing material 3 is shown in Figure 8-2. As can be observed, by

tripling the gas velocity were not observed significant differences between the data obtained. Thus, as was pointed by other authors (Kim and Deshusses, 2008; Piche et al., 2001) the oxygen mass transfer depends primarily on the superficial liquid velocity for each packing material. This implies that VOC treatment with biotrickling filtration was not affected by the gas velocity from the point of view of the oxygen transfer when the other conditions were kept constant.

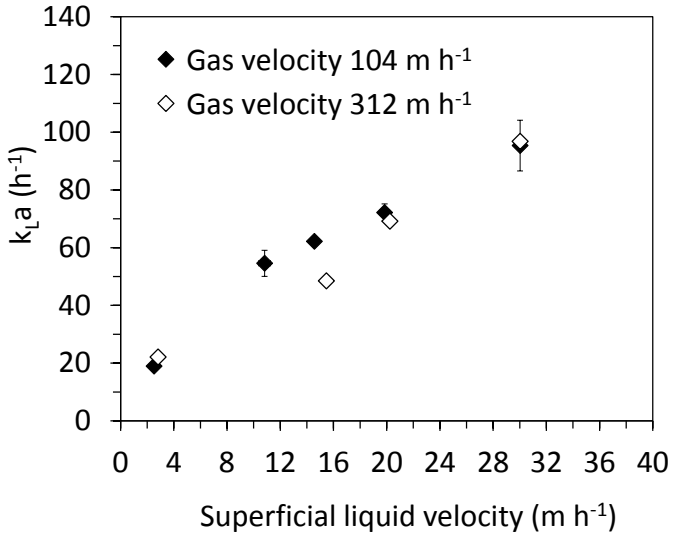

Figure 8-2 Influence of superficial liquid velocity and superficial air velocity on the oxygen mass transfer coefficient for the packing material number 3.

The behavior of each packing material on the oxygen mass transfer for the superficial liquid velocities was compared. The oxygen mass transfer coefficient obtained for low and high liquid velocities (3 and 30 m h^{-1}) for each packing material tested are shown in Figure 8-3 (6 and 30 m h^{-1} for packing material number 2).

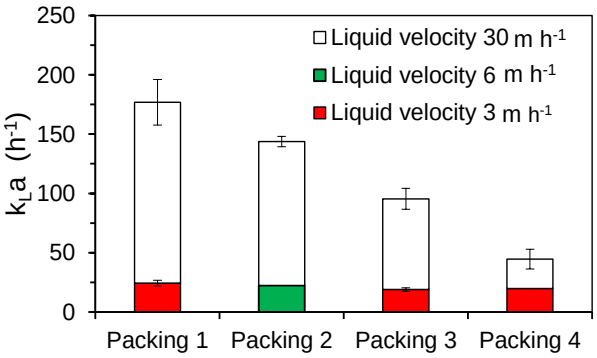

Figure 8-3 Influence of the liquid velocity on the oxygen mass transfer coefficient for each packing materials for high and low liquid velocities.

For the low liquid velocities, similar values of k_La were obtained. Thus, the influence of the specific surface area seems negligible under the tested conditions. However, for the liquid velocity of 30 m h^{-1}, large differences on the oxygen mass transfer coefficient were obtained for each packing material. This suggests that, at high liquid velocities, by increasing the specific surface area of the packing material is possible to enhance the oxygen mass transfer. So, the superficial liquid velocity is a key parameter in the operation of biotrickling filtration and oxygen mass transfer should be known for each packing material in order to optimize the performance of the process.

8.4 CONCLUSION

Results showed that oxygen mass transfer was strongly affected by superficial liquid velocities. No influence of gas velocity on the oxygen mass transfer was obtained. At low liquid velocities, no differences between packings were observed. At high liquid velocities, data show that higher values of specific surface area provide greater mass transfer coefficients for the tested range. Consequently, the study of oxygen mass transfer is a crucial factor in order to improve the biological performance of biotreatments for VOC elimination.

Acknowledgements

The research leading to these results has received funding from the People Programme (Marie Curie Actions) of the European Union's Seventh Framework Programme FP7/2007-2013/ under REA grant agreement nº 284949. Financial support from Ministerio de Ciencia e Innovación (Project CTM2010-15031/TECNO) and Generalitat Valenciana (ACOMP/2012/209), Spain, is also acknowledged. Pau San Valero acknowledges the Generalitat Valenciana, Spain (ACIF2011/067 contract).

8.5 REFERENCES

Alonso, C., Zhu, X., Suidan, M. T., Kim, B. R. and Kim, B. J. (1998). Modelling of the biodegradation process un a gas phase bioreactor-estimation of intrinsic parameters. In: F. E. Reynolds Jr. (Ed.), *Proc. 1998 USC-TRG Conference on Biofiltration* (pp. 211–218). Tustin, CA: The Reynolds Group.

Dorado, A. D., Rodriguez, G., Ribera, G., Bonsfills, A., Gabriel, D., Lafuente, J. and Gamisans, X. (2009). Evaluation of mass transfer coefficients in biotrickling filters: Experimental determination and comparison to correlations. *Chemical Engineering & Technology*, *32*(12), 1941–1950.

European Union. (2010). *Directive 2010/75/EU of the European Parliament and of the council of 24 November 2010 on industrial emissions (integrated pollution prevention and control) (Recast)*. *Official Journal of the European Union* (Vol. L334).

Kim, S. and Deshusses, M. A. (2008). Determination of mass transfer coefficients for packing materials used in biofilters and biotrickling filters for air pollution control. 1. Experimental results. *Chemical Engineering Science*, *63*(4), 841–855.

Kirchner, K., Wagner, S. and Rehm, H. J. (1992). Exhaust-gas purification using biocatalysts (fixed bacteria monocultures) -the influence of biofilm diffusion rate (O_2) on the overall reaction-rate. *Applied Microbiology and Biotechnology*, *37*(2), 277–279.

Piche, S., Grandjean, B. P. A., Iliuta, I. and Larachi, F. (2001). Interfacial mass transfer in randomly packed towers: A confident correlation for environmental applications. *Environmental Science & Technology*, *35*(24), 4817–4822.

Popat, S. C. and Deshusses, M. A. (2010). Analysis of the rate-limiting step of an anaerobic biotrickling filter removing TCE vapors. *Process Biochemistry*, *45*(4), 549–555.

9 DYNAMIC MATHEMATICAL MODELLING OF THE REMOVAL OF HYDROPHILIC VOCS BY BIOTRICKLING FILTERS

DYNAMIC MATHEMATICAL MODELLING OF THE REMOVAL OF HYDROPHILIC VOCs BY BIOTRICKLING FILTERS

Pau San-Valero, Josep M. Penya-roja, F. Javier Álvarez-Hornos, Paula Marzal & Carmen Gabaldón*

Research Group GI²AM, Department of Chemical Engineering, University of Valencia, Avda. Universitat s/n, 46100 Burjassot, Spain

*Corresponding author: carmen.gabaldon@uv.es

Abstract

A mathematical model for the simulation of the removal of hydrophilic compounds using biotrickling filtration was developed. The model takes into account that biotrickling filters operate by using an intermittent spraying pattern. During spraying periods, a mobile liquid phase was considered, while during non-spraying periods, a stagnant liquid phase was considered. The model was calibrated and validated with data from laboratory- and industrial-scale biotrickling filters. The laboratory experiments exhibited peaks of pollutants in the outlet of the biotrickling filter during spraying periods, while during non-spraying periods, near complete removal of the pollutant was achieved. The gaseous outlet emissions in the industrial biotrickling filter showed a buffered pattern; no peaks associated with spraying or with instantaneous variations of the flow rate or inlet emissions were observed. The model, which includes the prediction of the dissolved carbon in the water tank, has been proven as a very useful tool in identifying the governing processes of biotrickling filtration.

Keywords

Biotrickling filtration; air pollution control; volatile organic compounds; mathematical modelling

Int. J. Environ. Res. Public Health 2015, 12, 746-766

9.1 INTRODUCTION

Control of volatile organic compound (VOC) emissions from industry is nowadays a priority in air quality regulation. In the European Union (EU), Directive 1999/13/EC, recently modified by Directive 2010/75/EU, pursues the reduction of VOC emissions. According to data from the European Environment Agency, the sector of "solvents and product use" contributes 44% of the emissions of non-methane VOC in the EU; a reduction of 42% from 1990 to 2012 has been reported with a release of 2951 Gg in 2012 (European Environment Agency, 2014). The industrial use of solvents typically releases waste gas streams where the flow is high (>1000 $m^3\ h^{-1}$) and the VOC concentration is low (<5 g m^{-3}). Bioprocesses are best suited to the control of these emissions due to the low concentration of pollutants (Kennes et al., 2009). Among bioprocesses, biotrickling filtration is recommended for compounds with Henry's law constants below 0.1 (Kennes and Thalasso, 1998), such as ethanol, n-propanol or isopropanol, the main pollutants of the waste gas streams emitted from flexible food packaging industries (flexographic sector). A biotrickling filter (BTF) consists of a column filled with an inert packing material, where the biomass attaches to the media and develops a biofilm. In this configuration, the gas and liquid phases circulate through the column in co- or counter-current mode. Depending on the operation mode, the BTF process involves a continuous or intermittent trickling of water.

Despite the fact that BTFs have been successfully applied for the treatment of air pollutants, the use of BTFs depends on the increase of operational knowledge to allow the robustness of the performance. As has been recognized, the performance of BTF is markedly dependent on the operational conditions. Parameters, such as liquid velocity, gas velocity and empty bed residence time (EBRT) and inlet concentrations, may hinder the performance of field-scale BTFs (Webster et al., 1999; Zhu et al., 1998; Sempere et al., 2008). Thus, further research for a better understanding of the role of those parameters would be desirable (Kennes and Veiga, 2013). Several efforts have been made to adapt the operational conditions of laboratory experiments to emulate the operational conditions usually experienced in industrial applications (Sempere et al., 2008). One of the most common practices in industrial BTFs in comparison with laboratory studies is the use of intermittent trickling of water. San Valero et al. (2013) observed that a spraying regime of 15 min every 1.5 h resulted in peaks of concentration coinciding with the irrigation of the bed when treating isopropanol.

We concluded that the frequency of irrigation is a crucial parameter in terms of the achievement of low emissions under intermittent loading of highly-soluble compounds.

Biotrickling filtration involves a complex combination of several physical, chemical and biological processes; further investigation, in order to integrate the phenomena occurring during treatment, is required. Mathematical modelling is a fundamental tool in the development of an understanding of the process. Additionally, as pointed out by Lu et al. (2004), effective modelling can lead to the development of a trustworthy performance equation that decreases the time and cost of experimentation on the pilot scale. Thus, phenomenological models based on the main mechanisms on biofiltration seem to be useful in improving the understanding of BTFs and in identifying the governing processes involved in their operation. The phenomenological model most commonly used during the last few decades was developed by Ottengraf and van Den Oever (1983) for biofilters operating under steady-state conditions. Following this study, many models for biofilters have been reported in the literature, adding new phenomena, such as adsorption in the packing material and the inhibition kinetics of microbial growth, among others (Rene et al., 2013). As an example, Shareefdeen et al. (1993) included both oxygen and substrate inhibition effects; this model was improved by assuming the partial coverage of the support particles by biofilm and by modelling the adsorption on the uncovered particles by using the Freundlich isotherm (1994).

Most mathematical models of BTFs and trickle bed biofilters are based on mechanisms that have been used to describe biofilter behavior. Usually, a three-phase model (gas-liquid-biofilm) is used to describe these configurations. The main difference with biofilter models is related to the presence of a liquid phase, often simulated as an intermediate step between the gas phase and the biofilm. In steady state conditions, Mpanias and Baltzis (1998) were the first to develop a model that takes into account the kinetic limitations arising from the availability of VOCs and oxygen in BTF. This model was extended to VOC mixtures (2001). Concerning non-steady state conditions, Okkerse et al. (1999) presented a dynamic BTF model for the degradation of volatile acidifying pollutants, as well as mass accumulation and mass distribution along the column. Zhu et al. (1998) proposed a dynamic three-phase system with a non-uniform bacterial population to show the effect of mass transfer limitations due to the water phase in the reactor for the removal of diethyl ether. Kim and Deshusses (2003) developed a dynamic BTF model for the removal of H_2S with gas and liquid phase flowing counter-current, where the biofilm on the packing material was not completely

wetted. In this model, a fraction of the pollutant was transferred directly from the gas phase to the biofilm, while another fraction was transferred through the liquid phase to the biofilm. Recently, Almenglo et al. (2013) modified the Kim and Deshusses model by assuming a stagnant liquid fraction distributed homogeneously along the bed; mass balances in the biofilm were divided into "flowing" biofilm (which is in contact with flowing liquid) and "stagnant" biofilm (which is in contact with stagnant liquid). Lee and Heber (2010) proposed a model modified from that of Alonso et al. (1998) in order to develop a genetic algorithm to estimate the unknown parameters in ethylene removal. Iliuta et al. (2005) developed a predictive dynamic model in a trickle-bed bioreactor based on the macroscopic volume-averaged mass and momentum balance equations coupled with classical diffusion and bioreaction equations to illustrate the influence of biomass accumulation on a bioreactor for toluene removal. These authors showed that shifting from a biofilter to a trickle-bed bioreactor reduces the removal efficiency, due to an extra liquid-film mass transfer resistance step. However, despite the fact that these models provide valuable information on the understanding of the behavior of bioreactors, there is still a lack of information with respect to models adapted to industrial emissions characterized by an intermittent spraying pattern, variable gas flow rate and variable inlet concentration. In this regard, more effort is required to obtain more realistic simulations and to identify the main differences in the observed behavior between the laboratory scale and the industrial scale. As was pointed out by Devinny and Ramesh (2005), no single model has become generally accepted.

The aim of the present research is to go deeper into the intricacies of the treatment of hydrophilic compounds using biotrickling filtration technology. For this purpose, a mathematical model was developed to simulate the performance of BTFs, taking into account the main operational conditions found in the industry. The model presented herein was prepared for simulating systems with complex inlet concentration patterns, gas flow rates and cyclic conditions of spraying. An intermittent spraying regime implies that the liquid phase varies during the filter operation, making it necessary to distinguish two different situations, corresponding to spraying and non-spraying periods. In addition, the operation of BTF usually requires more than one spraying pattern during the same day related to periods with different feeding conditions or clogging control, among others. In this regard, the model is able to combine these two different patterns

The following objectives have been achieved: (1) developing a dynamic mathematical model based on different behaviors during spraying and non-spraying periods combined with variable inlet concentration and variable gas flow rate; (2) calibrating and validating the model with data from BTF at the laboratory scale using isopropanol as the target pollutant; and (3) validating the model with data from a BTF located in an industrial facility from the flexographic sector.

9.2 EXPERIMENTAL SECTION

9.2.1 Experimental setup and BTF operational conditions for the experiments at laboratory scale

Two sets of independent data were used to test the mathematical model. The first set corresponds to data from laboratory experiments using isopropanol as the target pollutant. The experiments were performed using a laboratory-scale BTF composed of three cylindrical methacrylate modules in series, with a total bed length of 100 cm and an internal diameter of 14.4 cm. The BTF was filled with a random packing material of 25 mm in diameter (Flexiring: superficial area (a) = 207 $m^2\ m^{-3}$; porosity of the packing material (θ_{PM}) = 0.92), using a volume of the bed of 16.32 L. The BTF had 20 cm of free spaces at the top and bottom of the column and was equipped with 3 equidistant sampling ports. The stream was contaminated with isopropanol, which was introduced through the bottom of the column. A recirculation solution was fed into the bioreactor in counter-current mode with respect to the air flow using a centrifugal pump at 2.5 L min^{-1} from a tank with 3.5 L of solution. An air stream polluted with VOCs was supplied to the BTF for 16 h per day (starting at 8:00 am), while the rest of the time (8 h), the BTF was supplied with clean air, maintaining a constant air flow rate. A BTF inoculated with activated sludge ran for more than 3 months with an inlet load (IL) of 30 g C $m^{-3}\ h^{-1}$, EBRT of 60 s and intermittent spraying. With this IL, two consecutive intermittent spraying patterns (Run 1 and Run 2) were applied during a minimum of a 2-week period. Table 9-1 summarizes the performance of the system during the last 5 days (from Monday to Friday) of each of the runs (1 and 2). Then, the inlet load was increased to 60 g C $m^{-3}\ h^{-1}$ for 2 weeks. Run 3 (Table 9-1) summarizes the performance of the system during the final week (from Monday to Wednesday). Each run started with clean water in the recirculation tank. No purges were undertaken until the end of each run. The pressure drop was negligible (<1 Pa m^{-1}). The liquid hold-up (θ_L) had an average value of 0.093 ±

0.003. The biofilm content was gravimetrically determined (mass contained in two rings extracted from each of the three sampling ports). The volume fraction of the biofilm (θ_B) calculated from the biofilm content of the bioreactor (specific gravity of 1) resulted in a value of 0.18 ± 0.04. The water content of the biofilm was measured as 95 ± 3%; 50 kg m^{-3} of biomass concentration (X_V), which was selected as the average value for modelling purposes.

Table 9-1 Overall performance of the laboratory-scale experiments. EBRT, empty bed residence time.

	Inlet load [a] (g C m^{-3} h^{-1})	**EBRT (s)**	**Spraying Pattern**	**Elimination Capacity [a] (g C m^{-3} h^{-1})**	**Removal Efficiency [a] (%)**
Run 1	32.6	60	1 h every 4 h	29.8	91
Run 2	32.0	60	30 min every 4 h	29.7	93
Run 3	59.6	60	1 h every 4 h	53.6	90

[a] Average value from periods during pollutant feeding (16 h d^{-1}).

9.2.2 Experimental setup and BTF operational conditions for the field scale

Data from an industrial BTF (VOCUS™, PAS Solutions BV, the Netherlands) located at a flexographic industry site were used. The waste gas stream was composed of a mixture of VOCs (63% ethanol, 22% ethyl acetate, 13% 1-ethoxy-2-propanol). The manufacturing shift of this industrial site was 18 h of emissions per day (from 6 to 24 h) during 5 days a week (working days), with several emission sources. The BTF system consisted of a packed reactor with a volume of 49 m^3 filled with polypropylene rings (Flexiring 50 mm: a = 102 m^2 m^{-3}; θ_{PM} = 0.93), plus a recirculation tank with a maximum water capacity of 15 m^3. The bioreactor was operated in counter-current mode; air from the factory was blown into the bottom of the column continuously (polluted air for 18 h per day and clean air for 6 h per day). The BTF began operating in June 2009. Two sets of data (from Monday to Thursday) with different spraying frequency (October 2009, and January 2011) were selected (Table 9-2). During weekends, clean air was blown on the BTF, and the spraying frequency was kept the same as those applied during non-VOC feeding periods in working days in order to promote the removal of the accumulated VOCs in the water tank. Volumes of water in the recirculation tank were 6.5 and 12.8 m^3 (25% of the volume renewed with fresh water on Sundays),

and the liquid flow rates were 30 and 32 $m^3\ h^{-1}$ for Run 4 and Run 5, respectively. The pressure drop was lower than 15 Pa m^{-1}. The system worked for more than 3 months under each of the selected conditions. Table 9-2 summarizes the performance of the system during the 4 days of each run. The volume fraction of the mobile liquid phase in the bioreactor was approached by measuring the quantity of accumulated water in the bioreactor during spraying; a value of 0.05 was obtained (θ_L).

Table 9-2 Overall performance of the industrial biotrickling filter (BTF).

	Date	Inlet Load[a] (g C $m^{-3}\ h^{-1}$)	Gas Flow Rate[a] ($m^{-3}\ h^{-1}$)	Spraying Pattern		Elimination Capacity [a] (g C $m^{-3}\ h^{-1}$)	Removal Efficiency [a] (%)
				0–6 am	6 am–12 pm		
Run 4	October 2009	27.5	1675	6 min every 21 min	6 min every 21 min	17.9	65
Run 5	January 2011	46.5	2717	6 min every 1 h	6 min every 3 h	29.1	63

[a] Average value from periods during pollutant feeding (18 h d^{-1}).

9.2.3 Analytical methods

In the laboratory experiments, the gas concentration of isopropanol was measured using a total hydrocarbon analyzer (Nira Mercury 901, Spirax Sarco, Spain). The response factor of the total hydrocarbon analyzer was determined by gas chromatography (model 7890, Agilent Technologies, USA). The determination of the total organic carbon (TOC) in water was measured using a total organic carbon analyzer (TOC-V_{CHS}, Shimadzu Corporation, Japan). At the industrial scale, the inlet and outlet gas VOC concentrations were continuously monitored using a total hydrocarbon analyzer (RS 53-T, Ratfisch Analysensysteme GmbH, Germany). The air flowed during the whole day, and the air flow rate was monitored continuously by using a pitot tube (19" pitot tube, Testo AG, Germany).

9.2.4 Model development

The model was based on the fact that BTFs are usually operated in intermittent spraying mode. The intermittent spraying regime implies two different behaviors of the system. Thus, a mobile liquid phase and a stagnant liquid phase were considered during the spraying period and non-spraying period, respectively. Thus, a three-phase model (gas-liquid-biofilm) is proposed here based on the mass balances of the gas and liquid phases and the biofilm. Two different systems of partial differential equations were used, depending on whether the spraying or the non-spraying period was simulated. The conceptual scheme of the BTF and the model derivation are shown in Figure 9-1. For model development, the following assumptions were made:

(1) The gas phase flows in a plug flow regime along the filter bed.

(2) Axial dispersion is neglected.

(3) The adsorption of pollutant in the packing material is negligible.

(4) The active biofilm is formed on the external surface of the packing material, and no reaction occurs in the pores. The biofilm covers the surface of the packing material, and its thickness (δ) is much smaller than the size of the solid particles, so a planar geometry is assumed.

(5) The packing material is completely covered by the biofilm.

(6) The biodegradation kinetics are described by a Monod expression, indicating the oxygen limitation.

(7) The diffusion inside of the biofilm is described by Fick's second law.

(8) A mobile liquid phase is assumed during the spraying period, and a stagnant liquid phase is considered during the non-spraying period.

(9) The gas-liquid interface is in equilibrium according to Henry's law.

(10) The mass flux at the gas-liquid and the liquid-biofilm interfaces can be expressed by mass transfer coefficients.

(11) The presence of biomass in the bioreactor increases resistance to the mass transfer between the gas and the liquid phase. Thus, the overall mass transfer coefficients experimentally determined in abiotic conditions are corrected by a factor (α_1) varying between 0 and 1.

(12) There is no reaction in the liquid phase.

According to the assumptions made above, the mass balances during both periods are described in the next subsection.

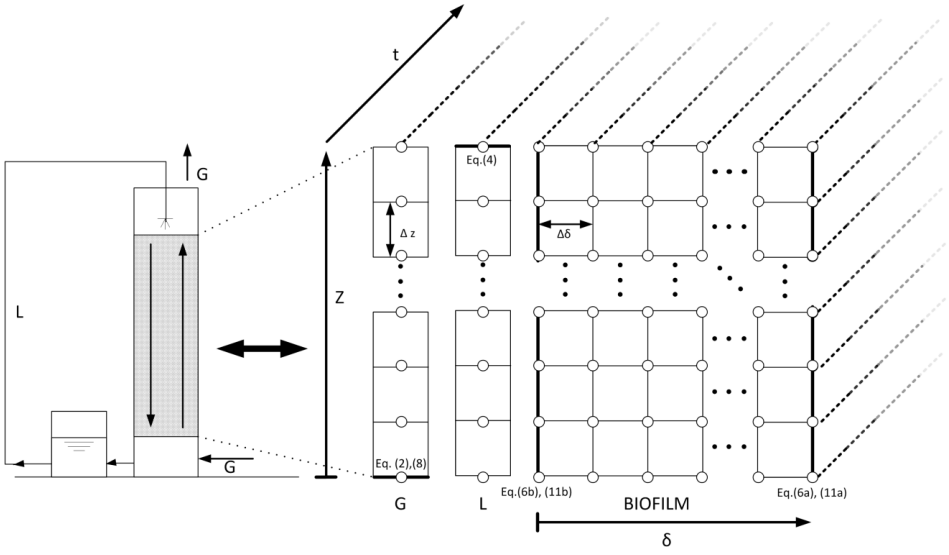

Figure 9-1 Conceptual scheme of the BTF and model derivation. Bold lines indicate the boundary conditions. Eq. means equation.

9.2.4.1 *Mass Balances during the Spraying Period*

During the spraying period, the pollutant and the oxygen are transferred from the gas phase to the mobile liquid phase and then to the biofilm, where the biodegradation takes place. The mass balance of the gas phase is described according to Equation (9-1) for a system in counter-current operation:

$$\theta_G \frac{\partial C_{G_i}}{\partial t} = -v_G \frac{\partial C_{G_i}}{\partial z} - \alpha_1 K_L a_i \left(\frac{C_{G_i}}{H_i} - C_{L_i} \right) \tag{9-1}$$

where *i* denotes the pollutant (*P*) or the oxygen (*O*). Thus, for component *i*, C_{Gi} and C_{Li} are the concentrations of gas and liquid phases, respectively; $K_L a_i$ is the overall mass transfer coefficient; H_i represents the dimensionless Henry's law constants expressed as the concentration of the gas phase/concentration of the liquid phase; *t* denotes time; *z* is the distance from the bottom of the column; v_G is the superficial air velocity; and θ_G is the porosity of the bed calculated as $\theta_G = \theta_{PM} - \theta_L - \theta_B$.

The boundary condition of Equation (9-1) is given by:

$$z = 0 \qquad C_G = C_{G_i}^{in} \tag{9-2}$$

where C_{Gi}^{in} is the inlet concentration of the component *i*.

The mass balance of the mobile liquid phase is given by:

$$\theta_L \frac{\partial C_{L_i}}{\partial t} = v_L \frac{\partial C_{L_i}}{\partial z} + \alpha_1 K_L a_i \left(\frac{C_{G_i}}{H_i} - C_{L_i} \right) - \frac{D_i a}{\beta} (C_{L_i} - S_{i,1}) \tag{9-3}$$

where for component *i*, D_i is the diffusion coefficient in water; $S_{i,1}$ is the concentration in the biofilm interface; v_L is the superficial liquid velocity; and β is the thickness of the liquid-biofilm interface.

The boundary condition of Equation (9-3) is given by the mass balance in the recirculation tank:

$$z = Z \qquad \frac{\partial C_{L_i}}{\partial t} = \frac{Q_L}{V_T} (C_{L_{i_{z=0}}} - C_{L_{i_{z=Z}}}) \tag{9-4}$$

where *Z* is the height of the column; Q_L is the liquid flow rate; and V_T is the volume of the recirculation tank. $C_{Li\ z=0}$ and $C_{Li\ z=Z}$ are the concentrations of the component *i* in the liquid phase at the bottom and top of the column, respectively.

The mass balance of the biofilm is given by:

$$\frac{\partial S_i}{\partial t} = f(X_v) D_i \frac{\partial^2 S_i}{\partial x^2} - \frac{\mu_{\max} X_v}{Y_i} \frac{S_P}{S_P + K_P} \frac{S_O}{S_O + K_O} \tag{9-5}$$

where S_i is the concentration inside the biofilm of component *i*; $f(X_v)$ is the correction factor of the diffusivities in water due to the biomass calculated by Fan's equation (Fan et al., 1990); X_v is the concentration of the biomass; μ_{max} is the specific growth rate of the biomass; K_P and K_O are the half-saturation constants of the pollutant and oxygen, respectively; and, for component *i*, Y_i is the yield coefficient.

The boundary conditions for the mass balance of the biofilm are given by:

$$x = \delta \qquad \frac{\partial S_i}{\partial x} = 0 \tag{9-6a}$$

$$x = 0 \qquad S_i = C_{L_i} \tag{9-6b}$$

where δ is the biofilm thickness.

9.2.4.2 *Mass Balances during the Non-Spraying Periods*

During the period without spraying, the pollutant and the oxygen are transferred from the gas phase to the stagnant liquid phase and then to the biofilm, where biodegradation takes place. The according mass balances are presented below.

The mass balance of the gas phase is given by Equation (9-7):

$$\theta_G \frac{\partial C_{G_i}}{\partial t} = -v_G \frac{\partial C_{G_i}}{\partial z} - \alpha_2 \alpha_1 K_L a_i \left(\frac{C_{G_i}}{H_i} - C_{L_i} \right) \tag{9-7}$$

where α_2 is a switch parameter that weights the gas-liquid mass transfer resistance. A value of 100 is assumed to indicate that the gas-liquid mass transfer resistance is negligible. A value of 1 indicates that a resistance to the gas-liquid mass transfer contributes to reducing the pollutant max flux diffusing to/from the biofilm.

The boundary condition of Equation (9-7) is given by:

$$z = 0 \qquad C_G = C_G^{in} \tag{9-8}$$

The mass balance of the stagnant liquid phase is given by:

$$\theta_L \frac{\partial C_{L_i}}{\partial t} = \alpha_2 \alpha_1 K_L a_i \left(\frac{C_{G_i}}{H_i} - C_{L_i} \right) - \frac{D_i a}{\beta} (C_{L_i} - S_{i,1}) \tag{9-9}$$

The mass balance in the biofilm is given by:

$$\frac{\partial S_i}{\partial t} = f(X_v) D_i \frac{\partial^2 S_i}{\partial x^2} - \frac{\mu_{\max} X_v}{Y_i} \frac{S_P}{S_P + K_P} \frac{S_O}{S_O + K_O} \tag{9-10}$$

with the boundary conditions:

$$x = \delta \qquad \frac{\partial S_i}{\partial x} = 0 \tag{9-11a}$$

$$x = 0 \qquad S_i = C_{L_i} \tag{9-11b}$$

9.2.4.3 *Numerical Solution*

The partial differential equations given above constitute two second-order nonlinear distributed systems. In order to solve them, the method of lines (MOL) was chosen. For a numerical problem solution, *Z* is divided into *N* sections with *N + 1* equi-spaced node points. Similarly, the biofilm thickness is divided into M sections with *M + 1* points, resulting in two ordinary differential equation (ODE) systems of *2(N + 1)(M + 3)* equations. The next step is to discretize the spatial variables. The parameters of *N* and *M* were optimized as 20 and 40, respectively. The resulting ODE systems were found to be stiff. Therefore, they were integrated using the *ode23t* function of MATLAB®.

9.3 RESULTS AND DISCUSSION

9.3.1 Model calibration

The calibration of the mathematical model presented herein was carried out with the experimental Run 1 (Table 9-1). Figure 9-2 shows the monitoring of the pollutant concentration in the gas phase (a.1) and the evolution of the dissolved carbon concentration in the water tank (a.2) from Monday to Friday (0 to 120 h). In Figure 9-2(a.1 and a.2), time 0 h refers to Monday 8:00 am. As an example of the daily patterns, data for Wednesday (48 to 72 h) is shown in Figure 9-2(b.1 and b.2). As is shown in Figure 9-2(a.1 and b.1), the outlet gas stream exhibited peaks of pollutant emission coinciding with the spraying periods (six peaks per day). During the periods without spraying, nearly complete removal of the pollutant was obtained. For every day, a similar dynamic pattern was observed. During the feeding of air polluted with VOC (0–16 h), the pollutant leak associated with the first spraying of each day (0 h) was much lower than the rest of the peaks. The leak increased during the second spraying (4 h), reaching a quasi-stable maximum during the third and fourth spraying (8 h, 12 h). After cutting off

the supply of VOC (at 16 h), the immediate peak (16 h) was similar to those obtained previously, but after some hours, the outlet gas emission during spraying was drastically reduced (20 h). The evolution of the peaks during the non-VOC feeding period indicated that the accumulated substrate in the system was consumed; the gas-phase leak at 20 h of each day was nearly in equilibrium with the organic liquid concentration in the tank. The dissolved carbon concentration in the water tank was monitored during spraying at working hours on alternate days (Figure 9-2(a.2, b.2)). As can be seen, the daily concentration increased with each spraying, indicating that the pollutant is absorbed in water. The outlet gas emissions of the second to fifth daily peaks were more than three-times higher than the predicted equilibrium concentration with the dissolved carbon concentration in the water. The variations of the liquid concentration in the recirculation tank between days indicated that the accumulated pollutant in water would be degraded in the BTF during spraying in night periods (16–24 h).

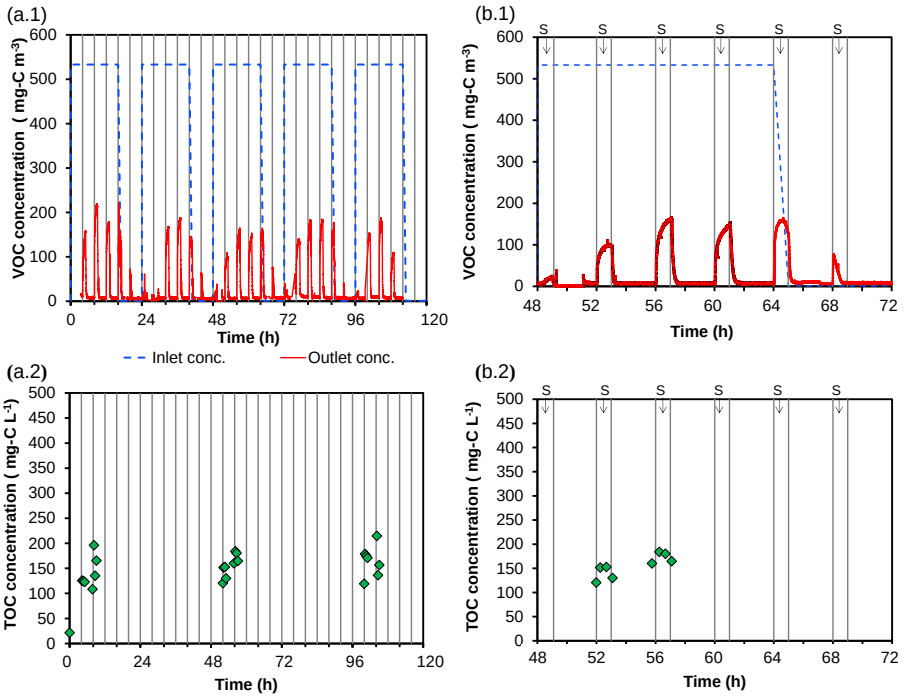

Figure 9-2 Experimental data of Run 1 (Monday to Friday), where each central line denotes a spraying: (a.1) concentration of VOC in the gas phase; (a.2) concentration of the dissolved carbon in the water tank. Wednesday results, where S denotes the spraying periods: (b.1) concentration of VOC in the gas phase; (b.2) concentration of the dissolved carbon in the water tank.

The parameters for the calibration of the model are summarized in Table 9-3. The values of physical constants, diffusivities in water and Henry's law constants have been taken from the literature. The overall mass transfer coefficients of the abiotic system were estimated using the experimental correlations proposed in San-Valero et al. (2014) for the operational conditions used in the present work. Biofilm thickness was assumed to be *60 μm*. The yield coefficient of the isopropanol was taken from the literature, and the yield coefficient of the oxygen was calculated using the stoichiometric balance.

Table 9-3 Parameters used in the modelling of BTF at the laboratory scale.

Parameters	Specific Value	Reference
Physical properties		
D_P (m^2 s^{-1})	1.13×10^{-9}	(Tucker and Nelken, 1982)
D_O (m^2 s^{-1})	2.0×10^{-9}	(Reid et al., 1987)
H_P	2.8×10^{-4}	(San-Valero et al., 2014)
H_O	31.4	(Sander, 2005)
K_La_P (s^{-1})	2.98×10^{-5}	Using correlation in (San-Valero et al., 2014)
K_La_O (s^{-1})	0.0126	Using correlation in (San-Valero et al., 2014)
Biofilm properties		
δ (m)	60×10^{-6}	This work
β (m)	3.8×10^{-6}	This work
Kinetic data		
f(Xv)	0.3495	(Fan et al., 1990)
Ko	0.26	(Shareefdeen and Baltzis, 1994)
Y_P	0.48	(Lu et al., 2004)
Yo	0.14	Stoichiometric balance
μ_{max} (s^{-1})	2×10^{-5}	This work
Ks_P (g C m^{-3})	350	This work

With this set of parameters, the calibration process started by determining the values of the thickness of the liquid-biofilm interface (β) and the biokinetic parameters (μ_{max}, K_{sP}) that predict the experimental evolution of the outlet concentration and the dissolved carbon in the water tank. During non-spraying, the mass transfer resistance between the gas and stagnant liquid was considered negligible (α_2 = 100), and during spraying, the gas-liquid mass transfer resistance

was assumed to be equal to that determined under abiotic conditions (α_1 = 1). The value proposed for μ_{max}, herein, 2 × 10^{-5} s^{-1}, appears to be in agreement with the values obtained in the literature for the treatment of isopropanol. Bustard *et al.* (2002) compiled data from different models proposed by different authors, with values ranging between 1.77 × 10^{-5} s^{-1} and 2.58 × 10^{-5} s^{-1}. The relative error deviation between experimental elimination capacity (EC) (29.8 g C m^{-3} h^{-1}) and simulated EC (31.8 g C m^{-3} h^{-1}) for Run 1 was 6.7%, indicating the feasibility of the model to reproduce the overall removal, although the dynamic pattern deviated from the experimental one. As an example, Figure 9-3 shows the results for Wednesday (48 to 72 h). The model predicts the existence of pollutant peaks associated with the mass transfer resistance of the gas-liquid film. The model predicts the sharp decrease of the gas-phase outlet concentration after spraying stops, corroborating that mass transfer resistance during non-spraying was negligible. The coupling of the spraying and non-spraying set of equations also predicts the periodical decrease of the dissolved carbon concentration in the water tank when the BTF works using clean air (from 64 to 72 h in Figure 9-3). This behavior is associated with the VOC desorption from the liquid to the gas phase and its biodegradation in the biofilm. However, the model underestimates the concentration of the outlet emissions in the case of the second to fifth peaks. In a second stage, the gas-liquid mass transfer flux was reduced by applying a correction factor in order to predict the maximum peak (α_1 = 0.23). As can be seen in Figure 9-3, this increase in the resistance to mass transfer overestimates the first two peaks after VOC feeding resumption after 8 h running with clean air. Experimental data indicated that the supply of VOCs, followed by long non-supply VOC periods (8 h per day), caused a cyclical variation in the resistance to mass transfer between the gas phase and liquid phase over time. This variation could be associated with a transient evolution in the physical properties due to biological reactions. For example, the accumulation of water and extracellular polymeric substances (EPS) could act as a periodical transfer barrier, deteriorating the removal efficiency of the system. When clean air was supplied, the accumulated VOC in the system could be biodegraded, and part of the formed EPS could disappear from the system, linked to the consumption by the microorganisms. In this regard, Zhang and Bishop (2003) suggested that EPS could be used as a substrate and concluded that EPS was biodegradable by its own producers, as well as by other microorganisms, during periods without feeding of VOC.

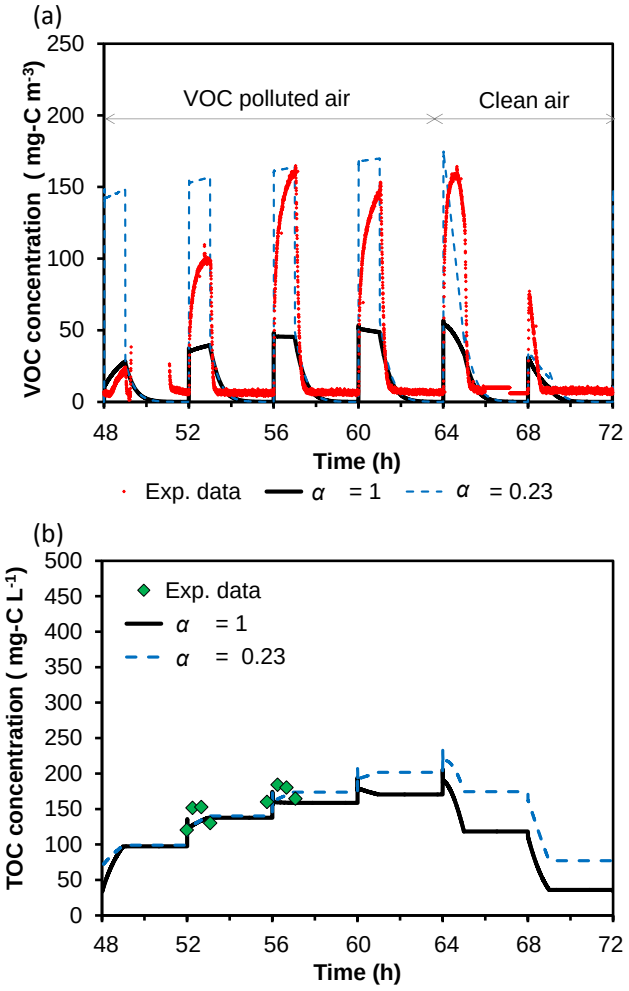

Figure 9-3 Influence of the parameter α_1 on the model predictions of Wednesday data (Run 1). (a) Outlet concentration of VOC in the gas phase. (b) Concentration of the dissolved carbon in the water tank.

The calibration of the model ends by fitting the daily variation of the correction factor of gas-liquid mass transfer resistance over time. The same daily variation was assumed for the five days of Run 1. The results of the model calibration are shown in Figure 9-4 (five days of Run 1). Figure 9-4(b.1 and b.2) zoom in on the plot of the Wednesday data (48 to 72 h), and values of α_1 are labelled. By using the proposed approach herein, the relative error (for the whole of Run 1) between experimental EC (29.8 g C m^{-3} h^{-1}) and simulated EC (30.5 g C

m^{-3} h^{-1}) was improved by 2.3%. The model is able to better predict the dynamic variations in the outlet gas-phase emissions and in the dissolved carbon concentration in the recirculation tank than in previous calibration steps.

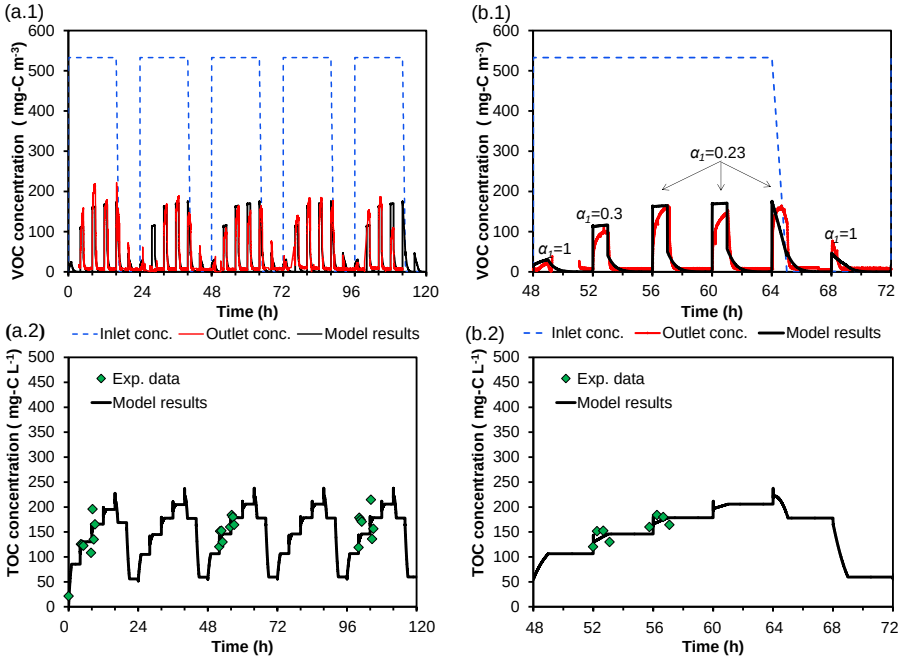

Figure 9-4 Weekly evolution of experimental data (Run 1) and model predictions for the treatment of isopropanol by a BTF. (a.1) concentration of VOC in the gas phase; (a.2) concentration of the dissolved carbon in the water tank. Wednesday results: (b.1) concentration of VOC in the gas phase; (b.2) concentration of the dissolved carbon in the water tank. Conc. means concentration and Exp. means experimental.

9.3.2 Model validation

The mathematical model was validated by using two sets of independent experiments at the laboratory scale (Run 2 and Run 3, Table 9-1) to check the capability of the model to predict the evolution of the system over five days and three days, respectively. Experimental data along with the results of the model simulations are shown in Figure 9-5. The model is capable of reproducing the cyclical performance by using a different spraying duration (Run 2) or inlet load (Run 3). The relative error between experimental EC and simulated EC was 3.7% and 2.4% for Run 2 and Run 3, respectively. In both cases, the model shows a daily

evolution of the outlet gas-phase concentrations: the gradual increase of the peaks when the air polluted with VOC is supplied to the BTF and its decrease when clean air is supplied; the model successfully predicts the available experimental data regarding outlet VOC emissions. The model also simulates the variations of the dissolved carbon in the water tank: the accumulation of dissolved carbon when the BTF is fed with VOC-polluted air and its decrease when clean air is used, showing good agreement with the available experimental TOC concentrations. For example, the model predicts the increase of the experimental organic carbon concentration from 55 (after purging the tank at 52 h) to ~400 mg C L^{-1} after the third daily spraying during Run 3. In spite of increasing the driving force, the intermediate purge had a negligible impact on the outlet VOC emissions (a similar experimental peak was obtained at the third daily spraying of Days 2 and 3). This corroborates that the gas-phase emission during spraying could be associated with the high resistance of the gas-liquid mass transfer.

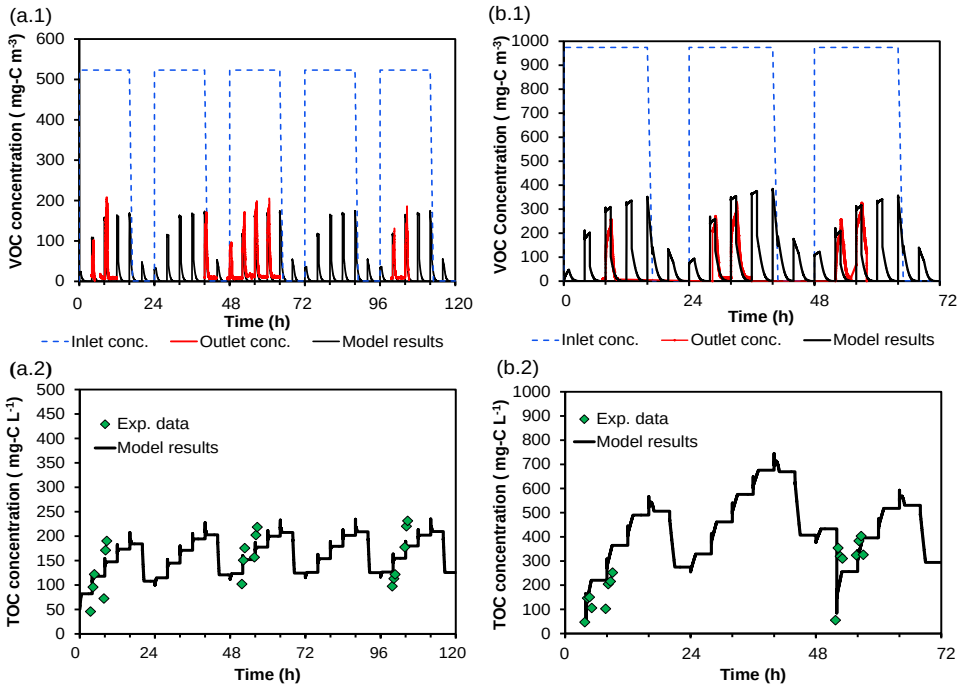

Figure 9-5 Weekly evolution of the experimental data and model predictions for the treatment of isopropanol by BTF (a) Run 2. (a.1) gas phase; (a.2) dissolved carbon in the water tank. (b) Run 3. (b.1) gas phase; (b.2) dissolved carbon in the water tank.

9.3.3 Model simulations

To assess the impact of the calibration parameters, μ_{max}, β and K_s, on the VOC outlet concentration and on the concentration of the dissolved carbon in the water tank, model simulations were carried out modifying by ±50% each parameter individually from the value listed in Table 3. The rest of the model parameters are listed in Table 9-3. Figure 9-6 shows the application of this study to Run 1 (Wednesday data, 48 to 72 h). When μ_{max} was increased to 50%, the model predicted lower values in the maximum concentration of the gas phase during the spraying periods (161 mg C m^{-3}). The predicted concentrations of the dissolved carbon in the water tank were lower (178 mg C L^{-1}) than those obtained with the optimal value (224 mg C L^{-1}) of μ_{max}, while during the periods fed with clean air, the dissolved carbon concentration decreased faster (24 mg C L^{-1}) than that obtained with the calibrated value (58 mg C L^{-1}). In contrast, when the μ_{max} was decreased by 50%, higher peaks were obtained during spraying periods (max peak 187 mg C m^{-3}). It is important to note that the decreasing of the outlet concentration after a spraying was slower than the experimental decrease, indicating that the process was controlled by the kinetics. The dissolved carbon concentration was higher (320 mg C L^{-1}) than that obtained with the optimal value of μ_{max}. When β was increased up to 50%, greater concentrations in the gas and in the liquid phase were obtained (max values 182 mg C m^{-3} and 281 mg C L^{-1}, respectively); while β was decreased by 50%, lower peaks in the outlet gas phase and a lower concentration in the water tank were achieved (max values 153 mg C m^{-3} and 140 mg C L^{-1}, respectively). The parameter β is related to the transfer of pollutant and oxygen between liquid and biofilm, and this analysis shows that this parameter is one of the most sensitive in the modelling of the treatment of isopropanol by BTF. When K_s was modified ±50%, the model appeared less sensitive to modifications of this parameter, obtaining a neglecting effect in the gas phase and less impact in the concentration of the dissolved carbon in the water tank than with the other parameters.

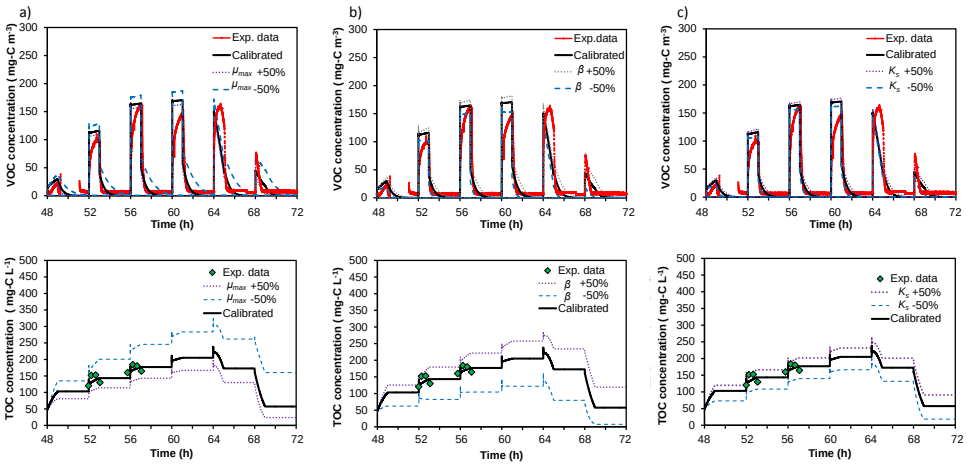

Figure 9-6 Effect of (a) μ_{max}, (b) β and (c) K_s on the outlet gas-phase concentration and on the dissolved carbon concentration in the recirculation tank. Experimental data correspond to the Wednesday data (48 to 72 h) of Run 1**.**

9.3.4 Model application to industrial unit processes

The model proposed herein was applied by using experimental data from two different periods from an industrial BTF located at a flexographic industry site (Run 4 and Run 5). Experimental data from both runs have a two-year spacing. Table 9-4 shows the VOC composition of the industrial emission and the diffusion coefficient in water and Henry's law constant for each compound that composed the VOC emission. Figure 9-7 shows the experimental data and the model simulations for both runs. In this figure, time 0 h refers to Monday 00:00 am. In contrast to those obtained in the laboratory experiments, the gaseous outlet emissions showed a buffered pattern, and no peaks associated with spraying or with instantaneous variations of the flow rate or inlet emissions were observed. During VOC inlet emissions coming from the factory (from 6:00 am to 12:00 pm), the outlet gas concentrations of the BTF were not clearly related to the spraying pattern; a continuous gradual increase of them was observed every day. During night periods (from 00:00 to 6:00 am), a slow decrease in the outlet emissions was observed; the VOC accumulated in the biofilm during periods receiving inlet emissions was not totally stripped or degraded over 6 hours, while when the bioreactor was operated with clear air for more than 24 h (weekends), the outlet gas concentration became negligible (data between 0 and 6 h in Figure 9-7). The

industrial BTF was acting as an absorption-desorption system during VOC feeding-non-VOC feeding cycles. This seems to indicate that there is a difference in the rate-limiting steps between the treatment of hydrophilic VOC by biotrickling filtration at the industrial scale and for laboratory units. This finding was one of the challenges of this work. Based on these two observations (no peaks during spraying and continuous outlet emissions during non-VOC feeding periods), it was assumed that: (1) there was an extra mass transfer resistance between the gas and liquid phases during non-spraying periods not observed in the laboratory experiments; and (2) a thick biofilm was developed.

Table 9-4 VOC composition and physical properties of the compounds of the industrial emission.

Compounds	Composition (%)	D_P ($m^2\ s^{-1}$) (Tucker and Nelken, 1982)	H_P (Sander, 2005)
Ethanol	63	1.48×10^{-9}	2.30×10^{-4}
Ethyl acetate	22	9.57×10^{-10}	6.40×10^{-3}
1-Ethoxy-2-propanol	13	8.49×10^{-10}	1.00×10^{-6} *

* Data estimated from (US EPA, 2013)

The simulation parameters for the application of the model to the industrial unit processes are listed in Table 9-3, except the overall mass transfer coefficients and the biofilm thickness. As the industrial BTF worked under conditions of variable gas velocities, the overall mass transfer coefficient for the pollutant was estimated for each simulated time point, applying the correlation proposed by San-Valero et al. (2014), using the gas velocity and the weighted average value of Henry's law constant of the VOC mixture (Equation (9-12)). This weighted average Henry's law constant was calculated using the percentage composition of each compound and its Henry's law constant (Table 9-4).

$$K_L a_P = \frac{H_P}{3600}\left(11.59\left(v_G 3600\right)^{0.85}\right) \tag{9-12}$$

The overall mass transfer of oxygen was experimentally determined in the laboratory, obtaining a value of 0.0066 s^{-1} for this packing material. The biofilm thickness (δ) was fitted to 500 µm in order to reproduce the slow desorption occurring during periods without supplying VOCs (every day from 0 am to 6 am). During spraying, it was assumed that there is similar mass transfer resistance to that in the laboratory systems (α_1 = 0.23). The emergence of the extra mass

transfer resistance during non-spraying was related to the creation of a stagnant liquid phase. The switch parameter α_2 was set to one to consider the resistance to mass transfer within the gas-liquid interface during non-spraying periods. Simulation of both runs started with clean water (VOC accumulated in the water tank during working days was removed at the weekend). In the case of Run 5, the recirculation tank on Wednesday at 4 pm (64 h of Run 5 in Figure 9-7) was renewed with fresh water; this was included in the simulation.

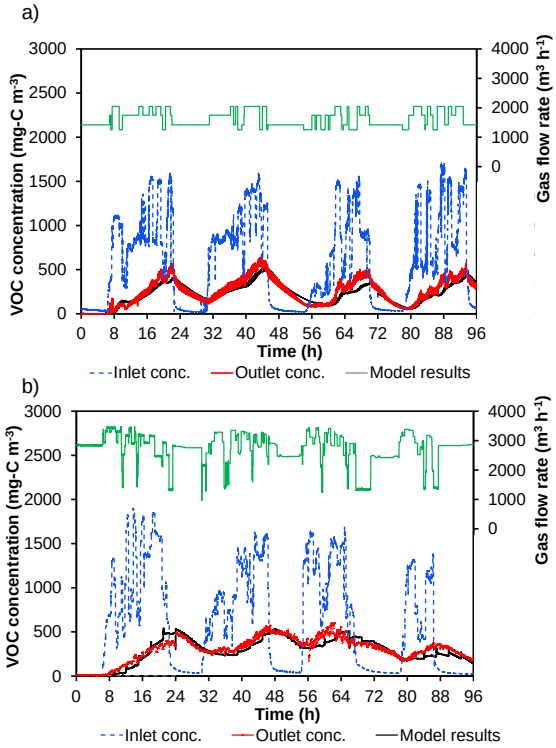

Figure 9-7 Experimental data and model results of the industrial BTF installed in a flexographic industry site: (a) Run 4 (b) Run 5.

As can be seen in Figure 9-7, the correspondence between the calculated and the experimental VOC emissions is quite good. Relative errors between simulated and experimental data were 1.6% and 2.2% for Run 4 and Run 5, respectively. During the course of the biological process, VOCs were degraded, but a part of the load is cyclically absorbed-desorbed following the daily cycles of VOC feeding-non VOC feeding. The thick biofilm works as the sink (every day from 6 am

to 12 pm) and source (every day from 0 am to 6 am) of the pollutant. The dynamic mathematical model approaches these phenomena through the existence of two resistances in series (gas-liquid, liquid-biofilm) that keep constant by operating the BTF with or without irrigation. This work appears as one of the first attempts to go more deeply into the modelling of the dynamic response associated with intermittent conditions (irrigation and inlet emissions), focusing on the observed differences between laboratory and industrial BTFs. In future work, the results of the model could be integrated into a software tool for the design and control of industrial BTFs.

9.4 CONCLUSIONS

A dynamic general model to simulate the removal of isopropanol emissions by biotrickling filtration has been developed. The model was built as a coupled set of equations for spraying and non-spraying periods in order to represent the intermittent irrigation usually performed in industrial applications. The model has been evaluated by using laboratory experiments working under intermittent spraying and intermittent VOC feeding to the bioreactor. The model predicts not only the overall performance, but also the outlet emission peaks occurring during spraying and the sharp decrease of gas-phase outlet concentration after spraying stops, indicating that mass transfer resistance during non-spraying was negligible. Practical applications of this model to predict the outlet VOC emissions in industrial BTF treating a mixture of pollutants were demonstrated. In this case, the thick biofilm and the mass transfer resistance between gas and stagnant liquid during non-spraying were the two main different characteristics from the model application to laboratory data.

9.5 NOMENCLATURE

a	Specific surface area of the packing material (m^{-1})
C	Concentration (g m^{-3})
D	Diffusion coefficient of substrates (m^2 s^{-1})
$f(X_v)$	Correction factor of diffusivity in biofilm according to Fan's equation
H	Henry's law constant
K_s	Half saturation rate constants of the substrate (g C m^{-3})
K_La	Overall mass transfer coefficients of the substrates (s^{-1})
M	Number of divisions along the biofilm

N Number of divisions along the column
Q Flow rate ($m^3\ s^{-1}$)
S Concentration in the biofilm ($g\ m^{-3}$)
t Time (s)
v Superficial velocity calculated as a fraction of Q and S ($m\ s^{-1}$)
V Volume (m^3)
x Coordinate for the depth in the biofilm, perpendicular to the biofilm surface
X_v Biomass concentration in the biofilm ($g\ m^{-3}$)
Y Yield coefficient (g of dry biomass synthesized per g consumed)
z Axial coordinate in the reactor
Z Height of the reactor (m)

Greek letters

α_1 Correction of the mass transfer coefficient between biotic and abiotic systems
α_2 Switch parameter of the model
β Thickness of the liquid-biofilm interface (m)
δ Thickness of the biofilm (m)
θ_B Volume fraction of the biofilm (–)
θ_G Porosity of the bioreactor (–)
θ_L Volume fraction of the liquid phase (–)
θ_{PM} Porosity of the packing material (–)
μ_{max} Maximum specific growth rate of the substratum (s^{-1})

Subscripts

i Substance (pollutant and oxygen)
G Gas
L Liquid
B Biofilm
P Pollutant
O Oxygen
R Reactor
T Tank

Acknowledgements

This project has received funding from the European Union's Seventh Framework Programme for research, technological development and demonstration under Grant Agreement No. 284949. Financial support from the Ministerio de Economía y Competitividad (Project CTM2010-15031/TECNO) and the Generalitat Valenciana (PROMETEO/2013/053), Spain, is also acknowledged. The authors would like to give special thanks to Dr. Sempere (PAS Solutions BV) for his consistent collaboration and support. Finally, Pau San Valero thanks the Ministerio de Educación, Cultura y Deporte, Spain, for her FPU contract (AP2010-2191).

Author contributions

San-Valero, Penya-roja and Gabaldón conceived and designed the laboratory experiments. San-Valero and Penya-roja performed the laboratory experiments. Penya-roja and Gabaldón performed the industrial experiments. All authors contributed to the mathematical modelling. San-Valero, Penya-roja, Álvarez-Hornos and Gabaldón ideated the model equations. Marzal assisted and supervised to the numerical solution of the model. San-Valero was responsible for generating the case studies of the model. San-Valero and Gabaldón drafted the manuscript, which was revised by all authors. All authors read and approved the final manuscript.

9.6 REFERENCES

Almenglo, F., Ramírez, M., Gómez, J. M., Cantero, D., Gamisans, X. and Dorado, A. D. (2013). Modeling and control strategies development for anoxic biotrickling filtration. In: L. Malhautier (Ed.), *Biotechniques for air pollution control and Bioenergy* (pp. 123–131). Paris: Presses de Mines.

Alonso, C., Suidan, M. T., Kim, B. R. and Kim, B. J. (1998). Dynamic mathematical model for the biodegradation of VOCs in a biofilter: biomass accumulation study. *Environmental Science & Technology*, *32*(20), 3118–3123.

Baltzis, B. C., Mpanias, C. J. and Bhattacharya, S. (2001). Modeling the removal of VOC mixtures in biotrickling filters. *Biotechnology and Bioengineering*, *72*(4), 389–401.

Bustard, M. T., Meeyoo, V. and Wright, P. C. (2002). Kinetic analysis of high-concentration isopropanol biodegradation by a solvent-tolerant mixed microbial culture. *Biotechnology and Bioengineering*, *78*(6), 708–713.

Devinny, J. S. and Ramesh, J. (2005). A phenomenological review of biofilter models. *Chemical Engineering Journal*, *113*(2-3), 187–196.

European Environment Agency. (2014). *European Union emission inventory report 1990–2012 under the UNECE Convention on Long-range Transboundary Air Pollution (LRTAP)*. *Technical report Nº 12/2014*. Luxembourg: Publications Office of the European Union.

Fan, L.-S., Leyva-Ramos, R., Wisecarver, K. D. and Zehner, B. J. (1990). Diffusion of phenol through a biofilm grown on activated carbon particles in a draft-tube three-phase fluidized-bed bioreactor. *Biotechnology and Bioengineering*, *35*(3), 279–286.

Iliuta, I., Iliuta, M. C. and Larachi, F. (2005). Hydrodynamics modeling of bioclogging in waste gas treating trickle-bed bioreactors. *Industrial & Engineering Chemistry Research*, *44*(14), 5044–5052.

Kennes, C., Rene, E. R. and Veiga, M. C. (2009). Bioprocesses for air pollution control. *Journal of Chemical Technology and Biotechnology*, *84*(10), 1419–1436.

Kennes, C. and Thalasso, F. (1998). Waste gas biotreatment technology. *Journal of Chemical Technology and Biotechnology*, *72*(4), 303–319.

Kennes, C. and Veiga, M. C. (2013). Biotrickling filters. In: C. Kennes and M. C. Veiga (Eds.), *Air pollution prevention and control: Bioreactors and Bioenergy*. United Kingdom: John Wiley & Sons, Ltd.

Kim, S. and Deshusses, M. A. (2003). Development and experimental validation of a conceptual model for biotrickling filtration of H_2S. *Environmental Progress*, *22*(2), 119–128.

Lee, S. H. and Heber, A. J. (2010). Ethylene removal using biotrickling filters: part II. Parameter estimation and mathematical simulation. *Chemical Engineering Journal*, *158*(2), 89–99.

Lu, C. Y., Chang, K. and Hsu, S. (2004). A model for treating isopropyl alcohol and acetone mixtures in a trickle-bed air biofilter. Process Biochemistry, 39(12), 1849–1858.

Mpanias, C. J. and Baltzis, B. C. (1998). An experimental and modeling study on the removal of mono-chlorobenzene vapor in biotrickling filters. *Biotechnology and Bioengineering*, *59*(3), 328–343.

Okkerse, W. J. H., Ottengraf, S. P. P., Osinga-Kuipers, B. and Okkerse, M. (1999). Biomass accumulation and clogging in biotrickling filters for waste gas treatment. Evaluation of a dynamic model using dichloromethane as a model pollutant. *Biotechnology and Bioengineering*, *63*(4), 418–430.

Ottengraf, S. P. and Van Den Oever, A. H. (1983). Kinetics of organic-compound removal from waste gases with a biological filter. *Biotechnology and Bioengineering*, *25*(12), 3089–3102.

Reid, R. C., Prausnitz, J. M. and Poling, B. E. (1987). *The properties of gases and liquids.* New York, EEUU: McGraw-Hill Book Company.

Rene, E. R., Veiga, M. C. and Kennes, C. (2013). Biofilters. In: C. Kennes and M. C. Veiga (Eds.), *Air Pollution Prevention and Control: Bioreactors and Bioenergy*. United Kingdom: John Wiley & Sons, Ltd.

Sander, R. (2005). Henry's law constants in NIST chemistry WebBook, NIST standard referencedatabase number 69. In: P. J. Linstrom and W. G. Mallard (Eds.), *National Institute of Standards and Technology*. Gaithersburg MD 208999, USA.

San-Valero, P., Penya-roja, J. M., Álvarez-Hornos, F. J. and Gabaldón, C. (2014). Modelling mass transfer properties in a biotrickling filter for the removal of isopropanol. *Chemical Engineering Science*, *108*(0), 47–56.

San-Valero, P., Penya-roja, J. M., Sempere, F. and Gabaldón, C. (2013). Biotrickling filtration of isopropanol under intermittent loading conditions. *Bioprocess and Biosystems Engineering*, *36*(7), 975–984.

Sempere, F., Gabaldón, C., Martínez-Soria, V., Marzal, P., Penya-roja, J. M. and Álvarez-Hornos, F. J. (2008). Performance evaluation of a biotrickling filter treating a mixture of oxygenated VOCs during intermittent loading. *Chemosphere*, *73*(9), 1533–1539.

Shareefdeen, Z. and Baltzis, B. C. (1994). Biofiltration of toluene vapor under steady-state and transient conditions -Theory and experimental results. *Chemical Engineering Science*, *49*(24A), 4347–4360.

Shareefdeen, Z., Baltzis, B. C., Oh, Y. S. and Bartha, R. (1993). Biofiltration of methanol vapor. *Biotechnology and Bioengineering*, *41*(5), 512–524.

Tucker, W. A. and Nelken, L. H. (1982). Diffusion coefficients in air and water. In: W. J. Lyman, W. F. Reehl, and D. H. Rosenblatt (Eds.), *Handbook of Chemical Property Estimation Methods*. American Chemical Society.

US EPA. (2013). *Estimation Programs Interface Suite™ for Microsoft® Windows, v 4.11*. Washington, DC, USA.: United States Environmental Protection Agency.

Webster, T. S., Cox, H. H. J. and Deshusses, M. A. (1999). Resolving operational and performance problems encountered in the use of a pilot/full-scale biotrickling fiber reactor. *Environmental Progress*, *18*(3), 162–172.

Zhang, X. Q. and Bishop, P. L. (2003). Biodegradability of biofilm extracellular polymeric substances. *Chemosphere*, *50*(1), 63–69.

Zhu, X. Q., Alonso, C., Suidan, M. T., Cao, H. W. and Kim, B. R. J. (1998). The effect of liquid phase on VOC removal in trickle-bed biofilters. *Water Science and Technology*, *38*(3), 315–322.

10 A TOOL FOR PREDICTING THE DYNAMIC RESPONSE OF BIOTRICKLING FILTERS FOR VOC REMOVAL

A TOOL FOR PREDICTING THE DYNAMIC RESPONSE OF BIOTRICKLING FILTERS FOR VOC REMOVAL

Pau San-Valero[a], Salvador Alcántara[b], Josep M. Penya-roja[a], F. Javier Álvarez-Hornos[a] & Carmen Gabaldón[a*]

[a] *Research Group GI²AM, Department of Chemical Engineering, University of Valencia, Avda. Universitat s/n, 46100 Burjassot, Spain*

[b] *PAS Solutions BV, P.O. Box 135, 8440 AC Heerenveen, The Netherlands*

*Corresponding author: carmen.gabaldon@uv.es

Abstract

This article presents the development of a MATLAB® computer program to simulate the performance of biotrickling filters. Since these filters behave differently during spraying and non-spraying cycles, the presented simulation tool is built on top of a mathematical description of each situation. The resulting variable-structure model is then used as the basis for simulation experiments. The model presented herein represents the first attempt to take into account the variable spraying pattern usually found in industrial installations. Overall, the software is flexible and easy to use, allowing the user to specify the emission concentration pattern, the gas concentration pattern, as well as the spraying cycle periods for up to two different emission patterns per day. The model is able to predict experimental data from a biotrickling filter treating isopropanol under intermittent conditions of loading and spraying. Simulation examples are then provided to study the effect of variable inlet concentrations and gas flow rates.

Keywords

Biotrickling filters, computer simulation, mathematical modelling, numerical analysis, VOC

Chem Eng Commun 2016, 203, 476-487

10.1 INTRODUCTION

Emission to the atmosphere, from a wide variety of sources, of volatile organic compounds (VOCs) remains one of the most important causes of air pollution. This has triggered significant research efforts to develop more cost-effective and environmentally friendly solutions for the treatment of air emissions of VOCs. In particular, there has been an increasing interest in biofiltration, especially since it has been classified as a best available technique (BAT) by the European Commission (2003). Among the biofiltration strategies, biotrickling filters (BTFs) constitute one of the most suitable biotechnologies for the treatment of VOCs. Biotrickling filters consist of a column filled with an inert packing material where the biomass attaches to the media and develops a biofilm. In this configuration, the gas and liquid phases circulate through the column in co- or counter-current mode. Thus, the pollutant and the oxygen are transferred from the gas phase to trickling liquid, and then to the biofilm, where biodegradation takes place.

Biotrickling filtration has been applied successfully to the treatment of VOCs at the laboratory, pilot, and industrial scales. However, to further improve the performance of BTFs for the treatment of VOCs it has become necessary to understand the intricacies of the processes involved as well as their rate-limiting steps (Popat and Deshusses, 2010). In this regard, biotrickling filtration involves a complex set of physico-chemical and biological mechanisms and, hence, mathematical models, in conjunction with computer-aided simulation, appear as fundamental tools to go deeper into the understanding of the involved governing processes.

Industrial processes that use solvents have fluctuating VOC emissions arising from the specific application and the unit operation dynamics of each particular industry (Rene et al., 2013). These result in emission levels whose variation in time is related to random fluctuations in the gas velocity and the inlet concentration profile. In addition, short-time shut-off periods associated with nights, weekends, and holiday closures further contribute to creating a variable pattern of VOC emissions at the industrial scale. This variability may sometimes hinder the performance of field-scale BTFs (Sempere et al., 2010). Also, operating BTFs under cyclic and discontinuous operation has traditionally produced some problems, as reported in Webster et al. (1999).

Intermittent water trickling, in contrast to continuous trickling, is also common practice in the operation of industrial BTFs. As shown in Sempere et al. (2008), intermittent trickling may improve the removal efficiency and better control the pressure drop. The final performance of the BTF is quite dependent on the rate of liquid trickling (Zhu et al., 1998). An intermittent spraying regime implies that the mobile liquid phase is not always present during the filter operation, making it necessary to distinguish two different situations, corresponding to spraying and non-spraying periods. Nevertheless, the modelling and simulation research presented in the literature so far tends to focus only on one particular case.

Several efforts have been made to model biofiltration processes. One of the most used models for the treatment of organic pollutants in waste gases in a gas–liquid biofilter has been developed by Ottengraf and van Den Oever (1983) in steady state conditions. Since then, there has been increasing interest in the application of dynamic models of biofilters and BTFs rather than of steady state models. Shareefdeen and Baltzis (1994) published one of the first attempts to describe the dynamic behaviour of biofilters, including the oxygen limitation in the biofilm and the phenomena of adsorption. Deshusses et al. (1995) proposed a model for the determination of the transient and steady-state conditions degrading the methyl ethyl ketone and methyl isobutyl ketone emissions in biofilters. Zarook et al. (1997) developed a transient biofiltration model that incorporates oxygen limitation effects, general mixing, and adsorption phenomena, as well as general biodegradation reaction kinetics. Thereafter, many researchers introduced variations of these models by taking new factors into consideration. Métris et al. (2001) used a simplication of the Zarook et al. (1997) model using CO_2 production to evaluate the response of the biofilters to starvation and shock loads in the biofiltration of toluene and xylene. Álvarez-Hornos et al. (2009) developed a dynamic model with a Haldane-type kinetic expression that considers oxygen limitation, (cross) inhibition effects due to high concentrations of substrates, and a general axial gradient equation for the biomass density. Many BTF models derive from biofilter models. Okkerse et al. (1999) presented a detailed dynamic model that includes the growth of methylene chloride degraders and inert biomass as well as the effect of the pH and dissolved oxygen. Kim and Deshusses (2003) presented a three-phase dynamic model to describe the biotrickling filtration of hydrogen sulfide with counter-current flows of a gas and a liquid. They assumed that the biofilm was not completely wetted by the liquid phase and thus, in some parts of the biofilm, the pollutant was transferred directly from the gas phase to the biofilm. In their review of biofilters and biotrickling

modelling, Devinny and Ramesh (2005) pointed out that no single model has become generally accepted. The complexity behind the operation of BTFs has made many researchers consider specific situations in their simulation studies (Lee and Heber, 2010; Mannucci et al., 2012). The increase in the number of factors taken into consideration in the mathematical models has necessitated greater efforts for their mathematical solution. In the case of the models of biotrickling filters, the presence of the liquid phase implies an increase of the level of complexity and for counter current operation, that which is usually found in the industry, the system of equations obtained can be relatively stiff and model instabilities could make their solution difficult (Deshusses and Shareefdeen, 2005). Even so, it has been recognized that realistic models adapted to the emissions of the industry are needed.

The aim of this paper is to present a more flexible tool to simulate the performance of BTFs. Based on the operational conditions commonly found in industry, the proposed model allows specifying variable inlet concentration patterns and gas velocities combined with different spraying patterns. These and other features provide the necessary flexibility to reproduce typical industrial use cases.

10.2 MODEL DEVELOPMENT

Industrial BTFs operate with intermittent water trickling. This means that the mobile liquid phase is only present at some times during the day, referred to here as the *spraying periods*. For the rest of the time, referred to as the *non-spraying periods*, the liquid phase remains as a stagnant phase. Figure 10-1 illustrates this concept. The modelling step has to take into account the principal mechanisms of the biofiltration process in each situation.In this configuration, the pollutant/oxygen is transferred from the gas phase to the liquid phase and then to the biofilm, as represented in Figure 10-2. The model has been developed following the general mass balances of the gas phase, liquid phase, and biofilm, by taking into account the most important phenomena compiled by Devinny and Ramesh (2005).

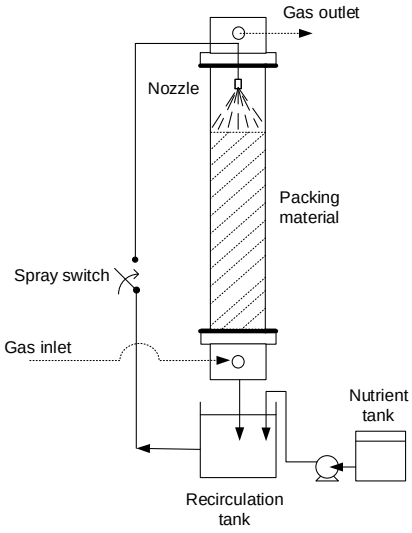

Figure 10-1 Diagram of a BTF. Liquid recirculation only happens during spraying periods.

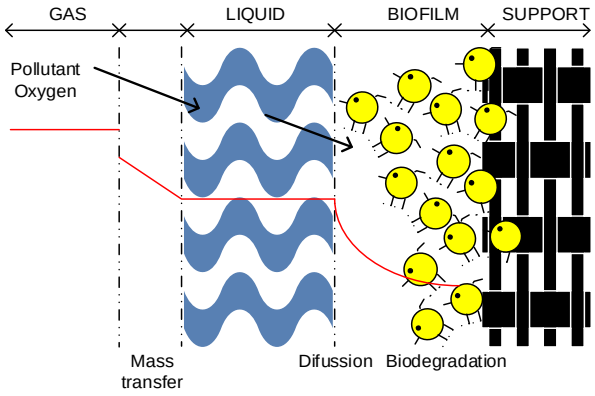

Figure 10-2 Mechanisms involved in the process of BTF.

For the derivation of the model, the following general assumptions have been made, based on consolidated models reported (Kim and Deshusses, 2003; Mpanias and Baltzis, 1998) and adapted to this model.

(1) The gas phase flows in a plug flow regime along the filter bed.

(2) Axial dispersion is neglected.

(3) The adsorption of the pollutant in the packing material is negligible.

(4) An active biofilm is formed on the external surface of the packing material and no reaction occurs in the pores. The biofilm covers the surface of the packing material and its thickness (δ) is much smaller than the size of the solid particles, so a planar geometry has been assumed.

(5) The packing material is completely covered by the biofilm.

(6) The diffusion of the biofilm is described by Fick's law.

(7) Ideal conditions of nutrients and pH are assumed.

(8) The system works under cycling conditions of spraying/non-spraying periods.

(9) The status reached at the end of one period determines the initial conditions for the next period.

(10) The biodegradation kinetics is described by a Monod expression, which takes into account oxygen limitation.

(11) The mass flux at the gas–liquid interface can be expressed by mass transfer coefficients.

(12) The mass flux at the liquid–biofilm interface can be expressed by mass transfer coefficients.

(13) There is no reaction in the liquid phase.

(14) The gas–liquid interface is in equilibrium according to Henry's law.

Based on the assumptions above, the mass balances for the different phases can be written as follows.

10.2.1 Spray mode

10.2.1.1 *Mass balance in the gas phase*

$$\theta_G \frac{\partial C_{G_P}}{\partial t} = -v_G \frac{\partial C_{G_P}}{\partial z} - \alpha_1 K_L a_P \left(\frac{C_{G_P}}{H_P} - C_{L_P} \right) \tag{10-1}$$

$$\theta_G \frac{\partial C_{G_O}}{\partial t} = -v_G \frac{\partial C_{G_O}}{\partial z} - \alpha_1 K_L a_O \left(\frac{C_{G_O}}{H_O} - C_{L_O} \right) \tag{10-2}$$

where, for the pollutant and oxygen, respectively, C_{GP} and C_{GO} are the concentrations in the gas phase, $K_L a_P$ and $K_L a_O$ are the overall mass transfer coefficients, α_1 is the correction factor of the overall mass transfer coefficients, H_P and H_O are the dimensionless Henry's law constants expressed as concentration of the gas phase/ concentration of the liquid phase, C_{LP} and C_{LO} are the concentration of the liquid phase. t denotes the time, z is the distance from the bottom of the column and v_G is the superficial air velocity given by

$$v_G = \frac{Q_G}{\frac{\pi D^2}{4}} \tag{10-3}$$

where Q_G is the volumetric gas flow rate and D is the column diameter.

θ_G is the porosity of the bioreactor and is given by

$$\theta_G = 1 - \left(1 - \theta_{PM}\right) - \theta_L - \theta_B \tag{10-4}$$

where θ_{PM} is the void fraction of the packing material, θ_L is the fraction occupied by the liquid film and θ_B is the fraction occupied by the biofilm.

The boundary conditions of equations (10-1) and (10-2) are

$$\begin{aligned} C_{G_P} &= C_{G_P}^{in} \quad at \quad z = 0 \\ C_{G_O} &= C_{G_O}^{in} \quad at \quad z = 0 \end{aligned} \tag{10-5}$$

where C^{in}_{GP} and C^{in}_{GO} are the inlet concentrations in the gas phase of the pollutant and the oxygen, respectively.

10.2.1.2 *Mass balance in the liquid phase*

$$\theta_L \frac{\partial C_{L_P}}{\partial t} = v_L \frac{\partial C_{L_P}}{\partial z} + \alpha_1 K_L a_P \left(\frac{C_{G_P}}{H_P} - C_{L_P} \right) - \frac{D_{w_P} A}{\beta} (C_{L_P} - S_{P_1}) \tag{10-6}$$

$$\theta_L \frac{\partial C_{L_O}}{\partial t} = v_L \frac{\partial C_{L_O}}{\partial z} + \alpha_1 K_L a_O \left(\frac{C_{G_O}}{H_O} - C_{L_O} \right) - \frac{D_{w_O} A}{\beta} (C_{L_O} - S_{O_1}) \tag{10-7}$$

where, for the pollutant and oxygen, respectively, S_{P_1} and S_{O_1} are the concentration in the biofilm interface, β is the thickness of the liquid-biofilm interface, D_{wP} and D_{wO} are the diffusion coefficient in water, A is the specific surface area, x is the axial position along the biofilm, and v_L is the superficial liquid velocity given by

$$v_L = \frac{Q_L}{\frac{\pi D^2}{4}} \tag{10-8}$$

where Q_L is the volumetric liquid flow rate.

The boundary conditions of Equations (10-6) and (10-7) are

$$\begin{aligned} \frac{\partial C_{L_P}}{\partial t} &= \frac{Q_L}{V_T} (C_{L_{P(z=0)}} - C_{L_{P(z=Z)}}) \quad at \quad z = Z \\ \frac{\partial C_{L_O}}{\partial t} &= \frac{Q_L}{V_T} (C_{L_{O(z=0)}} - C_{L_{O(z=Z)}}) \quad at \quad z = Z \end{aligned} \tag{10-9}$$

The boundary conditions given by Equation (10-9) correspond to the mass balances in the recirculation tank, where V_T is the water volume in the recirculation tank. It is assumed that the liquid inlet concentration in the column is equal to the concentration in the recirculation tank, and that the recirculated water depends on the liquid concentration at the bottom of the column.

10.2.1.3 *Mass balance in the biofilm*

$$\frac{\partial S_P}{\partial t} = D_{P_B}\frac{\partial^2 S_P}{\partial x^2} - \frac{\mu_{\max} X_v}{Y_P}\frac{S_P}{S_P + K_P}\frac{S_O}{S_O + K_O} \tag{10-10}$$

$$\frac{\partial S_O}{\partial t} = D_{O_B}\frac{\partial^2 S_O}{\partial x^2} - \frac{\mu_{\max} X_v}{Y_O}\frac{S_P}{S_P + K_P}\frac{S_O}{S_O + K_O} \tag{10-11}$$

where S_P and S_O are the concentrations in the biofilm. The boundary conditions are given by

$$\begin{aligned} \frac{\partial S_P}{\partial t} &= 0 \qquad at \qquad x = \delta \\ \frac{\partial S_O}{\partial t} &= 0 \qquad at \qquad x = \delta \end{aligned} \tag{10-12}$$

where X_V is the concentration of the biomass, μ_{max} is the specific growth rate of the biomass and, for the pollutant and oxygen, respectively, K_{S_P} and K_{S_O} are the half-saturation constants, Y_P and Y_O are the yield coefficients, and D_{P_B} and D_{O_B} are the effective diffusion coefficients inside the biofilm corrected by a factor ($f(X_V)$) calculated according to Fan's equation (Fan et al., 1990):

$$f(X_v) = \left(1 - \frac{0.43\left(X_v \cdot 10^{-3}\right)^{0.92}}{11.19 + 0.27\left(X_v \cdot 10^{-3}\right)^{0.99}}\right) \tag{10-13}$$

10.2.2 Non-spray mode

Analogously, the mass balances during non-spraying periods are

10.2.2.1 *Mass balance in the gas phase*

$$\theta_G \frac{\partial C_{G_P}}{\partial t} = -v_G \frac{\partial C_{G_P}}{\partial z} - \alpha_2 \alpha_1 K_L a_P \left(\frac{C_{G_P}}{H_P} - C_{L_P} \right) \tag{10-14}$$

$$\theta_G \frac{\partial C_{G_O}}{\partial t} = -v_G \frac{\partial C_{G_O}}{\partial z} - \alpha_2 \alpha_1 K_L a_O \left(\frac{C_{G_O}}{H_O} - C_{L_O} \right) \tag{10-15}$$

with the boundary conditions

$$\begin{aligned} C_{G_P} &= C_{G_P}^{in} \quad at \quad z = 0 \\ C_{G_O} &= C_{G_O}^{in} \quad at \quad z = 0 \end{aligned} \tag{10-16}$$

where α_2 is a switch model parameter (100 indicates that no mass transfer resistance is assumed between the gas and liquid phases, and 1 indicates that there is a mass transfer resistance).

10.2.2.2 *Mass balance in the liquid phase*

$$\theta_L \frac{\partial C_{L_P}}{\partial t} = \alpha_2 \alpha_1 K_L a_P \left(\frac{C_{G_P}}{H_P} - C_{L_P} \right) - \frac{D_{w_P} A}{\beta} (C_{L_P} - S_{P_1}) \tag{10-17}$$

$$\theta_L \frac{\partial C_{L_O}}{\partial t} = \alpha_2 \alpha_1 K_L a_O \left(\frac{C_{G_O}}{H_O} - C_{L_O} \right) - \frac{D_{w_O} A}{\beta} (C_{L_O} - S_{O_1}) \tag{10-18}$$

10.2.2.3 *Mass balance in the biofilm*

$$\frac{\partial S_P}{\partial t} = D_{P_B}\frac{\partial^2 S_P}{\partial x^2} - \frac{\mu_{\max} X_v}{Y_P}\frac{S_P}{S_P + K_P}\frac{S_O}{S_O + K_O} \tag{10-19}$$

$$\frac{\partial S_O}{\partial t} = D_{O_B}\frac{\partial^2 S_O}{\partial x^2} - \frac{\mu_{\max} X_v}{Y_O}\frac{S_P}{S_P + K_P}\frac{S_O}{S_O + K_O} \tag{10-20}$$

with the boundary conditions

$$\begin{aligned} \frac{\partial S_P}{\partial t} &= 0 \qquad at \qquad x = \delta \\ \frac{\partial S_O}{\partial t} &= 0 \qquad at \qquad x = \delta \end{aligned} \tag{10-21}$$

10.3 NUMERICAL SOLUTION

The partial differential equations (10-1), (10-2), (10-6), (10-7), (10-10), (10-11)(spray mode), and (10-14), (10-15), (10-17), (10-18), (10-19), and (10-20) (non-spray mode) constitute two second order nonlinear distributed systems. In order to solve them, the method of lines (MOL) (Schiesser, 1991, 1994; Schiesser and Griffiths, 2009) has been chosen. Although the finite difference method (FDM) has previously been used in the literature to simulate biofilter and biotrickling filters (Ikemoto et al., 2006; Álvarez-Hornos et al., 2009) in different ways, the MOL has some advantages that make it more suitable here. Apart from its simplicity, it allows taking advantage of the available ODE solvers. Note, in addition, that the overall MOL process can be regarded as an FDM procedure where the discretization in *t* is independent of that in *x, z,* which provides extra flexibility. Since the resulting systems have been found to be stiff, as is normally the case when applying the MOL (Schiesser, 1994), the *ode23t* solver from the MATLAB® has been selected for solving the corresponding equations. The *ode23t* is based on an implicit integration method and it is quite concerned with the stability issue. Other ODE solvers were tested, but the chosen solver gave the best results in practice.The MOL method is applied here following the steps:

- Generate a uniform grid in the spatial dimensions, i.e., $(x_i, z_j)_{i,j}$. *Z*, the height of the column (the z axis), is divided into *N* sections. Similarly, the biofilm thickness δ is divided into *M* sections with *M* + 1 points. The values of *N* = 20, *M* = 40 were used for the spatial discretization in each mode.
- For each node in the grid, replace the partial derivatives in the model equations with finite difference approximations.
- Solve the resulting system of ordinary differential equations (ODE) using standard numerical methods; note that the time variable *t* was left continuous in the first step.

10.4 DEVELOPED SOFTWARE TOOL

The main objective of this paper is to introduce a tool for the simulation of biotrickling filters using the mathematical models and numerical procedures described in the previous sections. This section describes the basic features implemented in the tool, focusing on its usability. The software has been developed in MATLAB®. It can be used with the basic MATLAB®package and it is available as a MATLAB package as well as a compiled standalone application. The graphical user interface (GUI) has been created using the GUIDE–MATLAB® toolbox. A screenshot of the GUI is shown in Figure 10-3. In the present example, the option two emissions pattern (per day) allows specifying two different patterns of inlet concentration, gas velocity, and spraying, over a period of 86,400 seconds (i.e., one day). When this option is marked, the user indicates the duration of the first pattern (< 86,400 seconds). The duration of the second pattern is then calculated automatically (86,400 seconds – time pattern 1). The resulting global daily pattern is the combination of the two specified patterns in series, and the total simulation time in this case equals the number of days specified by the user.

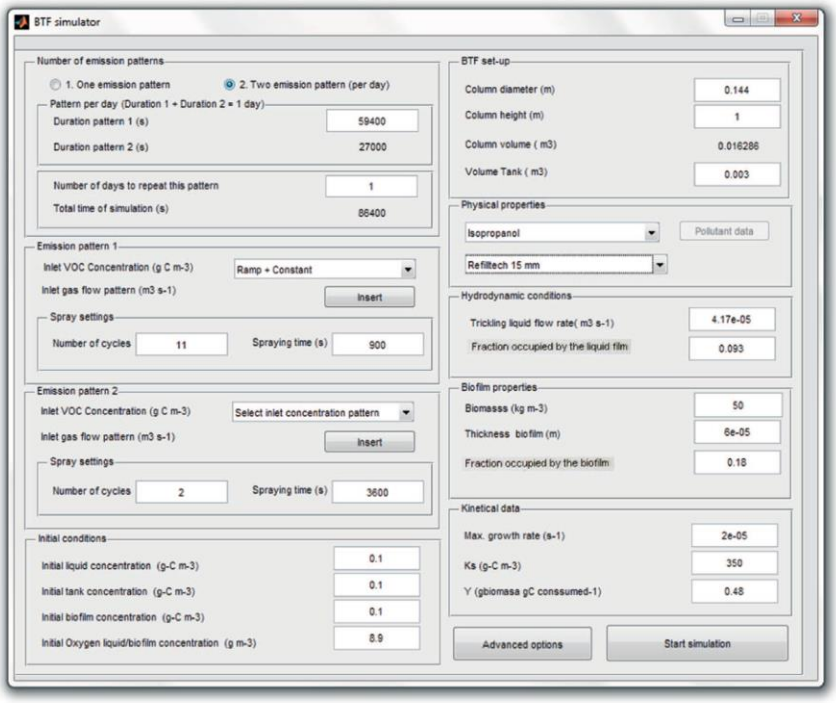

Figure 10-3 Main window of the GUI: Two emission patterns (per day).

The emission pattern and the spraying pattern are defined by the user by

- VOC inlet concentrations. For the inlet VOC concentration (C^{in}_{GP}) pattern, a drop-down list presents the user with the following options for the input profile:
  - Constant. The inlet concentration is assumed constant.
  - Ramp+Constant. A constant concentration is considered as before, but preceded by a ramp pofile until the final value is reached.
  - Pulse train. The inlet concentration oscillates between two values, describing a pulse train input signal.
  - Piecewise constant. The inlet concentration consists of a step (or staircase) function, i.e., it is piecewise constant having only finitely many pieces.

After making a choice, a dialog window allows introducing the defining parameters for each case. For instance, for the Ramp+Constant profile, Figure 10-4 shows the resulting dialog.

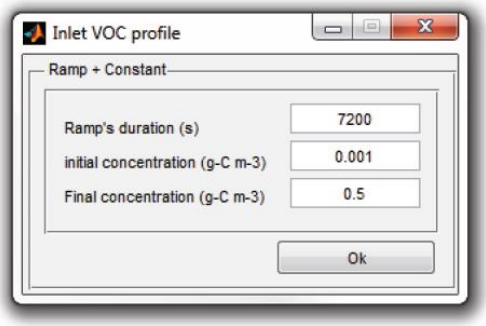

Figure 10-4 GUI of the MATLAB® tool. Dialog for the Ramp+Constant inlet VOC concentration profile.

In contrast with the inlet VOC concentration, the inlet oxygen concentration (C^{in}_{GO}) is assumed constant throughout the whole simulation (276 g m^{-3}).

- Inlet gas flow pattern. This consists of a step (or staircase) function, i.e., it is piecewise constant having only finitely many pieces.
- Spray settings. The spraying pattern will consist of an ON/OFF signal. As an example, the scheme of the spraying pattern for the option two emissions pattern (per day) is illustrated in Figure 10-5.

The spraying panel includes the following information:

- Number of spray cycles (n). Defines how many times to spray during each emission pattern.
- Spraying time (T_s). Duration of spraying, i.e., the duration of the ON part of one spray cycle.

The simulation requires the user to specify the initial conditions:

- Initial conditions for the simulation. This includes the VOC concentration in the liquid phase, the VOC concentration in the water tank and inside the biofilm, and the oxygen concentration in the liquid and inside the biofilm.

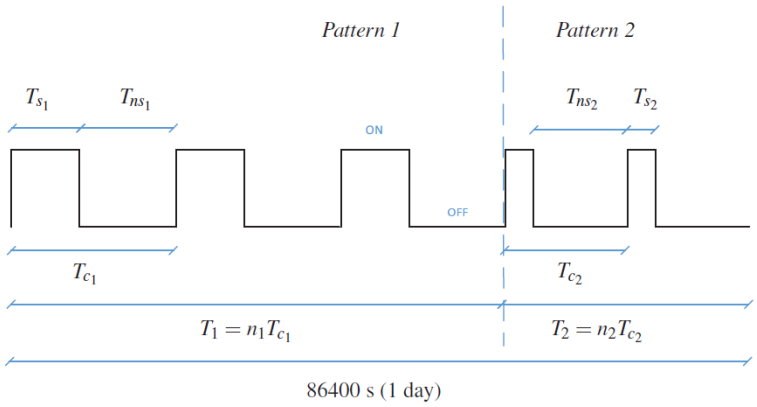

Figure 10-5 Spray cycle patterns for one day. Emission pattern 1 has three cycles (n_1=3), and emission pattern 2 has two (n_2=2) spray cycles. The user specifies T_{S_1}, n_1, T_1, T_{S_2}, and n_2. *Non-spray times* are given by $T_{nS_1} = (T_1 - n_1 T_{S_1})/n_1$) and $T_{nS_2} = (T_2 - n_2 T_{S_2})/n_2$ for emission pattern 1 and emission pattern 2, respectively

The input related to the BTF configuration, the pollutant and packing material data, and the model parameters are defined by the user:

- BTF setup. This part defines the characteristics of the BTF system, such as the column diameter, column height, and the volume of the water tank. This panel provides automatically the column volume of the reactors.

- Physical properties. The physical properties panel includes the selection of the pollutant and the selection of the packing material. The selection of the pollutant uses a pop-up menu where it is possible to choose from among some predefined VOCs, whose information includes the diffusion coefficient in water (D_{Pw}), the Henry's law constant (H_P) at 25◦C, and the chemical formula. Alternatively, the user can select a user defined pollutant by specifying its diffusion coefficient in water, its Henry's law constant, and its chemical formula. The selection of the packing material uses another pop-up menu in which there are some predefined packing materials for each of which there are provided its specific surface area (A), porosity (θ_{pm}), and specific coefficients to calculate the overall mass transfer coefficients ($K_L a_P$, $K_L a_O$) using the correlations proposed by San-

Valero et al. (2014). Alternatively, it is possible to a custom other packing material by specifying its specific surface area, porosity, and overall mass transfer coefficients.

- Hydrodynamic conditions such as the liquid flow rate and the fraction occupied by the liquid film (θ_L).
- Biofilm properties. In this panel there should be indicated its biomass density (X_v), the thickness of its biofilm (δ), and fraction occupied by the biofilm (θ_B).
- Kinetics data. In this panel the user indicates the kinetic parameters regarding the pollutant degradation (μ_{max}, K_s and Y_P). Regarding the oxygen parameters, K_O has been predefined from the literature as 0.26 g m^{-3} and Y_O is calculated by stoichiometry balance.
- Advanced options. This button opens a dialog where other properties related with the mass transfer can be defined.

After all the input data and parameters have been defined, the simulation is run by pressing the Start button. When it concludes, the results are presented to the user in a new window, shown in Figure 10-6. The main items are described next.

- A graph showing both the inlet and the outlet VOC concentrations in the gas phase.
- A graph showing the evolution of the VOC concentration in the liquid tank.

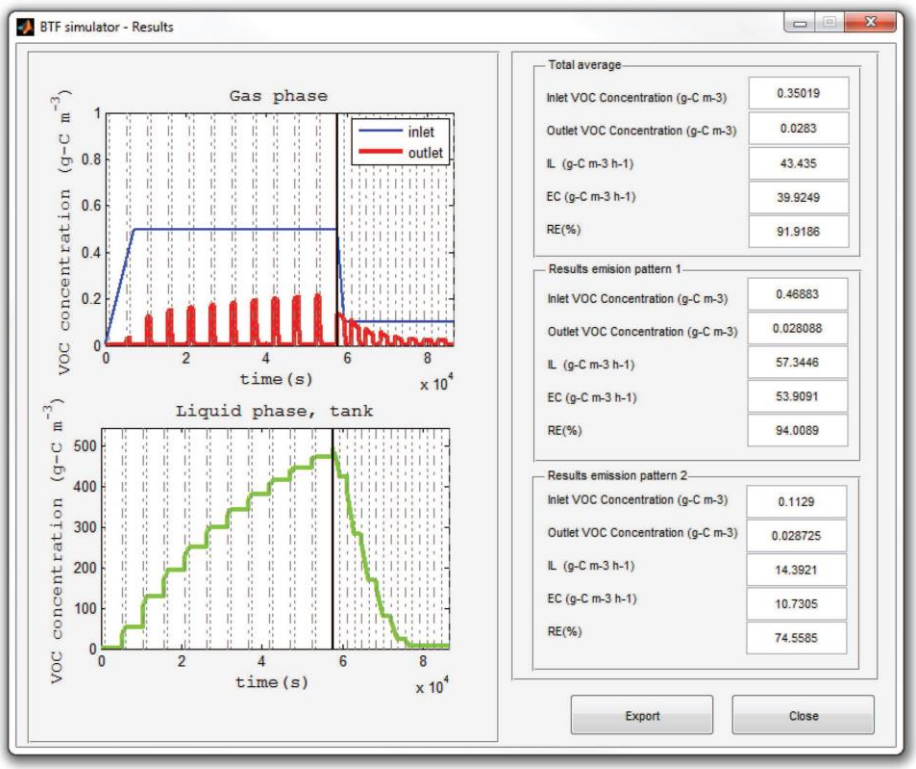

Figure 10-6 GUI of the MATLAB® tool (results window).

- Some relevant averages, over the whole simulation time, are displayed by this panel:
  - Inlet/Outlet VOC concentrations,
  - Inlet load (IL) defined as

$$IL\left(\frac{g-C}{m^3 h^1}\right)=\frac{\overline{C_G^{in}}\,\overline{Q_G}}{V_R}3600 \qquad (10\text{-}22)$$

where $\overline{C_G^{in}}$ is the average inlet concentration and $\overline{Q_G}$ is the average gas flow rate.

$$RE(\%) = \frac{\left(\overline{C_G^{in}} - \overline{C_G^{out}}\right)}{\overline{C_G^{in}}} 100 \quad (10\text{-}23)$$

where $\overline{C_G^{out}}$ is the average outlet concentration.

- Elimination Capacity (EC):

$$EC\left(\frac{g-C}{m^3 h^1}\right) = \frac{RE}{100} IL \quad (10\text{-}24)$$

- Panel with averages for the emission pattern 1 only.
- Panel with averages for the emission pattern 2 only.
- This button allows exporting the simulation results to a Comma-Separated Values (CSV) file.
- Closes the results window.

10.5 MODEL CALIBRATION AND VALIDATION

The model was calibrated and validated by using the experimental data corresponding to the dynamic response of a biotrickling filter treating isopropanol obtained by San-Valero et al. (2013). In this data, the BTF was operated under intermittent loading conditions and intermittent spraying frequency. These are the conditions typically found in the operation of industrial BTFs. During these experiments, it was observed that the discontinuous regime of spraying of the bed resulted in outlet emissions of isopropanol during spraying periods. Based on this observation, the effect of the spraying pattern was evaluated and it was pointed out that the spraying frequency is a critical parameter to achieve low emissions. The BTF was operated by using an IL of 32 g C m^{-3} h^{-1} and empty bed residence time (EBRT) of 30 s. The EBRT is defined as:

$$EBRT(s) = \frac{V_R}{Q_G} \quad (10\text{-}25)$$

These VOC feeding conditions were applied for a total duration of 57600 s (16 h) from 6:00 to 22:00 h. The rest of the day, the biotrickling filter remained without VOC supply and without spraying. The parameters used in the modelling of the BTF behaviour are summarized in Table 10-1. The experimental parameters were taken from the literature or experimentally determined. The calibrated parameters were determined to fit the transient response data of the biotrickling filter. An independent experiment with a spraying pattern of 15 min every 1.5 h was used in the calibration step. Thus, time durations of 900 and 4500 s for the spraying and non-spraying periods, respectively, were set. In this experiment, it was assumed that there was no mass transfer resistance at the gas–liquid interface (α_2=100). A comparison of the experimental results and the model predictions is shown in Figure 10-7.Figure 10-7 (a) displays the evolution of the inlet and outlet VOC concentrations while Figure 10-7(b) displays the evolution of the concentration of carbon dissolved in the water tank.

As is shown in Figure 10-7(a), the maximum concentrations of the pollutant are reached during the spraying periods, whereas during the non-spraying periods, nearly complete biodegradation of the pollutant is obtained. In addition, the peaks increase as the system gets filled with pollutant, reaching a stationary value for an outlet VOC concentration of around 0.2 g C m^{-3} after the third cycle. An EC of 27.2 g C m^{-3} h^{-1} is obtained for an IL of 32 g C m^{-3} h^{-1} during VOC feeding periods. The model successfully predicts the behaviour obtained, achieving maximum outlet concentrations during the spraying periods during the last cycles of the day. The experimental data fits the model prediction with a relative error of less that 3 % in the EC (EC of the model 28.0 g C m^{-3} h^{-1}). Also, the model prediction for the carbon dissolved in the water tank is in good agreement with the measured carbon in the water tank.

Table 10-1 Model parameters used in the mathematical model.

Variable	Specific Value	Units	Reference
Experimental parameters			
A_V	348	m^{-1}	San-Valero et al. (2013)
D	0.144	m	San-Valero et al. (2013)
D_{P_W}	1.13×10^{-9}	$m^2\ s^{-1}$	Tucker and Nelken (1982)
D_{O_W}	2×10^{-9}	$m^2\ s^{-1}$	Reid et al. (1987)
H_P	2.8×10^{-4}		San-Valero et al. (2014)
H_O	31.4		Sander (2005)
K_La_P	$K_La_P=\frac{H_P}{3600}\left(11.59\left(v_G3600\right)^{0.85}\right)$	s^{-1}	San-Valero et al. (2014)
K_La_O	1.15×10^{-2}	s^{-1}	San-Valero et al. (2014)
Q_L	41.7×10^{-6}	$m^3\ s^{-1}$	San-Valero et al. (2013)
V_R	0.0163	m^3	San-Valero et al. (2013)
V_T	0.003	m^3	San-Valero et al. (2013)
X_V	50×10^3	$g\ m^3$	This paper
Y_P	0.48	$\frac{g\ biomass}{g\ consumed}$	Lu et al. (2004)
Y_O	0.14	$\frac{g\ biomass}{g\ consumed}$	Stoichiometric balance
Z	1	m	San-Valero et al. (2013)
θ_B	0.18		This paper
θ_L	0.093		This paper
Calibration parameters			
K	350	$g\ C\ m^{-3}$	
$\alpha1$	0.23 (except for cycle 1 that takes $\alpha_1 = 1$)		
β	6.4×10^{-6}	m	
δ	60×10^{-6}	m	
μ_{max}	2×10^{-5}	s^{-1}	

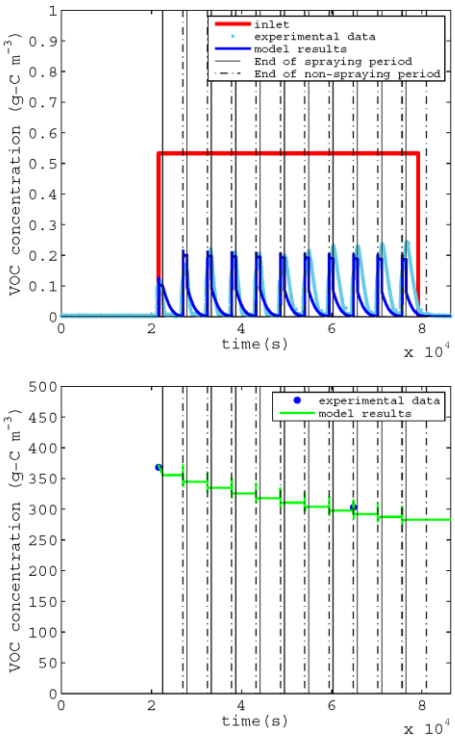

Figure 10-7 Model calibration with experimental data from San-Valero et al. (2013). a) Evolution of the concentration in the gas phase. b) Evolution of the dissolved organic carbon in the recirculation tank.

The validation of the model was carried out by using data from two experiments. The first experiment was carried out with a low spraying frequency of 15 min every 3 h, and a moderate IL=32 g C m^{-3} h^{-1}. The second experiment was carried out with double spraying frequency (15 min every 1.5h) and a double IL (65 g C m^{-3} h^{-1}). The experimental data and the model predictions are shown in Figure 10-8. Figure 10-8(a) displays the evolution of the inlet and outlet VOC concentrations for the first experiment while Figure 10-8(b) displays the evolution of the inlet and outlet VOC concentrations for the second experiment.

For the experiments carried out with a spraying regime of 15 min every 3 h and an IL of 32 g C m^{-3} h^{-1}, the relative error between the experimental and the simulated EC is 3.2 % (experimental EC of 28.8 g C m^{-3} h^{-1} and modelled EC of 29.7 g C m^{-3} h^{-1}). For the experiments carried out with a spraying regime of 15 min every 1.5 h and an IL of 65 g C m^{-3} h^{-1}, the error between the experimental and simulated EC is 4.0% (experimental EC of 50.3 g C m^{-3} h^{-1} and modelled EC of 52.3

g C m^{-3} h^{-1}). The modelled concentration of the dissolved carbon in the recirculation tank is in agreement with the measured values. As an example, for the series with a spraying regime of 15 min every 3 h and an IL of 32 g C m^{-3} h^{-1}, the measured dissolved carbon was 357 g C m^{-3} and the model predicted a value was 365 g C m^{-3}, with a relative error of 2.2 %.

So, the model has been proven suitable for describing the complex phenomena observed in the transient response of the biotrickling filter to variations of the spraying pattern.

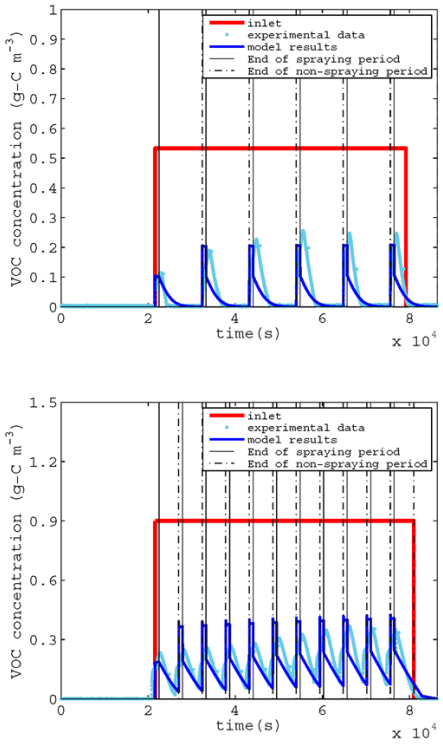

Figure 10-8 Model validation with experimental data from San-Valero et al. (2013). a) Spraying regime 15 min every 3h and IL 32 g C m^{-3} h^{-1}. b) Spraying regime 15 min every 1.5 h and IL 65 g C m^{-3} h^{-1}.

10.6 STUDY OF THE DYNAMIC RESPONSE OF THE BTF TO VARIABLE INLET CONCENTRATIONS AND GAS FLOW RATES

10.6.1 Dynamic response of the BTF to oscillating inlet concentrations

The effect of oscillating inlet VOC concentrations on the dynamic response of the BTF was investigated by using a periodic pulse train concentration pattern. The pulse train profile was used to study the influence of high shock loads during regular changes in the operation on the performance of the BTF. In particular, the selected inlet concentration took on two alternating values: C^{in}_P = 0.7 g C m^{-3} (for 7200 s) and C^{in}_P= 0.2 g C m^{-3} (for 3600 s). A linear transition with a duration of 15 min was used to connect the two different values. A constant EBRT of 60 s was applied. Also, durations of 0.25 and 1 h were specified for the spraying and non-spraying periods, respectively, and this pattern was applied for T = 59400 s. The simulation results are presented in Figure 10-9(a) for the gas phase and in Figure 10-9(b) for the liquid phase. Figure 10-9(a) shows that the concentration peaks not only depend on the spraying cycles but also on the pattern of the inlet concentration. An EC of 30 g C m^{-3} h^{-1} was obtained for an IL of 32 g C m^{-3} h^{-1}. The evolution of the VOC in the tank is presented in Figure 10-9(b). To observe the accumulation of dissolved carbonin the water tank, in this example the concentration of dissolved carbon in the tank was set to 0 g C m^{-3}. In this example, two different phenomena can be observed: absorption and desorption processes. These processes are markedly dependent on the equilibrium between the gas and liquid phases. As can be observed, when the inlet concentration increases during the spraying periods, a desorption of pollutant from the liquid phase to the gas phase is produced, and the opposite occurs when the inlet concentration increases. At the end of the period, the water contains 200 g C m^{-3} of dissolved carbon.

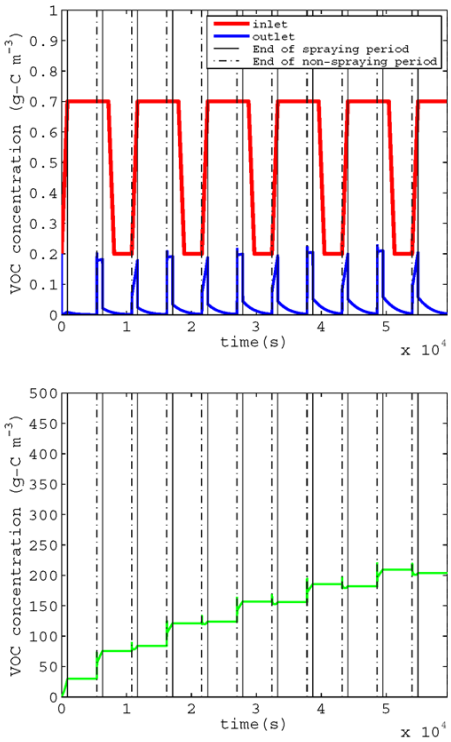

Figure 10-9 Dynamic response of the BTF to oscillating inlet concentration. a) Evolution of the concentration in the gas phase. b) Evolution of the dissolved organic carbon in the recirculation tank.

10.6.2 Dynamic response of the BTF to oscillating inlet concentration combined with spraying times during non-VOC feeding periods

The dynamic response of the BTF to oscillating inlet concentrations combined with spraying times during non-VOC feeding periods was investigated. An oscillating emission pattern was applied for a total of 59400 s per day. The inlet VOC concentration was exactly the same as the pulse train profile used in the previous example. A period without VOC feeding was applied for 27000 s with a Ramp+Constant profile of C_{GP} = 0.01 g C m^{-3} and a spraying time of 1 h every 4 h. The results for the gas and liquid phases, respectively, are shown in Figure 10-10(a) and Figure 10-10(b). The combination of different input profiles leads to some remarkable observations of the behaviour of the system. Namely, the presence of dissolved VOCs in the water recirculation tank, combined with the

spraying cycles during the shut-off periods, produces peaks of pollutant even in the absence of VOCs in the inlet stream. Also desorption is present during these periods. The decrease of these peaks during the shut-off periods are related to the transfer of VOCs to the column, where they get degraded.

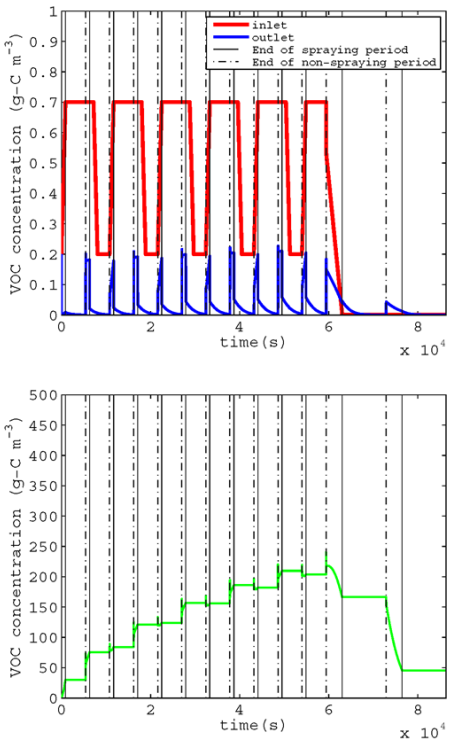

Figure 10-10 Dynamic response of the BTF to oscillating inlet concentration combined with spraying times during non-VOC feeding periods. a) Evolution of the concentration in the gas phase. b) Evolution of the dissolved organic carbon in the recirculation tank.

10.6.3 Dynamic response of the BTF to oscillating gas flow rates

The effect of the gas flow rate on the BTF was studied. A constant concentration of C_{GP} = 0.53 g C m^{-3} was selected. The gas flow rate took on two alternating values: 4.8 10^{-4} m^3 s^{-1} and 6.8 10^{-5} m^3 s^{-1}, each one applied for periods of 14400 s. Note that the average value of the EBRT is 60 seconds, as in the previously considered examples.The simulation results are shown in Figure 10-11. Figure 10-11(a) displays the evolution of the inlet and outlet VOC concentrations in the gas phase, Figure 10-11(b) displays the evolution of the concentration of

carbon dissolved in the water tank, and Figure 10-11(c) displays the oscillating EBRT pattern. As can be seen from Figure 10-11(a), the evolution of the peaks of the outlet gas concentration are different from those obtained in the previous examples. The gas velocity is directly related to the mass transfer of the pollutant between the gas and liquid phases, obtaining a greater mass transfer at large gas velocities, and thus, smaller EBRTs. The peaks in the outlet VOC concentration pattern obtained do oscillate according to the oscillating EBRT pattern. This contrasts with Figure 10-7(a), where the peaks increase until reaching a stationary state. These VOC emissions are related to an increase of the IL generated by an increase in the gas velocity and thus a decrease in the EBRT. As for the liquid phase, in Figure 10-11(b) it is possible to observe the influence of the gas velocity and EBRT on the absorption and desorption processes. In this situation, the increase in the amount of carbon dissolved in the water tank is combined with the desorption processes, producing oscillations as in the case of the outlet concentration.

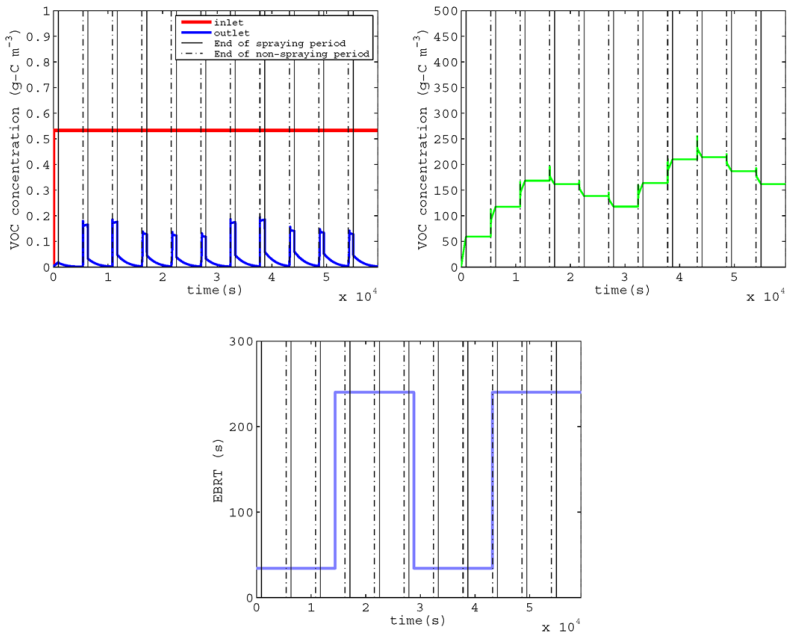

Figure 10-11 Dynamic response of the BTF to oscillating gas flow rates. a) Evolution of the concentration in the gas phase. b) Evolution of the dissolved organic carbon in the recirculation tank. c) Evolution of the EBRT.

10.7 CONCLUSIONS

BTFs usually employ alternating spraying and non-spraying periods. A software tool to simulate the behaviour of BTFs under this and other typical conditions found in industrial facilities has been presented. The partial differential equations of the BTF model have been solved numerically using the method of lines. In particular, the software also allows simulating the treatment of volatile organic compound (VOC) air emissions under variable inlet concentrations and gas velocities. The model was calibrated and validated by using data from a biotrickling filter treating isopropanol under intermittent conditions of loading and spraying. The capability of the model to reproduce the complex phenomena involved in the dynamic response of the treatment of hydrophilic compounds by biotrickling filters has been proven. Several examples demonstrate that the pattern of the outlet emissions depends on the pattern of the gas velocity and inlet concentration, showing the usefulness of the tool to assist in the design and operation of BTFs. The software tool presented herein will be the basis for implementing new features. For example, it would be interesting to allow multi-component mixtures in order to go deeper into the interactions between pollutants. This and other extensions are left for future research.

10.8 NOMENCLATURE

A	specific surface area of the packing material (m^{-1})
C	concentration (g m^{-3})
D	diffusion coefficient of substrates (m^2 s^{-1})
$f(Xv)$	correction factor of diffusivity in biofilm according to Equation (10-13)
H	Henry constant of the substrates
K_s	half saturation rate constants of substrate (g C m^{-3})
K_La	overall mass transfer coefficients of the substrates (s^{-1})
M	number of divisions along the biofilm
N	number of divisions along the column
Q	flow rate (m^3 s^{-1})
S	concentration in the biofilm (g m^{-3})
t	time (s)
v	superficial velocity (m s^{-1})
V	volume (m^3)
x	coordinate for the depth in the biofilm, perpendicular to the biofilm surface
X_v	biomass concentration in the biofilm (g m^{-3})
Y	yield coefficient (g of dry biomass synthesized per g consumed)

z	axial coordinate in the reactor
Z	height of the reactor (m)
C^{in}_{GP}	inlet VOC concentration (g C m^{-3})
C^{in}_{GO}	inlet oxygen concentration (g m^{-3})

Greek letters

β	liquid–biofilm interface (m)
δ	active biofilm thickness (m)
θ_B	fraction occupied by the biofilm
θ_G	porosity of the bioreactor
θ_L	fraction occupied by the liquid film
θ_{PM}	void fraction of the packing material
μ_{max}	maximum specific growth rate of the substratum (s^{-1})

Subscripts

G	gas
L	liquid
B	biofilm
P	pollutant
O	oxygen
R	reactor
T	tank
w	water

Acknowledgements

The research leading to these results has received funding from the People Programme (Marie Curie Actions) of the European Union's Seventh Framework Programme FP7/2007-2013/ under REA grant agreement number 284949. Financial support from the Ministerio de Economia y Competitividad (Project CTM2010-15031/TECNO) and the Generalitat Valenciana (PROMETEO/2013/053), Spain, is also acknowledged. Finally, Pau San Valero thanks the Ministerio de Educación, Cultura y Deporte, Spain, for her FPU contract (AP2010-2191).

10.9 REFERENCES

Álvarez-Hornos, F. J., Gabaldón, C., Martínez-Soria, V., Marzal, P. and Penya-roja, J.-M. (2009). Mathematical modeling of the biofiltration of ethyl acetate and toluene and their mixture. *Biochemical Engineering Journal*, *43*(2), 169–177.

Deshusses, M. A., Hamer, G. and Dunn, I. J. (1995). Behavior of biofilters for waste air biotreatment. 1. Dynamic-model development. *Environmental Science & Technology*, *29*(4), 1048–1058.

Deshusses, M. A. and Shareefdeen, Z. (2005). Modeling of biofilters and biotrickling filters for odor and VOC control Applications. In: Z. Shareefdeen and A. Singh (Eds.), *Biotechnology for Odor and Air Pollution Control* (pp. 213–231). Berlin/Heidelberg: Springer-Verlag.

Devinny, J. S. and Ramesh, J. (2005). A phenomenological review of biofilter models. *Chemical Engineering Journal*, *113*(2-3), 187–196.

European Commission. (2003). *IPPC Reference Document on Best Available Techniques in Common Waste Water and Waste Gas Treatment/Management Systems in the Chemical Sector*. (E. I. Bureau, Ed.). Sevilla.

Fan, L.-S., Leyva-Ramos, R., Wisecarver, K. D. and Zehner, B. J. (1990). Diffusion of phenol through a biofilm grown on activated carbon particles in a draft-tube three-phase fluidized-bed bioreactor. *Biotechnology and Bioengineering*, *35*(3), 279–286.

Ikemoto, S., Jennings, A. and Skubal, K. (2006). Modeling hydrophobic VOC biofilter treatment in the presence of nutrient stimulation and hydrophilic VOC inhibition. *Environmental Modelling & Software*, *21*(10), 1387–1401.

Kim, S. and Deshusses, M. A. (2003). Development and experimental validation of a conceptual model for biotrickling filtration of H_2S. *Environmental Progress*, *22*(2), 119–128.

Lee, S.-H., Li, C., Heber, A. J. and Zheng, C. (2010). Ethylene removal using biotrickling filters: Part I. Experimental description. *Chemical Engineering Journal*, *158*(2), 79–88.

Lu, C. Y., Chang, K. and Hsu, S. (2004). A model for treating isopropyl alcohol and acetone mixtures in a trickle-bed air biofilter. *Process Biochemistry*, *39*(12), 1849–1858.

Mannucci, A., Munz, G., Mori, G. and Lubello, C. (2012). Biomass accumulation modelling in a highly loaded biotrickling filter for hydrogen sulphide removal. *Chemosphere*, *88*(6), 712–7.

Métris, A., Gerrard, A. M., Cumming, R. H., Weigner, P. and Paca, J. (2001). Modelling shock loadings and starvation in the biofiltration of toluene and xylene. *Journal of Chemical Technology & Biotechnology*, *76*(6), 565–572.

Mpanias, C. J. and Baltzis, B. C. (1998). An experimental and modeling study on the removal of mono-chlorobenzene vapor in biotrickling filters. *Biotechnology and Bioengineering*, *59*(3), 328–343.

Okkerse, W. J. H., Ottengraf, S. P. P., Osinga-Kuipers, B. and Okkerse, M. (1999). Biomass accumulation and clogging in biotrickling filters for waste gas treatment. Evaluation of a dynamic model using dichloromethane as a model pollutant. *Biotechnology and Bioengineering*, *63*(4), 418–430.

Ottengraf, S. P. and Van Den Oever, A. H. (1983). Kinetics of organic-compound removal from waste gases with a biological filter. *Biotechnology and Bioengineering*, *25*(12), 3089–3102.

Popat, S. C. and Deshusses, M. A. (2010). Analysis of the rate-limiting step of an anaerobic biotrickling filter removing TCE vapors. *Process Biochemistry*, *45*(4), 549–555.

Reid, R. C., Prausnitz, J. M. and Poling, B. E. (1987). *The properties of gases and liquids.* New York, EEUU: McGraw-Hill Book Company.

Rene, E. R., Veiga, M. C. and Kennes, C. (2013). Biofilters. In: C. Kennes and M. C. Veiga (Eds.), *Air Pollution Prevention and Control: Bioreactors and Bioenergy*. United Kingdom: John Wiley & Sons, Ltd.

Sander, R. (2005). Henry's law constants in NIST chemistry WebBook, NIST standard referencedatabase number 69. In: P. J. Linstrom and W. G. Mallard (Eds.), *National Institute of Standards and Technology*. Gaithersburg MD 208999, USA.

San-Valero, P., Penya-roja, J. M., Álvarez-Hornos, F. J. and Gabaldón, C. (2014). Modelling mass transfer properties in a biotrickling filter for the removal of isopropanol. *Chemical Engineering Science*, *108*(0), 47–56.

San-Valero, P., Penya-roja, J. M., Sempere, F. and Gabaldón, C. (2013). Biotrickling filtration of isopropanol under intermittent loading conditions. *Bioprocess and Biosystems Engineering*, *36*(7), 975–984.

Schiesser, W. E. (1991). *The numerical method of lines*. Academic Press.

Schiesser, W. E. (1994). *Computational mathematics in engineering and applied sciences: ODEs, DAEs and PDEs*. Boca Raton: CRC Press.

Schiesser, W. E. and Griffiths, G. W. (2009). *A compendium of partial differential equations model: method of lines analysis with Matlab*. Cambridge, UK: Cambridge University Press.

Sempere, F., Gabaldón, C., Martínez-Soria, V., Marzal, P., Penya-roja, J. M. and Álvarez-Hornos, F. J. (2008). Performance evaluation of a biotrickling filter treating a mixture of oxygenated VOCs during intermittent loading. *Chemosphere*, *73*(9), 1533–1539.

Sempere, F., Martínez-Soria, V., Penya-roja, J.-M., Izquierdo, M., Palau, J. and Gabaldón, C. (2010). Comparison between laboratory and pilot biotrickling filtration of air emissions from painting and wood finishing. *Journal of Chemical Technology & Biotechnology*, *85*(3), 364–370.

Shareefdeen, Z. and Baltzis, B. C. (1994). Biofiltration of toluene vapor under steady-state and transient conditions -Theory and experimental results. *Chemical Engineering Science*, *49*(24A), 4347–4360.

Tucker, W. A. and Nelken, L. H. (1982). Diffusion coefficients in air and water. In: W. J. Lyman, W. F. Reehl, and D. H. Rosenblatt (Eds.), *Handbook of Chemical Property Estimation Methods*. New York: American Chemical Society.

Webster, T. S., Cox, H. H. J. and Deshusses, M. A. (1999). Resolving operational and performance problems encountered in the use of a pilot/full-scale biotrickling fiber reactor. *Environmental Progress*, *18*(3), 162–172.

Zarook, S. M., Shaikh, A. A. and Ansar, Z. (1997). Development, experimental validation and dynamic analysis of a general transient biofilter model. *Chemical Engineering Science*, *52*(5), 759–773.

Zhu, X. Q., Alonso, C., Suidan, M. T., Cao, H. W. and Kim, B. R. J. (1998). The effect of liquid phase on VOC removal in trickle-bed biofilters. *Water Science and Technology*, *38*(3), 315–322.

11 CONCLUSIONES Y PERSPECTIVAS

11.1 CONCLUSIONES

El objetivo fundamental de esta tesis doctoral ha sido el desarrollo de una herramienta matemática para la simulación del comportamiento transitorio del proceso de biofiltro percolador en el tratamiento de emisiones en aire de COV de elevada solubilidad en agua, bajo alimentación variable y discontinua de contaminante y utilizando patrones de riego intermitente. Las principales conclusiones que se extrae de cada uno de los artículos científicos que componen esta tesis doctoral (**capítulos 6–10**) se exponen a continuación:

1. Se investigó la respuesta de dos biofiltros percoladores empaquetados con dos materiales de relleno diferentes (estructurado y anillos de polipropileno de 15 mm) para el tratamiento de emisiones en aire de isopropanol. Se utilizaron patrones de riego intermitente (15 min cada 1.5 h) y de alimentación discontinuos (16 h por día, 5 días a la semana) con interrupciones asociadas a los periodos no productivos en fábrica. La respuesta de ambos biofiltros percoladores demostró la capacidad de esta tecnología para adaptarse a condiciones de operación propias de la industria. Se obtuvieron eficacias de eliminación completas con la aplicación de cargas volumétricas de entrada de hasta 30 g C m^{-3} h^{-1}. Así mismo se ha demostrado que el biofiltro percolador empaquetado con anillos de polipropileno es capaz de obtener una capacidad de eliminación máxima ligeramente superior (51 g C m^{-3} h^{-1}) que el biofiltro percolador empaquetado con el material de relleno estructurado (45 g C m^{-3} h^{-1}), bajo la máxima carga volumétrica de entrada (65 g C m^{-3} h^{-1}) y el mínimo tiempo de residencia de volumen vacío ensayado (14 s).

2. El patrón de emisión de contaminante en la fase gas del biofiltro percolador de laboratorio mostró que durante el riego se producía una emisión fugitiva de isopropanol. El estudio sobre su influencia en la operación de los biofiltros percoladores ha demostrado que disminuir la frecuencia de riego y expandirlo a los periodos de entrada de aire limpio al bioreactor, correspondientes a paradas prolongadas de fabricación de procesos 1 o 2 turnos diarios, permite eliminar el contaminante acumulado en la biopelícula y en el tanque de recirculación, mejorando la eficacia global del sistema. Esta forma de operar los biofiltros percoladores es una estrategia de optimización trasladable a la industria que permite aprovechar los ciclos de fabricación de las empresas para eliminar el compuesto orgánico acumulado en la fase

líquida y, por tanto, minimizar la emisión durante el riego en la corriente gaseosa depurada.

3. El sistema respondió satisfactoriamente a una interrupción en la alimentación de isopropanol de casi 2 meses de duración, obteniéndose eficacias de eliminación de 90 % tras 10 días desde la reanudación de la alimentación, similares a las obtenidas antes de dicha parada. Con este resultado se pone de manifiesto la robustez de esta tecnología para el tratamiento de compuestos orgánicos volátiles de elevada solubilidad en agua para aplicaciones industriales.

4. La transferencia de materia es un aspecto clave en la operación de los biofiltros percoladores. Por ello, en esta tesis doctoral se ha hecho énfasis en el estudio de transferencia de materia del contaminante orgánico y del oxígeno. El estudio de transferencia de materia de isopropanol llevado a cabo con un material de relleno estructurado y con los anillos de polipropileno de 25 mm ha demostrado que, en las condiciones estudiadas, la transferencia de isopropanol aumenta con la velocidad superficial de gas, siendo despreciable la influencia de la velocidad superficial de líquido y del material de relleno. Se ha propuesto una correlación empírica que depende de la velocidad superficial de gas. El estudio de la transferencia de oxígeno con tres materiales de relleno (material estructurado y anillos de polipropileno de 15 mm y de 25 mm) ha demostrado que, en las condiciones estudiadas, la transferencia de oxígeno se ve favorecida al incrementar la velocidad superficial de líquido. La influencia significativa del tipo de material de relleno y/o de la superficie específica del mismo en la transferencia de oxígeno se observó para velocidades superficiales de líquido superiores a 15 m h^{-1}. Se ha propuesto una correlación empírica que depende de la velocidad superficial de líquido para cada uno de los materiales de relleno ensayados. Por tanto, este estudio ha permitido calibrar los coeficientes de transferencia de materia. Estas correlaciones han sido incluidas en el modelo matemático desarrollado en esta tesis.

5. El estudio comparativo de transferencia de oxígeno entre los materiales de relleno utilizados en el laboratorio (material estructurado y anillos de polipropileno de 15 mm y de 25 mm de diámetro) y el material de relleno que se utiliza en biofiltros percoladores industriales (anillos de polipropileno de diámetro de 50 mm) ha demostrado que, en los intervalos de velocidad superficial de líquido utilizados en los biofiltros percoladores industriales (2–6

m h^{-1}), la transferencia de oxígeno no se ve favorecida por el tipo de material de relleno ni por el aumento de la superficie específica del material. Por tanto, durante el cambio de escala a la instalación industrial, utilizando los anillos de polipropileno de 50 mm, se obtendría una transferencia de oxígeno comparable a la obtenida con los materiales de relleno utilizados en el laboratorio.

6. El seguimiento de manera paralela de la evolución del patrón de emisión de contaminante de la fase gas y de la evolución de la concentración de carbono orgánico disuelto en el tanque de recirculación ha demostrado que la concentración máxima de contaminante en la fase gas a la salida del bioreactor durante el riego es superior a la concentración en equilibrio con el carbono orgánico disuelto en el tanque de recirculación. Esto evidencia que la fuga de contaminante durante el riego no está asociada sólo a la desorción de contaminante desde la fase líquida a la fase gas.

7. Se ha desarrollado un modelo dinámico de tres fases (gas–líquido–biopelícula) basado en el uso de condiciones cíclicas de periodos con riego y periodos sin riego. Durante los periodos con riego se ha considerado una fase líquida móvil mientras que en los periodos sin riego se ha considerado una fase líquida estancada. Este modelo es capaz de simular el comportamiento de los biofiltros percoladores que tratan COV de elevada solubilidad en agua bajo condiciones que utilizan riego intermitente y de carga volumétrica discontinua a nivel de laboratorio, y de carga discontinua y variable a nivel industrial.

8. La aplicación del modelo para la simulación del biofiltro percolador de laboratorio ha permitido demostrar que durante los periodos sin riego, la fase líquida estancada ofrece una resistencia despreciable a la transferencia de materia gas – líquido debido al fino espesor de la biopelícula. La emisión fugitiva de contaminante durante el riego solo se puede explicar si hay un aumento de la resistencia a la transferencia de materia desde la fase gas a la fase líquida móvil respecto a las transferencia de materia obtenida en condiciones abióticas que varía a lo largo del ciclo de producción asociado a cambios en las propiedades físicas de la biopelícula.

9. La aplicación del modelo ha permitido explicar que el uso de biofiltros percoladores a escala industrial para el tratamiento de COV de elevada solubilidad en agua está condicionado por el crecimiento excesivo de la biopelícula, lo que provoca que la resistencia a la transferencia desde la fase gas a la fase líquida durante el periodo de no riego no se pueda considerar

despreciable, contrariamente a lo que sucedía en los biofiltros percoladores de laboratorio. En consecuencia, el sistema actúa como fuente/sumidero, acumulando compuestos orgánicos en el interior de la biopelícula en los periodos de alimentación de contaminante al reactor, y desorbiéndolos en los periodos con aire limpio, siendo ésta la causa del patrón de emisión amortiguado que se observa en los biofiltros percoladores industriales.

10. La utilidad práctica del modelo ha quedado demostrada con su aplicación a la simulación del comportamiento de los biofiltros percoladores ante diferentes condiciones de operación típicas de la industria, como es la alimentación discontinua asociada a paradas de producción y variaciones en las concentraciones de entradas y caudales de gas producidos por los propios procesos de fabricación. La creación de una interfaz gráfica de comunicación con el usuario final ha supuesto el desarrollo de una herramienta útil para asistir en tareas de diseño y operación de los biofiltros percoladores, facilitando la transferencia del modelo al entorno industrial.

11.2 PERSPECTIVAS Y TRABAJO FUTURO

El trabajo de tesis doctoral realizado ha permitido profundizar en los principales mecanismos involucrados en la depuración de emisiones en aire de compuestos orgánicos volátiles de elevada solubilidad en agua en biofiltros percoladores. Los resultados experimentales han proporcionado una información valiosa en lo referente a la comprensión de este proceso cuando se trabaja en condiciones dinámicas de emisión de contaminante y riego del reactor, característica de los procesos industriales. En este sentido, a partir de la experiencia adquirida se proponen las siguientes líneas de trabajo futuro:

1. Estudio de las interacciones entre contaminantes durante la depuración de emisiones en aire de compuestos orgánicos volátiles de elevada solubilidad en agua mediante la inclusión en el modelo de nuevas cinéticas microbianas que incluyan la inhibición por sustrato e inhibición competitiva entre compuestos, entre otras.

2. Ampliación del modelo para estudiar la generación de productos intermedios en la depuración de emisiones en aire de compuestos orgánicos volátiles de elevada solubilidad en agua. En especial sería de interés incluir la generación de ácidos grasos volátiles en las etapas profundas de la biopelícula e

introducir la influencia que tiene la evolución del pH asociada a la producción de estos compuestos sobre el funcionamiento del sistema.

3. Aplicación del modelo a otro tipo de compuestos orgánicos volátiles de menor solubilidad en agua que los estudiados en la presente tesis doctoral a fin de ampliar su uso a otros sectores de interés industrial.
4. Transferencia de la herramienta generada al entorno industrial para ser utilizada como soporte en el diseño y operación de los biofiltros percoladores.

12 CONCLUSIONS AND PERSPECTIVES

12.1 CONCLUSIONS

The main objective of this work was the development of a mathematical tool for the simulation of the transient behaviour of the biotrickling filter process in the treatment of air emissions polluted with VOC of high water solubility, under variable and discontinuous pollutant feeding conditions, and using intermittent spraying patterns. The main conclusions are:

1. The response of two biotrickling filters filled with two different packing materials (structured and propylene rings of 15 mm) for the removal of isopropanol in waste gases was investigated. Intermittent spraying (15 min every 1.5 h) and discontinuous feeding (16 h per day; 5 days per week) associated with shut-off of the manufacturing processes were applied. The results demonstrated the capability of this technology to be applied to the typical operational conditions for industrial facilities. Complete removal up to an inlet load of 30 g C m^{-3} h^{-1} was obtained. At the highest inlet load (65 g C m^{-3} h^{-1}) and the minimum the minimum empty residence time applied (14 s), the biotrickling filter filled with propylene rings obtained a slightly higher elimination capacity (51 g C m^{-3} h^{-1}) than the biotrickling filter filled with the structured packing material (45 g C m^{-3} h^{-1}).

2. The outlet emission pattern showed a fugitive emission of pollutant in the gaseous stream during intermittent spraying. The study of their influence on the biotrickling filters operation demonstrated that overall system efficiency was improved by decreasing the spraying frequency and expanding the irrigation to periods when clean air is introduced. This fact promotes the biodegradation of the accumulated pollutant in the biofilm and in the recirculation tank. This operation mode of biotrickling filters is an optimisation strategy transferable to industry. This strategy takes advantage of production cycles of the companies to remove accumulated organic matter in the liquid phase. Therefore, pollutant emissions in the gaseous purified stream would be minimised.

3. A successful re-startup after nearly two months starvation period was obtained, achieving removal efficiencies of 90% after 10 days of the resumption of feeding of VOC. The elimination capacities obtained were similar to those obtained before the starvation period. These results corroborated the robustness of this technology for the treatment of volatile organic compounds of high water solubility in industrial applications.

4. Mass transfer is a key aspect in the operation of biotrickling filters. Thus, the study of mass transfer of the pollutant and of the oxygen has been emphasised here. The study of mass transfer of isopropanol using a structured packing material and propylene rings of 25 mm has been carried out. At the tested conditions, results demonstrated that the mass transfer coefficient of isopropanol increased with the superficial gas velocity, while the influence of the superficial liquid velocity and the packing material was negligible. An empirical correlation between the isopropanol mass transfer coefficient and the superficial gas velocity has been proposed. The study of the oxygen mass transfer with three packing materials (i.e. structured packing and propylene rings of 15 mm and 25 mm) was carried out. At the tested conditions, the results demonstrated that the mass transfer of oxygen is enhanced by increasing the superficial liquid velocity. Only for superficial liquid velocities greater than 15 m h^{-1} was the influence of packing material and/or its specific surface area on the oxygen mass transfer observed. An empirical correlation between oxygen mass transfer coefficients and superficial liquid velocity has been proposed for each of the tested packing materials. Thus, the obtained results enabled calibration of the mass transfer coefficients. These correlations have been included in the mathematical model developed here.

5. A comparative study of oxygen mass transfer between the packing materials applied in the laboratory (i.e. structured packing material and propylene rings of 15 mm and 25 mm diameter) and the packing material used in industry (i.e. propylene rings of 50 mm diameter) was carried out. In the range of superficial liquid velocities used in the industrial biotrickling filters (2–6 m h^{-1}), results showed that oxygen mass transfer is not enhanced for the type of packing material nor the increase of the specific surface area. Thus, a comparable mass transfer as that obtained at laboratory would be achieved during scaling-up to the industrial installation using the 50 mm propylene rings.

6. Parallel monitoring of the evolution of the emission pattern of pollutant in the gas phase and of the evolution of the dissolved organic carbon concentration in the recirculation tank was carried out for a laboratory biotrickling filter treating isopropanol. A higher concentration of pollutant in the outlet gaseous stream of the bioreactor than the predicted equilibrium concentration with the dissolved organic carbon in the recirculation tank has

been demonstrated. This fact indicates that leaks of pollutant during spraying cannot be only associated with desorption of the pollutant from the liquid phase to the gas phase.

7. A three-phase dynamic model (gas-liquid-biofilm) based on the use of cyclical conditions of spraying periods and non-spraying periods has been developed. During spraying periods, a mobile liquid phase was considered, while during non-spraying, a stagnant liquid phase was considered. The model is able to simulate the behaviour of biotrickling filters that treat VOC of high water solubility under intermittent spraying and discontinuous inlet loading at laboratory level as well as under intermittent spraying and discontinuous and variable inlet loading at industrial level.

8. A negligible mass transfer resistance at the stagnant liquid phase during non-spraying periods has been demonstrated by model application to simulation of laboratory biotrickling filters. Also, it was corroborated that the fugitive emission during spraying is only explained by an increase of the mass transfer resistance from the gas phase to the mobile liquid phase compared to the mass transfer resistance obtained in abiotic conditions. Variations of mass transfer resistance along the production cycles associated with variations of the physical properties of the biofilm were obtained.

9. Use of biotrickling filters in the industrial environment for treatment of VOC of high solubility in water conditioned by the excessive growth of the biofilm has been demonstrated. Thus, mass transfer resistance from the gas phase to the stagnant liquid phase during non-spraying periods could not be considered as negligible, compared to that obtained at laboratory scale. As a consequence, the system acts as a source/sink, accumulating organic compounds within the biofilm when polluted air is supplied and desorbing it in the periods when clean air is supplied. This phenomenon explains the buffered emission pattern of the industrial biotrickling filter.

10. The practical usefulness of the model has been demonstrated with the model application for simulating the behaviour of biotrickling filters under different typical industrial conditions, such as discontinuous loading associated with production closures and variations of the inlet concentration and gas flow rates due to the manufacturing processes. Creation of a graphical interface for communication with the end user resulted in a useful tool to assist in design tasks and operational tasks of biotrickling filters, facilitating model transfer to the industrial environment.

12.2 PERSPECTIVES AND FUTURE WORK

This dissertation has allowed for profound study of the main mechanisms involved in the treatment of air emissions of volatile organic compounds of high solubility in water. The experimental results provided valuable information regarding the understanding of this process when the system works under dynamic pollutant emission and spraying, as is the case for industrial processes. In this regard, from the experience acquired, the following future lines of work are proposed:

1. Study of the interactions between pollutants during the treatment of air emissions of volatile organic compounds of high solubility in water by the inclusion of new microbial kinetics in the model that would include the inhibition by substrate and competitive inhibition between compounds, among others.
2. Expansion of model to study the generation of intermediate products in the treatment of air emissions of volatile organic compounds of high water solubility. It would be interesting to include the generation of volatile fatty acids in the deeper parts of the biofilm and to introduce the influence of the evolution of the pH associated with the production of these compounds on system performance.
3. Application of the model to other kinds of volatile organic compounds with less volatility than those applied here, in order to expand its use to other sectors of industrial interest.
4. Transfer of the generated tool to the industrial environment in order to be used as support in the design and operation of biotrickling filters.

13 ANEXO

Bioprocess Biosyst Eng (2013) 36:975–984
DOI 10.1007/s00449-012-0833-y

ORIGINAL PAPER

Biotrickling filtration of isopropanol under intermittent loading conditions

Pau San-Valero · Josep M. Penya-Roja · Feliu Sempere · Carmen Gabaldón

Received: 7 September 2012 / Accepted: 17 September 2012 / Published online: 29 September 2012

Abstract This paper investigates the removal of isopropanol by gas-phase biotrickling filtration. Two plastic packing materials, one structured and one random, have been evaluated in terms of oxygen mass transfer and isopropanol removal efficiency. Oxygen mass transfer experiments were performed at gas velocities of 104 and 312 m h^{-1} and liquid velocities between 3 and 33 m h^{-1}. Both materials showed similar mass transfer coefficients up to liquid velocities of 15 m h^{-1}. At greater liquid velocities, the structured packing exhibited greater oxygen mass transfer coefficients. Biotrickling filtration experiments were carried out at inlet loads (IL) from 20 to 65 g C m^{-3} h^{-1} and empty bed residence times (EBRT) from 14 to 160 s. To simulate typical industrial emissions, intermittent isopropanol loading (16 h/day, 5 day/week) and intermittent spraying frequency (15 min/1.5 h) were applied. Maximum elimination capacity of 51 g C m^{-3} h^{-1} has been obtained for the random packing (IL of 65 g C m^{-3} h^{-1}, EBRT of 50 s). The decrease in irrigation frequency to 15 min every 3 h caused a decrease in the outlet emissions from 86 to 59 mg C Nm^{-3} (inlet of 500 mg C Nm^{-3}). The expansion of spraying to night and weekend periods promoted the degradation of the isopropanol accumulated in the water tank during the day, reaching effluent concentrations as low as 44 mg C Nm^{-3}. After a 7-week starvation period, the performance was recovered in less than 10 days, proving the robustness of the process.

P. San-Valero · J. M. Penya-Roja · F. Sempere · C. Gabaldón (✉)
Research Group GI^{2}AM, Department of Chemical Engineering, University of Valencia, Avda. Universitat s/n, 46100 Burjassot, Spain
e-mail: carmen.gabaldon@uv.es

Keywords Biotrickling filter · Intermittent loading · Isopropanol · Oxygen mass transfer · Volatile organic compounds

Introduction

Isopropanol is one of the main solvents used in chemical industries, and its manufacture worldwide exceeds 1×10^6 tonnes per year. This results in a significant production of solvent organic wastes, including emissions to the atmosphere as volatile organic compounds (VOC). Since the abatement of VOC is a factor in the protection of the environment and of public health in Europe [1], treatment technologies for VOC removal are required. When emissions are characterised by high flow rates and low VOC concentrations, biotreatments are suitable alternatives to conventional physicochemical technologies and have been classified as best available technologies (BAT) [2] owing to their low operational costs and the minimisation of negative cross-media effects [3]. Compared to a conventional biofilter, a biotrickling filter (BTF) allows better control of the physicochemical parameters, offers a smaller footprint and higher removal rates. The BTF uses an inert packing material and involves the continuous or intermittent trickling of water. In this configuration, the biomass attaches to the media and develops a biofilm; thus, the pollutant and the oxygen must be transferred from the gas phase to the trickling liquid and then to the biofilm, where the biodegradation takes place.

To enhance the performance of the BTF, it is necessary to understand the rate limiting steps of the process. One of the most important limiting factors may be the mass transfer from gas to liquid and biofilm [4–6]. However, correlations commonly used for absorption in chemical

processes do not correctly represent the phenomenon occurring in BTFs due to the different hydrodynamic conditions of chemical absorption. Absorption is marked by higher superficial velocities of the gas and liquid in comparison with BTF [7]. Treatment of hydrophilic compounds such as isopropanol, characterised by low Henry's constants, could typically be limited by oxygen transference. Consequently, oxygen mass transfer should be systematically studied in these cases [7].

Despite being widely used in industrial and chemical processes, there are no previous studies on the removal of isopropanol by biotrickling filtration. Literature data about the removal of isopropanol by biofilters is also scarce compared with other solvents [8, 9]. These works have been performed under continuous and constant loading; the removal of isopropanol under oscillating and/or discontinuous emissions has not been previously reported. Most gaseous emissions from industrial processes are intermittently generated due to short-time shut-off periods during the night and/or weekends. In fact, previous studies show that the operation of biofiltration under discontinuous VOC feeding regime can produce a degeneration of the system's performance, although the literature in this field is still limited. Cox and Deshusses [10] reported that non-use periods cause a starvation condition on the microorganisms, which has been identified as one of factors that causes a reduction in pollutant removal. These researchers observed that after 2 days of starvation, the endogenous respiration activity dropped by about 60 % and remained relatively constant thereafter.

The influence of long-term starvation periods, without VOC feeding, also requires further study to advance the applicability of this technology. In our previous work, the reacclimation period, after 3 weeks without VOC feeding, was lower than 24 h working at 60 s of empty bed residence time (EBRT) in a BTF treating a mixture of ethanol, ethyl acetate and methyl-ethyl ketone (MEK), and operating under discontinuous loading [11].

The purpose of the present study was to investigated the removal of isopropanol using a BTF, taking into consideration the following objectives: (1) to determine the oxygen mass transfer coefficient of a structured and a random packing material, establishing a relationship between the mass transfer coefficient, the trickling flow rate and the specific surface area; (2) to compare the performance of the process, in terms of EC and RE, under isopropanol discontinuous loading conditions at several EBRT by using two BTFs operating in parallel, one filled with the structured and the other with the random material; (3) to evaluate the influence of spraying frequency on the RE, and (4) to evaluate the response of the BTFs to a long-term starvation period representative of a holiday closure at an industrial site.

Materials and methods

Experimental setup for the determination of oxygen mass transfer

The system consisted of a column of methacrylate (14.4 cm internal diameter, 80 cm height) and a recirculation tank (10 L of water volume). The schematic of the experimental setup is shown in Fig. 1. The column was filled with two inert packing materials: a novel plastic cross-flow structured packing material (Odourpack, Pure Air Solution, The Netherlands) with 410 $m^2\ m^{-3}$ specific surface area and a random packing material (Refill-Tech, Italy) consisting of polypropylene rings with a nominal diameter of 5/8 in. and a specific surface area of 348 $m^2\ m^{-3}$. The packing height was 20 cm for the structured packing and 40 cm for the rings. The air stream (compressed, filtered and dried) was introduced through the bottom of the columns, with the flow rate adjusted using a mass flow controller (Bronkhorst Hi-Tec, The Netherlands). The experiments were carried out at two air superficial velocities of 104 and 312 m h^{-1}. The trickling water was recirculated using a centrifugal pump (HPR10/15, ITT, Great Britain) in counter-current mode with respect to the air flow rate, with a superficial velocity of the water between 3 and 33 m h^{-1}. The equipment is completed with a dissolved oxygen probe (Cellox® 325i, WTW, Germany). An internal pump installed in the recirculation tank ensured the ideal mixing condition. The experiments were carried out at room temperature (21.2 ± 0.7 °C).

For the determination of k_La, a dynamic method under inert conditions was used. The method consists of

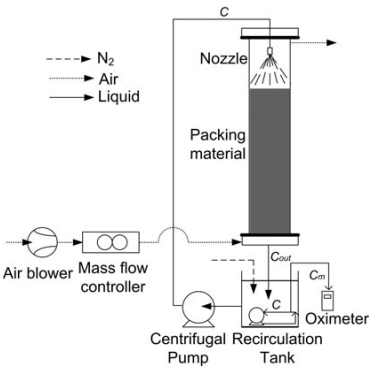

Fig. 1 Schematic of the experimental setup for the determination of k_La

measuring the increase in the oxygen concentration with time in a tank in which the oxygen has been previously displaced by bubbling nitrogen gas. The experiment starts when the air blower and the recirculation pump are switched on; oxygen is transferred from the air to the water in the packed column causing an increase in the dissolved oxygen concentration in the recirculation tank. Under these conditions, oxygen mass balances are as follows:

- In the packed column:

$$C_{\text{out}} = C^* - \frac{C^* - C}{\exp\left(\frac{L}{v}k_{\text{L}}a\right)} \quad (1)$$

where C_{out} is the predicted dissolved oxygen concentration at the bottom of the column, C is the predicted dissolved oxygen concentration in the recirculation tank, C^* is the oxygen solubility and L and v are the height of the column and the velocity of the trickling water, respectively.

- In the tank:

$$\frac{\mathrm{d}C}{\mathrm{d}t} = \frac{1}{\theta}(C_{\text{out}} - C) \quad (2)$$

where θ is the residence time in the tank.

The combination of Eqs. (1) and (2) permits obtaining the variation of the predicted oxygen concentration with time:

$$\frac{\mathrm{d}C}{\mathrm{d}t} = \frac{1}{\theta}\left(C^* - \left(\frac{C^* - C}{\exp\left(\frac{L}{v}k_{\text{L}}a\right)} - C\right)\right). \quad (3)$$

Because the dynamics of the probe is not fast enough, it is necessary to take into account the response time constant of the probe, τ, defined as time that the probe achieves 63 % of the end value measured when the probe is subjected to a step input assay [12]. The response time of the probe was determined by transferring the oxygen probe from an ideal mixed tank in which the dissolved oxygen concentration was displaced by bubbling nitrogen gas to a second tank which is saturated with dissolved oxygen. A first-order dynamic was assumed according to Eq. (4) [13].

$$\frac{\mathrm{d}C_{\text{m}}}{\mathrm{d}t} = \frac{(C - C_{\text{m}})}{\tau} \quad (4)$$

where C_{m} is the measured dissolved oxygen concentration in the recirculation tank by the oxygen probe.

The value of $k_{\text{L}}a$ of the packed column was calculated by minimising the sum of squares of the difference between the measured data recorded for dissolved oxygen concentration in the recirculation tank and the value obtained from the mathematical resolution of Eqs. (3) and (4).

Experimental setup for the removal of isopropanol

The experiment was performed using two identical laboratory-scale BTFs operating in parallel, named BTF1 and BTF2. The experimental setup is shown in Fig. 2. Each bioreactor was composed of three cylindrical methacrylate modules in series, with a total bed length of 100 cm and an internal diameter of 14.4 cm. BTF1 was filled with the structured material and BTF2 with the random packing, in each using a volume of 16.32 L. The bioreactors were also provided with 20 cm of top and bottom free spaces. The stream contaminated with isopropanol was introduced through the bottom of the column of the BTFs. A recirculation solution of 3 L, partially renewed every week, was fed into the bioreactor in counter-current mode with respect to the air flow using a centrifugal pump at 2.5–3 L min^{-1}. A nutrient solution buffered at pH 7 (21.65 g KNO_3 L^{-1}, 4.6 g $Na_3PO_4{\cdot}12H_2O$ L^{-1} and Ca, Fe, Zn, Co, Mn, Na, Ni, B, I, Se, Cr, Cu and vitamins at trace doses) was supplied to the recirculation tank using a peristaltic pump. The nutrient solution flow rate was set to maintain a supplied mass ratio of carbon and nitrogen (C/N) of 35, in order to assure that the nitrogen concentration in the recirculation solution was not limiting the biodegradation process. C/N mass ratios between 13 and 70 are suggested in the literature for the operation of bioreactors [14].

Influence of IL and EBRT on the removal of isopropanol

The operation of the bioreactors to determine the influence of IL and EBRT on the removal of isopropanol was structured in three phases (A, B, C) of a twofold step decrease in inlet concentration. Phase A started with

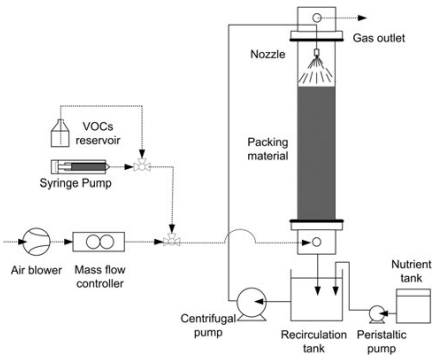

Fig. 2 Schematic of the experimental setup for the elimination of isopropanol

Table 1 Experimental plan for the removal of isopropanol under intermittent loading conditions

	Days	C_{in} (mg C Nm^{-3})	IL (g C m^{-3} h^{-1})	EBRT (s)
Phase A				
A-I	0–48	1,000	20	160
A-II	49–69	1,000	35	90
A-III	70–90	1,000	65	50
Phase B				
B-I	91–97	500	20	90
B-II	98–104	500	35	50
B-III	105–125	500	65	25
Phase C				
C-II	126–132	250	35	25
C-III	133–163	250	65	14

1,000 mg C Nm^{-3}. For each phase, several 1.8-fold IL step increases were carried out, resulting in EBRTs from 15 to 160 s. The design parameters of the experiments are summarised in Table 1. Intermittent feeding of VOC was programmed to simulate shift working conditions, which consisted of a regime of a period with VOC feeding of 16 h per day (from 6 to 22 h) for 5 days a week, and night and weekend periods without VOC supply. The air flow rate was kept constant during both periods. Water was trickled for 15 min every 1.5 h during the VOC feeding period. During non-VOC feeding periods, the trickling of water was stopped.

Influence of spraying frequency on the removal of isopropanol

The influence of the spraying frequency on the global performance of the system was evaluated by testing several patterns at an IL of 30 g C m^{-3} h^{-1} and EBRT of 60 s on the random packing material. Three frequency regimes were tested. Two of them were only applied during VOC feeding (16 h per day, 5 days per week) with trickling water frequencies of 15 min every 1.5 h or 15 min every 3 h; spraying was stopped during the night and weekend periods. The expansion of spraying to the non-VOC feeding periods was tested by trickling 15 min every 3 h over the whole day (24 h per day, 7 days per week).

Influence of long-term starvation on the removal of isopropanol

The influence of a long period without VOC feeding on the performance of the BTF was evaluated by stopping the supply of isopropanol for a period of 7 weeks. During this time, the air flow rate was maintained at an EBRT of 60 s and the water trickling was set to 15 min per day, to provide the minimum amount of nutrients and moisture that assures biomass viability. After that, the supply of isopropanol was restored using the same discontinuous VOC feeding mode (16 h per day, 5 days per week) that was applied before the VOC interruption; IL of 35 g C m^{-3} h^{-1}, EBRT of 60 s and a trickling water frequency of 15 min every 4 h were set.

Analytical methods

The oxygen concentration in the liquid was determined using a dissolved oxygen probe (Cellox® 325i, WTW, Germany). The concentration of isopropanol was measured using a total hydrocarbon analyser (Nira Mercury 901, Spirax Sarco, Spain). The response factor of the total hydrocarbon analyser was determined by gas chromatograph (model 7890, Agilent Technologies, EEUU). The CO_2 concentration was analysed using a nondispersive infrared carbon dioxide analyser (GMP222, Vaisala, Finland). The inlet and outlet gas streams were monitored daily. The pressure drop was monitored daily (MP101, KIMO Instruments, Spain). To determine the quality of the recirculation solution, conductivity and pH (ph/Cond 340i, WTW, Germany), soluble chemical oxygen demand (COD), nitrate and suspended solids (SS) concentrations were measured prior to the weekly purge. Soluble COD and nitrate concentrations were measured using Merck Speqtroquant kits (Merck KGaA, Germany): 114540 (COD) and 114773 (nitrate). The SS concentrations were determined according to the Standard Methods for Examination of Water and Wastewater [15].

Results and discussion

Determination of oxygen mass transfer coefficients

The determination of oxygen mass transfer coefficients was carried out for the two packing materials at several liquid velocities. The k_La coefficients were obtained using the least squares method to minimise the differences between the experimental data and the concentration of oxygen provided by the simple mathematical model established by Eqs. (3) and (4). The response time of the probe (τ) was determined earlier by means of a step input assay, resulting in a value of 19.4 ± 1.5 s. The effect of liquid velocity on mass transfer is shown in Fig. 3. The two packing materials presented a relationship between the liquid flow rate and the k_La values for a gas velocity of 104 m h^{-1} with similar values up to 15 m h^{-1}. For liquid velocities higher than this value, the structured material showed greater values of k_La. That difference cannot be explained by the slightly higher specific surface area of this material alone, but it

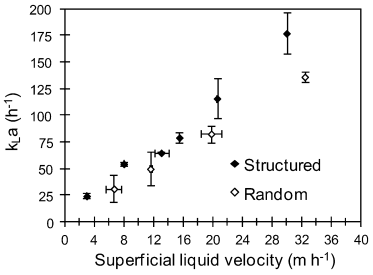

Fig. 3 Influence of superficial liquid velocity on the oxygen mass transfer coefficient in BTFs

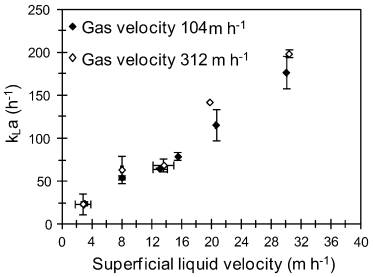

Fig. 4 Influence of superficial gas velocity on the oxygen mass transfer coefficient for the structured packing material

could be attributed to the different air and water flow paths in both materials. Selecting a liquid velocity of 10 m h^{-1} as representative of the operation of the BTFs in this study, a k_La approximately of 45 h^{-1} was obtained for both packing materials, without differences between them. The values obtained herein are of the same order of magnitude as those found by Kim and Deshusses [7] in previous papers. These authors reported a value of about 25 h^{-1} for liquid velocities around 10 m h^{-1} using 1 in. Pall rings (210 m^2 m^{-3}). These authors showed that Onda's correlation overestimated the k_La values on biotrickling filtration by a factor of about 20 [16], indicating the need for determining oxygen mass transfer in the typical range of velocities of biotreatments.

The influence of gas velocity on the oxygen mass transfer coefficients was determined with an additional test conducted at a gas velocity of 312 m h^{-1}. As an example, the results obtained for the structured packing material are shown in Fig. 4. As can be expected, these experiments demonstrated that k_La values were not significantly affected by gas velocities in the typical values of operation of BTFs.

Influence of inlet load and EBRT on the removal of isopropanol

The influence of inlet load on the removal of isopropanol in terms of EC and RE was evaluated. To simulate the emissions of industrial facilities, an intermittent VOC loading regime and a discontinuous trickling pattern were used. As an example, 24 h of a typically daily evolution of VOC concentration in the outlet gas stream of the BTF2 is shown in Fig. 5. This figure represents the outlet emission pattern for two different stages where inlet concentrations of 1,000 mg C Nm^{-3} (IL of 65 g C m^{-3} h^{-1}, stage A-III, Fig. 5a) and 500 mg C Nm^{-3} (IL of 35 mg C m^{-3}, stage B-II, Fig. 5b) were applied. As can be observed, the operating regime resulted in peaks of concentration coinciding with the irrigation of the bed (15 min every 1.5 h). These peaks are related to the accumulation of the pollutant in the trickling water and subsequent desorption when trickling starts, resulting in outlet emission peaks. The comparison between both stages shows the influence of loading in the emission pattern. In the periods between trickling, a complete removal of pollutant was achieved for the lowest loading condition (Fig. 5b), while leakage of pollutant occurred for the highest load (Fig. 5a).

The monitoring of the quality of the trickling water was carried out twice per week for the whole experimental period. The average values along with the standard deviation are shown in Table 2. As shown in Table 2, the pH and conductivity were kept at normal values for the development of the biological process during the whole period. Nitrate in the water tank was kept above 10 mg N L^{-1} making sure that nutrients were not limiting the bioprocess. Soluble COD values ranged between 700 and 1,800 mg COD L^{-1} depending on the loading conditions. The operational protocols regarding the quality of the trickling water included a weekly purge of 1.5 L of water. In all cases, solvent removal with the purge represents less than 5 % of the total amount of fed isopropanol during the week. In consequence, the organic carbon in the purge was considered negligible for evaluation of the BTF performance in terms of inlet load (IL), elimination capacity (EC) and removal efficiency (RE). About suspended solids, concentrations higher than 500 mg L^{-1} were only observed since month 3, indicating that significant detachment of solids from the packing materials started as the biofilm thickened. Average values of the suspended solids concentration from day 90 until the end of the experimentation period resulted in 3,151 and 1,022 mg L^{-1} for BTF1 and BTF2, respectively. The higher suspended solid concentrations in BTF1 than in BTF2 can be associated with the capability of the structured packing material to drag the biomass, in comparison with the random packing where biomass is detached with greater difficulty. In both bioreactors, the pressure drop was kept below

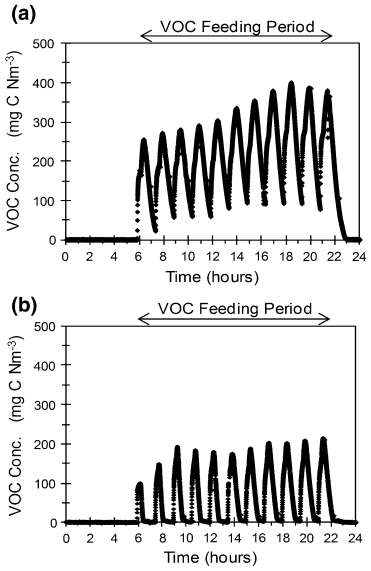

Fig. 5 Outlet pattern emission during 24 h monitoring of the biotrickling filtration of isopropanol under intermittent loading conditions for BTF2: **a** phase A-III, **b** phase B-II

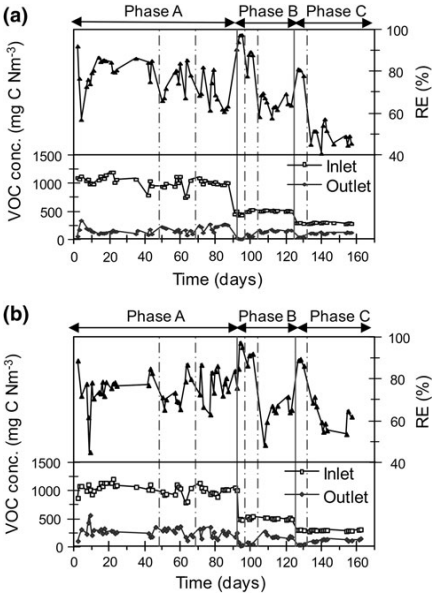

Fig. 6 Performance of the BTFs on the removal of isopropanol. The *discontinuous line* represents a 1.8-step increase in the inlet load: **a** BTF1, **b** BTF2

Table 2 Quality of trickling water during the whole experiment

	BTF1		BTF2	
	Average	SD	Average	SD
pH	8.91	0.23	9.01	0.23
Conductivity (mS cm^{-1})	5.22	1.33	5.23	1.14
Nitrate conc. (mg N L^{-1})	30	23	38	33
Soluble COD (mg L^{-1})	1,200	498	1,107	540

48 Pa m^{-1}, indicating that nonexcessive accumulation of biomass occurred. The accumulation of acetone as an intermediate product was not observed.

To quantify the outlet concentration of VOC, the most unfavourable conditions were selected. So, the average values of the previous 7 h during VOC feeding (from 15 to 22 h: last five spraying cycles) was used. The performance of BTF1 and BTF2 is shown in Fig. 6a, b, respectively. A similar evolution of both BTFs during the whole experiment was observed. The start-up was carried out using activated sludge from the secondary clarifier of the municipal wastewater treatment plant of Carlet (Spain). In order to simulate the procedure of the industrial BTFs, the inoculum was not previously adapted to degrade isopropanol. The systems were started by setting an EBRT of 160 s for BTF1 and 152 s for BTF2 and an inlet concentration of 1,000 mg C Nm^{-3} (phase A-I, day 0–48). After 4–6 days of operation, REs of 70 % were obtained. After that the performance was stable, with REs around 80 % for both BTFs. On day 49 (phase A-II) and on day 70 (phase A-III) the EBRT was consecutively decreased to 90 and 50 s, increasing the IL to 35 and 65 g C m^{-3} h^{-1}, respectively. During these stages, both BTFs presented similar variability in their performance with REs ranging between 60 and 85 %. In phase B, an inlet concentration of 500 mg C Nm^{-3} was set. REs greater than 90 % were achieved by applying ILs of 18 (phases B-I, days 91–97) and 33 g C m^{-3} h^{-1} (phase B-II, days 98–104). In phase B-III (days 105–125), with an IL of 64 g C m^{-3} h^{-1}, the REs significantly decreased to 60–70 %. Finally, the inlet concentration applied in phase C was 250 mg C Nm^{-3}. Working with an IL of 37 g C m^{-3} h^{-1} for BTF1, and 39 g C m^{-3} h^{-1} for BTF2 (days 126–132), high REs with values around 80 % for BTF1 and 88 % for BTF2 were observed. When the IL was increased to 65 g C m^{-3} h^{-1} (days 133–163), the performance of the BTFs decreased to

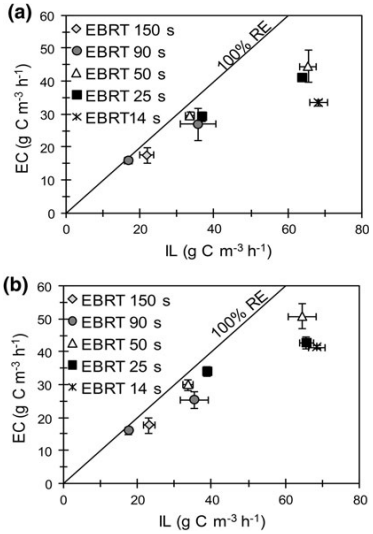

Fig. 7 Isopropanol elimination capacity versus inlet load: **a** BTF1; **b** BTF2

reach an RE of 49 % for BTF1 and 60 % for BTF2, coinciding with the minimum EBRT applied (14 s).

The elimination capacity versus the inlet load is presented in Fig. 7 for the different EBRTs (BTF1 in Fig. 7a and BTF2 in Fig. 7b). Both BTF performed near complete degradation up to a critical IL of 30 g C m^{-3} h^{-1} for all tested inlet concentrations (EBRT $>$ 25 s). Maximum ECs of 44.7 $\pm$ 5.3 and 50.8 $\pm$ 3.4 g C m^{-3} h^{-1} were obtained for BTF1 and BTF2, respectively (IL of 65 g C m^{-3} h^{-1} and EBRT of 50 s).

No data related to the biodegradation of isopropanol under intermittent loading conditions have previously been published in the literature. Previous studies on the removal of isopropanol under continuous loading conditions are also scarce and correspond with biofilters and trickled bed biofilters. Chang and Lu [8] found ECs between 45–89 g C m^{-3} h^{-1} for isopropanol loadings of 50–90 g C m^{-3} h^{-1} with EBRT of 20–30 s. Krailas et al. [9] reported a maximum isopropanol elimination capacity of 276 g m^{-3} h^{-1} (equivalent to 165 g C m^{-3} h^{-1}) and an acetone production rate of 56 g m^{-3} h^{-1} (equivalent to 35 g C m^{-3} h^{-1}) at an inlet load of 342 g m^{-3} h^{-1} (equivalent to 204 g C m^{-3} h^{-1}) using a biofilter. As can be seen, data reported in the present study show lower values of EC than those from the literature, due to the discontinuous operation used to mimic an industrial pattern. Results can also be compared with the removal of other hydrophilic compounds by biotrickling filtration, such as ethanol. Working under continuous loading conditions, Cox et al. [17] found a critical IL of 70 g ethanol m^{-3} h^{-1} (equivalent to 37 g C m^{-3} h^{-1}) at an EBRT of 57 s, and Morotti et al. [18] determined a maximum EC of 46 g ethanol m^{-3} h^{-1} (equivalent to 24 g C m^{-3} h^{-1}) using an EBRT of 66 s and an inlet concentration of 1,100 mg ethanol m^{-3}. Working under intermittent loading conditions, there are limited studies with BTF. In our previous work [19], a maximum EC of 48.5 g C m^{-3} h^{-1} was obtained with an IL of 70.5 g C m^{-3} h^{-1} and an EBRT of 40 s, treating a mixture 1:1 of ethyl acetate and ethanol working with fluctuating conditions for 12 h per day, 5 days at week using 1″ polypropylene rings as the packing material. Thus, the data presented in the present work are comparable with those previously reported for the fluctuating conditions of other oxygenated solvents, showing the capability of the system to adapt itself to the typical operation of industrial facilities characterised by discontinuous VOC emissions.

The variation in the rate of carbon dioxide production with its elimination capacity is shown in Fig. 8a, b for BTF1 and BTF2, respectively. No significant differences were obtained between the bioreactors. An average yield of 0.25 $\pm$ 0.09 and 0.29 $\pm$ 0.09 g C-CO_2 produced per g C degraded for BTF1 and BTF2 was obtained during the entire experiment, respectively. These values are similar to the data in the literature on treating oxygenated compounds. Sempere et al. [11] obtained an average yield coefficient between 0.18 and 0.40 g C-CO_2 produced per g C degraded treating a mixture of ethanol, ethyl acetate and methyl-ethyl ketone. Other researchers reported carbon mineralisation between 17 % [18] and 46 % [17] on treating ethanol.

Influence of spraying frequency on the removal of isopropanol

As discussed previously, the discontinuous regime of the spraying of the bed resulted in emissions of isopropanol during irrigation, increasing the average outlet concentrations in the emission. A minimum irrigation is required to supply the nutrients, but, due to the high solubility of non-degraded isopropanol in water, the accumulation in the trickling liquid caused a fugitive emission that could be minimised by optimising the frequency of the spraying. The effect of this variable on the average outlet concentration was evaluated for the random packing material. Three regimes of spraying were applied at IL of 32 g C m^{-3} h^{-1} and EBRT of 60 s. Figure 9a, b shows the results of spraying for 15 min every 1.5 h and every 3 h, respectively, only during the VOC feeding period (16 h per day). Figure 9c corresponds to a continuous trickling of 15 min every 3 h over a 24 h period, including the period without VOC.

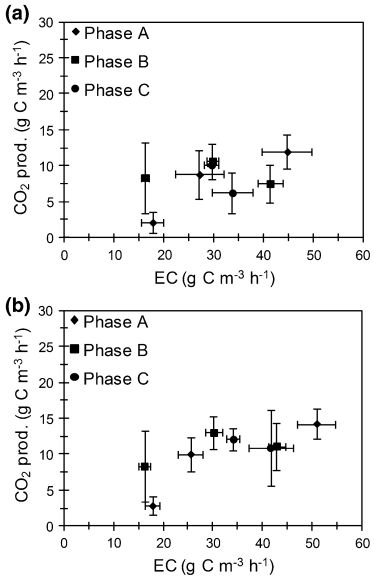

Fig. 8 Production of carbon dioxide versus elimination capacity of isopropanol: **a** BTF1, **b** BTF2

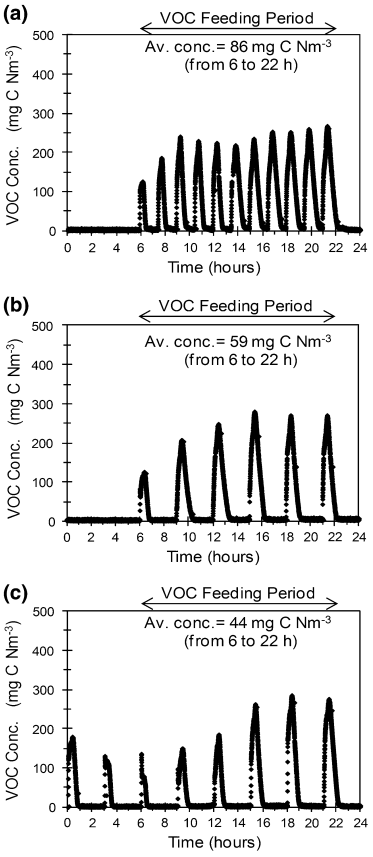

Fig. 9 Influence of the spraying regime on the outlet pattern emission: **a** spraying for 15 min every 1.5 h during VOC feeding period; **b** spraying for 15 min every 3 h during VOC feeding period; **c** 15 min every 3 h during 24 h

From Fig. 9a, b, it can be observed that by decreasing the spraying frequency per day it was possible to reduce the average daily outlet concentration from 86 to 59 mg C Nm^{-3} during the VOC feeding period. This decrease in the average daily outlet concentration is related to the fewer peaks of the spraying pattern of 15 min every 3 h. The expansion of spraying at nights (Fig. 9c) caused a decrease in the average outlet emission from 59 to 44 mg C Nm^{-3} during the isopropanol feeding period. Spraying during non-VOC feeding periods facilitated the VOC transfer to the biofilm and thus enhanced the degradation of the accumulated isopropanol in the water tank. Therefore, the transfer from water to the air during spraying decreases. These results indicated that for the removal of hydrophilic compounds, the spraying frequency is a critical parameter to achieve low emissions under discontinuous and oscillating patterns.

Influence of long-term starvation on the removal of isopropanol

The BTFs were submitted to a starvation period to simulate a holiday industrial closure, to evaluate their response after restoring VOC feeding. During the long-term starvation, the air flow rate was maintained at an EBRT of 60 s, and water trickling was set to 15 min per day to assure biomass viability conditions. The BTFs were kept under these conditions for up to 7 weeks. The VOC feeding was restored using the same intermittent pattern of 16 h per day that was applied before the VOC interruption. An IL of around 35 g C m^{-3} h^{-1}, EBRT of 60 s and a trickling water of 15 min every 4 h was set. The monitoring of the inlet and outlet VOC concentrations of BTF1 and BTF2 is presented in Fig. 10a, b, respectively, once the VOC

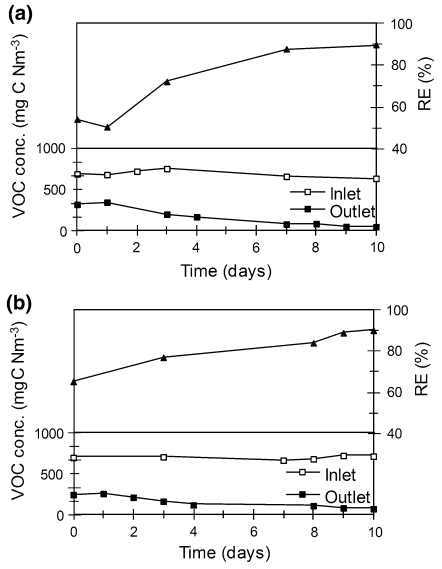

Fig. 10 Performance of the BTFs on the removal of isopropanol after 7 weeks of starvation: **a** BTF1; **b** BTF2

feeding was restored. As can be observed, REs of 80 % were obtained 5 days after the re-start up for both BTFs. After 10 days of operation, both BTFs achieved REs of 90 %, similar values to those obtained in phase B-II, indicating that the performance of the two bioreactors was fully recovered. These results show that the bacterial population can survive with endogenous metabolism for more than 7 weeks if proper adequate operational conditions are adjusted. Zhang and Bishop [20] suggested that extracellular polymeric substances can be a substrate during starving periods. Shorter starvation periods have also been tested on the degradation of other compounds in BTFs. Sempere et al. [11] reported on the successful re-acclimation of a BTF degrading a mixture of oxygenated compounds after a 3-week starvation period. Cox and Deshusses [10] found a great reactivation of toluene-degrading BTFs after periods of 2–9 days without VOC feeding. The long starvation period tested in this study is of interest due to the fact it has never previously been applied in biotrickling filtration. It demonstrates the sturdiness of the biofiltration techniques to adapt to conditions found in industrial facilities, avoiding the necessity for system re-inoculation with the subsequent saving of costs.

Conclusions

The removal of isopropanol in two biotrickling filters with two packing materials of similar specific surface area, one structured and one random, was investigated. Oxygen mass transfer coefficients were determined, showing similar values for liquid velocities up to 15 m h^{-1} at gas velocities of 104 and 312 m h^{-1}. At higher liquid velocities, the structured packing material showed a greater mass transfer coefficient attributed to the different air and water flow paths in both materials. Biotrickling filtration has been shown as an effective technology for the removal of isopropanol in waste gases under intermittent loading conditions (16 h per day, 5 days per week), typical of industrial sites with night and weekend shut-offs. Stable performance has been obtained with complete removal up to an inlet load of 30 g C m^{-3} h^{-1}. At high loads, the random packing material showed a slightly higher removal capacity. Due to the low Henry coefficient of isopropanol, it tends to accumulate in the water tank, causing a peak in the outlet emission during intermittent spraying. Thus, this fact indicates that the frequency of irrigation is a crucial parameter to achieve low emissions under intermittent loading of highly soluble compounds. Outlet emissions were reduced by half by decreasing the spraying frequency during isopropanol feeding and expanding the irrigation to nights and weekends. This strategy allows the minimisation of peak emissions from liquid-mass transfer during isopropanol feeding periods and promotes the biodegradation of isopropanol accumulated in water during nonfeeding periods. A fast re-start-up after a 7-week starvation period, one of the longest reported, corroborated that biotrickling filtration of soluble compounds under intermittent loading is a robust technology for industrial applications.

Acknowledgments The research leading to these results has received funding from the People Programme (Marie Curie Actions) of the European Union's Seventh Framework Programme FP7/2007-2013/under *REA* grant agreement no. 284949. Financial support from the Ministerio de Ciencia e Innovación (Project CTM2010-15031/TECNO) and Generalitat Valenciana (ACOMP/2012/209), Spain, is also acknowledged. Pau San-Valero acknowledges the Generalitat Valenciana, Spain (ACIF/2011/067 contract).

References

1. Council Directive 2010/75/EU of 24 November 2010 on industrial emissions (integrated pollution prevention and control). 17.12.2010. Official Journal of European Union
2. European Commission (2003) IPPC reference document on best available techniques in common wastewater and waste gas treatment/management systems in the chemical sector. Sevilla
3. Devinny JS, Deshusses MA, Webster TS (1999) Biofiltration for air pollution control. CRC-Lewis Publishers, Boca Raton

4. Popat SC, Deshusses MA (2010) Analysis of the rate-limiting step of an anaerobic biotrickling filter removing TCE vapors. Process Biochem 45:549–555
5. Kirchner K, Wagner S, Rehm HJ (1992) Exhaust-gas purification using biocatalysts (fixed bacteria monocultures)—the influence of biofilm diffusion rate (O_2) on the overall reaction-rate. Appl Microbiol Biotechnol 37:277–279
6. Barton JW, Davison BH, Klasson KT, Gable CC (1999) Estimation of mass transfer and kinetics in operating trickle-bed bioreactors for removal of VOCs. Environ Prog 18:87–92
7. Kim S, Deshusses MA (2008) Determination of mass transfer coefficients for packing materials used in biofilters and biotrickling filters for air pollution control. 1. Experimental results. Chem Eng Sci 63:841–855
8. Chang KS, Lu CS (2003) Biofiltration of isopropyl alcohol by a trickle-bed air biofilter. Biodegradation 14:9–18
9. Krailas S, Suppalak T, Meeyoo V (2004) Macrokinetic determination of isopropanol removal using a downward flow biofilter. Songklanakarin J Sci Technol 26:55–64
10. Cox HHJ, Deshusses MA (2002) Effect of starvation on the performance and re-acclimation of biotrickling filters for air pollution control. Environ Sci Technol 36:3069–3073
11. Sempere F, Gabaldón C, Martínez-Soria V, Marzal P, Penya-Roja JM, Alvarez-Hornos FJ (2008) Performance evaluation of a biotrickling filter treating a mixture of oxygenated VOCs during intermittent loading. Chemosphere 73:1533–1539
12. Van't Riet K (1979) Review of measuring methods and nonviscous gas–liquid mass transfer in stirred vessels. Ind Eng Chem Process Des Dev 18:357–364
13. Weiland P, Onken U (1981) Fluid dynamics and mass transfer in an airlift fermenter with external loop. Ger Chem Eng 4:42–50
14. Kennes C, Rene ER, Veiga MC (2009) Bioprocesses for air pollution control. J Chem Tech Biotechnol 84:1419–1436
15. Clesceri LS, Greenberg AE, Eaton AD (1998) Standard methods for the examination of water and wastewater. American Public Health Association, American Water Works Association and Water Environment Federation, Washington
16. Kim S, Deshusses MA (2008) Determination of mass transfer coefficients for packing materials used in biofilters and biotrickling filters for air pollution control—2: development of mass transfer coefficients correlations. Chem Eng Sci 63:856–861
17. Cox HHJ, Sexton T, Shareefdeen ZM, Deshusses MA (2001) Thermophilic biotrickling filtration of ethanol vapors. Environ Sci Technol 35:2612–2619
18. Morotti K, Ramirez AA, Jones JP, Heitz M (2011) Analysis and comparison of biotreatment of air polluted with ethanol using biofiltration and biotrickling filtration. Environ Technol 33:1967–1973
19. Sempere F, Gabaldón C, Martínez-Soria V, Penya-Roja JM, Álvarez-Hornos FJ (2009) Evaluation of a combined activated carbon prefilter and biotrickling filter system treating variable ethanol and ethyl acetate gaseous emissions. Eng Life Sci 9:317–323
20. Zhang XQ, Bishop PL (2003) Biodegradability of biofilm extracellular polymeric substances. Chemosphere 50:63–69

Chemical Engineering Science 108 (2014) 47–56

Contents lists available at ScienceDirect

Chemical Engineering Science

journal homepage: www.elsevier.com/locate/ces

Modelling mass transfer properties in a biotrickling filter for the removal of isopropanol

Pau San-Valero, Josep M. Penya-Roja, F. Javier Álvarez-Hornos, Carmen Gabaldón *

Research Group GI²AM, Department of Chemical Engineering, University of Valencia, Avda. Universitat s/n, 46100 Burjassot, Spain

HIGHLIGHTS

- Dimensionless Henry's law constant of isopropanol rises by a factor of 1.8 per 10 °C.
- Mass transfer of isopropanol is highly influenced by temperature.
- Isopropanol mass transfer coefficient increases with gas velocity.
- Oxygen mass transfer coefficient depends on packing material and liquid velocity.
- Power law correlations appear suitable to model both mass transfer coefficients.

ARTICLE INFO

Article history:
Received 9 August 2013
Received in revised form
21 November 2013
Accepted 23 December 2013
Available online 31 December 2013

Keywords:
Bioreactors
Mass transfer
Mathematical modelling
Bioprocess
Hydrodynamics

ABSTRACT

A study was carried out to model mass transfer properties in biotrickling filters, treating isopropanol as the target pollutant. This study was extended to the mass transfer of oxygen related to the fact that the treatment of hydrophilic compounds by biotrickling filtration is often limited by oxygen. A simple method for each compound was developed based on their physical properties. The influence of temperature on Henry's law constant of isopropanol was determined. An increase of 1.8 per 10 °C for the dimensionless Henry's law constant was obtained. The determination of the overall mass transfer coefficients of isopropanol ($K_G a$) was carried out, obtaining values between 500 and 1800 h^{-1} for gas velocities of 100 and 300 m h^{-1}. No significant influences were observed for either the liquid velocity or packing material. Also, the determination of overall mass transfer coefficients of oxygen ($K_L a$) were carried out, obtaining values between 20 and 200 h^{-1} depending on the packing material for liquid velocities between 2 and 33 m h^{-1}. Structured packing materials exhibited greater mass transfer coefficients, while for random packing materials, the mass transfer coefficients clearly benefited from the high specific surface area. Mathematical correlations found in the literature were compared with the empirical data, showing that neither was capable of reproducing the mass transfer coefficients obtained empirically. Thus, empirical relationships between the mass transfer coefficients and the gas and liquid velocities are proposed to characterise the system.

1. Introduction

In recent decades, there has been an emergent interest in research into biotreatment as an alternative for the treatment of volatile organic compounds (VOC), which includes the biotrickling filter as one of the most applicable technologies (Devinny et al., 1999). The use of biotrickling filtration for the treatment of VOC it is frequent and has been shown to be capable of achieving high removal efficiencies. Considering that biotrickling filtration involves a series of complex physical, chemical and biological processes, further work is needed to determine the mechanisms that contribute to the observed behaviour (Iranpour et al., 2005). The most representative mechanisms in a biotrickling filter are mass transfer, diffusion and biological degradation. Typically, the process may be limited by mass transfer as well as kinetics. Unfortunately, research has been mainly focused on biodegradation kinetics rather than mass transfer (Dorado et al., 2009; Lebrero et al., 2012) and, despite being a key step in the process, the optimisation of mass transfer between the gas and the liquid/biofilm remains one of the most difficult aims to achieve. Relating to this, several authors (Dorado et al., 2009; Kim and Deshusses, 2008a) have emphasised the need to determine the mass transfer coefficients in order to develop simulations for the design and optimisation of biotrickling filters. Also, determining the mass

* Corresponding author. Tel.: +34 96 354 34 37; fax: +34 96 354 48 98.
E-mail address: carmen.gabaldon@uv.es (C. Gabaldón).

0009-2509/$ - see front matter © 2014 Elsevier Ltd. All rights reserved.
http://dx.doi.org/10.1016/j.ces.2013.12.033

transfer coefficient would facilitate the selection of the packing material and the modelling of bioreactors used for air pollution control.

As pointed by other authors (Dorado et al., 2009; Kim and Deshusses, 2008a; Pérez et al., 2006), the hydrodynamic conditions used in biofiltration are markedly different than those used in absorption processes, so the typical correlations used in these systems are not useful for predicting the phenomena occurring in biotrickling filters. Dorado et al. (2009) confirmed that using experimental global mass transfer coefficients appears to be the most suitable way to represent mass transfer in biotrickling filter systems; they pointed out the need for using the target pollutant for the determination of mass transfer coefficients.

Isopropanol is a hydrophilic compound typified by its high volatility and relatively low hazardous properties in comparison with other solvents. As a result, it is one of the most commonly used solvents in chemical industries as coating, printing, cleaning, among others, resulting in a large amount of emissions to the atmosphere that should be treated. Due to its low Henry's law constant in comparison with Henry's law constant of oxygen, its treatment by biofiltration implies that the process could be typically limited by the low concentration of oxygen in the biofilm. This could imply that that the penetration depth of oxygen in water or the biofilm is lower than that of the pollutant, causing anaerobic zones in the deeper parts of the biofilm close to the substratum (Shareefdeen and Singh, 2005). Experiments based on the physical properties of the gas and liquid phases have shown that the volumetric mass transfer coefficient could be influenced by the liquid phase at a similar level of contribution than the influence of the gas (Pérez et al., 2006). So, both influences should be assessed in order to characterise and improve the process.

The purpose of this research was to determine the mass transfer coefficients for the treatment of hydrophilic compounds using isopropanol and oxygen as reference components for various packing materials. To carry out this purpose, the following objectives were developed: (1) to establish a simple method to determine the mass transfer coefficients of typical hydrophilic compounds using isopropanol as the target pollutant, (2) to establish a simple method to determine the mass transfer coefficients of oxygen, (3) to determine the influence of gas and liquid velocities on the mass transfer coefficients and (4) to establish a mathematical relationship between the mass transfer coefficients and the operational conditions.

2. Materials and methods

2.1. Theory

The overall mass transfer coefficient expressed in the liquid phase is defined as a function of the individual mass transfer coefficients, and is related to the overall mass transfer coefficient expressed in the gas phase

$$\frac{1}{K_L a}=\frac{1}{HK_G a}=\frac{1}{k_L a}+\frac{1}{Hk_G a} \quad (1)$$

Depending on Henry's law constant of the substance, the main resistance to the transfer could be controlled only by one of these phases. Liss and Slater (1974) established that for Henry's law constants over 250 atm (mole fraction)$^{-1}$, the main resistance is controlled by the liquid film, while for Henry's law constants between 1 and 250 atm (mole fraction)$^{-1}$, the main resistance is a mix between the two phases, and for Henry's law constants up to 1 atm (mole fraction)$^{-1}$, the resistance is controlled by the gas film. Due to the existing differences between Henry's law constant of isopropanol (0.460 ± 0.124 atm (mole fraction)$^{-1}$ (Sander, 2005)) and oxygen (43922 ± 1679 atm (mole fraction)$^{-1}$), two different methods were developed to measure the mass transfer coefficients for each compound.

2.2. Determination of the mass transfer coefficient of isopropanol

2.2.1. Experimental set-up

As shown in Fig. 1, the system consisted of a column of methacrylate (14.4 cm internal diameter, 120 cm height) and a recirculation tank (5 L water volume). Two packing materials, one random (Flexiring 25 mm) and one structured (PAS Winded Media), were investigated; the characteristics of these materials are shown in Table 1. The packing height was 100 cm. The air stream (compressed, filtered and dried) was introduced through the bottom of the column, with the flow rate adjusted using a mass flow controller (Bronkhorst Hi-Tec, The Netherlands). The experiments were carried out at three superficial air velocities around 100, 150 and 300 m h^{-1} and the trickling water was recirculated using a centrifugal pump (HPR10/15, ITT, Great Britain) in counter-current mode with respect to the air flow rate, with a superficial water velocity of 2, 4, 7 and 13 m h^{-1}. The operational conditions were selected in order to evaluate the wide range used in biotrickling filters. The experiments were carried out at room temperature (21.5 ± 1.3 °C). For isopropanol, these changes in temperature imply variations in Henry's law constants

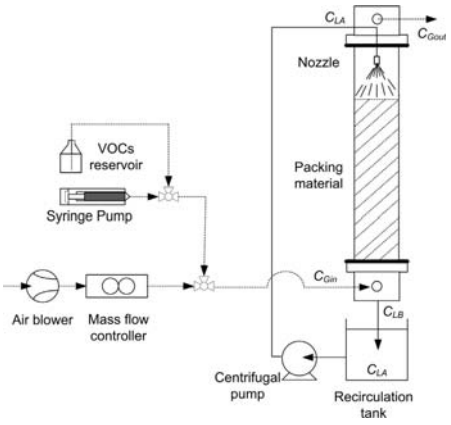

Fig. 1. Experimental set-up for the determination of the mass transfer coefficient of isopropanol.

Table 1
Characteristics of the packing materials.

Packing material		Diameter[a] (mm)	Density[a] (kg m^{-3})	Bed porosity[a] (%)	Specific surface area[a] (m^2 m^{-3})
PAS Winded Media[b]	Structured	–	–	93	410
Flexiring	Random	25	71	92	207[c]
Refilltech	Random	15	110.7	91	348

[a] Data provided by the suppliers.
[b] Packing material supplied by PAS Solutions BV.
[c] Larachi et al. (2008).

of up to 20–25% (Sander, 2005); thus, the dependence of H on temperature had to be obtained for an accurate study of mass transfer.

The concentration of isopropanol was measured using a total hydrocarbon analyser (Nira Mercury 901, Spirax Sarco, Spain). The response factor of the total hydrocarbon analyser was determined by gas chromatography (model 7890, Agilent Technologies, EEUU). The determination of the total organic carbon (TOC) in water was measured using a total organic carbon analyser (TOC−V_{CHS}, Shimadzu Corporation, Japan).

2.2.2. Experimental procedure

A method under inert conditions was used for the determination of the overall mass transfer coefficients of isopropanol. This method consisted of monitoring the concentration of isopropanol in the gas phase during entire experiment and periodically taking samples from the bottom of the column and water tank. To minimise the effect of adsorption in the packing surface and the absorption in the water inside the reactor, the system was previously wetted and saturated with isopropanol. When the inlet concentration was equal to the outlet concentration, a continuous trickle began from the tank to the top of the column. The first 20 min of each experiment were neglected to ensure that stable conditions were achieved. After 20 min, the gas concentration as well as the liquid concentration at the bottom of the column and in the tank were considered as the initial points of the experiment and were used to estimate the value of the mass transfer coefficients. Under these conditions, mass balances of isopropanol were developed based on the following assumptions: (1) the behaviour of the column was described as a plug flow regime; (2) the water tank was perfectly mixed; (3) reaction in pipes was negligible, so, the concentration of the water tank was the same as the concentration of the inlet of the column.

2.2.2.1. Mass balance in the packed column. For each time point and for a differential column of the reactor, the total amount of carbon transferred from the gas to the liquid phase in the column is defined by

$$dC_{G,IPA} = -\frac{Q_L}{Q_G} dC_{L,IPA} \tag{2}$$

where $C_{G,IPA}$ and $C_{L,IPA}$ are the gas/liquid concentrations and Q_G and Q_L are the volumetric flow rates in the gas/liquid phases, respectively.

From the integration of Eq. (2), the following equation is obtained:

$$C_{L_B,IPA} = C_{L_A,IPA} + \frac{Q_G}{Q_L}(C_{G_{in},IPA} - C_{G_{out},IPA}) \tag{3}$$

To determine the outlet concentration in the gas phase, the mass balance is described as:

$$Q_G dC_{G,IPA} = -H_{IPA} K_G a (C^*_{L,IPA} - C_{L,IPA}) dV_c \tag{4}$$

where V_c is the volume of the column, H_{IPA} is the dimensionless Henry's law constant of isopropanol expressed as concentration of gas phase/concentration of the liquid phase and $C^*_{L,IPA}$ is defined by Henry's Law according to the following equation:

$$C^*_{L,IPA} = \frac{C_{G,IPA}}{H_{IPA}} \tag{5}$$

Taking into account Eq. (5) and that the cross-sectional area of the column is constant, Eq. (4) can be written as follows:

$$Q_G \frac{dC_{G,IPA}}{dz} = -H_{IPA} K_G a S \left(\frac{C_{G,IPA}}{H_{IPA}} - C_{L,IPA}\right) \tag{6}$$

where S and z are the surface and the distance from the bottom of the column, respectively. The following boundary conditions were assumed. At the bottom of the column ($z=0$)

$$C_{G,IPA} = C_{G_{in},IPA}$$
$$C_{L,IPA} = C_{L_B,IPA} \tag{7}$$

while at the top of the column ($z=Z$)

$$C_{G,IPA} = C_{G_{out},IPA}$$
$$C_{L,IPA} = C_{L_A,IPA} \tag{8}$$

where $C_{G_{in},IPA}$ and $C_{G_{out},IPA}$ are the inlet/outlet concentrations in the gas phase and $C_{L_A,IPA}$ and $C_{L_B,IPA}$ are the liquid concentrations at the top and at the bottom of the column. The concentration at the top of the column is assumed to be equal to the concentration in the tank. Integrating Eq. (6) and with the conditions presented in Eqs. (7) and (8), the following equation was obtained:

$$\ln \frac{(C_{G_{out},IPA} - H_{IPA} C_{L_A,IPA})}{(C_{G_{in},IPA} - H_{IPA} C_{L_B,IPA})} = -\left(1 + H_{IPA}\frac{Q_G}{Q_L}\right)\frac{K_G a}{Q_G} SZ \tag{9}$$

Combining Eqs. (9) and (3), the outlet concentration is described by:

$$C_{G_{out},IPA} = \frac{\left(1 - H_{IPA}\frac{Q_G}{Q_L}\right)\exp\left(-\left(1 + H_{IPA}\frac{Q_G}{Q_L}\right)\frac{K_G a}{Q_G} SZ\right) C_{G_{in},IPA} + \left(1 - \exp\left(-\left(1 + H_{IPA}\frac{Q_G}{Q_L}\right)\frac{K_G a}{Q_G} SZ\right)\right) H_{IPA} C_{L_A,IPA}}{1 - H_{IPA}\frac{Q_G}{Q_L}\exp\left(-\left(1 + H_{IPA}\frac{Q_G}{Q_L}\right)\frac{K_G a}{Q_G} SZ\right)} \tag{10}$$

2.2.2.2. Mass balance in the tank. The variation of $C_{L_A,IPA}$ and $C_{L_B,IPA}$ is described by the mass balance in the tank as follows:

$$\frac{dC_{L_A,IPA}}{dt} = \frac{Q_L}{V_T}(C_{L_B,IPA} - C_{L_A,IPA}) \tag{11}$$

where V_T is the volume of the tank.

As was previously mentioned, the variations in temperature during the experiment imply variations in Henry's law constants up to 20–25% (Sander, 2005). For this reason, the estimation of the parameters was divided into two stages. First, the estimation of $K_G a$ and H was carried out for the experiments with Flexiring 25 mm. These fitted values of H were related to the temperature and an empirical correlation between H and T was obtained. Second, the empirical correlation between H and T was used in each experiment of the structured packing material, thus the $K_G a$ was the only parameter to be fitted in this step.

2.3. Determination of the mass transfer coefficient of oxygen

2.3.1. Experimental set-up

As is shown in Fig. 2, a similar set-up as that used for the determination of the mass transfer coefficient of isopropanol was used but with a volume of 10 L in the recirculation tank. In this case, the study was extended to three packing materials, two random (Flexiring 25 mm and Refilltech 15 mm) and one structured (PAS Winded Media); the characteristics are shown in

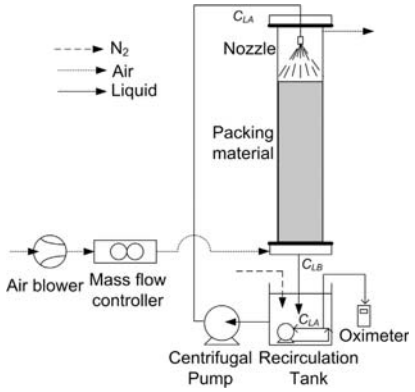

Fig. 2. Experimental set-up for the determination of the mass transfer coefficient of oxygen.

Table 1. The packing height was 40 cm for the random packing materials and 20 cm for the structured packing material. The experiments were carried out at two superficial air velocities of 104 m h^{-1} and 312 m h^{-1}. The trickling water was recirculated using a centrifugal pump with a superficial water velocity between 3 and 33 m h^{-1}. The equipment was supplemented with a dissolved oxygen probe (Cellox® 325i, WTW, Germany) to measure the dissolved oxygen concentration in the tank. An internal pump installed in the recirculation tank ensured the ideal mixing conditions. The experiments were carried out at room temperature (21.2 ± 0.7 °C). For oxygen, this implies variations in Henry's law constant up to 2% (Sander, 2005), thus the dependence of H on temperature was neglected.

2.3.2. Experimental procedure

For the determination of K_La, a dynamic method under inert conditions was used as described elsewhere (San-Valero et al., 2013). The method consisted of measuring the increase in the oxygen concentration over time in a tank in which the oxygen was previously displaced by bubbling nitrogen gas. The experiment started when the air blower and the recirculation pump were switched on; oxygen was transferred from the air to the water in the packed column, causing an increase in the dissolved oxygen concentration in the recirculation tank. The oxygen mass balances were developed using the same assumptions as isopropanol.

2.3.2.1. Mass balance in the packed column.

$$C_{L_B,OXY} = C^*_{L,OXY} - \frac{C^*_{L,OXY} - C_{L_A,OXY}}{\exp(\frac{Z}{v}K_La)} \tag{12}$$

where $C_{L_B,OXY}$ is the predicted dissolved oxygen concentration at the bottom of the column, $C_{L_A,OXY}$ is the predicted dissolved oxygen concentration in the recirculation tank, $C^*_{L,OXY}$ is the oxygen solubility and Z and v are the height of the column and the velocity of the trickling water, respectively.

In the tank:

$$\frac{dC_{L_A,OXY}}{dt} = \frac{Q_L}{V_T}(C_{L_B,OXY} - C_{L_A,OXY}) \tag{13}$$

The combination of Eqs. (12) and (13) permits obtaining the variation of the predicted oxygen concentration over time (Van't Riet, 1979):

$$\frac{dC_{L_A,OXY}}{dt} = \frac{Q_L}{V_T}\left(C^*_{L,OXY} - \frac{C^*_{L,OXY} - C_{L_A,OXY}}{\exp(\frac{Z}{v}K_La)} - C_{L_A,OXY}\right) \tag{14}$$

The response time constant of the probe, τ, is defined as the time at which the probe achieves 63% of the end value measured when the probe is subjected to a step input assay (Van't Riet, 1979). It was determined by transferring the oxygen probe from an ideal mixed tank in which the dissolved oxygen concentration was displaced by bubbling nitrogen gas to a second tank which was saturated with dissolved oxygen. First order dynamics were assumed a according to Eq. (15) (Weiland and Onken, 1981)

$$\frac{dC_{L_m,OXY}}{dt} = \frac{(C_{L_A,OXY} - C_{L_m,OXY})}{\tau} \tag{15}$$

where $C^*_{L_m,OXY}$ is the dissolved oxygen concentration in the recirculation tank measured by the oxygen probe.

The value of K_La of the packed column was calculated by minimising the sum of squares of the difference between the measured data recorded for the dissolved oxygen concentration in the recirculation tank and the value obtained from the mathematical resolution of Eqs. (14) and (15).

3. Results and discussion

3.1. Determination of the mass transfer coefficient of isopropanol

3.1.1. Correlation between Henry's law constant and the temperature

The determination of the mass transfer coefficient of isopropanol was carried out for two packing materials: Flexiring 25 mm and PAS Winded Media. As the influence of the temperature on Henry's law constant of isopropanol should not be neglected, the first set of experiments with the packing material Flexiring 25 mm were used for the estimation of K_Ca and H. This estimation allowed for obtaining the exact temperature dependence of the system with Henry's law constant. The values of $H^*_{298\ K}$ and the enthalpy of the solution divided by the ideal gas law constant were obtained by using the least squares method in order to minimise the differences between the experimental data and the Van't Hoff equation. The parameters $H^*_{298\ K}$ and the enthalpy of the solution divided by the ideal gas law constant obtained are shown as

$$H^*_{T,IPA} = 146\exp\left(5501\left(\frac{1}{T} - \frac{1}{298}\right)\right) \tag{16}$$

where $H^*_{T,IPA}$ is Henry's law constant expressed in M atm^{-1} and T is the temperature expressed in K. The dimensionless Henry's law

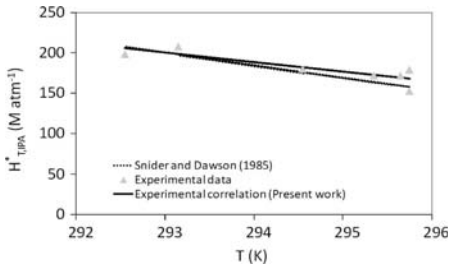

Fig. 3. Dependence of Henry's law constant on temperature.

constant could be related with Henry's law constant expressed in M atm^{-1} by the following equation:

$$H_{IPA} = \frac{1}{H^{*}_{T,IPA} RT} \tag{17}$$

where R is the universal gas constant (0.082 atm K^{-1} M^{-1}).

Fig. 3 shows the experimental data with the results provided by the empirical correlation described by the Eq. (16). The available data from literature is also plotted (Snider and Dawson, 1985). The general variation range of the dimensionless Henry's law constant for VOC from 1.12 to 3.55 per 10 °C rise in temperature, with an average value of 1.88 found by Staudinger and Roberts (2001). The empirical correlation of Eq. (16) presented an increase in the dimensionless Henry's law constant of 1.8 per each 10 °C while Snider and Dawson (1985) provides a variation of 2.25 per 10 °C rise. It is common to find some discrepancies in the literature for the same compound related with the influence of non-temperature effects on Henry's law constant such as pH, dissolved salts, etc (Staudinger and Roberts, 1996). Regarding this, Staudinger and Roberts (2001) pointed out that it appears prudent to determine the exact temperature of each case. Thus, the empirical correlation obtained in Eq. (16) was used to obtain the value of H in the experiments carried out with the structured packing material.

3.1.2. $K_C a$ calculations

Typical examples of the raw data obtained from the experiments for each packing material and the results of the data obtained with the mathematical model are shown in Fig. 4. The experiment presented in Fig. 4A corresponds to one test carried out with the packing material Flexiring 25 mm operating at a gas velocity of 180 m h^{-1} and a liquid velocity of 6.3 m h^{-1} while the experiment presented in Fig. 4B corresponds to one test carried out with the packing material PAS Winded Media operating at a gas velocity of 180 m h^{-1} and a liquid velocity of 1.8 m h^{-1}. These examples were representative of all tests done. The goodness of fit of the experimental data and the data provided by the

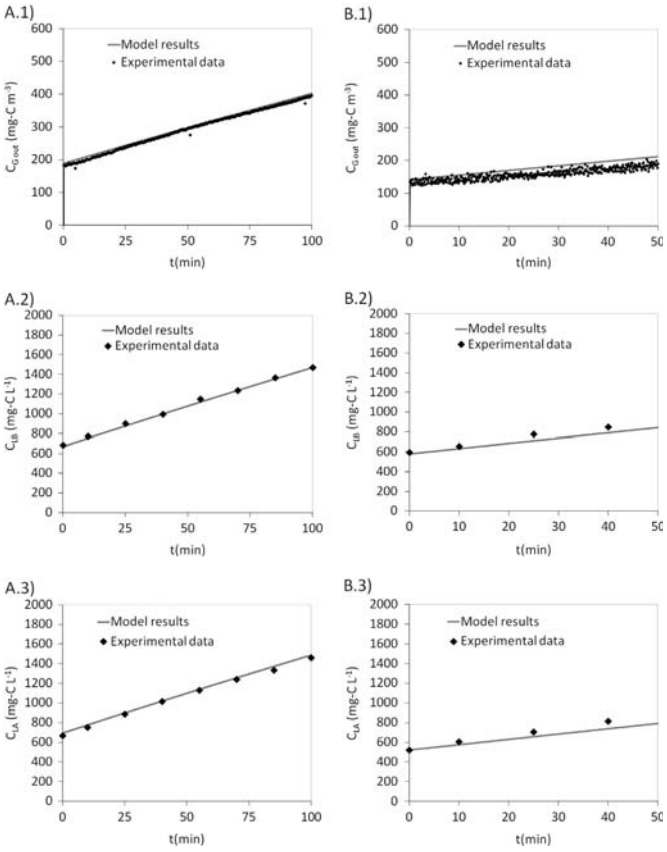

Fig. 4. Experimental data and model results for the experiments of the mass transfer coefficient of isopropanol. (A) Flexiring 25 mm: (1) $C_{G_{out}}$ (2) C_{L_B} (3) C_{L_A} and (B) PAS Winded Media: (1) $C_{G_{out}}$ (2) C_{L_B} (3) C_{L_A}.

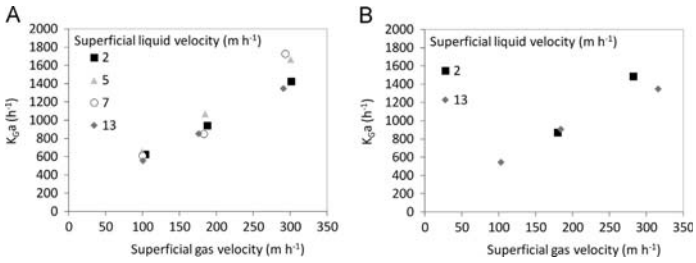

Fig. 5. Influence of the superficial gas and liquid velocities on the mass transfer coefficient of isopropanol (A) Flexiring 25 mm and (B) PAS Winded Media.

mathematical model were tested by using the relative error of the concentration of each phase. An average value of the relative error of 6% for the gas phase and an average error of 5% for the liquid phase (C_{L_4}, C_{L_8}) were obtained. The relative error obtained indicated that the method was accurate for the determination of the mass transfer coefficient of isopropanol.

The effect of the gas and liquid velocities for both packing materials is shown in Fig. 5. Depending on the packing material and the conditions, K_Ga values were obtained in a range between 500 and 1800 h^{-1} for gas velocities between 100 and 300 m h^{-1} and for liquid velocities between 2 and 13 m h^{-1}. These data are on the same order of magnitude as the data presented by Kim and Deshusses (2008a). These authors showed that for biotrickling filters operating at a typical range of gas velocities below 500 m h^{-1}, the k_Ga values were between 500 and 2000 h^{-1}. As shown in Fig. 5, the mass transfer coefficient of isopropanol was strongly influenced by the gas velocity. As an example, a 50% variation in the gas velocity would imply a variation of around 40% in the mass transfer coefficient. This behaviour is in agreement with that found by other authors in the literature (Dorado et al., 2009; Kim and Deshusses, 2008a; Piche et al., 2001). To evaluate the effect of the liquid velocity on the mass transfer coefficient of isopropanol, further experiments were carried out at several liquid velocities. No significant influence of the liquid velocity was observed. This could have occurred since the packing material was completely wet. Kim and Deshusses (2008a) observed that when wetting was almost complete, the effect of liquid velocity was slight or constant. The same behaviour was observed by Piche et al. (2001). No differences between packing materials were found (Fig. 5). Regarding this, Dorado et al. (2009) suggested that when pollutant diffusion is in the gas phase, as is the case with isopropanol, neither the liquid side resistance nor the packing material characteristics affect the global system performance.

3.2. Determination of the mass transfer coefficient of oxygen

The determination of the mass transfer coefficient of oxygen was extended to the three packing materials shown in Table 1 at several liquid velocities (from 2 to 33 m h^{-1}) and two gas velocities (104 and 312 m h^{-1}). The K_La coefficients were obtained using the least squares method in order to minimise the differences between the experimental data and the concentration of oxygen provided by the mathematical model established by Eqs. (14) and (15). The response time of the probe (τ) was determined by means of a step input assay, resulting in a value of 19.4 ± 1.5 s (San-Valero et al., 2013).

A typical example of the raw data obtained during one of the experiments and the result of the mathematical procedure described above is shown in Fig. 6. The same mathematical procedure was used for all packing materials, so only one example

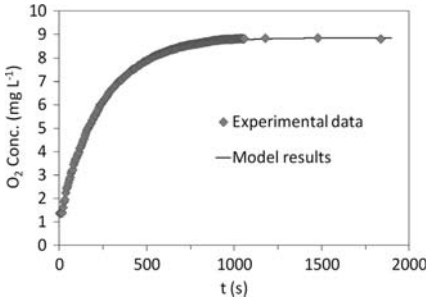

Fig. 6. Experimental data and model results for the experiments of the mass transfer coefficients of oxygen.

is shown as a representative of the other packing materials. This corresponds to one test carried out with the packing material Flexiring 25 mm operating at a gas velocity of 104 m h^{-1} and a liquid velocity of 11 m h^{-1}. Similarly to the experiments using isopropanol, the experimental data and the data provided by the mathematical model were evaluated by using the relative error of the concentrations, obtaining an average value less than 2% for all tests done. This confirms that the method was accurate for the determination of the mass transfer coefficient of oxygen.

The effect of the gas and liquid velocities on the mass transfer coefficient is shown in Fig. 7 for each packing material. Depending on the packing material and the conditions, K_La values were obtained in a range between 20 and 200 h^{-1} for liquid velocities between 2 and 33 m h^{-1}. These results are consistent with the data obtained by other authors (Kim and Deshusses, 2008a; Piche et al., 2001). As may be seen in this figure, oxygen transfer was enhanced at high liquid velocities. A clear dependence can be observed between the global coefficients and liquid velocities. In addition, these data show that there was not a significant influence of gas velocity on the mass transfer coefficient of oxygen. This is in accordance with the literature (Piche et al., 2001; Kim and Deshusses, 2008a), and is related to the fact that oxygen is a poorly soluble gas in water and the main resistance is located in the liquid phase, in contrast to what occurs with isopropanol.

The influence of the packing material was extended to three materials: two random with different specific surface area and one structured. The experimental data from San-Valero et al. (2013) are compiled herein for this purpose. The most important differences in the behaviour of the packing material were observed at liquid velocities above 15 m h^{-1}. This could be due to the fact that turbulence is higher at higher liquid velocities than at lower liquid

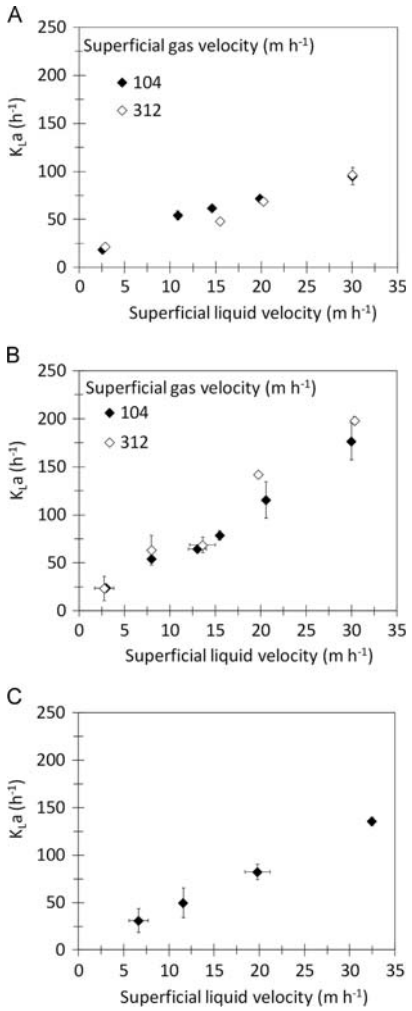

Fig. 7. Influence of gas and liquid velocities on the mass transfer coefficients of oxygen. (A) Flexiring 25 mm (B) PAS Winded Media and (C) Refilltech 15 mm.

velocities, thus increasing the interfacial area and facilitating the mass transfer of oxygen between phases, in contrast to the mass transfer of isopropanol where the main resistance was located in the gas phase. For the comparison between packing materials, a velocity of 30 m h^{-1} was chosen since this was the velocity where differences were most evident. In this regard, the structured packing material with a specific surface area of 410 m^3 m^{-2} exhibited the maximum mass transfer coefficient of oxygen with a value around 175 h^{-1}. For the random packing materials, K_La values of 130 and 100 h^{-1} were obtained for Refilltech 15 mm and Flexiring 25 mm, with specific surface areas of 348 and 207 m^3 m^{-1}, respectively. These data show that a high specific surface area improves the mass transfer of oxygen. The structured packing material exhibited a higher mass transfer coefficient than those obtained with the random packing material with a similar specific surface area. This could be attributed to the effect of different flow paths within the packing materials on the mass transfer of oxygen. Random packing materials could promote channelling more readily than structured packing materials.

3.3. Mathematical correlation

Mathematical correlations were developed in order to characterise the influence of the gas and liquid velocities on the mass transfer coefficients of isopropanol and oxygen. For the mass transfer of isopropanol, non-significant influences of the packing materials and liquid velocities were observed. Thus, the experimental data can be fitted to a relationship between the mass transfer coefficient and the gas velocity. For the mass transfer of oxygen, two important influences were observed, i.e. the packing material and the liquid velocity. So, it was considered necessary to develop empirical correlations for each of the packing materials. Power law relationships according to Eqs. (18) and (19) between gas or liquid velocity and K_Ga or K_La could be the most suitable way to represent this phenomenon for isopropanol and for oxygen:

$$K_Ga_{IPA} = c_1 v_G^{c_2} \tag{18}$$

$$K_La_{OXY} = c_1 v_L^{c_2} \tag{19}$$

where K_Ga and K_La are expressed in h^{-1}, and v_G and v_L in m h^{-1}.

The parameters obtained for each correlation are shown in Table 2. In order to analyse the accuracy of the empirical correlations proposed herein, the observed and predicted values of the mass transfer coefficient for isopropanol and oxygen are presented in Fig. 8. In both cases, the experimental data fit ($r^2 > 0.94$) the predicted data; the greatest observed difference was 20% for the entire data set. These uncertainties are similar to those reported by other authors (Kim and Deshusses, 2008b; Onda et al., 1968).

The most general correlations were those proposed by Onda et al. (1968) and Van Krevelen and Hoftijzer (1948) for conventional absorption packing columns. These correlations are described as follows:

Onda

$$k_G = 5.23\frac{D_G}{d_p^2 a_p}\left(\frac{\rho_G v_G}{\mu_G a_p}\right)^{0.7}\left(\frac{\mu_G}{\rho_G D_G}\right)^{1/3} \tag{20}$$

$$k_L = 0.0051(a_p d_p)^{0.4}\left(\frac{\mu_L g}{\rho_L}\right)^{1/3}\left(\frac{\rho_L v_L}{a_e \mu_L}\right)^{2/3}\left(\frac{\mu_L}{\rho_L D_L}\right)^{-0.5} \tag{21}$$

Table 2
Empirical coefficients for the correlations described by Eqs. (18) and (19).

Packing material	K_Ga isopropanol (h^{-1})		
	c_1 ($m^{-c_2}h^{(c_2-1)}$)	c_2 (dimensionless)	r^2
PAS Winded Media Flexiring 25 mm	11.59	0.85	0.94
	K_La oxygen (h^{-1})		
	c_1 ($m^{-c_2}h^{(c_2-1)}$)	c_2 (dimensionless)	r^2
Flexiring 25 mm	10.72	0.65	0.99
PAS Winded Media	9.54	0.84	0.95
Refilltech 15 mm	5.29	0.93	0.99

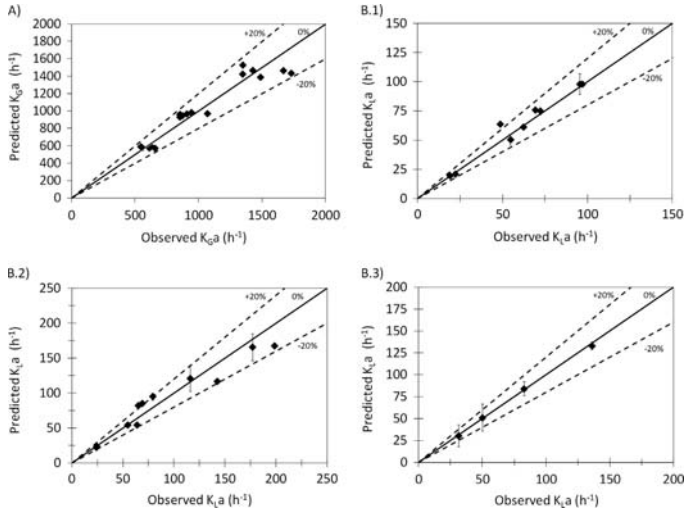

Fig. 8. Comparison of correlation results and experimental data for mass transfer coefficients: (A) Isopropanol and (B) oxygen: (1) Flexiring 25 mm (2) PAS Winded Media (3) Refilltech 15 mm. Dotted lines indicate an uncertainty of ±20%.

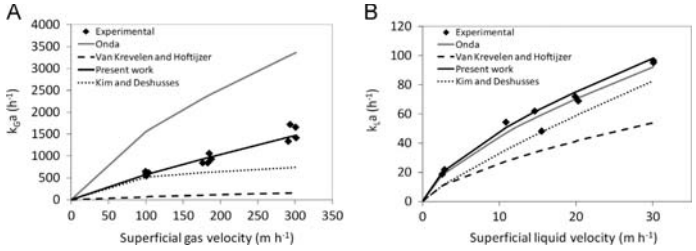

Fig. 9. Comparison between experimental data and empirical correlations for Flexiring 25 mm. (A) Isopropanol and (B) oxygen.

Van Krevelen and Hoftijzer

$$k_G = 0.2\frac{D_G}{d_c}\left(\frac{\rho_G v_G}{\mu_G a_p}\right)^{0.8}\left(\frac{\mu_G}{\rho_G D_G}\right)^{1/3} \quad (22)$$

$$k_L = 0.015 D_L\left(\frac{\mu_L^2}{\rho_L^2 g}\right)^{-1/3}\left(\frac{\rho_L v_L}{a_e \mu_L}\right)^{2/3}\left(\frac{\mu_L}{\rho_L D_L}\right)^{1/3} \quad (23)$$

The assumed supposition that the main resistance to the mass transfer of isopropanol is in the gas phase and for oxygen is in the liquid phase was checked applying the Onda and Van Krevelen and Hoftijzer equations, taking into account both resistances and neglecting one of them for each compound. The error committed neglecting one of the phases was very small (in all cases less than 6%). The hydrodynamics under which these correlations were developed are markedly different than these used in biofiltration, characterised by lower gas and liquid velocities. For this reason, Kim and Deshusses (2008b) developed specific correlations for biotrickling filters for different packing materials.

Kim and Deshusses (For Pall ring 1")

$$\log(k_G a) = 2.05 + 0.33\log(v_G) \quad (24)$$

$$\log(k_L a) = 0.69 + 0.83\log(v_L) \quad (25)$$

The results obtained herein were compared with these three correlations for the experiments with Flexiring 25 mm. In the case of the equations proposed by Onda and Van Krevelen and Hoftijzer, the wetted area and the effective gas-liquid interface were considered the same as that of the packing material. In the case of Kim and Deshusses, since Pall rings 1" and Flexiring 25 mm have a similar specific surface area, the values of the coefficients proposed in their research were used for comparison purposes.

Fig. 9 shows the comparison between the experimental data and correlations for the packing material Flexiring 25 mm. For the mass transfer coefficient of isopropanol (Fig. 9A) it is clear that neither correlation found in the literature was capable of simulating the mass transfer coefficients obtained experimentally. The Onda equation overestimated the values of $K_G a$ by a factor between 2 and 3, while the values provided by the Van Krevelen

and Hoftijzer equation underestimated the experimental data. In the case of the equation from Kim and Deshusses, the experimental data were successfully predicted only at low gas velocities.

For the mass transfer coefficient of oxygen, the prediction of the Onda correlation fit accurately with the experimental data, and the results predicted by Kim and Deshusses were slightly smaller in comparison. In this case, the results of Van Krevelen and Hoftijzer were clearly quite different from the empirical data.

These results show how theoretical and general correlations are not accurate for the prediction of the mass transfer coefficients in biotrickling filters. So, as was proposed by Dorado et al. (2009), using experimental global mass transfer coefficients appears the most suitable way to represent mass transfer. The correlations proposed in this paper are useful for the mathematical modelling of the treatment of vapour emissions of isopropanol with biotrickling filters.

4. Conclusions

Mass transfer properties for isopropanol and oxygen were determined for several packing materials in the liquid and gas velocity ranges typically used in biotrickling filtration. Henry's law constant of isopropanol was clearly influenced by the temperature in the ambient range. An empirical correlation based on the Van't Hoff equation was obtained by using experiments with the random packing material Flexiring 25 mm. This correlation was validated with the experiments carried out with the structured packing material PAS Winded Media. The influence of the gas and liquid velocities and the packing materials on the mass transfer coefficients of isopropanol and oxygen was determined. The mass transfer coefficient of isopropanol increased almost linearly with gas velocity, while the influences of the liquid velocity and packing material were not significant. The mass transfer coefficient of oxygen was influenced by the packing material and by the liquid velocity. No significant influence of the gas velocity was observed. Based on the data obtained in the present study, power law relationships between the mass transfer coefficient and the gas and liquid velocities were proposed in each case. Three mathematical correlations found in the literature were compared with the empirical data; none of the correlations were capable of reproducing the mass transfer coefficients obtained empirically.

The data presented in this paper contain valuable information for modelling the mass transfer coefficients of isopropanol and oxygen. This information is useful for mathematical modelling of physical phenomena that take place during the removal of isopropanol by biotrickling filtration. This paper provides a simple methodology that can be extended to any hydrophilic volatile organic compound.

Nomenclature

a	specific interfacial area
a_e	effective specific interfacial area
a_p	packing specific surface area
C	mass concentration
c_1	empirical coefficient of power law
c_2	empirical coefficient of power law
D	diffusion coefficient
d_c	column inner diameter
d_p	particle diameter
H	Henry's law constant
K	overall mass transfer coefficient
k	individual mass transfer coefficient
Q	volumetric flow rate
S	surface of the column
t	time
V	volume
V_R	volume of the reactor
V_T	volume of the tank
z	distance from the bottom of the column
Z	height of the column
ρ	density
τ	response time of the probe
μ	viscosity

Subscripts

G	gas
IPA	isopropanol
L	liquid
OXY	oxygen

Sub-subscripts

A	inlet to the column of the liquid phase
B	outlet of the column of the liquid phase
in	inlet to the column of the gas phase
m	measured
out	outlet of the column of the gas phase

Acknowledgements

The research leading to these results has received funding from the People Programme (Marie Curie Actions) of the European Union's Seventh Framework Programme FP7/2007-2013/ under REA grant agreement no. 284949. Financial support from the Ministerio de Economía y Competitividad (Project CTM2010-15031/TECNO) and Generalitat Valenciana (PROMETEO/2013/053) Spain is also acknowledged. Joaquim Castro Blanch is also acknowledged for his laboratory support. Pau San-Valero acknowledges the Ministerio de Educación, Cultura y Deporte Spain for her FPU contract (AP2010-2191).

References

Devinny, J.S., Deshusses, M.A., Webster, T.S., 1999. Biofiltration for air pollution control. CRC-Lewis Publishers, Boca Raton.

Dorado, A.D., Rodriguez, G., Ribera, G., Bonsfills, A., Gabriel, D., Lafuente, J., Gamisans, X., 2009. Evaluation of mass transfer coefficients in biotrickling filters: experimental determination and comparison to correlations. Chem. Eng. Technol. 32, 1941–1950.

Iranpour, R., Cox, H.H. J., Deshusses, M.A., Schroeder, E.D., 2005. Literature review of air pollution control biofilters and biotrickling filters for odor and volatile organic compound removal. Environ. Prog. 24, 254–267.

Kim, S., Deshusses, M.A., 2008a. Determination of mass transfer coefficients for packing materials used in biofilters and biotrickling filters for air pollution control. 1. Experimental results. Chem. Eng. Sci. 63, 841–855.

Kim, S., Deshusses, M.A., 2008b. Determination of mass transfer coefficients for packing materials used in biofilters and biotrickling filters for air pollution control – 2: development of mass transfer coefficients correlations. Chem. Eng. Sci. 63, 856–861.

Larachi, F., Lévesque, S., Grandjean, B.P. A., 2008. Seamless mass transfer correlations for packed beds bridging random and structured packings. Ind. Eng. Chem. Res. 47, 3274–3284.

Lebrero, R., Estrada, J.M., Muñoz, R., Quijano, G., 2012. Toluene mass transfer characterization in a biotrickling filter. Biochem. Eng. J. 60, 44–49.

Liss, P.S., Slater, P.G., 1974. Flux of gases across the air-sea interface. Nature 247, 181–184.

Onda, K., Takeuchi, H., Okumoto, Y., 1968. Mass transfer coefficients between gas and liquid phases in packed columns. J. Chem. Eng. Jpn. 1 (1), 56–62.

Pérez, J., Montesinos, J.L., Gòdia, F., 2006. Gas–liquid mass transfer in an up-flow cocurrent packed-bed biofilm reactor. Biochem. Eng. J. 31 (3), 188–196.

Piche, S., Grandjean, B.P. A., Iliuta, I., Larachi, F., 2001. Interfacial mass transfer in randomly packed towers: a confident correlation for environmental applications. Environ. Sci. Technol. 35, 4817–4822.

Sander, R., 2005. Henry's law constants in NIST chemistry WebBook, NIST standard referencedata base number 69, in: Linstrom, P. J., Mallard, W. G. (Eds), National Institute of Standards and Technology. Gaithersburg, MD, USA.

San-Valero, P., Penya-Roja, J.M., Sempere, F., Gabaldon, C., 2013. Biotrickling filtration of isopropanol under intermittent loading conditions. Bioprocess. Biosyst. Eng. 36, 975–984.

Shareefdeen, Z., Singh, A., 2005. Biotechnology for odor and air pollution control. Springer, Heidelberg, Germany.

Snider, J.R., Dawson, G.A., 1985. Tropospheric light alcohols, carbonyls, and acetonitrile: Concentrations in the southwestern United States and Henry's Law data. J. Geophys. Res.: Atmos. 90, 3797–3805.

Staudinger, J., Roberts, P.V., 1996. A critical review of Henry's law constants for environmental applications. Crit. Rev. Environ. Sci. Technol. 26, 205–297.

Staudinger, J., Roberts, P.V., 2001. A critical compilation of Henry's law constant temperature dependence relations for organic compounds in dilute aqueous solutions. Chemosphere 44, 561–576.

Van Krevelen, D.W., Hoftijzer, P.J., 1948. Kinetics of simultaneous absorption and chemical reaction. Chem. Eng. Prog. 44, 529–536.

Van't Riet, K., 1979. Review of measuring methods and results in nonviscous gas-liquid mass transfer in stirred vessels. Indus. Eng. Chem. Process Des. Dev. 18 (3), 357–364.

Weiland, P., Onken, U., 1981. Fluid dynamics and mass transfer in an airlift fermenter with external loop. German Chem. Eng. 4, 42–50.

Available online at www.sciencedirect.com

SciVerse ScienceDirect

Procedia Engineering 42 (2012) 1726 – 1730

Procedia Engineering

www.elsevier.com/locate/procedia

20th International Congress of Chemical and Process Engineering CHISA 2012
25 – 29 August 2012, Prague, Czech Republic

Study of mass oxygen transfer in a biotrickling filter for air pollution control

P. San-Valero, C. Gabaldón, J. Penya-roja a* and M.C. Pérez

Univ. Valencia, Dep. Chemical Engineering, Av. de la Universidad s/n, 46100, Burjassot, Spain

Abstract

Biotrickling filtration is a potential and cost effective alternative for the treatment of volatile organic compound (VOC) emissions in air, so it is necessary to deepen into the key aspects of design and operation for the optimization of this technology. One of these factors is the oxygen mass transfer of the process. This study would facilitate the selection of the packing material and the mathematical modelling and simulation of bioreactors. Four plastic packing materials with a different specific surface area have been evaluated in terms of oxygen mass transfer. For the tested range of superficial liquid velocities, data show a relationship between the k_La and the superficial liquid velocity in all packing materials used, except for the biggest plastic rings. No significant differences in mass transfer coefficients at low liquid velocities were observed, however dependency between oxygen transfer and specific surface area increased considerably for high liquid velocities. No significant influences of the superficial air velocity were observed.

Keywords: Mass transfer; biotrickling filter; oxygen; volatile organic compounds

1. Introduction

The abatement of volatile organic compound (VOC) emissions is a factor of protection of the environment and public health in Europe [1]. As a consequence of these increasingly restrictive environmental regulations, treatment technologies for VOC removal are required. Since late 1990s there

*Corresponding author. J. Penya-roja. Tel.: +34-96-3543695; fax: +34-96-3544898.
E-mail address: Josep.penarrocha@uv.es.

1877-7058 © 2012 Published by Elsevier Ltd.
doi:10.1016/j.proeng.2012.07.565

has been an emergent interest of research towards the biotrickling filter (BTF), which allows better control of the pH and offers smaller footprint compared to conventional biofilters. BTF uses an inert packing material and involves continuous or intermittent trickling of water. In this configuration, the biomass attaches to the media and develops a biofilm, thus, the pollutant and the oxygen will be transferred from the gas phase to the trickling liquid and then to the biofilm, where the biodegradation takes place. As it was pointed out [2,3] the mass transfer could be limiting the performance of the process, so the choice of a suitable packing is very important. In the same way, oxygen limitation could be occur [3,4]. This limitation could be especially vital for the treatment of high loads of VOCs hydrophilic compounds due to their higher partition coefficient than partition coefficient of the oxygen. In order to optimize the cost and efficiency of the BTF at industrial scale, a good gas-liquid contact is necessary. Determining the mass transfer coefficient would facilitate the selection of the packing material and the modelling of bioreactors used for air pollution control. Correlations commonly used for chemical absorption processes do not represent correctly the phenomenon occurred in BTFs due to the different hydrodynamic conditions of chemical absorption [5,6].

2. Materials and methods

In this study, a dynamic method was used for the determination of k_La. This method consists of measuring the evolution of the concentration of dissolved oxygen in the recirculation tank in which the oxygen has been previously displaced by bubbling nitrogen gas. The system consisted of a column of methacrylate (14.4 cm internal diameter, 80 cm height) and a recirculation tank. The column was filled with different propylene packing materials to be tested. In this case one structured and three random packing materials with different size and superficial area have been used as can be seen in Table 1.

Table 1. Characteristics of the packing materials used*

			Size (mm)	Superficial area (m^2 m^{-3})
Packing 1		Structured	----	410
Packing 2	Plastic Rings	Random	15	348
Packing 3	Plastic Rings	Random	25	207
Packing 4	Plastic Rings	Random	50	110

* All packing materials were supplied by Pure Air Solutions, The Netherlands.

As shown in Figure 1, the air stream was introduced through the bottom of the column. The flow rate was adjusted using a mass flow controller (Bronkhorst Hi-Tec, The Netherlands). The experiments were carried out for two air superficial velocities of 104 m h^{-1} and 312 m h^{-1} to evaluate the influence of air flow rate. The trickling water was recirculated in counter current mode, with a water superficial velocity between 3 and 33 m h^{-1}. The oxygen concentration in the liquid was determined using a dissolved oxygen probe (Cellox® 325i, WTW, Germany), for which the response time was considered.

The value of k_La was calculated adjusting experimental data of dissolved oxygen concentration in the recirculation tank with theoretical values obtained from the oxygen mass balance in the tank, using the following equations:

$$dC/dt = 1/\theta\ (C^* - (C^*-C)/exp(L/v^*k_La)-C) \quad (1)$$

$$dC_{med}/dt = (C-C_m)/\tau \quad (2)$$

where C is the real dissolved oxygen concentration in the recirculation tank, C_m is the measured dissolved oxygen concentration in the recirculation tank, C^* is the oxygen solubility experimentally determined, θ is the hydraulic residence time in the tank, τ is the response time constant of the probe (time that the probe achieves the 63.2% of the final value) and L and v are the height of the column and the velocity of the trickling water, respectively.

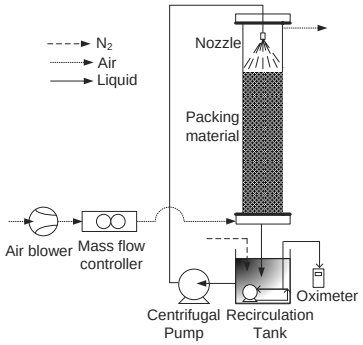

Fig. 1. Experimental setup

3. Results and discussion

The determination of oxygen mass transfer coefficients was carried out for each packing material at several liquid velocities, where k_La coefficients were obtained using least squares method to minimize the differences between the experimental data and the concentration of oxygen provided by the simple mathematical model established by the equations (1) and (2). Previously, the response time of the probe (τ) was determined by means of a step input assay, resulting in a value of 19.4 ±1.5 s.

For the tested range of superficial liquid velocities, data show a clear dependence of the k_La with the superficial liquid velocity for all tested packing material, except for the biggest plastic rings. As an example, besides, the influence of superficial liquid velocity versus the mass transfer coefficient for the two gas velocity tested in packing material 3 is shown in Figure 2. As can be observed, by tripling the gas velocity were not observed significant differences between the data obtained. Thus, as was pointed by other authors [5,7] the oxygen mass transfer depends primarily on the superficial liquid velocity for each packing material. This implies that VOC treatment with biotrickling filtration was not affected by the gas velocity from the point of view of the oxygen transfer when the other conditions were kept constant.

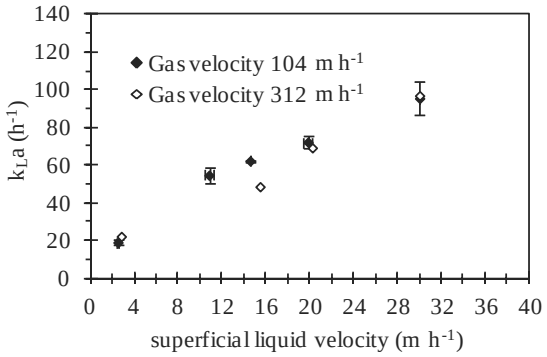

Fig. 2. Influence of superficial liquid velocity and superficial air velocity on the oxygen mass transfer coefficient for the packing material number 3.

The behavior of each packing material on the oxygen mass transfer for the superficial liquid velocities was compared. The oxygen mass transfer coefficient obtained for low and high liquid velocities (3 and 30 m h^{-1}) for each packing material tested are shown in Figure 3 (6 and 30 m h^{-1} for packing material number 2).

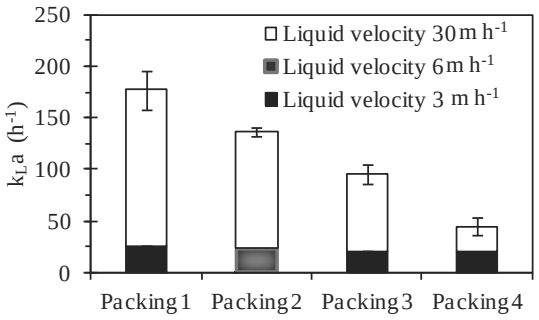

Fig. 3. Influence of the liquid velocity on the oxygen mass transfer coefficient for each packing materials for high and low liquid velocities.

.

For the low liquid velocities, similar values of k_La were obtained. Thus, the influence of the specific surface area seems negligible under the tested conditions. However, for the liquid velocity of 30 m h^{-1}, large differences on the oxygen mass transfer coefficient were obtained for each packing material. This suggests that, at high liquid velocities, by increasing the specific surface area of the packing material is possible to enhance the oxygen mass transfer. So, the superficial liquid velocity is a key parameter in the operation of biotrickling filtration and oxygen mass transfer should be known for each packing material in order to optimize the performance of the process.

4. Conclusion

Results showed that oxygen mass transfer was strongly affected by superficial liquid velocities. No influence of gas velocity on the oxygen mass transfer was obtained. At low liquid velocities, no differences between packings were observed. At high liquid velocities, data show that higher values of specific surface area provide greater mass transfer coefficients for the tested range. Consequently, the study of oxygen mass transfer is a crucial factor in order to improve the biological performance of biotreatments for VOC elimination.

Acknowledgements

The research leading to these results has received funding from the People Programme (Marie Curie Actions) of the European Union's Seventh Framework Programme FP7/2007-2013/ under *REA* grant agreement nº 284949. Financial support from Ministerio de Ciencia e Innovación (Project CTM2010-15031/TECNO) and Generalitat Valenciana (ACOMP/2012/209), Spain, is also acknowledged. Pau San Valero acknowledges the Generalitat Valenciana, Spain (ACIF2011/067 contract).

References

[1] Council Directive 2010/75/EU of 24 November 2010 on industrial emissions (integrated pollution prevention and control). 2010.

[2] Popat SC, Deshusses MA. Analysis of the rate-limiting step of an anaerobic biotrickling filter removing TCE vapors. *Process Biochem* 2010;**45:**549-555.

[3] Kirchner K, Wagner S, Rehm HJ. Exhaust-Gas Purification using Biocatalysts (Fixed Bacteria Monocultures) - the Influence of Biofilm Diffusion Rate (O_2) on the overall Reaction-Rate. *Appl Microbiol Biotechnol.* 1992;**37:**277-279.

[4] Alonso C, Zhu X, Suidan MT, Kim BR, Kim BJ. Modelling of the biodegradation process in a gas phase bioreactor-estimation of intrinsic parameters. In: F.E. Reynolds Jr, editors. *Proc 1998 USC-TRG Conf. Biofiltration*, Tustin: The Reynolds Group; 1998; p.211-218.

[5] Kim S, Deshusses MA. Determination of mass transfer coefficients for packing materials used in biofilters and biotrickling filters for air pollution control. 1. Experimental results. *Chem Eng Sci* 2008;**63:**841-855.

[6] Dorado AD, Rodriguez G, Ribera G, Bonsfills A, Gabriel D, Lafuente J, et al. Evaluation of Mass Transfer Coefficients in Biotrickling Filters: Experimental Determination and Comparison to Correlations. *Chem Eng Technol* 2009;**32:**1941-1950.

[7] Piche S, Grandjean BPA, Iliuta I, Larachi F. Interfacial mass transfer in randomly packed towers: A confident correlation for environmental applications. *EnvironSci Technol* 2001;**35:**4817-4822.

Int. J. Environ. Res. Public Health **2015**, *12*, 746-766; doi:10.3390/ijerph120100746

OPEN ACCESS

International Journal of
Environmental Research and Public Health
ISSN 1660-4601
www.mdpi.com/journal/ijerph

Article

Dynamic Mathematical Modelling of the Removal of Hydrophilic VOCs by Biotrickling Filters

Pau San-Valero, Josep M. Penya-roja, F. Javier Álvarez-Hornos, Paula Marzal and Carmen Gabaldón *

Research Group GI^{2}AM, Department of Chemical Engineering, University of Valencia, Avda. Universitat s/n, 46100 Burjassot, Spain; E-Mails: pau.valero@uv.es (P.S.); josep.penarrocha@uv.es (J.M.P.); Francisco.j.alvarez@uv.es (F.J.A.-H.); paula.marzal@uv.es (P.M.)

* Author to whom correspondence should be addressed; E-Mail: carmen.gabaldon@uv.es; Tel.: +34-96-354-3437; Fax: +34-96-354-4898.

Academic Editor: Christian Kennes

Received: 26 September 2014 / Accepted: 23 December 2014 / Published: 14 January 2015

Abstract: A mathematical model for the simulation of the removal of hydrophilic compounds using biotrickling filtration was developed. The model takes into account that biotrickling filters operate by using an intermittent spraying pattern. During spraying periods, a mobile liquid phase was considered, while during non-spraying periods, a stagnant liquid phase was considered. The model was calibrated and validated with data from laboratory- and industrial-scale biotrickling filters. The laboratory experiments exhibited peaks of pollutants in the outlet of the biotrickling filter during spraying periods, while during non-spraying periods, near complete removal of the pollutant was achieved. The gaseous outlet emissions in the industrial biotrickling filter showed a buffered pattern; no peaks associated with spraying or with instantaneous variations of the flow rate or inlet emissions were observed. The model, which includes the prediction of the dissolved carbon in the water tank, has been proven as a very useful tool in identifying the governing processes of biotrickling filtration.

Keywords: biotrickling filtration; air pollution control; volatile organic compounds; mathematical modelling

1. Introduction

Control of volatile organic compound (VOC) emissions from industry is nowadays a priority in air quality regulation. In the European Union (EU), Directive 1999/13/EC, recently modified by Directive 2010/75/EU, pursues the reduction of VOC emissions. According to data from the European Environment Agency, the sector of "solvents and product use" contributes 44% of the emissions of non-methane VOC in the EU; a reduction of 42% from 1990 to 2012 has been reported with a release of 2951 Gg in 2012 [1]. The industrial use of solvents typically releases waste gas streams where the flow is high (>1000 $m^3 \cdot h^{-1}$) and the VOC concentration is low (<5 $g \cdot m^{-3}$). Bioprocesses are best suited to the control of these emissions due to the low concentration of pollutants [2]. Among bioprocesses, biotrickling filtration is recommended for compounds with Henry's law constants below 0.1 [3], such as ethanol, n-propanol or isopropanol, the main pollutants of the waste gas streams emitted from flexible food packaging industries (flexographic sector). A biotrickling filter (BTF) consists of a column filled with an inert packing material, where the biomass attaches to the media and develops a biofilm. In this configuration, the gas and liquid phases circulate through the column in co- or counter-current mode. Depending on the operation mode, the BTF process involves a continuous or intermittent trickling of water.

Despite the fact that BTFs have been successfully applied for the treatment of air pollutants, the use of BTFs depends on the increase of operational knowledge to allow the robustness of the performance. As has been recognized, the performance of BTF is markedly dependent on the operational conditions. Parameters, such as liquid velocity, gas velocity and empty bed residence time (EBRT) and inlet concentrations, may hinder the performance of field-scale BTFs [4–6]. Thus, further research for a better understanding of the role of those parameters would be desirable [7]. Several efforts have been made to adapt the operational conditions of laboratory experiments to emulate the operational conditions usually experienced in industrial applications [6]. One of the most common practices in industrial BTFs in comparison with laboratory studies is the use of intermittent trickling of water. San Valero *et al.* [8] observed that a spraying regime of 15 min every 1.5 h resulted in peaks of concentration coinciding with the irrigation of the bed when treating isopropanol. We concluded that the frequency of irrigation is a crucial parameter in terms of the achievement of low emissions under intermittent loading of highly-soluble compounds.

Biotrickling filtration involves a complex combination of several physical, chemical and biological processes; further investigation, in order to integrate the phenomena occurring during treatment, is required. Mathematical modelling is a fundamental tool in the development of an understanding of the process. Additionally, as pointed out by Lu *et al.* [9], effective modelling can lead to the development of a trustworthy performance equation that decreases the time and cost of experimentation on the pilot scale. Thus, phenomenological models based on the main mechanisms on biofiltration seem to be useful in improving the understanding of BTFs and in identifying the governing processes involved in their operation. The phenomenological model most commonly used during the last few decades was developed by Ottengraf and Van Den Oever [10] for biofilters operating under steady-state conditions. Following this study, many models for biofilters have been reported in the literature, adding new phenomena, such as adsorption in the packing material and the inhibition kinetics of microbial growth, among others [11]. As an example, Shareefdeen *et al.* [12] included both oxygen and substrate inhibition

effects; this model was improved by assuming the partial coverage of the support particles by biofilm and by modelling the adsorption on the uncovered particles by using the Freundlich isotherm [13].

Most mathematical models of BTFs and trickle bed biofilters are based on mechanisms that have been used to describe biofilter behavior. Usually, a three-phase model (gas-liquid-biofilm) is used to describe these configurations. The main difference with biofilter models is related to the presence of a liquid phase, often simulated as an intermediate step between the gas phase and the biofilm. In steady state conditions, Mpanias and Baltzis [14] were the first to develop a model that takes into account the kinetic limitations arising from the availability of VOCs and oxygen in BTF. This model was extended to VOC mixtures [15]. Concerning non-steady state conditions, Okkerse *et al.* [16] presented a dynamic BTF model for the degradation of volatile acidifying pollutants, as well as mass accumulation and mass distribution along the column. Zhu *et al.* [5] proposed a dynamic three-phase system with a non-uniform bacterial population to show the effect of mass transfer limitations due to the water phase in the reactor for the removal of diethyl ether. Kim and Deshusses [17] developed a dynamic BTF model for the removal of H_2S with gas and liquid phase flowing counter-current, where the biofilm on the packing material was not completely wetted. In this model, a fraction of the pollutant was transferred directly from the gas phase to the biofilm, while another fraction was transferred through the liquid phase to the biofilm. Recently, Almenglo *et al.* [18] modified the Kim and Deshusses model by assuming a stagnant liquid fraction distributed homogeneously along the bed; mass balances in the biofilm were divided into "flowing" biofilm (which is in contact with flowing liquid) and "stagnant" biofilm (which is in contact with stagnant liquid). Lee and Heber [19] proposed a model modified from that of Alonso *et al.* [20] in order to develop a genetic algorithm to estimate the unknown parameters in ethylene removal. Iliuta *et al.* [21] developed a predictive dynamic model in a trickle-bed bioreactor based on the macroscopic volume-averaged mass and momentum balance equations coupled with classical diffusion and bioreaction equations to illustrate the influence of biomass accumulation on a bioreactor for toluene removal. These authors showed that shifting from a biofilter to a trickle-bed bioreactor reduces the removal efficiency, due to an extra liquid-film mass transfer resistance step. However, despite the fact that these models provide valuable information on the understanding of the behavior of bioreactors, there is still a lack of information with respect to models adapted to industrial emissions characterized by an intermittent spraying pattern, variable gas flow rate and variable inlet concentration. In this regard, more effort is required to obtain more realistic simulations and to identify the main differences in the observed behavior between the laboratory scale and the industrial scale. As was pointed out by Devinny and Ramesh [22], no single model has become generally accepted.

The aim of the present research is to go deeper into the intricacies of the treatment of hydrophilic compounds using biotrickling filtration technology. For this purpose, a mathematical model was developed to simulate the performance of BTFs, taking into account the main operational conditions found in the industry. The model presented herein was prepared for simulating systems with complex inlet concentration patterns, gas flow rates and cyclic conditions of spraying. An intermittent spraying regime implies that the liquid phase varies during the filter operation, making it necessary to distinguish two different situations, corresponding to spraying and non-spraying periods. In addition, the operation of BTF usually requires more than one spraying pattern during the same day related to periods with different feeding conditions or clogging control, among others. In this regard, the model is able to combine these two different patterns.

The following objectives have been achieved: (1) developing a dynamic mathematical model based on different behaviors during spraying and non-spraying periods combined with variable inlet concentration and variable gas flow rate; (2) calibrating and validating the model with data from BTF at the laboratory scale using isopropanol as the target pollutant; and (3) validating the model with data from a BTF located in an industrial facility from the flexographic sector.

2. Experimental Section

2.1. Experimental Set-Up and BTF Operational Conditions for the Experiments at Laboratory Scale

Two sets of independent data were used to test the mathematical model. The first set corresponds to data from laboratory experiments using isopropanol as the target pollutant. The experiments were performed using a laboratory-scale BTF composed of three cylindrical methacrylate modules in series, with a total bed length of 100 cm and an internal diameter of 14.4 cm. The BTF was filled with a random packing material of 25 mm in diameter (Flexiring: superficial area (a) = 207 $m^2 \cdot m^{-3}$; porosity of the packing material (θ_{PM}) = 0.92), using a volume of the bed of 16.32 L. The BTF had 20 cm of free spaces at the top and bottom of the column and was equipped with 3 equidistant sampling ports. The stream was contaminated with isopropanol, which was introduced through the bottom of the column. A recirculation solution was fed into the bioreactor in counter-current mode with respect to the air flow using a centrifugal pump at 2.5 $L \cdot min^{-1}$ from a tank with 3.5 L of solution. An air stream polluted with VOCs was supplied to the BTF for 16 h per day (starting at 8:00 am), while the rest of the time (8 h), the BTF was supplied with clean air, maintaining a constant air flow rate. A BTF inoculated with activated sludge ran for more than 3 months with an inlet load (IL) of 30 g–$C \cdot m^{-3} \cdot h^{-1}$, EBRT of 60 s and intermittent spraying. With this IL, two consecutive intermittent spraying patterns (Run 1 and Run 2) were applied during a minimum of a 2-week period. Table 1 summarizes the performance of the system during the last 5 days (from Monday to Friday) of each of the runs (1 and 2). Then, the inlet load was increased to 60 g–$C \cdot m^{-3} \cdot h^{-1}$ for 2 weeks. Run 3 (Table 1) summarizes the performance of the system during the final week (from Monday to Wednesday). Each run started with clean water in the recirculation tank. No purges were undertaken until the end of each run. The pressure drop was negligible (<1 $Pa \cdot m^{-1}$). The liquid hold-up (θ_L) had an average value of 0.093 ± 0.003. The biofilm content was gravimetrically determined (mass contained in two rings extracted from each of the three sampling ports). The volume fraction of the biofilm (θ_B) calculated from the biofilm content of the bioreactor (specific gravity of 1) resulted in a value of 0.18 ± 0.04. The water content of the biofilm was measured as 95 ± 3%; 50 $kg \cdot m^{-3}$ of biomass concentration (X_V), which was selected as the average value for modelling purposes.

Table 1. Overall performance of the laboratory-scale experiments. EBRT, empty bed residence time.

	Inlet load [a] (g–C·m^{-3}·h^{-1})	EBRT (s)	Spraying Pattern	Elimination Capacity [a] (g–C·m^{-3}·h^{-1})	Removal Efficiency [a] (%)
Run 1	32.6	60	1 h every 4 h	29.8	91
Run 2	32.0	60	30 min every 4 h	29.7	93
Run 3	59.6	60	1 h every 4 h	53.6	90

[a] Average value from periods during pollutant feeding (16 h·d^{-1}).

2.2. Experimental Set-Up and BTF Operational Conditions for the Field Scale

Data from an industrial BTF (VOCUS^{TM}, PAS Solutions BV, the Netherlands) located at a flexographic industry site were used. The waste gas stream was composed of a mixture of VOCs (63% ethanol, 22% ethyl acetate, 13% 1-ethoxy-2-propanol). The manufacturing shift of this industrial site was 18 h of emissions per day (from 6 to 24 h) during 5 days a week (working days), with several emission sources. The BTF system consisted of a packed reactor with a volume of 49 m^3 filled with polypropylene rings (Flexiring 50 mm: a = 102 m^2·m^{-3}; θ_{PM} = 0.93), plus a recirculation tank with a maximum water capacity of 15 m^3. The bioreactor was operated in counter-current mode; air from the factory was blown into the bottom of the column continuously (polluted air for 18 h per day and clean air for 6 h per day). The BTF began operating in June 2009. Two sets of data (from Monday to Thursday) with different spraying frequency (October 2009, and January 2011) were selected (Table 2). During weekends, clean air was blown on the BTF, and the spraying frequency was kept the same as those applied during non-VOC feeding periods in working days in order to promote the removal of the accumulated VOCs in the water tank. Volumes of water in the recirculation tank were 6.5 and 12.8 m^3 (25% of the volume renewed with fresh water on Sundays), and the liquid flow rates were 30 and 32 m^3·h^{-1} for Run 4 and Run 5, respectively. The pressure drop was lower than 15 Pa·m^{-1}. The system worked for more than 3 months under each of the selected conditions. Table 2 summarizes the performance of the system during the 4 days of each run. The volume fraction of the mobile liquid phase in the bioreactor was approached by measuring the quantity of accumulated water in the bioreactor during spraying; a value of 0.05 was obtained (θ_L).

Table 2. Overall performance of the industrial biotrickling filter (BTF).

	Date	Inlet Load [a] (g–C·m^{-3}·h^{-1})	Gas Flow Rate [a] (m^{-3}·h^{-1})	Spraying Pattern		Elimination Capacity [a] (g–C·m^{-3}·h^{-1})	Removal Efficiency [a] (%)
				0–6 am	6 am–12 pm		
Run 4	October 2009	27.5	1675	6 min every 21 min	6 min every 21 min	17.9	65
Run 5	January 2011	46.5	2717	6 min every 1 h	6 min every 3 h	29.1	63

[a] Average value from periods during pollutant feeding (18 h·d^{-1}).

2.3. Analytical Methods

In the laboratory experiments, the gas concentration of isopropanol was measured using a total hydrocarbon analyzer (Nira Mercury 901, Spirax Sarco, Spain). The response factor of the total hydrocarbon analyzer was determined by gas chromatography (model 7890, Agilent Technologies, USA). The determination of the total organic carbon (TOC) in water was measured using a total organic carbon analyzer (TOC-VCHS, Shimadzu Corporation, Japan). At the industrial scale, the inlet and outlet gas VOC concentrations were continuously monitored using a total hydrocarbon analyzer (RS 53-T, Ratfisch Analysensysteme GmbH, Germany). The air flowed during the whole day, and the air flow rate was monitored continuously by using a pitot tube (19″ pitot tube, Testo AG, Germany).

2.4. Model Development

The model was based on the fact that BTFs are usually operated in intermittent spraying mode. The intermittent spraying regime implies two different behaviors of the system. Thus, a mobile liquid phase and a stagnant liquid phase were considered during the spraying period and non-spraying period, respectively. Thus, a three-phase model (gas-liquid-biofilm) is proposed here based on the mass balances of the gas and liquid phases and the biofilm. Two different systems of partial differential equations were used, depending on whether the spraying or the non-spraying period was simulated. The conceptual scheme of the BTF and the model derivation are shown in Figure 1. For model development, the following assumptions were made:

(1) The gas phase flows in a plug flow regime along the filter bed.
(2) Axial dispersion is neglected.
(3) The adsorption of pollutant in the packing material is negligible.
(4) The active biofilm is formed on the external surface of the packing material, and no reaction occurs in the pores. The biofilm covers the surface of the packing material, and its thickness (δ) is much smaller than the size of the solid particles, so a planar geometry is assumed.
(5) The packing material is completely covered by the biofilm.
(6) The biodegradation kinetics are described by a Monod expression, indicating the oxygen limitation.
(7) The diffusion inside of the biofilm is described by Fick's second law.
(8) A mobile liquid phase is assumed during the spraying period, and a stagnant liquid phase is considered during the non-spraying period.
(9) The gas-liquid interface is in equilibrium according to Henry's law.
(10) The mass flux at the gas-liquid and the liquid-biofilm interfaces can be expressed by mass transfer coefficients.
(11) The presence of biomass in the bioreactor increases resistance to the mass transfer between the gas and the liquid phase. Thus, the overall mass transfer coefficients experimentally determined in abiotic conditions are corrected by a factor (α_1) varying between 0 and 1.
(12) There is no reaction in the liquid phase.

According to the assumptions made above, the mass balances during both periods are described in the next subsection.

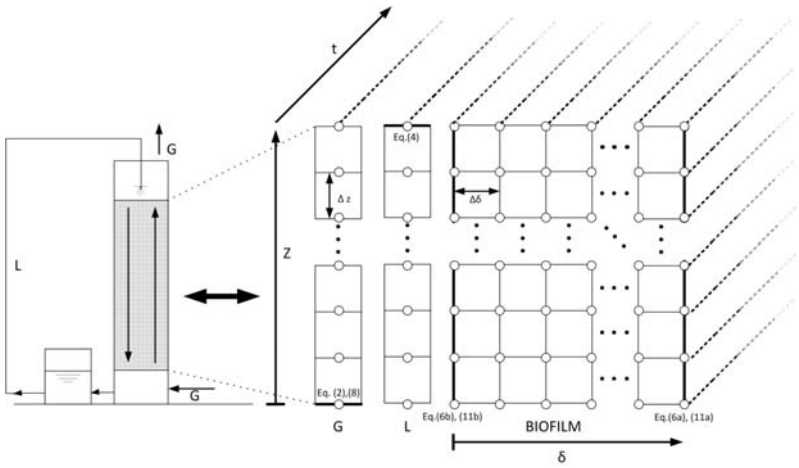

Figure 1. Conceptual scheme of the BTF and model derivation. Bold lines indicate the boundary conditions. Eq. means equation.

2.4.1. Mass Balances during the Spraying Period

During the spraying period, the pollutant and the oxygen are transferred from the gas phase to the mobile liquid phase and then to the biofilm, where the biodegradation takes place. The mass balance of the gas phase is described according to Equation (1) for a system in counter-current operation:

$$\theta_G \frac{\partial C_{G_i}}{\partial t} = -v_G \frac{\partial C_{G_i}}{\partial z} - \alpha_1 K_L a_i \left(\frac{C_{G_i}}{H_i} - C_{L_i} \right) \quad (1)$$

where i denotes the pollutant (P) or the oxygen (O). Thus, for component i, C_{Gi} and C_{Li} are the concentrations of gas and liquid phases, respectively; $K_L a_i$ is the overall mass transfer coefficient; H_i represents the dimensionless Henry's law constants expressed as the concentration of the gas phase/concentration of the liquid phase; t denotes time; z is the distance from the bottom of the column; v_G is the superficial air velocity; and θ_G is the porosity of the bed calculated as $\theta_G = \theta_{PM} - \theta_L - \theta_B$.

The boundary condition of Equation (1) is given by:

$$z = 0 \qquad C_G = C_{G_i}^{in} \quad (2)$$

where $C_{G_i}^{in}$ is the inlet concentration of the component i.

The mass balance of the mobile liquid phase is given by:

$$\theta_L \frac{\partial C_{L_i}}{\partial t} = v_L \frac{\partial C_{L_i}}{\partial z} + \alpha_1 K_L a_i \left(\frac{C_{G_i}}{H_i} - C_{L_i} \right) - \frac{D_i a}{\beta} (C_{L_i} - S_{i,1}) \quad (3)$$

where for component i, D_i is the diffusion coefficient in water; $S_{i,1}$ is the concentration in the biofilm interface; v_L is the superficial liquid velocity; and β is the thickness of the liquid-biofilm interface.

The boundary condition of Equation (3) is given by the mass balance in the recirculation tank:

$$z = Z \qquad \frac{\partial C_{L_i}}{\partial t} = \frac{Q_L}{V_T}(C_{L_{i z=0}} - C_{L_{i z=Z}}) \tag{4}$$

where Z is the height of the column; Q_L is the liquid flow rate; and V_T is the volume of the recirculation tank. $C_{Li\,z=0}$ and $C_{Li\,z=Z}$ are the concentrations of the component i in the liquid phase at the bottom and top of the column, respectively.

The mass balance of the biofilm is given by:

$$\frac{\partial S_i}{\partial t} = f(X_v) D_i \frac{\partial^2 S_i}{\partial x^2} - \frac{\mu_{\max} X_v}{Y_i} \frac{S_P}{S_P + K_P} \frac{S_O}{S_O + K_O} \tag{5}$$

where S_i is the concentration inside the biofilm of component i; $f(X_v)$ is the correction factor of the diffusivities in water due to the biomass calculated by Fan's equation [23]; X_v is the concentration of the biomass; μ_{max} is the specific growth rate of the biomass; K_P and K_o are the half-saturation constants of the pollutant and oxygen, respectively; and, for component i, Y_i is the yield coefficient.

The boundary conditions for the mass balance of the biofilm are given by:

$$x = \delta \qquad \frac{\partial S_i}{\partial x} = 0 \tag{6a}$$

$$x = 0 \qquad S_i = C_{L_i} \tag{6b}$$

where δ is the biofilm thickness.

2.4.2. Mass Balances during the Non-Spraying Periods

During the period without spraying, the pollutant and the oxygen are transferred from the gas phase to the stagnant liquid phase and then to the biofilm, where biodegradation takes place. The according mass balances are presented below.

The mass balance of the gas phase is given by Equation (7):

$$\theta_G \frac{\partial C_{G_i}}{\partial t} = -v_G \frac{\partial C_{G_i}}{\partial z} - \alpha_2 \alpha_1 K_L a_i \left(\frac{C_{G_i}}{H_i} - C_{L_i} \right) \tag{7}$$

where α_2 is a switch parameter that weights the gas-liquid mass transfer resistance. A value of 100 is assumed to indicate that the gas-liquid mass transfer resistance is negligible. A value of 1 indicates that a resistance to the gas-liquid mass transfer contributes to reducing the pollutant max flux diffusing to/from the biofilm.

The boundary condition of Equation (7) is given by:

$$z = 0 \qquad C_G = C_G^{in} \tag{8}$$

The mass balance of the stagnant liquid phase is given by:

$$\theta_L \frac{\partial C_{L_i}}{\partial t} = \alpha_2 \alpha_1 K_L a_i \left(\frac{C_{G_i}}{H_i} - C_{L_i} \right) - \frac{D_i a}{\beta} (C_{L_i} - S_{i,1}) \tag{9}$$

The mass balance in the biofilm is given by:

$$\frac{\partial S_i}{\partial t} = f(X_v) D_i \frac{\partial^2 S_i}{\partial x^2} - \frac{\mu_{\max} X_v}{Y_i} \frac{S_P}{S_P + K_P} \frac{S_O}{S_O + K_O} \quad (10)$$

with the boundary conditions:

$$x = \delta \qquad \frac{\partial S_i}{\partial x} = 0 \quad (11a)$$

$$x = 0 \qquad S_i = C_{L_i} \quad (11b)$$

2.4.3. Numerical Solution

The partial differential equations given above constitute two second-order nonlinear distributed systems. In order to solve them, the method of lines (MOL) was chosen. For a numerical problem solution, Z is divided into N sections with $N + 1$ equi-spaced node points. Similarly, the biofilm thickness is divided into M sections with $M + 1$ points, resulting in two ordinary differential equation (ODE) systems of $2(N + 1)(M + 3)$ equations. The next step is to discretize the spatial variables. The parameters of N and M were optimized as 20 and 40, respectively. The resulting ODE systems were found to be stiff. Therefore, they were integrated using the ode23t function of Matlab.

3. Results and Discussion

3.1. Model Calibration

The calibration of the mathematical model presented herein was carried out with the experimental Run 1 (Table 1). Figure 2 shows the monitoring of the pollutant concentration in the gas phase (a.1) and the evolution of the dissolved carbon concentration in the water tank (a.2) from Monday to Friday (0 to 120 h). In Figure 2 (a.1 and a.2), time 0 h refers to Monday 8:00 am. As an example of the daily patterns, data for Wednesday (48 to 72 h) is shown in Figure 2 (b.1 and b.2). As is shown in Figure 2 (a.1 and b.1), the outlet gas stream exhibited peaks of pollutant emission coinciding with the spraying periods (six peaks per day). During the periods without spraying, nearly complete removal of the pollutant was obtained. For every day, a similar dynamic pattern was observed. During the feeding of air polluted with VOC (0–16 h), the pollutant leak associated with the first spraying of each day (0 h) was much lower than the rest of the peaks. The leak increased during the second spraying (4 h), reaching a quasi-stable maximum during the third and fourth spraying (8 h, 12 h). After cutting off the supply of VOC (at 16 h), the immediate peak (16 h) was similar to those obtained previously, but after some hours, the outlet gas emission during spraying was drastically reduced (20 h). The evolution of the peaks during the non-VOC feeding period indicated that the accumulated substrate in the system was consumed; the gas-phase leak at 20 h of each day was nearly in equilibrium with the organic liquid concentration in the tank. The dissolved carbon concentration in the water tank was monitored during spraying at working hours on alternate days (Figure 2 (a.2, b.2)). As can be seen, the daily concentration increased with each spraying, indicating that the pollutant is absorbed in water. The outlet gas emissions of the second to fifth daily peaks were more than three-times higher than the predicted equilibrium concentration with the dissolved carbon concentration in the water. The variations

of the liquid concentration in the recirculation tank between days indicated that the accumulated pollutant in water would be degraded in the BTF during spraying in night periods (16–24 h).

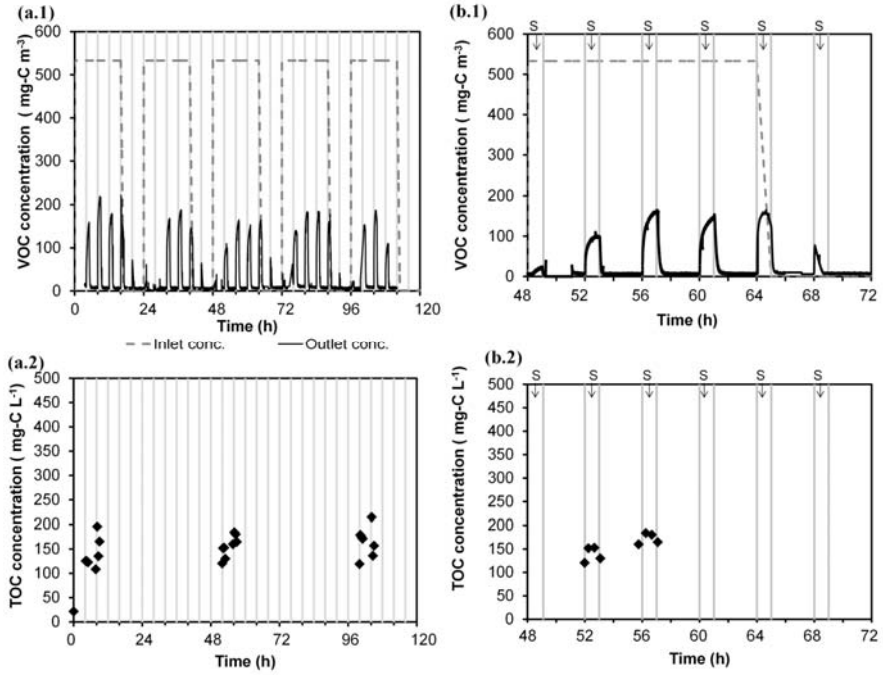

Figure 2. Experimental data of Run 1 (Monday to Friday), where each central line denotes a spraying: (**a.1**) concentration of VOC in the gas phase; (**a.2**) concentration of the dissolved carbon in the water tank. Wednesday results, where S denotes the spraying periods: (**b.1**) concentration of VOC in the gas phase; (**b.2**) concentration of the dissolved carbon in the water tank.

The parameters for the calibration of the model are summarized in Table 3. The values of physical constants, diffusivities in water and Henry's law constants have been taken from the literature. The overall mass transfer coefficients of the abiotic system were estimated using the experimental correlations proposed in San-Valero *et al.* [24] for the operational conditions used in the present work. Biofilm thickness was assumed to be 60 μm. The yield coefficient of the isopropanol was taken from the literature, and the yield coefficient of the oxygen was calculated using the stoichiometric balance.

Table 3. Parameters used in the modelling of BTF at the laboratory scale.

Parameters	Specific Value	Reference
Physical properties		
D_P ($m^2 \cdot s^{-1}$)	1.13×10^{-9}	[25]
D_O ($m^2 \cdot s^{-1}$)	2.0×10^{-9}	[26]
H_P	2.8×10^{-4}	[24]
H_O	31.4	[27]
K_La_P (s^{-1})	2.98×10^{-5}	Using correlation in [24]
K_La_O (s^{-1})	0.0126	Using correlation in [24]
Biofilm properties		
δ (m)	60×10^{-6}	This work
β (m)	3.8×10^{-6}	This work
Kinetic data		
$f(Xv)$	0.3495	[23]
Ko	0.26	[12]
Y_P	0.48	[11]
Yo	0.14	Stoichiometric balance
μ_{max} (s^{-1})	2×10^{-5}	This work
Ks_P ($g–C \cdot m^{-3}$)	350	This work

With this set of parameters, the calibration process started by determining the values of the thickness of the liquid-biofilm interface (β) and the biokinetic parameters (μ_{max}, Ks_P) that predict the experimental evolution of the outlet concentration and the dissolved carbon in the water tank. During non-spraying, the mass transfer resistance between the gas and stagnant liquid was considered negligible ($\alpha_2 = 100$), and during spraying, the gas-liquid mass transfer resistance was assumed to be equal to that determined under abiotic conditions ($\alpha_1 = 1$). The value proposed for μ_{max}, herein, 2×10^{-5} s^{-1}, appears to be in agreement with the values obtained in the literature for the treatment of isopropanol. Bustard *et al.* [28] compiled data from different models proposed by different authors, with values ranging between 1.77×10^{-5} s^{-1} and 2.58×10^{-5} s^{-1}. The relative error deviation between experimental elimination capacity (EC) (29.8 g–C m^{-3} h^{-1}) and simulated EC (31.8 g–C m^{-3} h^{-1}) for Run 1 was 6.7%, indicating the feasibility of the model to reproduce the overall removal, although the dynamic pattern deviated from the experimental one. As an example, Figure 3 shows the results for Wednesday (48 to 72 h). The model predicts the existence of pollutant peaks associated with the mass transfer resistance of the gas-liquid film. The model predicts the sharp decrease of the gas-phase outlet concentration after spraying stops, corroborating that mass transfer resistance during non-spraying was negligible. The coupling of the spraying and non-spraying set of equations also predicts the periodical decrease of the dissolved carbon concentration in the water tank when the BTF works using clean air (from 64 to 72 h in Figure 3). This behavior is associated with the VOC desorption from the liquid to the gas phase and its biodegradation in the biofilm. However, the model underestimates the concentration of the outlet emissions in the case of the second to fifth peaks. In a second stage, the gas-liquid mass transfer flux was reduced by applying a correction factor in order to predict the maximum peak ($\alpha_1 = 0.23$). As can be seen in Figure 3, this increase in the resistance to mass transfer overestimates the first two peaks after VOC feeding resumption after 8 h running with clean air. Experimental data indicated that the supply of VOCs, followed by long non-supply VOC periods (8 h

per day), caused a cyclical variation in the resistance to mass transfer between the gas phase and liquid phase over time. This variation could be associated with a transient evolution in the physical properties due to biological reactions. For example, the accumulation of water and extracellular polymeric substances (EPS) could act as a periodical transfer barrier, deteriorating the removal efficiency of the system. When clean air was supplied, the accumulated VOC in the system could be biodegraded, and part of the formed EPS could disappear from the system, linked to the consumption by the microorganisms. In this regard, Zhang and Bishop [29] suggested that EPS could be used as a substrate and concluded that EPS was biodegradable by its own producers, as well as by other microorganisms, during periods without feeding of VOC.

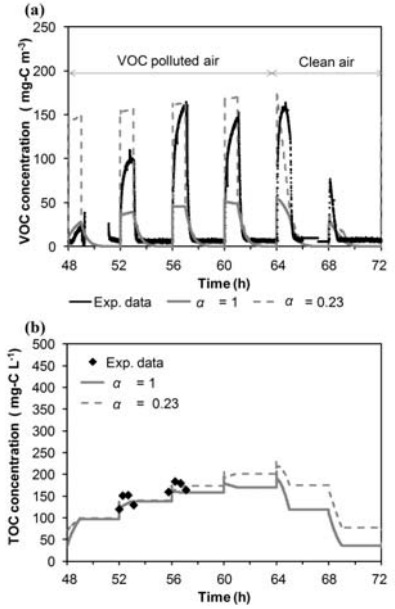

Figure 3. Influence of the parameter α_1 on the model predictions of Wednesday data (Run 1). (**a**) Outlet concentration of VOC in the gas phase. (**b**) Concentration of the dissolved carbon in the water tank.

The calibration of the model ends by fitting the daily variation of the correction factor of gas-liquid mass transfer resistance over time. The same daily variation was assumed for the five days of Run 1. The results of the model calibration are shown in Figure 4 (five days of Run 1). Figure 4 (b.1 and b.2) zoom in on the plot of the Wednesday data (48 to 72 h), and values of α_1 are labelled. By using the proposed approach herein, the relative error (for the whole of Run 1) between experimental EC (29.8 g–C·m^{-3}·h^{-1}) and simulated EC (30.5 g–C·m^{-3}·h^{-1}) was improved by 2.3%. The model is able to better predict the dynamic variations in the outlet gas-phase emissions and in the dissolved carbon concentration in the recirculation tank than in previous calibration steps.

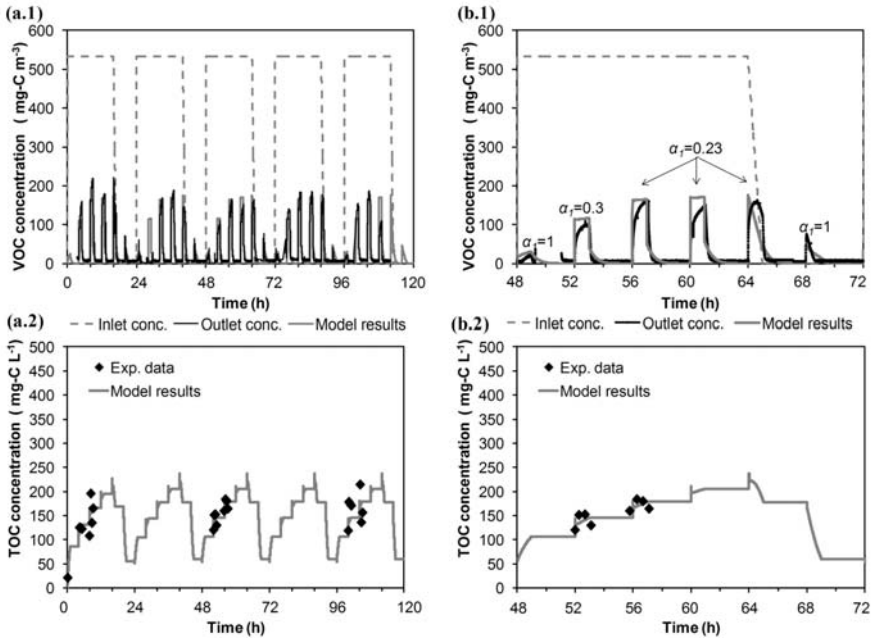

Figure 4. Weekly evolution of experimental data (Run 1) and model predictions for the treatment of isopropanol by a BTF. (**a.1**) concentration of VOC in the gas phase; (**a.2**) concentration of the dissolved carbon in the water tank. Wednesday results: (**b.1**) concentration of VOC in the gas phase; (**b.2**) concentration of the dissolved carbon in the water tank. Conc. means concentration and Exp. means experimental.

3.2. Model Validation

The mathematical model was validated by using two sets of independent experiments at the laboratory scale (Run 2 and Run 3, Table 1) to check the capability of the model to predict the evolution of the system over five days and three days, respectively. Experimental data along with the results of the model simulations are shown in Figure 5. The model is capable of reproducing the cyclical performance by using a different spraying duration (Run 2) or inlet load (Run 3). The relative error between experimental EC and simulated EC was 3.7% and 2.4% for Run 2 and Run 3, respectively. In both cases, the model shows a daily evolution of the outlet gas-phase concentrations: the gradual increase of the peaks when the air polluted with VOC is supplied to the BTF and its decrease when clean air is supplied; the model successfully predicts the available experimental data regarding outlet VOC emissions. The model also simulates the variations of the dissolved carbon in the water tank: the accumulation of dissolved carbon when the BTF is fed with VOC-polluted air and its decrease when clean air is used, showing good agreement with the available experimental TOC concentrations. For example, the model predicts the increase of the experimental organic carbon concentration from 55 (after purging the tank at 52 h) to

~400 mg–C·L^{-1} after the third daily spraying during Run 3. In spite of increasing the driving force, the intermediate purge had a negligible impact on the outlet VOC emissions (a similar experimental peak was obtained at the third daily spraying of Days 2 and 3). This corroborates that the gas-phase emission during spraying could be associated with the high resistance of the gas-liquid mass transfer.

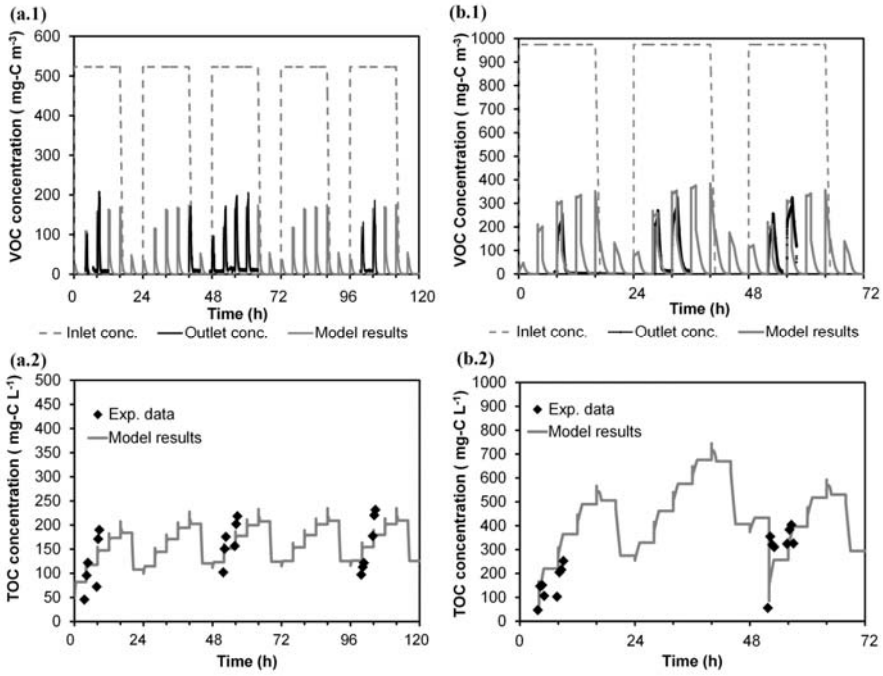

Figure 5. Weekly evolution of the experimental data and model predictions for the treatment of isopropanol by BTF (**a**) Run 2. (**a.1**) gas phase; (**a.2**) dissolved carbon in the water tank. (**b**) Run 3. (**b.1**) gas phase; (**b.2**) dissolved carbon in the water tank.

3.3. Model Simulations

To assess the impact of the calibration parameters, μ_{max}, β and K_s, on the VOC outlet concentration and on the concentration of the dissolved carbon in the water tank, model simulations were carried out modifying by ±50% each parameter individually from the value listed in Table 3. The rest of the model parameters are listed in Table 3. Figure 6 shows the application of this study to Run 1 (Wednesday data, 48 to 72 h). When μ_{max} was increased to 50%, the model predicted lower values in the maximum concentration of the gas phase during the spraying periods (161 mg–C·m^{-3}). The predicted concentrations of the dissolved carbon in the water tank were lower (178 mg–C·L^{-1}) than those obtained with the optimal value (224 mg–C·L^{-1}) of μ_{max}, while during the periods fed with clean air, the dissolved

carbon concentration decreased faster (24 mg–C·L^{-1}) than that obtained with the calibrated value (58 mg–C·L^{-1}). In contrast, when the μ_{max} was decreased by 50%, higher peaks were obtained during spraying periods (max peak 187 mg–C·m^{-3}). It is important to note that the decreasing of the outlet concentration after a spraying was slower than the experimental decrease, indicating that the process was controlled by the kinetics. The dissolved carbon concentration was higher (320 mg–C·L^{-1}) than that obtained with the optimal value of μ_{max}. When β was increased up to 50%, greater concentrations in the gas and in the liquid phase were obtained (max values 182 mg–C·m^{-3} and 281 mg–C·L^{-1}, respectively); while β was decreased by 50%, lower peaks in the outlet gas phase and a lower concentration in the water tank were achieved (max values 153 mg–C·m^{-3} and 140 mg–C·L^{-1}, respectively). The parameter β is related to the transfer of pollutant and oxygen between liquid and biofilm, and this analysis shows that this parameter is one of the most sensitive in the modelling of the treatment of isopropanol by BTF. When K_s was modified ±50%, the model appeared less sensitive to modifications of this parameter, obtaining a neglecting effect in the gas phase and less impact in the concentration of the dissolved carbon in the water tank than with the other parameters.

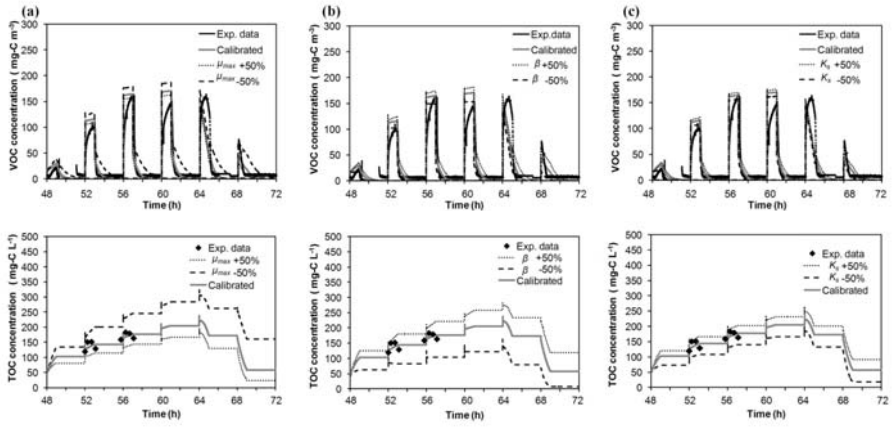

Figure 6. Effect of (**a**) μ_{max}, (**b**) β and (**c**) K_s on the outlet gas-phase concentration and on the dissolved carbon concentration in the recirculation tank. Experimental data correspond to the Wednesday data (48 to 72 h) of Run 1.

3.4. Model Application to Industrial Unit Processes

The model proposed herein was applied by using experimental data from two different periods from an industrial BTF located at a flexographic industry site (Run 4 and Run 5). Experimental data from both runs have a two-year spacing. Table 4 shows the VOC composition of the industrial emission and the diffusion coefficient in water and Henry's law constant for each compound that composed the VOC emission. Figure 7 shows the experimental data and the model simulations for both runs. In this figure, time 0 h refers to Monday 00:00 am. In contrast to those obtained in the laboratory experiments, the

gaseous outlet emissions showed a buffered pattern, and no peaks associated with spraying or with instantaneous variations of the flow rate or inlet emissions were observed. During VOC inlet emissions coming from the factory (from 6:00 am to 12:00 pm), the outlet gas concentrations of the BTF were not clearly related to the spraying pattern; a continuous gradual increase of them was observed every day. During night periods (from 00:00 to 6:00 am), a slow decrease in the outlet emissions was observed; the VOC accumulated in the biofilm during periods receiving inlet emissions was not totally stripped or degraded over 6 hours, while when the bioreactor was operated with clear air for more than 24 h (weekends), the outlet gas concentration became negligible (data between 0 and 6 h in Figure 7). The industrial BTF was acting as an absorption-desorption system during VOC feeding-non-VOC feeding cycles. This seems to indicate that there is a difference in the rate-limiting steps between the treatment of hydrophilic VOC by biotrickling filtration at the industrial scale and for laboratory units. This finding was one of the challenges of this work. Based on these two observations (no peaks during spraying and continuous outlet emissions during non-VOC feeding periods), it was assumed that: (1) there was an extra mass transfer resistance between the gas and liquid phases during non-spraying periods not observed in the laboratory experiments; and (2) a thick biofilm was developed.

Table 4. VOC composition and physical properties of the compounds of the industrial emission.

Compounds	Composition (%)	D_P ($m^2 \cdot s^{-1}$) [25]	H_P [27]
Ethanol	63	1.48×10^{-9}	2.30×10^{-4}
Ethyl acetate	22	9.57×10^{-10}	6.40×10^{-3}
1-Ethoxy-2-propanol	13	8.49×10^{-10}	1.00×10^{-6} *

* Data estimated from [30]

The simulation parameters for the application of the model to the industrial unit processes are listed in Table 3, except the overall mass transfer coefficients and the biofilm thickness. As the industrial BTF worked under conditions of variable gas velocities, the overall mass transfer coefficient for the pollutant was estimated for each simulated time point, applying the correlation proposed by San-Valero *et al.* [24], using the gas velocity and the weighted average value of Henry's law constant of the VOC mixture (Equation (12)). This weighted average Henry's law constant was calculated using the percentage composition of each compound and its Henry's law constant (Table 4).

$$K_L a_P = \frac{H_P}{3600}\left(11.59\left(v_G 3600\right)^{0.85}\right) \quad (12)$$

The overall mass transfer of oxygen was experimentally determined in the laboratory, obtaining a value of 0.0066 s^{-1} for this packing material. The biofilm thickness (δ) was fitted to 500 μm in order to reproduce the slow desorption occurring during periods without supplying VOCs (every day from 0 am to 6 am). During spraying, it was assumed that there is similar mass transfer resistance to that in the laboratory systems (α_1 = 0.23). The emergence of the extra mass transfer resistance during non-spraying was related to the creation of a stagnant liquid phase. The switch parameter α_2 was set to one to consider the resistance to mass transfer within the gas-liquid interface during non-spraying periods. Simulation of both runs started with clean water (VOC accumulated in the water tank during working days was removed at the weekend). In the case of Run 5, the recirculation tank on Wednesday at 4 pm (64 h of Run 5 in Figure 7) was renewed with fresh water; this was included in the simulation.

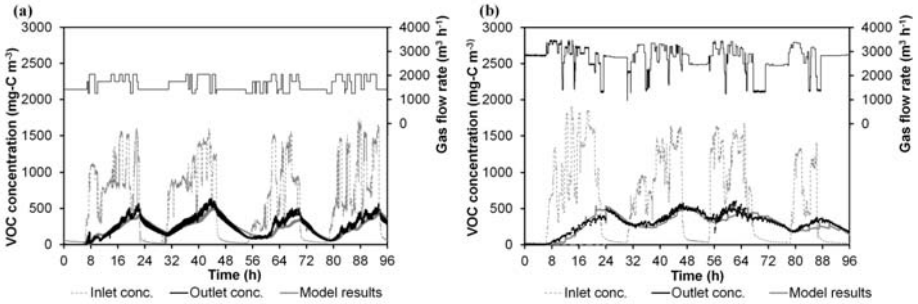

Figure 7. Experimental data and model results of the industrial BTF installed in a flexographic industry site: (**a**) Run 4 (**b**) Run 5.

As can be seen in Figure 7, the correspondence between the calculated and the experimental VOC emissions is quite good. Relative errors between simulated and experimental data were 1.6% and 2.2% for Run 4 and Run 5, respectively. During the course of the biological process, VOCs were degraded, but a part of the load is cyclically absorbed-desorbed following the daily cycles of VOC feeding-non VOC feeding. The thick biofilm works as the sink (every day from 6 am to 12 pm) and source (every day from 0 am to 6 am) of the pollutant. The dynamic mathematical model approaches these phenomena through the existence of two resistances in series (gas-liquid, liquid-biofilm) that keep constant by operating the BTF with or without irrigation. This work appears as one of the first attempts to go more deeply into the modelling of the dynamic response associated with intermittent conditions (irrigation and inlet emissions), focusing on the observed differences between laboratory and industrial BTFs. In future work, the results of the model could be integrated into a software tool for the design and control of industrial BTFs.

4. Conclusions

A dynamic general model to simulate the removal of isopropanol emissions by biotrickling filtration has been developed. The model was built as a coupled set of equations for spraying and non-spraying periods in order to represent the intermittent irrigation usually performed in industrial applications. The model has been evaluated by using laboratory experiments working under intermittent spraying and intermittent VOC feeding to the bioreactor. The model predicts not only the overall performance, but also the outlet emission peaks occurring during spraying and the sharp decrease of gas-phase outlet concentration after spraying stops, indicating that mass transfer resistance during non-spraying was negligible. Practical applications of this model to predict the outlet VOC emissions in industrial BTF treating a mixture of pollutants were demonstrated. In this case, the thick biofilm and the mass transfer resistance between gas and stagnant liquid during non-spraying were the two main different characteristics from the model application to laboratory data.

Nomenclature

a	Specific surface area of the packing material (m^{-1})
C	Concentration ($g \cdot m^{-3}$)
D	Diffusion coefficient of substrates ($m^2 \cdot s^{-1}$)
$f(X_v)$	Correction factor of diffusivity in biofilm according to Fan's equation
H	Henry's law constant
K_s	Half saturation rate constants of the substrate ($g–C \cdot m^{-3}$)
K_La	Overall mass transfer coefficients of the substrates (s^{-1})
M	Number of divisions along the biofilm
N	Number of divisions along the column
Q	Flow rate ($m^3 \cdot s^{-1}$)
S	Concentration in the biofilm ($g \cdot m^{-3}$)
t	Time (s)
v	Superficial velocity calculated as a fraction of Q and S ($m \cdot s^{-1}$)
V	Volume (m^3)
x	Coordinate for the depth in the biofilm, perpendicular to the biofilm surface
X_v	Biomass concentration in the biofilm ($g \cdot m^{-3}$)
Y	Yield coefficient (g of dry biomass synthesized per g consumed)
z	Axial coordinate in the reactor
Z	Height of the reactor (m)
Greek letters	
α_1	Correction of the mass transfer coefficient between biotic and abiotic systems
α_2	Switch parameter of the model
β	Thickness of the liquid-biofilm interface (m)
δ	Thickness of the biofilm (m)
θ_B	Volume fraction of the biofilm (–)
θ_G	Porosity of the bioreactor (–)
θ_L	Volume fraction of the liquid phase (–)
θ_{PM}	Porosity of the packing material (–)
μ_{max}	Maximum specific growth rate of the substratum (s^{-1})
Subscripts	
i	Substance (pollutant and oxygen)
G	Gas
L	Liquid
B	Biofilm
P	Pollutant
O	Oxygen
R	Reactor
T	Tank

Acknowledgements

This project has received funding from the European Union's Seventh Framework Programme for research, technological development and demonstration under Grant Agreement No. 284949. Financial support from the Ministerio de Economía y Competitividad (Project CTM2010-15031/TECNO) and the Generalitat Valenciana (PROMETEO/2013/053), Spain, is also acknowledged. The authors would like to give special thanks to Dr. Sempere (PAS Solutions BV) for his consistent collaboration and support. Finally, Pau San Valero thanks the Ministerio de Educación, Cultura y Deporte, Spain, for her FPU contract (AP2010-2191).

Author Contributions

San-Valero, Penya-roja and Gabaldón conceived and designed the laboratory experiments. San-Valero and Penya-roja performed the laboratory experiments. Penya-roja and Gabaldón performed the industrial experiments. All authors contributed to the mathematical modelling. San-Valero, Penya-roja, Álvarez-Hornos and Gabaldón ideated the model equations. Marzal assisted and supervised to the numerical solution of the model. San-Valero was responsible for generating the case studies of the model. San-Valero and Gabaldón drafted the manuscript, which was revised by all authors. All authors read and approved the final manuscript.

Conflicts of Interest

The authors declare no conflict of interest.

References

1. European Environment Agency (EEA). *European Union Emission Inventory Report 1990–2012 under the UNECE Convention on Long-Range Transboundary Air Pollution (LRTAP) (Technical Report N° 12/2014)*; Publications Office of the European Union: Luxembourg city, Luxembourg, 2014.
2. Kennes, C.; Rene, E.R.; Veiga, M.C. Bioprocesses for air pollution control. *J. Chem. Technol. Biotechnol*. **2009**, *84*, 1419–1436.
3. Kennes, C.; Thalasso, F. Review: Waste gas biotreatment technology. *J. Chem. Technol. Biotechnol.* **1998**, *72*, 303–319.
4. Webster, T.S.; Cox, H.H.J.; Deshusses, M.A. Resolving operational and performance problems encountered in the use of a pilot/full-scale biotrickling fiber reactor. *Environ. Prog.* **1999**, *18*, 162–172.
5. Zhu, X.Q.; Alonso, C.; Suidan, M.T.; Cao, H.W.; Kim, B.J.; Kim, B.R. The effect of liquid phase on VOC removal in trickle-bed biofilters. *Water Sci. Technol.* **1998**, *38*, 315–322.
6. Sempere, F.; Gabaldón, C.; Martínez-Soria, V.; Marzal, P.; Penya-roja, J.M.; Alvarez-Hornos, F.J. Performance evaluation of a biotrickling filter treating a mixture of oxygenated VOCs during intermittent loading. *Chemosphere* **2008**, *73*, 1533–1539.

7. Kennes, C.; Veiga, M.C. Biotrickling filters. In *Air pollution prevention and control. Bioreactors and Bioenergy*; Kennes, C., Veiga, M.C., Eds.; John Wiley & Sons, Ltd.: Oxford, UK, 2013; pp. 121–138.
8. San-Valero, P.; Penya-Roja, J.M.; Sempere, F.; Gabaldon, C. Biotrickling filtration of isopropanol under intermittent loading conditions. *Bioprocess Biosyst. Eng.* **2013**, *36*, 975–984.
9. Lu, C.Y.; Chang, K.; Hsu, S. A model for treating isopropyl alcohol and acetone mixtures in a trickle-bed air biofilter. *Process Biochem.* **2004**, *39*, 1849–1858.
10. Ottengraf, S.P.; Van Den Oever, A.H. Kinetics of organic-compound removal from waste gases with a biological filter. *Biotechnol. Bioeng.* **1983**, *25*, 3089–3102.
11. Rene, E.R.; Veiga, M.C.; Kennes, C. Biofilters. In *Air Pollution Prevention and Control: Bioreactors and Bioenergy*; Kennes, C., Veiga, M.C, Eds.; John Wiley & Sons, Ltd.: Oxford, UK, 2013; pp. 59–120.
12. Shareefdeen, Z.; Baltzis, B.C.; Oh, Y.S.; Bartha, R. Biofiltration of methanol vapor. *Biotechnol. Bioeng.* **1993**, *41*, 512–524.
13. Shareefdeen, Z.; Baltzis, B.C. Biofiltration of toluene vapor under steady-state and transient conditions—Theory and experimental results. *Chem. Eng. Sci.* **1994**, *49*, 4347–4360.
14. Mpanias, C.J.; Baltzis, B.C. An experimental and modeling study on the removal of mono-chlorobenzene vapor in biotrickling filters. *Biotechnol. Bioeng.* **1998**, *59*, 328–343.
15. Baltzis, B.C.; Mpanias, C.J.; Bhattacharya, S. Modeling the removal of VOC mixtures in biotrickling filters. *Biotechnol. Bioeng.* **2001**, *72*, 389–401.
16. Okkerse, W.J.H.; Ottengraf, S.P.P.; Osinga-Kuipers, B.; Okkerse, M. Biomass accumulation and clogging in biotrickling filters for waste gas treatment. Evaluation of a dynamic model using dichloromethane as a model pollutant. *Biotechnol. Bioeng.* **1999**, *63*, 418–430.
17. Kim, S.; Deshusses, M.A. Development and experimental validation of a conceptual model for biotrickling filtration of H_2S. *Environ. Prog.* **2003**, *22*, 119–128.
18. Almenglo, F.; Ramírez, M.; Gómez, J.M.; Cantero, D.; Gamisans, X.; Dorado, A.D. Modeling and control strategies development for anoxic biotrickling filtration. In *Biotechniques for Air Pollution Control and Bioenergy*; Malhautier, L., Ed.; Presses de Mines: Paris, France, 2013; pp. 123–131.
19. Lee, S.H.; Heber, A.J. Ethylene removal using biotrickling filters: Part II. Parameter estimation and mathematical simulation. *Chem. Eng. J.* **2010**, *158*, 89–99.
20. Alonso, C.; Suidan, M.T.; Kim, B.R.; Kim, B.J. Dynamic mathematical model for the biodegradation of VOCs in a biofilter: Biomass accumulation study. *Environ. Sci. Technol.* **1998**, *32*, 3118–3123.
21. Iliuta, I.; Iliuta, M.C.; Larachi, F. Hydrodynamics modeling of bioclogging in waste gas treating trickle-bed bioreactors. *Ind. Eng. Chem. Res.* **2005**, *44*, 5044–5052.
22. Devinny, J.S.; Ramesh, J. A phenomenological review of biofilter models. *Chem. Eng. J.* **2005**, *113*, 187–196.
23. Fan, L.S.; Leyva-Ramos, R.; Wisecarver, K.D.; Zehner, B.J. Diffusion of phenol through a biofilm grown on activated carbon particles in a draft-tube three-phase fluidized-bed bioreactor. *Biotechnol. Bioeng.* **1990**, *35*, 279–286.

24. San-Valero, P.; Penya-Roja, J.M.; Álvarez-Hornos, F.J.; Gabaldón, C. Modelling mass transfer properties in a biotrickling filter for the removal of isopropanol. *Chem. Eng. Sci.* **2014**, *108*, 47–56.
25. Tucker, W.A.; Nelken, L.H. Diffusion coefficients in air and water. In *Handbook of Chemical Property Estimation Methods*; Lyman, W.J., Reehl, W.F., Rosenblatt, D.H., Eds.; American Chemical Society: New York, NY, USA, 1982.
26. Reid, R.C.; Prausnitz, J.M.; Poling, B.E. *The Properties of Gases and Liquids*; McGraw-Hill Book Company: New York, NY, USA, 1987.
27. Sander, R. Henry's law constants. In *NIST Chemistry Webbook, NIST Standard Reference Database Number 69*; Linstrom, P.J., Mallard, W.G., Eds.; National Institute of Standards and Technology: Gaithersburg, MD, USA, 2005.
28. Bustard, M.T.; Meeyoo, V.; Wright, P.C. Kinetic analysis of high-concentration isopropanol biodegradation by a solvent-tolerant mixed microbial culture. *Biotechnol. Bioeng.* **2002**, *78*, 708–713.
29. Zhang, X.Q.; Bishop, P.L. Biodegradability of biofilm extracellular polymeric substances. *Chemosphere* **2003**, *50*, 63–69.
30. US EPA. *Estimation Programs Interface Suite™ for Microsoft® Windows, V 4.11*; United States Environmental Protection Agency: Washington, DC, USA, 2013.

Chemical Engineering Communications, 203:476–487, 2016

ISSN: 0098-6445 print/1563-5201 online
DOI: 10.1080/00986445.2015.1025954

Taylor & Francis
Taylor & Francis Group

A Tool for Predicting the Dynamic Response of Biotrickling Filters for VOC Removal

PAU SAN-VALERO[1], SALVADOR ALCÁNTARA[2], JOSEP M. PENYA-ROJA[1], F. JAVIER ÁLVAREZ-HORNOS[1], and CARMEN GABALDÓN[1]

[1]*Research Group GI²AM, Department of Chemical Engineering, University of Valencia, Avda. Universitat s/n, Burjassot, Spain*
[2]*PAS Solutions BV, AC Heerenveen, The Netherlands*

This article presents the development of a MATLAB® computer program to simulate the performance of biotrickling filters. Since these filters behave differently during spraying and nonspraying cycles, the presented simulation tool is built on top of a mathematical description of each situation. The resulting variable-structure model is then used as the basis for simulation experiments. The model presented herein represents the first attempt to take into account the variable spraying pattern usually found in industrial installations. Overall, the software is flexible and easy to use, allowing the user to specify the emission concentration pattern, the gas concentration pattern, as well as the spraying cycle periods for up to two different emission patterns per day. The model is able to predict experimental data from a biotrickling filter treating isopropanol under intermittent conditions of loading and spraying. Simulation examples are then provided to study the effect of variable inlet concentrations and gas flow rates.

Keywords: Biotrickling filters; Computer simulation; Mathematical modeling; Numerical analysis; VOC

Introduction

Emission to the atmosphere, from a wide variety of sources, of volatile organic compounds (VOCs) remains one of the most important causes of air pollution. This has triggered significant research efforts to develop more cost-effective and environmentally friendly solutions for the treatment of air emissions of VOCs. In particular, there has been an increasing interest in biofiltration, especially since it has been classified as a best available technique (BAT) by the European Commission, (2003). Among the biofiltration strategies, biotrickling filters (BTFs) constitute one of the most suitable biotechnologies for the treatment of VOCs. Biotrickling filters consist of a column filled with an inert packing material where the biomass attaches to the media and develops a biofilm. In this configuration, the gas and liquid phases circulate through the column in co- or countercurrent mode. Thus, the pollutant and the oxygen are transferred from the gas phase to trickling liquid, and then to the biofilm, where biodegradation takes place.

Biotrickling filtration has been applied successfully to the treatment of VOCs at the laboratory, pilot, and industrial scales. However, to further improve the performance of BTFs for the treatment of VOCs it has become necessary to understand the intricacies of the processes involved as well as their rate-limiting steps (Popat and Deshusses, 2010). In this regard, biotrickling filtration involves a complex set of physicochemical and biological mechanisms and, hence, mathematical models, in conjunction with computer-aided simulation, appear as fundamental tools to go deeper into the understanding of the involved governing processes.

Industrial processes that use solvents have fluctuating VOC emissions arising from the specific application and the unit operation dynamics of each particular industry Rene et al., (2013). These result in emission levels whose variation in time is related to random fluctuations in the gas velocity and the inlet concentration profile. In addition, short-time shut-off periods associated with nights, weekends, and holiday closures further contribute to creating a variable pattern of VOC emissions at the industrial scale. This variability may sometimes hinder the performance of field-scale BTFs (Sempere et al., 2010). Also, operating BTFs under cyclic and discontinuous operation has traditionally produced some problems, as reported in Webster et al., (1999).

Intermittent water trickling, in contrast to continuous trickling, is also common practice in the operation of industrial BTFs. As shown in Sempere et al., (2008), intermittent trickling may improve the removal efficiency and better control the pressure drop. The final performance of the BTF is quite dependent on the rate of liquid trickling (Zhu et al., 1998). An intermittent spraying regime implies that the mobile liquid phase is not always present during the filter operation, making it necessary to distinguish two different situations, corresponding to *spraying* and *nonspraying*

Address correspondence to Carmen Gabaldón, Research Group GI²AM, Department of Chemical Engineering, University of Valencia, Avda. Universitat s/n, 46100 Burjassot, Spain. E-mail: carmen.gabaldon@uv.es

Color versions of one or more of the figures in the article can be found online at www.tandfonline.com/gcec.

periods. Nevertheless, the modeling and simulation research presented in the literature so far tends to focus only on one particular case.

Several efforts have been made to model biofiltration processes. One of the most used models for the treatment of organic pollutants in waste gases in a gas–liquid biofilter has been developed by Ottengraf and Van Den Oever, (1983) in steady-state conditions. Since then, there has been increasing interest in the application of dynamic models of biofilters and BTFs rather than of steady-state models. Shareefdeen and Baltzis, (1994) published one of the first attempts to describe the dynamic behavior of biofilters, including the oxygen limitation in the biofilm and the phenomena of adsorption. Deshusses et al., (1995) proposed a model for the determination of the transient and steady-state conditions degrading the methyl ethyl ketone and methyl isobutyl ketone emissions in biofilters. Zarook et al., (1997) developed a transient biofiltration model that incorporates oxygen limitation effects, general mixing, and adsorption phenomena, as well as general biodegradation reaction kinetics. Thereafter, many researchers introduced variations of these models by taking new factors into consideration. Métris et al., (2001) used a simplication of the Zarook et al., (1997) model using CO_2 production to evaluate the response of the biofilters to starvation and shock loads in the biofiltration of toluene and xylene. Álvarez-Hornos et al., (2009) developed a dynamic model with a Haldane-type kinetic expression that considers oxygen limitation, (cross) inhibition effects due to high concentrations of substrates, and a general axial gradient equation for the biomass density. Many BTF models derive from biofilter models. Okkerse et al., (1999) presented a detailed dynamic model that includes the growth of methylene chloride degraders and inert biomass as well as the effect of the pH and dissolved oxygen. Kim and Deshusses, (2003) presented a three-phase dynamic model to describe the biotrickling filtration of hydrogen sulfide with counter-current flows of a gas and a liquid. They assumed that the biofilm was not completely wetted by the liquid phase and thus, in some parts of the biofilm, the pollutant was transferred directly from the gas phase to the biofilm. In their review of biofilters and biotrickling modeling, Devinny and Ramesh, (2005) pointed out that no single model has become generally accepted. The complexity behind the operation of BTFs has made many researchers consider specific situations in their simulation studies Lee and Heber, 2010, Mannucci et al., (2012).

The increase in the number of factors taken into consideration in the mathematical models has necessitated greater efforts for their mathematical solution. In the case of the models of biotrickling filters, the presence of the liquid phase implies an increase of the level of complexity and for counter-current operation, that which is usually found in the industry, the system of equations obtained can be relatively *stiff* and model instabilities could make their solution difficult (Deshusses and Shareefdeen, 2005). Even so, it has been recognized that realistic models adapted to the emissions of the industry are needed.

The aim of this paper is to present a more flexible tool to simulate the performance of BTFs. Based on the operational conditions commonly found in industry, the proposed model allows specifying variable inlet concentration patterns and gas velocities combined with different spraying patterns. These and other features provide the necessary flexibility to reproduce typical industrial use cases.

Model Development

Industrial BTFs operate with intermittent water trickling. This means that the mobile liquid phase is only present at some times during the day, referred to here as the *spraying periods*. For the rest of the time, referred to as the *nonspraying periods*, the liquid phase remains as a stagnant phase. Figure 1 illustrates this concept. The modeling step has to take into account the principal mechanisms of the biofiltration process in each situation. In this configuration, the pollutant/oxygen is transferred from the gas phase to the liquid phase and then to the biofilm, as represented in Figure 2. The model has been developed following the general mass balances of the gas phase, liquid phase, and biofilm, by taking into account the most important phenomena compiled by Devinny and Ramesh, (2005).

For the derivation of the model, the following general assumptions have been made, based on consolidated models reported Kim and Deshusses, 2003, Mpanias and Baltzis, (1998) and adapted to this model.

1. The gas phase flows in a plug flow regime along the filter bed.
2. Axial dispersion is neglected.

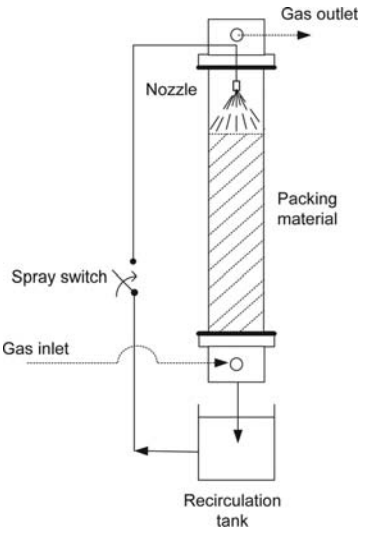

Fig. 1. Diagram of a BTF. Liquid recirculation only happens during spraying periods.

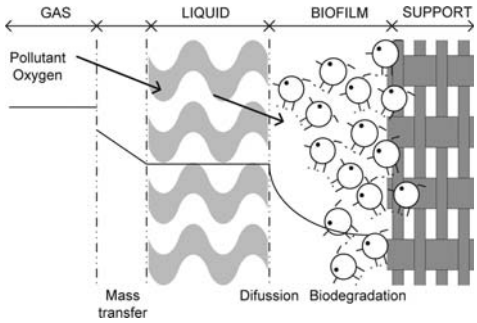

Fig. 2. Mechanisms involved in the process of BTF.

3. The adsorption of the pollutant in the packing material is negligible.
4. An active biofilm is formed on the external surface of the packing material and no reaction occurs in the pores. The biofilm covers the surface of the packing material and its thickness (δ) is much smaller than the size of the solid particles, so a planar geometry has been assumed.
5. The packing material is completely covered by the biofilm.
6. The diffusion of the biofilm is described by Fick's law.
7. Ideal conditions of nutrients and pH are assumed.
8. The system works under cycling conditions of spraying/nonspraying periods.
9. The status reached at the end of one period determines the initial conditions for the next period.
10. The biodegradation kinetics is described by a Monod expression, which takes into account oxygen limitation.
11. The mass flux at the gas–liquid interface can be expressed by mass transfer coefficients.
12. The mass flux at the liquid–biofilm interface can be expressed by mass transfer coefficients.
13. There is no reaction in the liquid phase.
14. The gas–liquid interface is in equilibrium according to Henry's law.

Based on the assumptions above, the mass balances for the different phases can be written as follows:

Spray Mode

Mass Balance in the Gas Phase

$$\theta_G \frac{\partial C_{G_P}}{\partial t} = -v_G \frac{\partial C_{G_P}}{\partial z} - \alpha_1 K_L a_P \left(\frac{C_{G_P}}{H_P} - C_{L_P} \right) \quad (1)$$

$$\theta_G \frac{\partial C_{G_O}}{\partial t} = -v_G \frac{\partial C_{G_O}}{\partial z} - \alpha_1 K_L a_O \left(\frac{C_{G_O}}{H_O} - C_{L_O} \right) \quad (2)$$

where for the pollutant and oxygen, respectively, C_{G_P} and C_{G_O} are the concentrations in the gas phase, $K_L a_P$ and $K_L a_O$ are the overall mass transfer coefficients, α_1 is the correction factor of the overall mass transfer coefficients, H_P and H_O are the dimensionless Henry's law constants expressed as concentration of the gas phase/concentration of the liquid phase, and C_{L_P} and C_{L_O} are the concentration of the liquid phase. t denotes the time, z is the distance from the bottom of the column and v_G is the superficial air velocity given by

$$v_G = \frac{Q_G}{\frac{\pi D^2}{4}} \quad (3)$$

where Q_G is the volumetric gas flow rate and D is the column diameter.

θ_G is the porosity of the bioreactor and is given by

$$\theta_G = 1 - (1 - \theta_{pm}) - \theta_L - \theta_B \quad (4)$$

where θ_{pm} is the void fraction of the packing material, θ_L is the fraction occupied by the liquid film, and θ_B is the fraction occupied by the biofilm.

The boundary conditions of Equations (1) and (2) are

$$\begin{aligned} C_{G_P} &= C_{G_P}^{in} \quad \text{at } z = 0 \\ C_{G_O} &= C_{G_O}^{in} \quad \text{at } z = 0 \end{aligned} \quad (5)$$

where $C_{G_P}^{in}$ and $C_{G_O}^{in}$ are the inlet concentrations in the gas phase of the pollutant and the oxygen, respectively.

Mass Balance in the Liquid Phase

$$\theta_L \frac{\partial C_{L_P}}{\partial t} = v_L \frac{\partial C_{L_P}}{\partial z} + \alpha_1 K_L a_P \left(\frac{C_{G_P}}{H_P} - C_{L_P} \right) - \frac{D_{w_P} A}{\beta} (C_{L_P} - S_{P_1}) \quad (6)$$

$$\theta_L \frac{\partial C_{L_O}}{\partial t} = v_L \frac{\partial C_{L_O}}{\partial z} + \alpha_1 K_L a_O \left(\frac{C_{G_O}}{H_O} - C_{L_O} \right) - \frac{D_{w_O} A}{\beta} (C_{L_O} - S_{O_1}) \quad (7)$$

where for the pollutant and oxygen, respectively, S_{P_1} and S_{O_1} are the concentration in the biofilm interface, β is the thickness of the liquid–biofilm interface, D_{w_P} and D_{w_O} are the diffusion coefficient in water, A is the specific surface area, x is the axial position along the biofilm, and v_L is the superficial liquid velocity given by

$$v_L = \frac{Q_L}{\frac{\pi D^2}{4}} \quad (8)$$

where Q_L is the volumetric liquid flow rate.

The boundary conditions of Equations (6) and (7) are

$$\begin{aligned} \frac{\partial C_{L_P}}{\partial t} &= \frac{Q_L}{V_T} (C_{L_{P(z=0)}} - C_{L_{P(z=Z)}}) \quad \text{at } z = Z \\ \frac{\partial C_{L_O}}{\partial t} &= \frac{Q_L}{V_T} (C_{L_{O(z=0)}} - C_{L_{O(z=Z)}}) \quad \text{at } z = Z \end{aligned} \quad (9)$$

The boundary conditions given by Equation (9) correspond to the mass balances in the recirculation tank, where V_T is the water volume in the recirculation tank. It is assumed that the liquid inlet concentration in the column is equal to the concentration in the recirculation tank, and that the recirculated water depends on the liquid concentration at the bottom of the column.

Mass Balance in the Biofilm

$$\frac{\partial S_P}{\partial t} = D_{P_B}\frac{\partial^2 S_P}{\partial x^2} - \frac{\mu_{\max} X_v}{Y_P}\frac{S_P}{S_P + K_P}\frac{S_O}{S_O + K_O} \tag{10}$$

$$\frac{\partial S_O}{\partial t} = D_{O_B}\frac{\partial^2 S_O}{\partial x^2} - \frac{\mu_{\max} X_v}{Y_O}\frac{S_P}{S_P + K_P}\frac{S_O}{S_O + K_O} \tag{11}$$

where S_P and S_O are the concentrations in the biofilm. The boundary conditions are given by

$$\begin{aligned} \frac{\partial S_P}{\partial t} &= 0 \quad \text{at} \quad x = \delta \\ \frac{\partial S_O}{\partial t} &= 0 \quad \text{at} \quad x = \delta \end{aligned} \tag{12}$$

where X_v is the concentration of the biomass, $\mu_{\max}$ is the specific growth rate of the biomass and for the pollutant and oxygen, respectively, K_{S_P} and K_{S_O} are the half-saturation constants, Y_P and Y_O are the yield coefficients, and D_{P_B} and D_{O_B} are the effective diffusion coefficients inside the biofilm corrected by a factor ($f(X_v)$), calculated according to Fan's equation (Fan et al., 1990):

$$f(X_v) = \left(1 - \frac{0.43(X_v 10^{-3})^{0.92}}{11.19 + 0.27(X_v 10^{-3})^{0.99}}\right) \tag{13}$$

Nonspray Mode

Analogously, the mass balances during nonspraying periods are:

Mass Balance in the Gas Phase

$$\theta_G\frac{\partial C_{G_P}}{\partial t} = -v_G\frac{\partial C_{G_P}}{\partial z} - \alpha_2\alpha_1 K_L a_P\left(\frac{C_{G_P}}{H_P} - C_{L_P}\right) \tag{14}$$

$$\theta_G\frac{\partial C_{G_O}}{\partial t} = -v_G\frac{\partial C_{G_O}}{\partial z} - \alpha_2\alpha_1 K_L a_O\left(\frac{C_{G_O}}{H_O} - C_{L_O}\right) \tag{15}$$

with the boundary conditions

$$\begin{aligned} C_{G_P} &= C_{G_P}^{in} \quad \text{at} \quad z = 0 \\ C_{G_O} &= C_{G_O}^{in} \quad \text{at} \quad z = 0 \end{aligned} \tag{16}$$

where α_2 is a switch model parameter (100 indicates that no mass transfer resistance is assumed between the gas and liquid phases, and 1 indicates that there is a mass transfer resistance).

Mass Balance in the Liquid Phase

$$\theta_L\frac{\partial C_{L_P}}{\partial t} = \alpha_2\alpha_1 K_L a_P\left(\frac{C_{G_P}}{H_P} - C_{L_P}\right) - \frac{D_{w_P}A}{\beta}(C_{L_P} - S_{P_1}) \tag{17}$$

$$\theta_L\frac{\partial C_{L_O}}{\partial t} = \alpha_2\alpha_1 K_L a_O\left(\frac{C_{G_O}}{H_O} - C_{L_O}\right) - \frac{D_{w_O}A}{\beta}(C_{L_O} - S_{O_1}) \tag{18}$$

Mass Balance in the Biofilm

$$\frac{\partial S_P}{\partial t} = D_{P_B}\frac{\partial^2 S_P}{\partial x^2} - \frac{\mu_{\max} X_v}{Y_P}\frac{S_P}{S_P + K_P}\frac{S_O}{S_O + K_O} \tag{19}$$

$$\frac{\partial S_O}{\partial t} = D_{O_B}\frac{\partial^2 S_O}{\partial x^2} - \frac{\mu_{\max} X_v}{Y_O}\frac{S_P}{S_P + K_P}\frac{S_O}{S_O + K_O} \tag{20}$$

with the boundary conditions

$$\begin{aligned} \frac{\partial S_P}{\partial t} &= 0 \quad \text{at} \quad x = \delta \\ \frac{\partial S_O}{\partial t} &= 0 \quad \text{at} \quad x = \delta \end{aligned} \tag{21}$$

Numerical Solution

The partial differential Equations (1), (2), (6), (7), (10), (11) (spray mode) and (14), (15), (17), (18), (19), and (20) (nonspray mode) constitute two-second-order nonlinear distributed systems. In order to solve them, the method of lines (MOL) Schiesser, 1991, Schiesser, 1994, Schiesser and Griffiths, (2009) has been chosen. Although the finite difference method (FDM) has previously been used in the literature to simulate biofilters and biotrickling filters (Ikemoto et al., 2006, Álvarez-Hornos et al., 2009) in different ways, the MOL has some advantages that make it more suitable here. Apart from its simplicity, it allows taking advantage of the available ODE solvers. Note, in addition, that the overall MOL process can be regarded as an FDM procedure where the discretization in t is independent of that in x, z, which provides extra flexibility. Since the resulting systems have been found to be *stiff*, as is normally the case when applying the MOL (Schiesser, 1994), the ODE23t solver from the MATLAB® has been selected for solving the corresponding equations. The ODE23t is based on an implicit integration method and it is quite concerned with the stability issue. Other ODE solvers were tested, but the chosen solver gave the best results in practice. The MOL method is applied here following the steps:

- Generate a uniform grid in the spatial dimensions, i.e., $(x_i, z_j)_{i,j}$. Z, the height of the column (the z axis), is divided into N sections. Similarly, the biofilm thickness δ is divided into M sections with $M+1$ points. The values of $N=20$, $M=40$ were used for the spatial discretization in each mode.

- For each node in the grid, replace the partial derivatives in the model equations with finite difference approximations.
- Solve the resulting system of ordinary differential equations (ODEs) using standard numerical methods; note that the time variable t was left continuous in the first step.

Developed Software Tool

The main objective of this paper is to introduce a tool for the simulation of biotrickling filters using the mathematical models and numerical procedures described in the previous sections. This section describes the basic features implemented in the tool, focusing on its usability. The software has been developed in MATLAB®. It can be used with the basic MATLAB® package and it is available as a MATLAB package as well as a compiled standalone application. The graphical user interface (GUI) has been created using the GUIDE–MATLAB® toolbox. A screenshot of the GUI is shown in Figure 3. In the present example, the option *two emissions pattern (per day)* allows specifying two different patterns of inlet concentration, gas velocity, and spraying, over a period of 86,400 s (i.e., 1 day). When this option is marked, the user indicates the duration of the first pattern ($<86{,}400$ s). The duration of the second pattern is then calculated automatically (86,400 s – time pattern 1). The resulting global daily pattern is the combination of the two specified patterns in series, and the total simulation time in this case equals the number of days specified by the user.

The emission pattern and the spraying pattern are defined by the user by

- VOC inlet concentrations. For the inlet VOC concentration ($C^{in}_{G_p}$) pattern, a drop-down list presents the user with the following options for the input profile:
  – Constant. The inlet concentration is assumed constant.

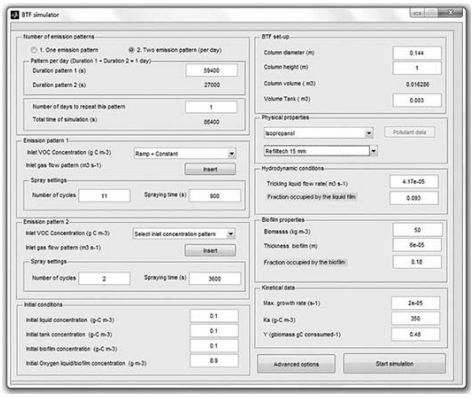

Fig. 3. Main window of the GUI: two emission patterns (per day).

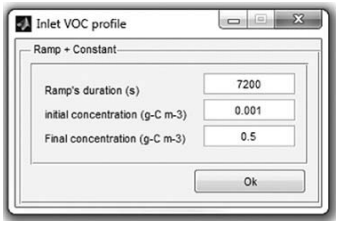

Fig. 4. GUI of the MATLAB tool. Dialog for the Ramp+Constant inlet VOC concentration profile.

  – Ramp+Constant. A constant concentration is considered as before, but preceded by a ramp pofile until the final value is reached.
  – Pulse train. The inlet concentration oscillates between two values, describing a pulse train input signal.
  – Piecewise constant. The inlet concentration consists of a step (or staircase) function, i.e., it is piecewise constant having only finitely many pieces.

After making a choice, a dialog window allows introducing the defining parameters for each case. For instance, for the Ramp+Constant profile, Figure 4 shows the resulting dialog.

In contrast with the inlet VOC concentration, the inlet oxygen concentration (C^{in}_{Go}) is assumed constant throughout the whole simulation ($276\,\mathrm{g\,m^{-3}}$).

- Inlet gas flow pattern. This consists of a step (or staircase) function, i.e., it is piecewise constant having only finitely many pieces.
- Spray settings. The spraying pattern will consist of an ON/OFF signal. As an example, the scheme of the spraying pattern for the option *two emissions pattern (per day)* is illustrated in Figure 5.
  The spraying panel includes the following information:
  – Number of spray cycles (n). Defines how many times to spray during each emission pattern.

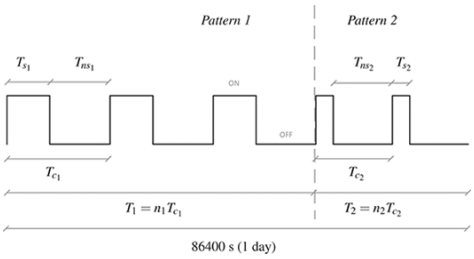

Fig. 5. Spray cycle patterns for 1 day. Emission pattern 1 has three cycles ($n_1 = 3$), and emission pattern 2 has two ($n_2 = 2$) spray cycles. The user specifies $T_{s_1}, n_1, T_1, T_{s_2}$, and n_2. *Nonspray times* are given by $T_{ns_1} = (T_1 - n_1 T_{s_1})/n_1)$ and $T_{ns_2} = (T_2 - n_2 T_{s_2})/n_2$ for emission pattern 1 and emission pattern 2, respectively.

– Spraying time (T_s). Duration of spraying, i.e., the duration of the ON part of one spray cycle.

The simulation requires the user to specify the initial conditions:

- Initial conditions for the simulation. This includes the VOC concentration in the liquid phase, the VOC concentration in the water tank and inside the biofilm, and the oxygen concentration in the liquid and inside the biofilm.

The input related to the BTF configuration, the pollutant and packing material data, and the model parameters are defined by the user:

- BTF setup. This part defines the characteristics of the BTF system, such as the column diameter, column height, and the volume of the water tank. This panel provides automatically the column volume of the reactors.
- Physical properties. The physical properties panel includes the selection of the pollutant and the selection of the packing material. The selection of the pollutant uses a pop-up menu where it is possible to choose from among some predefined VOCs, whose information includes the diffusion coefficient in water (D_{P_w}), the Henry's law constant (H_P) at 25°C, and the chemical formula. Alternatively, the user can select a user defined pollutant by specifying its diffusion coefficient in water, its Henry's law constant, and its chemical formula. The selection of the packing material uses another pop-up menu in which there are some predefined packing materials for each of which there are provided its specific surface area (A), porosity (θ_{pm}), and specific coefficients to calculate the overall mass transfer coefficients (K_La_P, K_La_O) using the correlations proposed by San-Valero et al., (2014). Alternatively, it is possible to a custom other packing material by specifying its specific surface area, porosity, and overall mass transfer coefficients.
- Hydrodynamic conditions such as the liquid flow rate and the fraction occupied by the liquid film (θ_L).
- Biofilm properties. In this panel there should be indicated its biomass density (Xv), the thickness of its biofilm (δ), and fraction occupied by the biofilm (θ_B).
- Kinetics data. In this panel the user indicates the kinetic parameters regarding the pollutant degradation (μ_{max}, K_s and Y_P). Regarding the oxygen parameters, K_O has been predefined from the literature as 0.26 g m^{-3} and Y_O is calculated by stoichiometry balance.
- Advanced options. This button opens a dialog where other properties related with the mass transfer can be defined.

After all the input data and parameters have been defined, the simulation is run by pressing the Start button. When it concludes, the results are presented to the user in a new window, shown in Figure 6. The main items are described next.

- A graph showing both the inlet and the outlet VOC concentrations in the gas phase.
- A graph showing the evolution of the VOC concentration in the liquid tank.
- Some relevant averages, over the whole simulation time, are displayed by this panel:
  – Inlet/Outlet VOC concentrations,

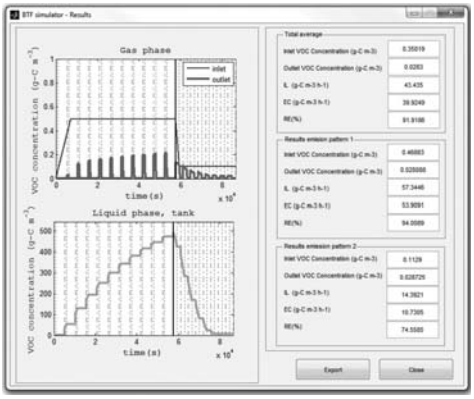

Fig. 6. GUI of the MATLAB tool (results window).

– Inlet load (IL) defined as

$$IL(\frac{g-C}{m^3\ h^1}) = \frac{\overline{C_G^{in}}\overline{Q_G}}{V_R}3600 \tag{22}$$

where $\overline{C_G^{in}}$ is the average inlet concentration and $\overline{Q_G}$ is the average gas flow rate.

– Removal efficiency (RE):

$$RE(\%) = \frac{\overline{C_G^{in}} - \overline{C_G^{out}}}{\overline{C_G^{in}}}100 \tag{23}$$

where $\overline{C_G^{out}}$ is the average outlet concentration.

– Elimination capacity (EC):

$$EC(\frac{g-C}{m^3\ h^1}) = \frac{RE}{100}IL \tag{24}$$

- Panel with averages for the emission pattern 1 only.
- Panel with averages for the emission pattern 2 only.
- This button allows exporting the simulation results to a *Comma-Separated Values* (CSV) file.
- Closes the results window.

Model Calibration and Validation

The model was calibrated and validated by using the experimental data corresponding to the dynamic response of a biotrickling filter treating isopropanol obtained by San-Valero et al., (2013). In this data, the BTF was operated under intermittent loading conditions and intermittent spraying frequency. These are the conditions typically found in the operation of industrial BTFs. During these experiments, it was observed that the discontinuous regime of spraying of the bed resulted in outlet emissions of isopropanol during spraying periods. Based on this observation, the effect of

the spraying pattern was evaluated and it was pointed out that the spraying frequency is a critical parameter to achieve low emissions. The BTF was operated by using an IL of 32 g-Cm^{-3} h^{-1} and empty bed residence time (EBRT) of 30 s. The EBRT is defined as

$$EBRT(s) = \frac{V_R}{Q_G} \quad (25)$$

These VOC feeding conditions were applied for a total duration of 57,600 s (16 h) from 6:00 to 22:00 h. The rest of the day, the biotrickling filter remained without VOC supply and without spraying. The parameters used in the modeling of the BTF behavior are summarized in Table 1. The experimental parameters were taken from the literature or experimentally determined. The calibrated parameters were determined to fit the transient response data of the biotrickling filter. An independent experiment with a spraying pattern of 15 min every 1.5 h was used in the calibration step. Thus, time durations of 900 and 4500 s for the spraying and nonspraying periods, respectively, were set. In this experiment, it was assumed that there was no mass transfer resistance at the gas–liquid interface ($\alpha_2 = 100$). A comparison of the experimental results and the model predictions is shown in Figure 7. Figure 7(a) displays the evolution of the inlet and outlet VOC concentrations while Figure 7(b) displays the evolution of the concentration of carbon dissolved in the water tank.

As is shown in Figure 7(a), the maximum concentrations of the pollutant are reached during the spraying periods, whereas during the nonspraying periods, nearly complete biodegradation of the pollutant is obtained. In addition,

Table 1. Model parameters used in the mathematical model

Variable	Specific value	Units	References
Experimental parameters			
A_v	348	m^{-1}	San-Valero et al., (2013)
D	0.144	m	San-Valero et al., (2013)
D_{P_w}	1.13×10^{-9}	m^2 s^{-1}	Tucker and Nelken, (1982)
D_{O_w}	2×10^{-9}	m^2 s^{-1}	Reid et al., (1987)
H_P	2.8×10^{-4}		San-Valero et al., (2014)
H_O	31.4		Sander, (2005)
$K_L a_P$	$\frac{H_P}{3600}\left(11.59(v_G 3600)^{0.85}\right)$	s^{-1}	San-Valero et al., (2014)
$K_L a_0$	1.15×10^{-2}	s^{-1}	San-Valero et al., (2014)
Q_L	41.7×10^{-6}	m^3 s^{-1}	San-Valero et al., (2013)
V_R	0.0163	m^3	San-Valero et al., (2013)
V_T	0.003	m^3	San-Valero et al., (2013)
X_v	50×10^3	g m^{-3}	This paper
Y_P	0.48	$\frac{gbiomass}{gconsumed}$	Lu et al., (2004)
Y_O	0.14	$\frac{gbiomass}{gconsumed}$	Stoichiometric balance
Z	1	m	San-Valero et al., (2013)
θ_B	0.18		This paper
θ_L	0.093		This paper
Calibration parameters			
K_{s_P}	350	g-C m^{-3}	
α_1	0.23 (except for cycle 1 that takes $\alpha_1 = 1$)		
β	6.4×10^{-6}	m	
δ	60×10^{-6}	m	
μ_{max}	2×10^{-5}	s^{-1}	

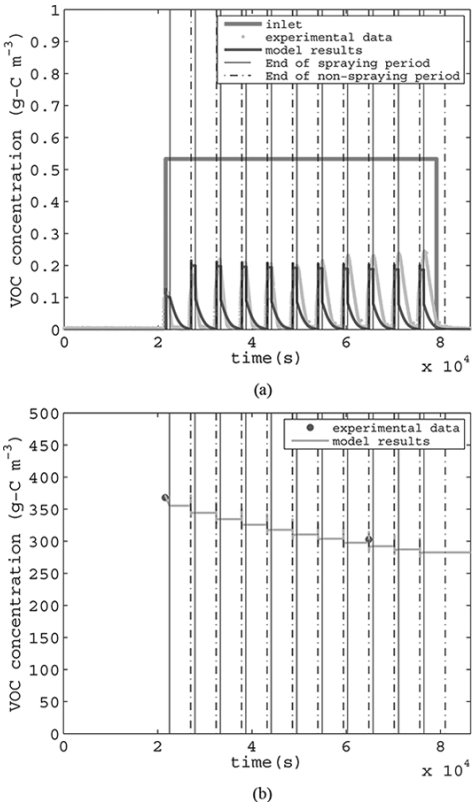

Fig. 7. Model calibration with experimental data from San-Valero et al., (2013). (a) Evolution of the concentration in the gas phase. (b) Evolution of the dissolved organic carbon in the recirculation tank.

the peaks increase as the system gets filled with pollutant, reaching a stationary value for an outlet VOC concentration of around 0.2 g-Cm^{-3} after the third cycle. An EC of 27.2 g-Cm^{-3} h^{-1} is obtained for an IL of 32 g-Cm^{-3} h^{-1} during VOC feeding periods. The model successfully predicts the behavior obtained, achieving maximum outlet concentrations during the spraying periods during the last cycles of the day. The experimental data fit the model prediction with a relative error of less than 3% in the EC (EC of the model 28.0 g-Cm^{-3} h^{-1}). Also, the model prediction for the carbon dissolved in the water tank is in good agreement with the measured carbon in the water tank.

The validation of the model was carried out by using data from two experiments. The first experiment was carried out with a low spraying frequency of 15 min every 3 h, and a moderate IL = 32 g-Cm^{-3} h^{-1}. The second experiment was carried out with double spraying frequency (15 min every 1.5 h) and a double IL (65 g-Cm^{-3} h^{-1}). The experimental data and the model predictions are shown in Figure 8. Figure 8(a) displays the evolution of the inlet and outlet VOC concentrations for the first experiment while Figure 8(b) displays the evolution of the inlet and outlet VOC concentrations for the second experiment.

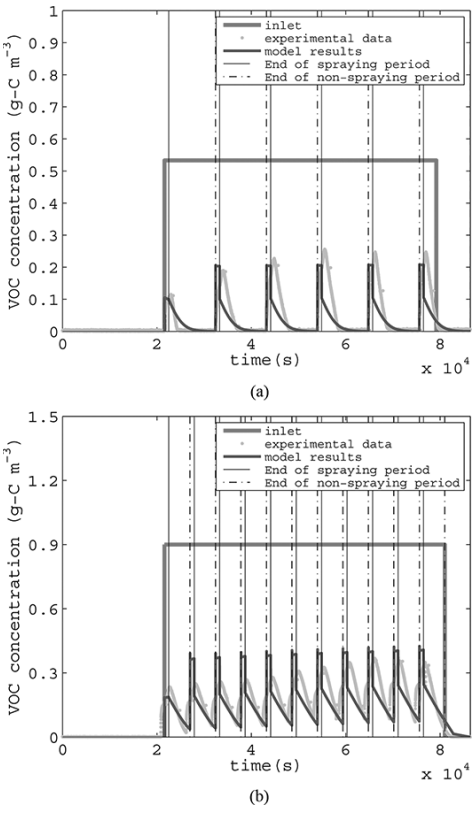

Fig. 8. Model validation with experimental data from San-Valero et al., (2013). (a) Spraying regime 15 min every 3 h and IL 32 g—C m^{-3}. (b) Spraying regime 15 min every 1.5 h and IL 65 g—C m^{-3}.

For the experiments carried out with a spraying regime of 15 min every 3 h and an IL of 32 g-Cm^{-3} h^{-1}, the relative error between the experimental and the simulated EC is 3.2% (experimental EC of 28.8 g-Cm^{-3} h^{-1} and modeled EC of 29.7 g-Cm^{-3} h^{-1}). For the experiments carried out with a spraying regime of 15 min every 1.5 h and an IL of 65 g-Cm^{-3} h^{-1}, the error between the experimental and simulated EC is 4.0% (experimental EC of 50.3 g-Cm^{-3} h^{-1} and modeled EC of 52.3 g-Cm^{-3} h^{-1}). The modeled concentration of the dissolved carbon in the recirculation tank is in agreement with the measured values. As an example, for the series with a spraying regime of 15 min every 3 h and an IL of 32 g-Cm^{-3} h^{-1}, the measured dissolved carbon was 357 g-Cm^{-3} and the model predicted a value was 365 g-Cm^{-3}, with a relative error of 2.2%.

So, the model has been proven suitable for describing the complex phenomena observed in the transient response of the biotrickling filter to variations of the spraying pattern.

Study of the Dynamic Response of the BTF to Variable Inlet Concentrations and Gas Flow Rates

Dynamic Response of the BTF to Oscillating Inlet Concentrations

The effect of oscillating inlet VOC concentrations on the dynamic response of the BTF was investigated by using a periodic pulse train concentration pattern. The pulse train profile was used to study the influence of high shock loads during regular changes in the operation on the performance of the BTF. In particular, the selected inlet concentration took on two alternating values: $C_{Gp}^{in} = 0.7$ g-Cm^{-3} (for 7200 s) and $C_{Gp}^{in} = 0.2$ g-Cm^{-3} (for 3600 s). A linear transition with a duration of 15 min was used to connect the two different values. A constant EBRT of 60 s was applied. Also, durations of 0.25 and 1 h were specified for the spraying and nonspraying periods, respectively, and this pattern was applied for $T = 59{,}400$ s. The simulation results are presented in Figure 9(a) for the gas phase and in Figure 9(b) for the liquid phase. Figure 9(a) shows that the concentration peaks not only depend on the spraying cycles but also on the pattern of the inlet concentration. An EC of 30 g-Cm^{-3} h^{-1} was obtained for an IL of 32 g-Cm^{-3} h^{-1}. The evolution of the VOC in the tank is presented in Figure 9(b). To observe the accumulation of dissolved carbon in the water tank, in this example the concentration of dissolved carbon in the tank was set to 0 g-Cm^{-3}. In this example, two different phenomena can be observed: absorption and desorption processes. These processes are markedly dependent on the equilibrium between the gas and liquid phases. As can be

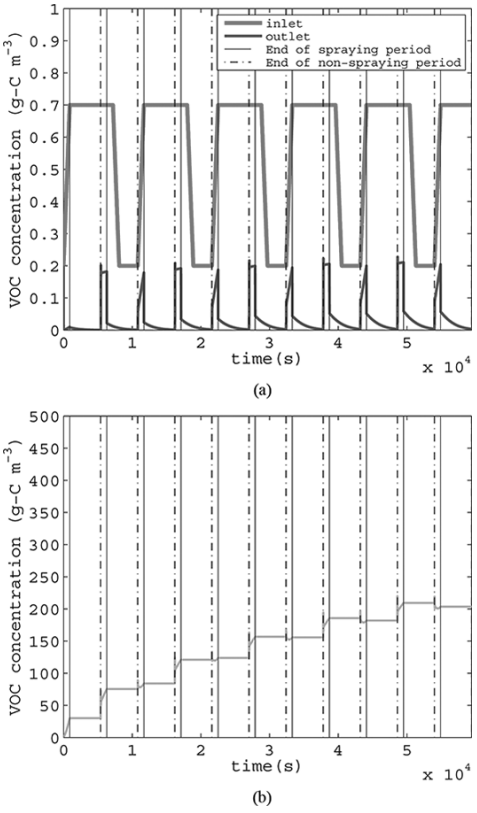

Fig. 9. Dynamic response of the BTF to oscillating inlet concentration. (a) Evolution of the concentration in the gas phase. (b) Evolution of the dissolved organic carbon in the recirculation tank.

observed, when the inlet concentration increases during the spraying periods, a desorption of pollutant from the liquid phase to the gas phase is produced, and the opposite occurs when the inlet concentration increases. At the end of the period, the water contains 200 g-Cm^{-3} of dissolved carbon.

Dynamic Response of the BTF to Oscillating Inlet Concentration Combined with Spraying Times during Non-VOC Feeding Periods

The dynamic response of the BTF to oscillating inlet concentrations combined with spraying times during non-VOC feeding periods was investigated. An oscillating emission pattern was applied for a total of 59,400 s per day. The inlet VOC concentration was exactly the same as the pulse train profile used in the previous example. A period without VOC feeding was applied for 27,000 s with a Ramp+ Constant profile of $C_{G_P} = 0.01$ g-Cm^{-3} and a spraying time of 1 h every 4 h. The results for the gas and liquid phases, respectively, are shown in Figures 10(a) and 10(b). The combination of different input profiles leads to some remarkable observations of the behavior of the system. Namely, the presence of dissolved VOCs in the water recirculation tank, combined with the spraying cycles during the shut-off periods, produces peaks of pollutant even in the absence of VOCs in the inlet stream. Also desorption is present during these periods. The decrease of these peaks during the

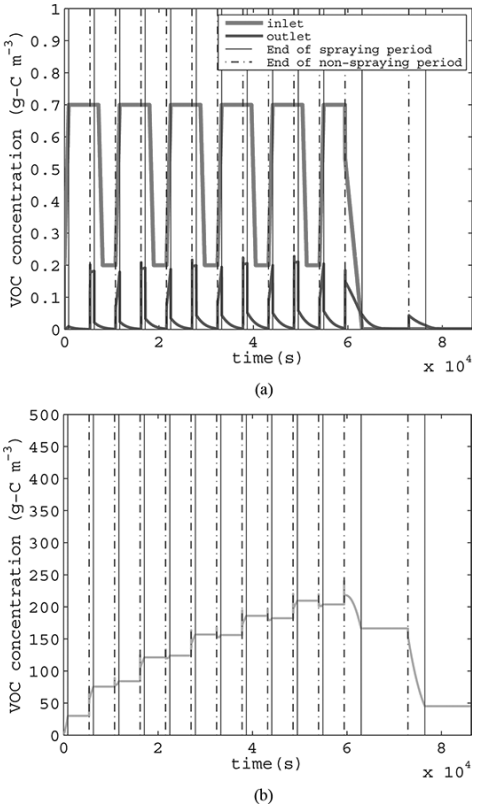

Fig. 10. Dynamic response of the BTF to oscillating inlet concentration combined with spraying times during non-VOC feeding periods. (a) Evolution of the concentration in the gas phase. (b) Evolution of the dissolved organic carbon in the recirculation tank.

shut-off periods are related to the transfer of VOCs to the column, where they get degraded.

Dynamic Response of the BTF to Oscillating Gas Flow Rates

The effect of the gas flow rate on the BTF was studied. A constant concentration of $C_{G_P} = 0.53\,\text{g-Cm}^{-3}$ was selected. The gas flow rate took on two alternating values: $4.8\ 10^{-4}\ \text{m}^3\ \text{s}^{-1}$ and $6.8\ 10^{-5}\ \text{m}^3\ \text{s}^{-1}$, each one applied for periods of 14,400 s. Note that the average value of the EBRT is 60 s, as in the previously considered examples. The simulation results are shown in Figure 11. Figure 11(a) displays the evolution of the inlet and outlet VOC concentrations in the gas phase, Figure 11(b) displays the evolution of the concentration of carbon dissolved in the water tank, and Figure 11(c) displays the oscillating EBRT pattern. As can be seen from Figure 11(a), the evolution of the peaks of the outlet gas concentration are different from those obtained in the previous examples. The gas velocity is directly related to the mass transfer of the pollutant between the gas and liquid phases, obtaining a greater mass transfer at large gas velocities, and thus, smaller EBRTs. The peaks in the outlet VOC concentration pattern obtained do oscillate according to the oscillating EBRT pattern. This contrasts with Figure 7(a), where the peaks increase until reaching a stationary state. These VOC emissions are related to an increase of the IL generated by an increase in the gas velocity and thus a decrease in the EBRT. As for the liquid phase, in Figure 11(b) it is possible to observe the influence of the gas velocity and EBRT on the absorption and desorption processes. In this situation, the increase in the amount of carbon dissolved in the water tank is combined with the desorption processes, producing oscillations as in the case of the outlet concentration.

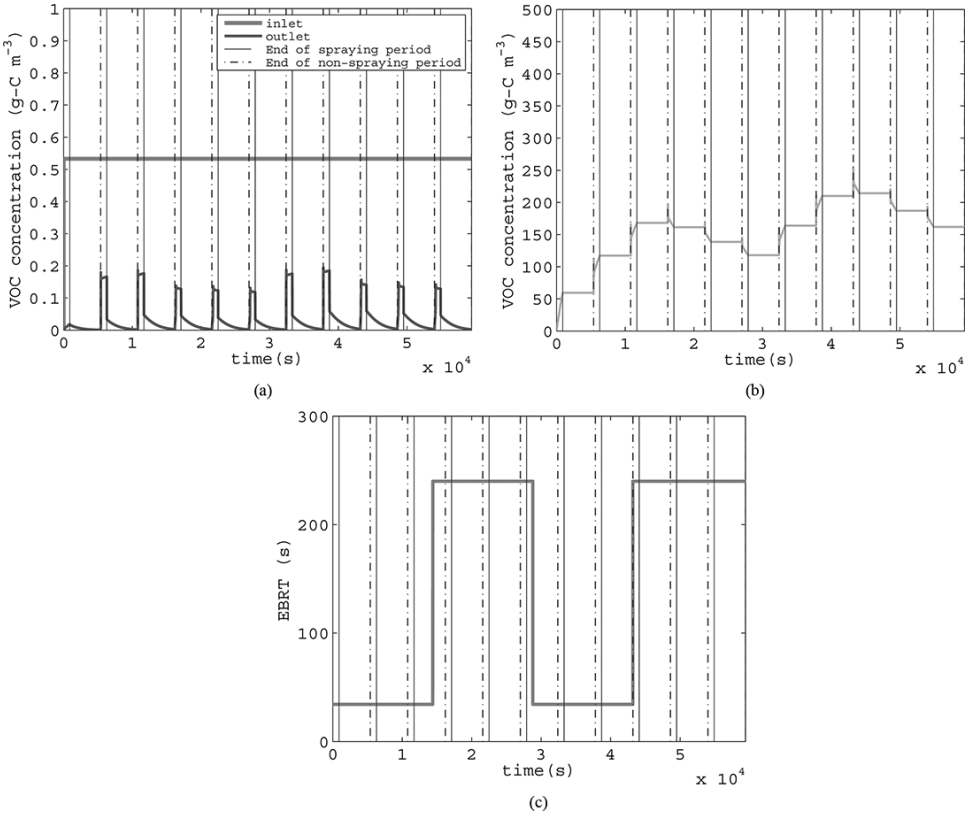

Fig. 11. Dynamic response of the BTF to oscillating gas flow rates. (a) Evolution of the concentration in the gas phase. (b) Evolution of the dissolved organic carbon in the recirculation tank. (c) Evolution of the EBRT.

Conclusions

BTFs usually employ alternating spraying and nonspraying periods. A software tool to simulate the behavior of BTFs under this and other typical conditions found in industrial facilities has been presented. The partial differential equations of the BTF model have been solved numerically using the method of lines. In particular, the software allows simulating the treatment of VOC air emissions under variable inlet concentrations and gas velocities. The model was calibrated and validated by using data from a biotrickling filter treating isopropanol under intermittent conditions of loading and spraying. The capability of the model to reproduce the complex phenomena involved in the dynamic response of the treatment of hydrophilic compounds by biotrickling filters has been proven. Several examples demonstrate that the pattern of the outlet emissions depends on the pattern of the gas velocity and inlet concentration, showing the usefulness of the tool to assist in the design and operation of BTFs. The software tool presented herein will be the basis for implementing new features. For example, it would be interesting to allow multicomponent mixtures in order to go deeper into the interactions between pollutants. This and other extensions are left for future research.

Funding

The research leading to these results has received funding from the People Programme (Marie Curie Actions) of the European Union's Seventh Framework Programme FP7/2007-2013/under REA grant agreement number 284949. Financial support from the Ministerio de Economia y Competitividad (Project CTM2010-15031/TECNO) and the Generalitat Valenciana (PROMETEO/2013/053), Spain, is also acknowledged. Finally, Pau San Valero thanks the Ministerio de Educación, Cultura y Deporte, Spain, for her FPU contract (AP2010-2191).

Nomenclature

A	specific surface area of the packing material (m^{-1})
C	concentration (g m^{-3})
D	diffusion coefficient of substrates (m^2 s^{-1})
$f(X_v)$	correction factor of diffusivity in biofilm according to Equation 13
H	Henry constant of the substrates
K_s	half saturation rate constants of substrate (g-C m^{-3})
K_La	overall mass transfer coefficients of the substrates (s^{-1})
M	number of divisions along the biofilm
N	number of divisions along the column
Q	flow rate (m^3 s^{-1})
S	concentration in the biofilm (g m^{-3})
t	time (s)
v	superficial velocity (m s^{-1})
V	volume (m^3)
x	coordinate for the depth in the biofilm, perpendicular to the biofilm surface
X_v	biomass concentration in the biofilm (g m^{-3})
Y	yield coefficient (g of dry biomass synthesized per g consumed)
z	axial coordinate in the reactor
Z	height of the reactor (m)
$C_{G_P}^{in}$	inlet VOC concentration (g-C m^{-3})
$C_{G_O}^{in}$	inlet oxygen concentration (g m^{-3})

Greek letters

β	liquid–biofilm interface (m)
δ	active biofilm thickness (m)
θ_B	fraction occupied by the biofilm
θ_G	porosity of the bioreactor
θ_L	fraction occupied by the liquid film
θ_{pm}	void fraction of the packing material
μ_{max}	maximum specific growth rate of the substratum (s^{-1})

Subscripts

G	gas
L	liquid
B	biofilm
P	pollutant
O	oxygen
R	reactor
T	tank
w	water

References

Álvarez-Hornos, F.-J., Gabaldón, C., Martnez-Soria, V., Marzal, P., and Penya-roja, J. M. (2009). Mathematical modeling of the biofiltration of ethyl acetate and toluene and their mixture, *Biochem. Eng. J.*, **43**(2), 169–177.

Deshusses, M.-A., Hamer, G., and Dunn, I.-J. (1995). Behavior of biofilters for waste air biotreatment. 1. Dynamic model development. *Environ. Sci. Tech.*, **29**(4), 1048–1058.

Deshusses, M.-A., and Shareefdeen, Z., (2005). Modeling of biofilters and biotrickling filters for odor and VOC control applications. In Shareefdeen, Z. and Singh, A., editors, *Biotechnology for Odor and Air Pollution Control*, Springer-Verlag, Berlin.

Devinny, J.-S., and Ramesh, J. (2005). A phenomenological review of biofilter models. *Chem. Eng. J.*, **113**(2–3), 187–196.

European Commission. (2003). IPPC reference document on best available techniques in common waste water and waste gas treatment/management systems in the chemical sector, Technical report, European Commission.

Fan, L.-S., Leyva-Ramos, R., Wisecarver, K. D., and Zehner, B. J. (1990). Diffusion of phenol through a biofilm grown on activated carbon particles in a draft-tube three-phase fluidized-bed bioreactor, *Biotechnol. Bioeng.*, **35**(3), 279–286.

Ikemoto, S., Jennings, A. A., and Skubal, K. L. (2006). Modeling hydrophobic VOC biofilter treatment in the presence of nutrient stimulation and hydrophilic VOC inhibition, *Environ. Model. Software*, **21**(10), 1387–1401.

Kim, S., and Deshusses, M. A. (2003). Development and experimental validation of a conceptual model for biotrickling filtration of H_2S, *Environ. Prog.*, **22**(2), 119–128.

Lee, S.-H., and Heber, A.-J. (2010). Ethylene removal using biotrickling filters: Part II. Parameter estimation and mathematical simulation, *Chem. Eng. J.*, **158**(2), 89–99.

Lu, C., Chang, K., and Hsu, S. (2004). A model for treating isopropyl alcohol and acetone mixtures in a trickle-bed air biofilter, *Process Biochem.*, **39**(12), 1849–1858.

Mannucci, A., Munz, G., Mori, G., and Lubello, C. (2012). Biomass accumulation modelling in a highly loaded biotrickling filter for hydrogen sulphide removal, *Chemosphere*, **88**(6), 712–717.

Mpanias, C. J., and Baltzis, B. C. (1998). An experimental and modeling study on the removal of mono-chlorobenzene vapor in biotrickling filters, *Biotechnol. Bioeng.*, **59**(3), 328–343.

Métris, A., Gerrard, A. M., Cumming, R. H., Weigner, P., and Paca, J. (2001). Modelling shock loadings and starvation in the biofiltration of toluene and xylene, *J. Chem. Technol. Biot.*, **76**(6), 565–572.

Okkerse, W. J.-H., Ottengraf, S. P.-P., Osinga-Kuipers, B., and Okkerse, M. (1999). Biomass accumulation and clogging in biotrickling filters for waste gas treatment. Evaluation of a dynamic model using dichloromethane as a model pollutant, *Biotechnol. Bioeng.*, **63**(4), 418–430.

Ottengraf, S. P.-P., and Van Den Oever, A. H.-C. (1983). Kinetics of organic compound removal from waste gases with a biological filter, *Biotechnol. Bioeng.*, **25**(12), 3089–3102.

Popat, S.-C., and Deshusses, M.-A. (2010). Analysis of the rate-limiting step of an anaerobic biotrickling filter removing TCE vapors, *Process Biochem.*, **45**(4), 549–555.

Reid, R. C., Prausnitz, J. M., and Polling, B. (1987). *The Properties of Gases and Liquids*, McGraw-Hill Book Company, New York.

Rene, E. R., Veiga, M. C., and Kennes, C. (2013). Biofilters, in Veiga, M. C., and Kennes, C., editors, *Air Pollution Prevention and Control: Bioreactors and Bioenergy*, John Wiley & Sons, Chichester:UK, pp. 59–119.

San-Valero, P., Penya-roja, J., Sempere, F., and Gabaldón, C. (2013). Biotrickling filtration of isopropanol under intermittent loading conditions, *Bioproc. Biosyst. Eng.*, **36**(7), 975–984.

San-Valero, P., Penya-roja, J. M., Álvarez Hornos, F. J., and Gabaldón, C. (2014). Modelling mass transfer properties in a biotrickling filter for the removal of isopropanol, *Chem. Eng. Sci.*, **108**(0), 47–56.

Sander, R. (2005). Henry's law constants in NIST Chemistry WebBook, in: Linstrom, P. and Mallard, W., editors, *NIST Standard Reference Database Number 69*, National Institute of Standards and Technology, Gaithersburg MD, 20899.

Schiesser, W.-E. (1991). *The Numerical Method of Lines*, Academic Press, San Diego.

Schiesser, W. E. (1994). *Computational Mathematics in Engineering and Applied Science: ODEs, DAEs and PDEs*, CRC Press, Boca Raton.

Schiesser, W.-E., and Griffiths, G. W. (2009). *A Compendium of Partial Differential Equation Models: Method of Lines Analysis with Matlab*, Cambridge University Press, Cambridge, UK.

Sempere, F., Gabaldón, C., Martnez-Soria, V., Marzal, P., Penya-roja, J. M., and Álvarez Hornos, F. J. (2008). Performance evaluation of a biotrickling filter treating a mixture of oxygenated VOCs during intermittent loading, *Chemosphere*, **73**(9), 1533–1539.

Sempere, F., Martnez-Soria, V., Penya-roja, J. M., Izquierdo, M., Palau, J., and Gabaldón, C. (2010). Comparison between laboratory and pilot biotrickling filtration of air emissions from painting and wood finishing, *J. Chem. Technol. Biot.*, **85**(3), 364–370.

Shareefdeen, Z., and Baltzis, B. C. (1994). Biofiltration of toluene vapor under steady-state and transient conditions- Theory and experimental results, *Chem. Eng. Sci.*, **49**(24A), 4347–4360.

Tucker, W. A., and Nelken, L. H. (1982). Diffusion coefficients in air and water, in: Lyman, W. J., Reehl, W. F., and Rosenblatt, D. H., editors, *Handbook of Chemical Property Estimation Methods*, chapter 17, American Chemical Society, New York.

Webster, T.-S., Cox, H. H.-J., and Deshusses, M.-A. (1999). Resolving operational and performance problems encountered in the use of a pilot/full-scale biotrickling fiber reactor, *Environ Prog*, **18**(3), 162–172.

Zarook, S.-M., Shaikh, A.-A., and Ansar, Z. (1997). Development, experimental validation and dynamic analysis of a general transient biofilter model, *Chem. Eng. Sci.*, **52**(5), 759–773.

Zhu, X. Q., Alonso, C., Suidan, M. T., Cao, H. W., Kim, B. J., and Kim, B. R. (1998). The effect of liquid phase on VOC removal in trickle-bed biofilters, *Water. Sci. Technol.*, **38**(3), 315–322.